FUNCTIONAL BRAIN CONNECTIVITY ASSOCIATED WITH REPETITIVE BEHAVIOR IN AUTISM SPECTRUM DISORDER

by

Kenton Hayes MacDowell

A Dissertation Submitted to the Faculty of

The Charles E. Schmidt College of Science

in Partial Fulfillment of the Requirements for the Degree of

Doctor of Philosophy

Florida Atlantic University

Boca Raton, FL

August 2021

FUNCTIONAL BRAIN CONNECTIVITY ASSOCIATED WITH REPETITIVE

BEHAVIOR IN AUTISM SPECTRUM DISORDER

by

Kenton Hayes MacDowell

This dissertation was prepared under the direction of the candidate's dissertation advisor, Dr. Summer L. Sheremata, Center for Complex Systems and Brain Sciences, and has been approved by the members of his supervisory committee. It was submitted to the faculty of the Charles E. Schmidt College of Science and was accepted in partial fulfillment of the requirements for the degree of Doctor of Philosophy.

SUPERVISORY COMMITTEE:

Summer Sheremata (Jul 13, 2021 16:23 EDT)

Summer L. Sheremata, Ph.D.
Dissertation Advisor

Ali A. Danesh, PhD (Jul 19, 2021 16:29 EDT)

Ali A. Danesh, Ph.D.

Gary W Perry (Jul 22, 2021 11:16 EDT)

Gary W. Perry, Ph.D.
Chair, Center for Complex Systems and Brain Sciences

Mark A Halko, PhD (Jul 19, 2021 19:04 EDT)

Mark A. Halko, Ph.D.

Teresa Wilcox, Ph.D.
Interim Dean, The Charles E. Schmidt College of Science

Robert W. Stackman Jr. (Jul 22, 2021 15:11 EDT)

Robert W. Stackman, Ph.D.
Dean, Graduate College

July 22, 2021

Date

ACKNOWLEDGEMENTS

Let it be first humbly requested that the particular order of the acknowledgments in this section be tolerated, if not forgiven; it was arrived at in terms of narrative development rather than relative importance, chronology, professional or other relational category, alphabetical precedence, or any other such matter, all of which I deemed to be, if not also incalculable, at the very least, meaningless.

Thank you to Dr. Douglas Broadfield for fostering my incipient interest in the mysteries of the brain by assisting me and exhorting me to start by learning about the things that are *not* mysteries about the brain, an essential prerequisite to probing its mysteries, and for recognizing that my unbridled enthusiasm could be bridled, and shaped into an actual productive enterprise, the latter having been confirmed if this is being read by any individual not on my advisory committee. Not only because the story in my case is so succinct, thank you to Dr. W. Scott McGraw, in whose undergraduate class in primate evolution and adaptation in 2012 I was introduced to my first scholarly brush with neuroscience in the form of my term paper entitled *The Evolution of the Anthropoid Brain*, establishing a proto-incipient interest in the mysteries of the brain, and there prior, to L. J. for recommending the popular science book *The Female Brain*, whereunto was eagerly directed the incipientest of brainular interest.

And thus let me thank, and to an extent that far exceeds the obviousness of so doing in a doctoral thesis acknowledgements section, my advisory committee. Dr. Sheremata, my committee chair, provided endless advice, insight, and support, as well as the gentle, and sometimes slightly less gentle, guidance necessary to shape my exuberant reading, writing, and tinkering with of scripts into an ostensibly coherent scientific effort; I wouldn't have believed it possible myself had I not seen it with my own eyes, and am not certain that even in such a case modest observational rigor isn't due. Dr. Danesh, with his insights into the lived, human experiences manifest by autism spectrum disorder, both in those diagnosed with it and in those touched by anyone else who has been diagnosed, as well as his broad knowledge of the brain science as it stands today in research on the disorder, likewise would elicit incredulity whereupon all of the above he also added inexhaustibly kind encouragement through every stage of the project, had I not also borne witness to it so perpetually. My committee has indeed been a dynamo like no other, which Dr. Halko has illustriously completes

iv

Systems and Brain Sciences, and especially the co-director Ms. Thamsten, without whom I surely would have missed one too many a deadline, repeatedly, to see this project through to the end.

Second-to-last, but least only in average body mass, I thank Anne, Banjo, Bebop and Rocksteady, Cali, Cookie and Crème, Eve, Gremlin and Bonsai, Joseph, Koyaanisqatsi, Nehushtan, Pablo and Frida, Peanut and Butterscotch, Peppermint, Reynolds and Cyril, Simone and Jean-Paul, and Vader, who have vouchsafed me, in the form of their defense, due to the surpassing virtue of their innocence, my cause and struggle. I ask anyone reading this consider looking into TNVR programs if feral cats overpopulate their locale.

For he gave me sound knowledge of what exists,

that I might know the structure of the universe and the force of its elements,

The beginning and the end and the midpoint of times,

the changes in the sun's course and the variations of the seasons,

Cycles of years, positions of stars,

natures of living things, tempers of beasts,

Powers of the winds and thoughts of human beings,

uses of plants and virtues of roots—

Whatever is hidden or plain I learned,

for Wisdom, the artisan of all, taught me.

Book of Wisdom, 7:17-22

ABSTRACT

Author: Kenton Hayes MacDowell

Title: Functional brain connectivity associated with repetitive behavior in autism
                     spectrum disorder

Institution: Florida Atlantic University

Dissertation Advisor: Dr. Summer L. Sheremata

Degree: Doctor of Philosophy

Year: 2021

The high prevalence of autism spectrum disorder (ASD) results in large costs to individuals, families, and society. Among diagnosed individuals, restrictive and repetitive behaviors (RRBs) correlate with functional impairments substantially impacting wellbeing but remain less studied than social and communication deficits. Brain resting-state functional connectivity (fc) measures intrinsic, potentially RRB-associated neural dynamics. Here, whole-brain (WB), and iterated seed-based (SB)fc guided by the preceding WBfc and *a priori* hypotheses was performed. Combined results were used to model a brain network beginning with qualitative assessment of its potential functional association with RRBs. Once rigorously defined, the network was used to inform construction of a dynamical systems model of brain activity hypothesized to correlate with RRB severity. Qualitative model behavior tracked expectations of real cortical activity in RRB presentation. Model numerical output was found to correlate with behavioral measures of RRBs to a significantly greater degree than the underlying brain connectivity values themselves did. Some summary measures of model output were also found to correlate significantly, though near threshold, with severity measures in the other two ASD core deficit domains, and particularly, far more extensively than should be expected given the underlying brain connectivity values themselves were apparently effectively wholly uncorrelated with the measures. Significant findings are: (1) dynamical modeling of brain activity can identify significant correlations with symptom manifestation that fc alone cannot; (2) dynamical modeling of brain activity could potentially increase understanding of ASD's extensive heterogeneity across symptom domains; (3) extensive overlap between the constructed network and known RRB-implicated brain divisions was identified, with cerebellum, increasingly implicated in distributed neocortical functional differences in RRBs in humans and animal models, centrally connected to

multiple such divisions; (4) further overlap is found via striatal circuitry, implicated in multiple RRB-like behaviors previously, and forming at least $^1/_3$ of the functional basis for the network's hypothetical relationship with RRBs; (5) ASD-associated angular gyrus, PFC, ACC overlap was found. This successful tandem application of fc, dynamical modeling, and neurocognitive network theory illustrates the need for broad theoretical approaches in illuminating ASD heterogeneity and the neurocognitive underpinnings of specific ASD presentations.

For my family.

FUNCTIONAL BRAIN CONNECTIVITY ASSOCIATED WITH REPETITIVE BEHAVIOR IN AUTISM SPECTRUM DISORDER

LIST OF TABLES

LIST OF FIGURES

CHAPTER 1

BACKGROUND

1.1 OVERVIEW OF ASD

Autism spectrum disorder is a neurodevelopmental disorder characterized by core deficits in social, language and nonverbal communication, and repetitive behavior domains [1]. Estimates for the prevalence of the disorder range from 0.6%, based on a review of studies from 14 countries, to 2.76%, by the National Center for Health Statistics [2], and the prevalence appears to be increasing through time [3]. The disorder has a significant genetic basis, consistently identified in twin studies [4], and has in fact been argued to be one of the most genetically influenced among those mental disorders with complex etiologies [5]. ASD-associated impairments result in substantial costs; including explicit and implicit costs to those with an ASD diagnosis, their family, social support structure, and the wider community, including government subsidies and unsubsidized healthcare costs, a per-capita lifetime total of well over two-million dollars has been estimated, with total costs in the United States over the next decade reaching over ten-trillion dollars [2]. Furthering our understanding of the disorder, then, is of great importance to both those with the disorder and society as a whole, especially because treatment options for the disorder remain relatively circumscribed: Treatment at present is largely in the form of behavioral therapy, dietary restrictions [6, 7], and, despite the implication of nearly every major neurotransmitter system with wide cerebral distribution, two antipsychotic medications, risperidone and aripiprazole, these to treat aggression, and no other FDA-approved pharmacotherapeutic interventions [8]. Recently, however, consistent with the implication of the nonapeptide oxytocin in some autism symptoms [9], a selective vasopressin V1a receptor antagonist is in phase 2 clinical trials with apparent efficacy in treating social and language, but not specifically repetitive behavior, deficits in ASD [10]. Vasopressin is a related nonapeptide hormone that also functions as a neurotransmitter implicated in social interactions.

The disorder was first described be Leo Kanner in 1943 [11, 12], but its precise symptomatological extent, along with how to approach research of the disorder with this issue in mind, continues to be debated. While both clinical and basic research has repeatedly found that the symptoms in different deficit categories in ASD are related to one another, and it presents as a coherent disorder, it is

characterized by substantial heterogeneity in multiple domains; it, therefore, consists of "dissimilar parts that are somehow connected [13, p. 123]." As a spectrum disorder, significant variability in the overall level of impairment between diagnosed individuals is an inherent property. However, significant differences in the severity of the individual symptoms, even between those within the same core deficit category, occur at any given level of overall impairment. Nevertheless, it is noted, "whereas there is striking behavioral heterogeneity among individuals with ASD, research continues to reinforce the concept that, as a group, individuals with ASD are characterized by a particular set of symptoms that differentiate them from other diagnostic groups [14, p. 5]," suggesting it is reasonable to construe ASD as a discrete disorder as long as its great diversity is appreciated.

1.1.1 Symptom manifestation

Despite many identified biological correlates in the brain and other organ systems, ASD is behaviorally defined [15–17]. Hence, the significance to individuals diagnosed with the disorder and to their family, friends, and caretakers lies in the distress caused by these behavioral symptoms. Symptoms within all three core deficit categories can result in significant difficulties with daily tasks, but individuals diagnosed with ASD are most frequently noted to demonstrate diminished social skills, including impairments in peer interactions. [18].

An extensive collection of examples of common difficulties faced by individuals with ASD can be found in [19]. In addition to the distinguishing (i.e., diagnostic) deficits characteristic of ASD, additional commonly observed symptoms are summarized: self-harm, abnormal aggressive behavior, anxiety, problems with sleep, problems with eating, and uncooperative behavior. Further behaviors commonly observed in individuals with ASD include "hand flapping, tip-toe walking, body rocking, echolalia . . . , or spinning objects [19, p. 411]." Some of the many other symptoms or difficulties sometimes observed include:

- Poor performance in school

- Attachment to odd objects, such as household tools instead of stuffed animals

- Fascination with specific objects

- Increased or decreased sensitivity to certain stimuli

- Seeking of specific sensory experiences (a behavior sometimes called "stimming")

- Comorbidity with disorders such as ADHD, anxiety spectrum disorders, gastrointestinal disturbances, and others

- Unusual emotional responses to other people

- Curtness in contravention of social norms

- A preference for simpler types of humor

- Missing joking behavior/taking a joke literally

- Great variation in different measures of cognitive performance, e.g., between verbal and performance IQ scores

- Being overwhelmed when performing complex tasks

- Sensory abnormalities, for example, hypersensitivity to auditory stimuli is observed in around one-fifth of children with ASD [20]

Relevant to this thesis is that these examples are all presented in the context of a review of evidence bearing on the plausibility of brain connectivity-based explanations for the symptoms of ASD [19]. While differences in brain connectivity are proposed to result in the symptoms of ASD, including those above, the differences in brain connectivity are not ultimately the cause of ASD, that is, they are likely to arise from some more fundamental biological mechanism. However, understanding the relationship between brain connectivity differences and ASD symptoms helps characterize the pathophysiology of the disorder which, in turn, can better inform potential clinical interventions. Even so, the high degree of variability in the presentation of the disorder complicates such research, and because the current level of knowledge regarding its fundamental nature still leaves us uncomfortably far from "knowing what we don't know [21]," a full appreciation of its complexity is a prerequisite for designing contextualizable research methodologies at this stage.

1.1.2 Diagnostic criteria

ASD in the DSM-5 [22, p. 50] is placed under the neurodevelopmental disorders. It comprises three severity categories based on the level of impairment, from minor, to requiring substantial assistance in daily tasks. The diagnostic criteria consist of four symptom categories, listed in figure 1.1.

Previously, in the DSM-IV-TR, and relevant to the discussion on heterogeneity (section 1.3), three separate disorders were defined under the autism diagnostic umbrella: autistic disorder, Asperger's syndrome, and pervasive developmental disorder, not otherwise specified [23]. This scheme is discrete too from the non-diagnostic, but common in the literature, distinction between "high-functioning autism (HFA)," typified by average intelligence but with the pervasive symptoms of ASD, and

(A) Persistent, pervasive, and sustained impairment in reciprocal social communication and social interaction

(B) Restricted and repetitive behavior, interests, or activities that are typically abnormal in intensity or focus

(C) Symptoms are present from early childhood

(D) Symptoms limit or impair everyday functioning

Figure 1.1: Diagnostic criteria for ASD separated into categories as given in the DSM-5 [22, pp. 53–54]

"low-functioning autism," which also includes intellectual disability and more severe impairment in daily activities. HFA-associated deficits include a lack of behavioral and cognitive flexibility, the performance of behavioral rituals, a poor grasp of abstract use of language, poor executive function, and dysregulation of temper, all of which can contribute to difficulties in daily life, school, and work [24], but without significant intellectual impairment, and with a relatively preserved ability to care for oneself.

While the DSM-5 definition, notably its collapse of the social and language core deficit categories into a single communication/social interaction category, is the one used in clinical practice in the United States at the time of this writing, the ABIDE II dataset used in this study utilized DSM-IV-TR criteria for inclusion of subjects (see section 2.1). Because this thesis considers the three core deficit categories as recognizably distinct in terms of behavioral measures, and not as groupings fundamental to the nature or definition of the disorder itself, "core deficits" will be used to denote social, language, and repetitive behavior domains.

Causes of the disorder

A vast swathe of research literature on risk factors and etiology, beyond genetic and broad environmental factors, exists, but with very little apparent cohesion between the mechanisms across the many proposals [12]. Some proposed risk factors and causes include exposure to heavy metals and other pollutants, vaccines (thoroughly debunked although of apparently intransigent popular interest [25]), other medications, and dietary factors, including the popular gluten/casein theory, likewise lacking high-quality evidentiary support in the literature [26].

One risk factor, however, has in fact been identified as significant and consistent: male gender.

This too, however, comes with a substantial caveat. Anatomical differences in the brain are more pronounced in females with ASD diagnoses than in males [27], suggesting that the disorder may, contrary to being more common in males, be underdiagnosed in females. Borderline personality disorder, which has been asserted to share fundamental cognitive mechanisms with ASD, may likewise be overdiagnosed in females while the true gender ratio may be closer to unity [28] (see also section 1.3). Conversely, however, the greatly increased risk for comorbid ASD in fragile x syndrome, an x-linked disorder, does provide one causative mechanism in which male karyotype does in fact increase the predicted incidence of ASD. That is, assuming fragile x syndrome increases the ASD risk in male and female karyotypes equally, its x-linked genetic mechanism would be expected to result in twice as many boys as girls receiving an ASD diagnosis comorbid to fragile x syndrome if survival rates for fragile x syndrome are equivalent for male and female karyotypes.

1.2 ASD RESEARCH—SUMMARY AND NEUROCOGNITIVE APPROACH

1.2.1 Brief history

Our understanding of ASD has evolved substantially since it was first recognized as a discrete disorder. The earliest propositions regarding its origins include that poor/distant parenting causes ASD, whereas it is now known to be a disorder of neural development substantially correlated with genetic factors [29].

Clinical and behavioral observations, neuroimaging studies (section 1.4.1), and human and animal [30] genetic studies have revealed several promising avenues for further research, if no final and coherent conclusion as yet. As research has proliferated, so too have efforts to account for the broad range of observations in terms of cohesive theories, several of which will now be discussed.

1.2.2 Contemporary theories

Attempts at theoretical syntheses of the extant ASD research literature may be termed "theories of autism." Such theories may consider only one, multiple, or ostensibly all of the relevant research domains, e.g., psychological, genetic, neurological, neurocognitive, etc. In any case, they share the common feature of an attempt to explain or "reduce" many apparently disparate findings to single explanatory mechanisms, or a few closely related mechanisms. Such attempts serve to generate new hypotheses as well as summarize results relevant to their proposed mechanism. Given that the precise clinical boundaries circumscribing ASD are not universally agreed upon [4], at least in terms sufficient to account for the substantially affirmed heterogeneity in the presentation of the disorder,

a single theory that unites all features of ASD is not now tenable, but theoretical syntheses are still important in that they render comprehensible what might at first seem an ever-expanding body of incongruous findings. An elaboration of several prominent such theories follows, and they are summarized in tables 1.1, 1.2 and 1.3.

Amygdala theory of autism

The *amygdala* theory of autism was one of the first popular theories. It is both simple, given its implication of a single anatomical area (the amygdala, or nucleus amygdalodeum), and powerful, in that multiple aspects of ASD symptomatology can be accounted for by it. Nevertheless, as could be expected, its simplicity also limits the extent to which it can account for all the features of a disorder as heterogeneous as ASD.

A central role for the amygdala in the cognitive activity required for social intelligence is posited under the theory to underly ASD social deficits [31]. Medical case studies and lesion studies, perhaps the oldest form of evidence of the functional organization of nervous systems, support this scheme: amygdala injuries cause impairments in emotion perception, the ability to discern between appropriate and inappropriate social actions via connections to orbitofrontal cortex, and, via connections to superior temporal gyrus, the ability to perceive faces. This evidence, along with evidence of pathology in cell density in the amygdala in ASD, motivated the early fMRI study of activation in the "social brain" in [31] which found further evidence for the role of the amygdala in ASD deficits.

Connectivity between the amygdala and neocortex is a potential source of emotion-related deficits in ASD [32, 33]. Differences between putatively typical and ASD innate versus conditioned fear responses may be attributable to pathological connectivity of this nature [32]. The amygdala is further implicated in deficits in empathy, of particular relevance given that psychopathy and ASD present with opposite impairments in empathy (p. 15) [34]. The amygdala may be involved in the increased prevalence of anxiety (p. 17) among those with ASD based on increased activation of right amygdala and left middle temporal gyrus in subjects diagnosed with ASD correlating with increased anxiety [35].

Recent directions include viewing the role of the amygdala in mammalian evolutionary history as part of a "relevance detector" apparatus in light of its role in contributing to rapid arousal in response to threats and in associating stimuli with rewards and adding emotional salience to memory. Abnormalities in the circuits required for the amygdala to serve this function causes aberrant processing of self-relevant information, leading to the diminished emotional competencies of individuals with ASD compared to controls [36]. Of particular relevance to the present study, analysis of

6

Table 1.1: Theories of autism primarily associated with their neural substrate.

Theory	Consistent observations	Challenges
Amygdala	Pervasive emotion-associated deficits in ASD; many observed differences in amygdala structure/function; frequent anxiety comorbidity	Limited by narrow focus; cannot account for RRBs nor sensory abnormalities
Neural circuit	Histological verification, mechanism for observed widespread disruptions in connectivity	Accounts for fundamental neuroanatomical aberrations, but abstruse without specifically identifying cortex-wide patterns of changes; hence, includes connectopathy at all spatial scales, increasing power but decreasing succinctness, but also common etiopathogenetic mechanism (disrupted synaptogenesis and function)
Mirror neuron	Consistent with deficits in social reciprocity	Many; mirror neuron system theoretical in humans, few reproducible, and many incompatible, results
Putative cerebellar	One of the most consistently implicated structures in ASD neuropathology, multiplex functionality suggests high likelihood of at least some major involvement in at least some ASD deficits	Extremely broad, given cerebellum contains ∼50% of CNS neurons, but therefore also extremely probable to be significant, though not entire, part of ASD pathophysiology; discretizing role is hence predominant challenge; is also not etiologically fundamental

Table 1.2: Theories of autism primarily associated with their behavioral or cognitive aspects.

Theory	Consistent observations	Challenges
Social motivation	Direct cognitive explanation for one/two of the core deficits	Fails to sufficiently account for RRBs, reduced social motivation does not account for all observed social deficits, e.g., even when desiring social interactions, individuals with ASD may be less successful
Metarepresentation	Accounts for social deficits even when social interaction is desired—failure to reconstruct minds of others makes social interactions both more difficult and also therefore more frequently undesirable and frustrating	Fails to account for RRBs, less explanatory power for high-functioning adult individuals with ASD

Table 1.3: Theories of autism primarily associated with their evolutionary or evolutionary-psychology explanations.

Theory	Consistent observations	Challenges
Extreme male brain	Succinct summary of a vast array of symptoms/deficits, consistent with higher male diagnosis rates	Belies gender and sexual heterogeneity, i.e., oversimplifies due to broadness; does not straightforwardly account for sensory abnormalities or profound language impairments
Assortative mating	Provides an adaptive explanation that accounts for most/all ASD deficits in some form	Fails to account for severe forms of the disorder which seem plainly maladaptive and not necessarily associated with associated constructs like "detail orientation"

data from ABIDE showed decreased functional connectivity between amygdala and thalamus (bilaterally) and right putamen [37]. Recently, despite the inherent circumscription of the amygdala theory's explanatory power when considered in isolation, functional connectivity between amygdala and multiple targets across the brain was found to vary with ASD diagnosis and sex [38]. Thus, while this theory suffers from important limitations, as expected given the constraints on technology, methods, and the vastly lesser extent of the size of the research literature at the time of its formulation, rather than being discarded, the role of amygdala in ASD deficits would best be incorporated into whatever other neuroanatomical and functional theories of ASD are conceived or refined. For example, differences in both amygdala, in the "limbic" system, and the putative "social brain," in neocortex, have been posited to explain ASD social deficits separately, but functional connectivity differences *between* them have been found to correlate with ASD social deficits [39]. Hence, while the amygdala theory cannot be conceived at this point as in contention as an exhaustive neuropathophysiological account of ASD, amygdala's well-established correlation with certain ASD features demonstrates the practical benefits attempts at theoretical synthesis can lend in guiding research efforts.

Neural circuit theories of autism

Neural circuit theories of autism propose that the formation of excitatory—inhibitory circuits is disrupted early in development in ASD, later causing downstream disruptions in large cognitive networks that integrate information and activity across multiple domains. That is, "noise" in neural circuits due to atypical excitatory, inhibitory, and general synaptic function is integrated at the larger scale of cognition, leading to the observed deficits in attention, learning, social cognition and related domains, and frequent comorbidity with epilepsy. For example, such malformation of neural circuits has been observed in the neural circuit for social attention perception in ASD [40]. Because of the profound implications local disruption of neural circuits has on whole-brain connectivity patterns, this theory unifies putative central mechanisms in ASD pathophysiology across temporal and spatial dimensions of neurodevelopment. Beginning with alterations in the function of molecular mechanisms at the outset of ontogenesis underlying the proliferation of connections between the smallest wholly discrete functional units of the nervous system, neurons, and extending through the lifespan given the centrality of synaptic plasticity in dynamic adaptations to experiences, and throughout the nervous system given the dependence of transcortical brain networks, thought to underlie cognition, on an appropriate course of synaptogenesis to establish their substrate, these theories propose a single pathogenetic origin of ASD neural and behavioral features that itself arises from some combination of genetic etiologies, and therefore encompasses the greatest extent of explanatory levels while remaining consistent with the extant suite of observations. Because these theories seem to offer the most plausible framework of all the ASD theories from a neurocognitive perspective, and are especially relevant to functional connectivity analyses such as used in this thesis, they will be discussed in particular detail.

Early theoretical justification of a network- and circuit-based explanation for ASD came in the form of artificial neural network models. Cortical feature maps satisfactorily provide a mechanism that would explain why disruptions in connectivity could lead to a neurological disease states such as ASD, while likewise admitting of the potential for "multiple etiologies [41, p. 1139]." The discrete phrase "neural circuit theory of autism" originated from the same paper [41], establishing a family of theories all oriented towards aberrations at the columnar and minicolumnar levels; the predictions made by this initial conjecture have been verified in subsequent research. Fundamentally, the explanations have in common that they propose that integration of sensory and other information is disrupted in cortex due to aberrant micro-scale connectivity of this type, causing ASD symptoms. Cortical maps associated with stimulus features were implicated as directions of future research interest.

Multiple genetic mechanisms are known to be involved in synaptic development, perhaps most prominently in ASD those involving fragile x mental retardation protein, a mutation in the gene coding for which can cause fragile x syndrome, a disorder presenting with frequent comorbid ASD. Fundamental to this and other genetic mechanisms, periods during which activity dependent plasticity (ADP) has outsized influence over widespread areas of the nervous system associated with ontogenetic timing of maximal plasticity to environmental factors are termed critical periods. As much of nervous system ontogenesis is hierarchical in nature and critical periods coincide with many important stages in typical development, an ASD etiology of anomalies within critical periods would succeed in explaining neurodevelopmental aspects of the disorder that persist throughout life [42]. More fundamentally, neural circuit theories implicate some combination of alterations in all of synaptogenesis and concomitant minicolumnar malformation, hierarchical "amplification" of these micro-scale aberrations throughout cortex, and thus, finally, an imbalance between various modes of cortical activity, such as, for example, between excitatory and inhibitory modulation within and between regions of cortex.

The implication of a simple ratio between excitation and inhibition by necessity must be complicated in a homeostatic perspective; not only may different brain regions be differentially affected, down to the level of the microcircuit and across cortical, subcortical, brain stem, and cerebellar structures, but even cellular compartments *within* microcircuits may experience differential excitatory and inhibitory regimes, and in turn send accordingly modulated efferents to further targets. [43] follows [42] in focusing on monogenic ASDs (e.g. fragile x syndrome) due to the greater potential for resolving fine variances in excitation and inhibition using translational models. Specifically, 10 monogenic syndromes are included for review: *ARX* mutations, Dravet syndrome, tuberous sclerosis, fragile x syndrome, Angelman syndrome, Rett syndrome, *NRXN1* mutations, *GPHN* mutations, *SHANK* mutation/Phelan McDermid syndrome, and *CNTNAP2* mutations. These etiologies are most directly associated with multiple mechanisms of neuronal development, allowing targeted inquiry as to the specific disruptions caused by the associated gene mutations with mechanisms of "neurogenesis, migration, differentiation, and/or function of cortical interneurons [43, p. 685]," which includes the influence (or ability/lack of ability to mitigate deficits through intervention) of activity dependent plasticity. The complex and extensive pleiotropies associated with single-gene alterations demonstrate a mechanism by which disrupted neural develop may itself induce widespread downstream changes dynamically within a homeostatic milieu. This allows recurrent disruptions to "reverberate" given the fundamental interconnectedness of nervous systems and the multiple hierarchical levels of functioning that are interdependent. [43] further follows [42] by expanding exclusively on the balance

between excitatory and inhibitory circuits in ASD, specifically weighing subsequent evidence against the initial postulation that ASD is substantially a disorder of hyperexcitability, with the strongest lines of evidence observed being diminished GABAergic activity and comorbidity with epilepsy. Additionally, the relative paucity of inhibition is supposed to contribute to a relatively "noisy" cognition, driving the impairments seen in ASD. Ultimately, a "homeostatic view [43, p. 684]" is taken to synthesize and reconcile the apparently opposing excess excitation/excess inhibition views. While an exhaustive review of the multiple nuanced mechanisms at genetic, molecular, and cellular levels would prove excessive in light of the explicitly neurocognitive focus of this thesis directed towards the domain of functional connectivity, the current literature provides broad support for a fundamentally circuit-derived, neurodevelopmentally realized disruption of widely distributed cognitive networks underlying ASD.

Neuroanatomical evidence of synaptic changes in ASD has also been corroborated by analysis of ASD brains postmortem. Neocortical mini-columns of both glutamatergic and GABAergic neurons had fewer vertical arrays, and the peripheral neuropil space was comparatively disordered in ASD brains. Animal models corroborate the relevance of this difference; in musine *Fmr1* knockout models, there were regionally variable increases and decreases in glutamic acid decarboxylase concentration. In addition to the implications for impoverished inhibition due to lower GABA levels, hyperconnectivity in excitatory connections has been observed anatomically in these models [42].

There is also direct anatomical evidence of pathological synaptic formation in ASD in humans. Greater dendritic spine density in projection neurons in cortex in ASD, observed to be elongated and with tortuous morphology in fragile x syndrome, is observed; Decreased synaptic pruning may account for these structural differences in the synapse. Such malformation of dendritic arbors is also observed in other neurological disease states. *Fmr1* knockout mice provide a plausible mechanism; dendritic spines in these models are observed to frequently fail to stabilize. As both dynamic and stabilizing processes are necessary for optimal ADP in dendrites, this will cause fewer mature synaptic connections to form. *Fmr1* knockout also reduces axonal dynamism in mice, consistent with hypothesized excessive stability of brain structure and function in ASD [42].

This model suggests some potential therapeutic avenues for treating ASD. Metabolic glutamate receptor agonists cause learning and memory deficits, and GABAergic modulation can offset hypoinhibition; the positive allosteric modulator acamprosate demonstrates preliminary evidence of improving social and communication deficits in subjects diagnosed with ASD. The implication of critical periods also suggests that early intervention and environmental enrichment can offset some neurodevelopmental disruptions in ASD, and in fact, early deprivation may in fact cause ASD-as-

sociated traits, as in the Romanian orphan study [44]; this condition was reversed in some cases by environmental enrichment. Therapeutic routes contingent on continuing technical innovations, such as optogenetic control, have also been noted for their potential in light of these theories [42].

Intrinsic to critical period dysfunction, as implicated in multiple ASD-associated mechanisms, is disruption first in subcortical, then in sensory, and finally in association areas of the brain. This essential schematic suggests that investigation of sensory system dysfunction is likely to be fruitful for the enhancement of understanding deficits in higher-level cognitive processes as well. Despite this, popular conception, and the preponderance of research, focuses on deficits in social cognition. This focus, though less exclusive recently, is inappropriate wherever it deemphasizes the role of other neurocognitive mechanisms as multiple lines of evidence implicate sensory systems not just as of potential explanatory importance, but also as potential therapeutic targets; sensory deprivation induces some ASD-like symptoms that are partially reversed via therapeutic intervention in the form of environmental enrichment. A potential confound in this approach is the heterogeneity of ASD present at nearly every conceivable level of every major dimension. Multiple single genes are associated with presence of ASD traits in ASD manifestations with associated somatic abnormalities (syndromic ASD) beyond the therapeutic threshold. While these genes do share fundamental roles in neurodevelopment, the existence of non-overlapping genetic causes of autism, let alone that majority of ASD cases are not the result of single gene mutations, nor present with readily identifiable somatic phenotypes (syndromic), at least cautions against overly optimistic assumptions regarding the extent of the portability of therapeutic interventions that are successful in specialized cases to ASD more generally [45].

Recent efforts have increasingly confidently and clearly recognized that a unifying ensemble of synaptogenopathic alterations in experience-dependent neuroplastic mechanisms of ontogenesis involving cortex of the frontal lobe and the sensory periphery, incorporating to-this-point-known associations between ASD and a slew of genetic, metabolic, immunological, neurotransmissive, and ensuing connectopathic modifications from putatively typical development and cognition, underlies, substantially, at least, in its totality, both the existence and nature of the many particular manifestations, and the accordingly comprehensively multiplex heterogeneity of the disorder [46]. The devisement and particularization of suchlike an amalgamated etiopathogenic machinery in the disorder, dreamed up specifically for and in view of the multifarity of its germaneness to many big chunks of the multitudinous peculiar symptom instantiations seen totally within the confines of the disorder's diagnostic criteria, is an exercise of substantial nuance, and further one subject to near constant refinements given the rapid pace of literature and associated improvements in technology,

13

methods, potential subject access to healthcare and research settings, and so on. The asserted mechanism itself is, chiefly, lower than hypothetically canonical microglial influence on synaptic pruning due to ASD-associated genetic alterations to synaptic function, mainly exuberant synaptogenesis followed by excessive fixity of established synapses, results in a cascade of macroscopic differences in connectivity associated with ASD that are not necessarily expediently compartmentalizable into categories "hyperconnectivity" and "hypoconnectivity." A mechanism suchlike the above has two attractive properties in terms of putative "theories of autism:" First, it has broad, deep explanatory power given its combined syntheticity and fundamentality, and second, could be plausibly generative of a whole host of (heterogeneous) disorder presentations. Theories conforming to generic schema of this nature that at present remain, at the very least, *consistent with* the observational evidence putatively bearing on their soundness are those with the most substantial plausibility within and across explanatory modes. Effectively, they are the most parsimonious consistent theoretical forms.

Relevant to the present experiment, various anatomical and functional neural circuits have been proposed as underlying RRB, both in ASD, and as a general symptom presentation in psychopathology: "[A] circuit-oriented approach is likely to provide great utility towards understanding the complex and heterogeneous phenomena of RRB appearing in ASD and related neurodevelopmental disorders [47, p. 153]." In even less oblique terms, "ASDs are disorders of connectivity [46, p. 10]." A summary of implicated circuits is given in section 1.4.3.

Social motivation theory of autism

The *social motivation* theory of autism [9, 18, 48–54] posits that social deficits of individuals diagnosed with ASD are the result of atypical reward processing in the brain [51]. Unlike the prior two theories, it is formulated in behavioral and cognitive terms, though this nevertheless allows the incorporation of neural data within such a context.

In relevant behavioral experiments, children with high-functioning ASD have been found to be less likely to approach avatars with positive expressions than controls [50]. One possible explanation for this, incorporating underlying neural systems explanations within the social motivation framework, is that lower levels of activation in the reward system in response to social stimuli, potentially due to aberrant function of neural systems that utilize oxytocin, and their relationship with the "reward hormone" dopamine via the mesocorticolimbic dopamine circuit, reduce cognitive salience of positive social stimuli. [9]. Some lines of inquiry have yielded results contrary to the social motivation theory. In an EEG study, early-stage face perception and recognition of emotion in facial expression were *inversely* related to extent of social motivation [53]. While this theory is appealing

for covering two of the core deficits, if ASD communication deficits are conceived as ultimately social in nature, it insufficiently addresses the third (restrictive and repetitive behavior, RRB).

Extreme male brain theory of autism

The *extreme male brain* theory of autism posits that a putative autistic cognitive phenotype is effectively an exaggeration of the typical male cognitive phenotype in comparison to the typical female cognitive phenotype. The most central difference between the two gender-typical cognitive phenotypes under this theory is the extent of preference for empathizing (female) versus systemizing (male), and indeed, the extreme male brain theory of autism is expansion of the *empathizing-systemizing* theory of autism. "Systemizing" is the preference for and ability to interpret phenomena as logical and orderly, characterized by predictable patterns. Empathy, the ability to recognize the internal states of others, differs from systemizing in that the phenomena it successfully characterizes are much more variable and "complex." The "autistic brain" is idiomatically "the ultimate pattern detector [55, p. 172]." While this formulation has many faults, it shares important fundamental aspects with evolutionary cognitive explanations, paradigmatically, the assortative mating theory discussed below, which further provides an explicitly adaptive explanation for RRBs. Such adaptive explanations form a major part of the theoretical context in which RRB deficits can be explained.

The original formulation of this theory, by [55], views both the mean difference between men and women, and between individuals with ASD and putatively typical individuals, as comprising spectra with no clear delineation or explicit breakpoints. [55] suggests multifactorial contributions to the ASD neuropsychological phenotype, including genetic, hormonal (specifically degree of fetal testosterone exposure), and social factors. While the extreme male brain theory, like autism itself, is defined in psychological or cognitive, and not neurobiological, terms, [55] notes that to at least some extent, the neuroanatomical differences associated with ASD as compared with putatively cognitively typical individuals are coterminous with the differences between biological males and females. Specifically, [55] enumerates anterior cingulate cortex, superior temporal gyrus, prefrontal cortex, and thalamus as larger in females and putatively typical individuals, and amygdala and cerebellum, as well as overall brain size, as large in males and individuals with ASD diagnoses.

[56] attempts to resolve the plausibility of the extreme male brain theory by testing its predictive power with respect to a mental rotation task. Performance on this spatial task is broken into rotational components (slope of the function of reaction time and error rate vs. degree of rotation) and non-rotational components (intercept of the function). The non-rotational component involves all cognitive requirements of the task other than the rotation itself.

The process of computing the task stimuli recruits the occipital lobe for encoding visual information, the parietal lobe for receiving this information and processing it in three dimensions, and the right frontal lobe for the final determination of a response to the task. Adult males outperform adult females on average on this task primarily due to improved performance on the rotational aspects. Individuals diagnosed with ASD, however, were previously shown to have an advantage primarily in the *non*-rotational component. Some fMRI data suggests that this is due to a systemizing advantage, as lower frontal activity was observed in subjects diagnosed with ASD during a rotational task, and higher frontal activity was observed in female subjects. [56] corroborates this interpretation of the fMRI data by combining a mental rotation task with a systemizing test based on an assessment of physics intuition (intuitive physics test). The results of this experiment suggest that it is in fact a systemizing advantage that leads to better performance specifically due to the non-rotational components of the task; the incongruous results with the prior male vs. female comparison could be due to insufficient angles of rotation in the task. Proxy measures for circulating testosterone (time awake) suggest that task performance improves with circulating testosterone levels, but not prenatal testosterone exposure. [57] likewise finds that prenatal testosterone exposure does not correlate with performance on systemizing tasks, but across three spatial tasks concludes, explicitly in contradiction to [56], that the "male advantage" and "ASD advantage" are distinct for rotation tasks.

"Classical" autism is fourfold as common in males, the deprecated Asperger's Syndrome, ninefold [55]. While sources supporting the extreme male brain theory consider the differential diagnosis rates to be supportive of the theory, [16] argues for the plausibility of a reversal of this causality; a predisposition towards viewing the autistic phenotype as fundamentally "male" contributes to this very differential, and indeed, explicitly articulating ASD in such terms may further reinforce this pattern. In any case, the others point out, reasonably, that popular interpretation may adversely affect quality of life for girls and women diagnosed with ASD due to prevailing institutional gender norms and their implicit effect on factors such as social support and quality of medical treatment.

[58] finds evidence for increased digit length in family members of individuals diagnosed with ASD, but not a decreased 2D:4D ratio specifically, the traditional proxy for prenatal testosterone exposure. As digit length is controlled by both genetic and hormonal factors, this association may form a putative basis for understanding the genetic and hormonal factors involved in ASD.

[55] points out certain types of apparent empathy deficits associated with ASD, and specifically cites an impoverished theory of mind as an earlier theoretical model of autism writ large; [59] corroborates this mechanism, but whereas [55] does emphasize that empathy can be divided into

16

cognitive empathy (that is, theory of mind), and affective empathy, [59] points out that affective empathy does not seem to be diminished in ASD.

Hans Asperger originally postulated a nascent form of the extreme male brain theory to explain ASD, but he lacked substantial behavioral and neurobiological data, or the theoretical framework of the empathizing/systemizing dichotomy. The extreme male brain theory does not predict every observed symptom associated with ASD, but does purport to explain all of the symptoms common to *all* ASD diagnoses [60].

Assortative mating theory of autism

The *assortative mating* theory of autism [61–63], related to the hyper-systemizing theory of autism, itself a refinement of the extreme male brain theory, posits a fundamentally evolutionary mechanism to account for the symptoms and prevalence of ASD. Systemizing is a cognitive process fundamentally tied to likelihood and variance within the outcome space of given events or processes: It allows the estimation of the likelihood of certain outcomes based on prior conditions and their associated outcomes. A conceptual break with its progenitor theories, especially now, seems a prudent revision to be explicitly made to the theory: Recent results have suggested a lack of sex-effects in the repetitive and adaptive symptom and behavior domains [64], themselves the category of ASD deficits most directly associated with the theory. This in addition to the fact the putative "male brain," or any other such conceptualization in terms of gross population-level demographics, is, despite lay literature entitled contrariwise [65], not a thing discrete nor a notion substantially demonstrated to this point to exist, as such.

Philosophically, [62] distinguishes between the classes of phenomena that systemizing and empathizing are respectively capable of successfully apprehending as non-agentive and agentive. Agentive changes occur when they are the result of the intention of a cognitively endowed entity. From the fundamentally utilitarian articulation that "[b]eing able to anticipate change ...allows the organism to avoid negative consequences or benefit from positive change [62, p. 866]," it is simple to conclude that, to whatever extent systemizing and empathizing are in competition for (metabolic, cognitive) resources, there exists variation on which natural selection can act. Game-theoretic analyses could therefore determine an evolutionarily stable strategy based on the utility of varying combinations of the strength of these faculties. Assortative mating, the tendency of sexually reproducing species to self-organize into reproductive pairings consisting of similarly fit individuals, may thus take stock of the relative and absolute levels of systemizing/empathizing faculties among potential pairings.

While agentive and non-agentive changes do exist along a continuum of complexity, with agentive

17

changes tending towards more complex, [62] notes that humans, in light of their high level of social sophistication, have an innate apparatus for dealing with qualitatively agentive changes: This apparatus includes amygdala, orbitofrontal cortex, medial frontal cortex, and superior temporal sulcus as part of its "wiring (section 1.4.3)." In fact, this very sociality, [62] posits, may facilitate positive assortative mating between high, but not extreme, systemizers; it is the offspring of such parents who are likely to have ASD. Evidence for this theory comes in the form of a higher prevalence of relatives of individuals diagnosed with ASD in careers where systemizing ability is beneficial (e.g. engineers, scientists) [61, 62, 66].

However, [67] suggests that the return on systemizing cognitive styles (quantitative ability) is increasing over time, and that even the increased diagnosis rates of ASD do not offset the countervailing increase in such returns. Thus, the assortative mating theory may in fact provide an example of natural selection increasing fitness due to changing environments (e.g., prevalence of various types of careers, skills necessary to "survive in the modern world"). Because ASD is rare, relatively smaller changes in the variance of the distribution lead to relatively larger percentage changes in the number of ASD cases. However, other evidence, with some differing underlying methods, suggests an absence of any effect of systemizing preference on partner selection [68]. This discrepancy warrants further investigation, as assortative mating sufficient to significantly increased ASD prevalence would have to overcome the tendency of offspring's phenotypes to regress towards the mean.

The family of theories is of substantial overall interest to ASD research writ large because it purports to engender *all* of the core deficits of the disorder. Succinctly, "the Empathizing–Systemizing theory is successful in interpreting the core features of autism, both social and non-social, compared to other current theories of autism [69, p. 321]." The same source concludes that an explicit measure of systemizing must at least be included in a successful diagnostic measure of ASD.

Mirror neuron theory of autism

The *mirror neuron* theory of autism contends dysfunction in the mirror neuron system homologs and analogs in humans contributes to the theory of mind deficits (cf. *mindblindness* theory of autism) and deficits in social attention and responses. A thorough conceptual account of the mirror neuron theory is given by [70].

The mirror neuron system (MNS) was first described on the basis of functional activation of its neurons in macaques. The putative neuronal population fired in the course of both the performance and observation of a given action (even if that action was performed by a human in recordings of monkeys). This suggests that these neurons and the system comprising them were necessary for

social motor learning and its underlying cognitive processes. Since its discovery in monkeys, multiple neuroimaging methods have elucidated the structural and functional properties of the analogous system in humans. Given the remarkable phylogenetic conservatism typifying interspecific nervous system variation, it is unsurprising that such a functional neural domain would likewise arise in human cortex. The homologous cortical domain in humans to F5 in the macaque is Broca's area, which also suggests a role of the putative MNS in language evolution or production [71].

[72] gives cortical regions that contribute to the MNS as pars opercularis, inferior frontal cortex, inferior parietal lobule, and superior temporal sulcus. In the experiment in that paper, multiple areas of the cortical sheet were found to be thinner in subjects with an ASD diagnosis as compared to matched controls exhibiting typical development. These areas included the above mentioned putative MNS regions as well as those associated with sensory and motor areas subserving facial expression recognition and production, as well as in areas of prefrontal cortex, anterior cingulate, medial parietal cortex, the supramarginal gyrus, and the middle and inferior portions of the temporal cortex, which in sum contribute broadly to social cognition. Importantly, thinning only in the MNS regions was correlated with ASD trait extent, and thinning in none of the areas was associated with differences in IQ, suggesting unique importance of the MNS in ASD etiology.

Contemporaneous fMRI evidence also provides early support for the mirror neuron theory of autism as well. [73] suggests a corticolimbic functional network that integrates parts of the putative MNS. Subjects made or observed facial expressions while in the MRI scanner in their task, which was supposed to require social cognition and mimicry components, which relate ASD and the MNS. While task performance could not be measured in the scanner, some subjects performed the test out of the scanner to verify compliance with instructions. Additionally, eye movements were tracked in this additional phase to ensure that the results did not primarily reflect differences in attention. Areas activated in the subjects exhibiting typical development included striate and extrastriate, primary motor, and premotor cortex; bilateral pars opercularis and pars triangularis; structures of the limbic system; and cerebellum. In the subjects with ASD, striate cortex was also activated, with the fusiform gyrus specifically reported; face premotor regions; and amygdala. Activation of the pars opercularis, however, was not reported in the ASD group. This lack of activation in the human homolog of the macaque MNS implicates that system in some ASD deficits. Furthermore, the subjects diagnosed with ASD exhibited relatively greater activation of left anterior parietal and right visual association cortex, and less in the insular area, periamygdaloid complex, ventral striatum, and thalamus. Thus, it appears that the subject diagnosed with ASD are relying on cortical areas to overcome functional connectopathy in regions of the insula integrating limbic and

cortical areas. Further implicating the pars opercularis as figuring in the deficits of ASD, activation in this structure was negatively correlated with ADOS-G and ADI-R social subscale scores.

A slightly larger, roughly contemporaneous group of subjects diagnosed with ASD of group size of 16 provided results in a similar vein, implicating a similar array of MNS-associated neural structures, using a task in which an image of a hand either displayed a specific finger being raised, or used one of two different symbolic cues to indicate a finger, which the subject is to raise in response [74]. The salience of this stimulus regime is that it separates an identical motor task (finger raising) into an imitative (cued by a depiction of the action being performed) and a non-imitative (symbolically indicated) version.

Currently, however, there is a lack of confirmatory evidence for the mirror neuron theory. For example, the MNS or its homologs are present in some species which are generally not presumed to possess theory of mind [75]. Further objections to the theorization emerged alongside its increasing prevalence in neuroimaging literature [76]. First, the mirror neuron system is a circumscribed neural system with relatively specific functions. While imitation deficits are observed in ASD (including imitative behavior not typically seen, such as echolalia), MNS dysfunction fails to account for the vast majority of deficits observed in ASD, and thus fails to provide sufficient mechanistic relevance to merit the inclusive label "theory of autism." Furthermore, activation of the putative mirror neuron system is not associated with other sensory and integral social components of collective motor learning, meaning it does not even satisfactorily account for the primary phenomenon it would be invoked to. Finally, the mirror neuron system, despite the straightforward implication of its name, appears to subserve a subtler array of functions than explicit mimicry, all of this leaving the theory "ambitious but underspecified [76, p. 228]."

Metarepresentation theory of autism

The *metarepresentation* theory of autism proposes that deficits in theory of mind in individuals diagnosed with ASD undergird the suite of ASD-associated traits [17]. This early theory was one of the first attempts to characterize ASD in terms of a central mechanism that ostensibly accounted for diverse features of the disorder, and hence was one of the first "theories of autism;" "[s]o far, nobody has had any idea of how to characterize such mechanisms in even quasi-computational terms [17, p. 38]." In seeking to explain the broad swathe of ASD-associated social deficits, a general inability of individuals diagnosed with ASD to ascribe emotional states to other people succeeds in accounting for many. The data presented as supporting the theory were the results of a "false belief" task, in which subjects, either children diagnosed with ASD or else those of putatively typical

neurocognitive development, were asked to infer where a doll (agent) would look for a marble that had been moved without the knowledge of the doll. The children diagnosed with ASD demonstrated inferior performance on this task without other obvious cognitive impairments. [77] notes that children with Down's syndrome outperform children with ASD despite having lower intelligence quotients. While little of this is surprising in light of the above-discussed theories of autism, the theory of mind and metarepresentation theories were fundamentally novel approaches, seeking to explain ASD in terms of discrete cognitive mechanisms that differ in their function in individuals diagnosed with ASD as compared with those exhibiting putatively typical neurocognition.

Learning based on feedback from task responses differed between ASD and intellectually impaired nonautistic subjects based in a task in which subjects chose one of two boxes, both opaque in the first condition, and both with a window facing only the subject in the second [78]. In each case, a prize was in one of the boxes, and the subjects were rewarded with this prize if they chose the empty box. Once the windowed boxes were substituted, the task became trivial; subjects were even advised of this fact. Furthermore, the task was performed either with or without a putative opponent, who reaped the prize whenever the subject did not. The nonautistic subjects demonstrated improved performance when an opponent was present while the subjects diagnosed with ASD did not. This suggests a more fundamental processing error than simply lacking the cognitive apparatus to represent the cognitive states of others (the opponent), as the authors suggest, because otherwise task performance would improve in the no opponent condition. No competitive motivation (or "set [78, p. 502]") occurs in the subjects diagnosed with ASD either as it seemed do for nonautistic subjects. [78] instead suggests an explanation of mental disengagement, in which the salience of the prize dominates among participants diagnosed with ASD. In fact, participants diagnosed with ASD frequently chose the box with the prize in the windowed condition for every trial, meaning that their trial success rate was 0% and they never earned a single prize. Evidence for this contention came additionally in an experimental task in which subjects had to first eschew the most direct physical route to grab a marble inside a contraption in the form of a box with a knob and lever on respective sides and a platform inside supporting the marble. Reaching directly for the marble caused the platform to drop and render the marble inaccessible. Rather, the knob allowed a one-step acquisition. The second and decisive portion came when the knob solution was inactivated, leaving only the switch solution which required coordination between the subject's two hands to use the switch to deactivate the beam that senses the subject's hand and trips the mechanism to block access to the marble. Despite the mechanism's tendency towards arcaneness, the results were unambiguous: subjects diagnosed with ASD compared to subjects diagnosed with intellectual disability and preschool aged subjects of

putatively typical development faltered markedly on the switch portion of the task, reinforcing the notion that the saliency of the marble was disruptive to the efforts of a subject diagnosed with ASD in a specific manner and to a significant degree. As the switch protocol involved no other humans directly, this potentially contradicts the metarepresentation theory, while still allowing the general conceptual mechanism to be involved with, if not fundamental to, ASD deficits. This observation is also consistent with a central role of RRBs and related behaviors in the presentation of ASD broadly.

Cerebellar theory of autism

A putative *cerebellar* theory of autism would assert the cerebellum is the focal structure of ASD pathophysiology. Such a theory definitely exists, with all the necessary features of a putative theory of autism, implicitly [79], but exists as a discrete phrase similar to the other theories discussed only marginally (but also definitely) explicitly. For example, it has been stated, with explicit reference to the phrase "cerebellar theory of autism," that it is "probably the most unlikely neurobiological hypothesis of autism, as on first observation autistic individuals hardly show any of the traditional signs of cerebellar abnormalities [80, p. 108];" it has in stark contrast, however, also been observed that "[a]lterations to the cerebellum are . . . one of the most consistently reported pathological findings in post-mortem studies in ASD [47, p. 165]." This assertion can be found verbatim elsewhere as well [81]. While relevant context will be established next, first, a superficial discrimination between these contrasting, broad, albeit for the moment, isolated claims, is informed by the facts that, first, the cerebellum-negative claim is caveated by both resting on a *lack* of observations and the restriction of the type of observation that would be considered positive to "traditional signs" of cerebellar pathology, and second, the cerebellum-positive claim is 13 years more recent and specifically a review of neuroimaging in autism. In the same reference, similar aberrance is noted to be the *most* commonly observed in basal ganglia specifically for RRBs across disorders. The numerous intrinsic functional relationships between these two structures, mediated by their mutual broad, substantial impact on neocortical function [82], likewise suggests strongly that alterations to their function comprise an important aspect of ASD pathophysiology across ASD core deficit categories. Further supporting this relationship is the fact that cerebellar lesions have been associated with cognitive deficits similar to those seen in ASD and in other neurodevelopmental disorders (ADHD, dyslexia), and that the earliness of such lesions is associated with the severity thereunto [83], implying a specifically developmental component, consistent with the disorder classification of ASD.

The aforementioned context provides theoretical and practical direction to the present study more than does the mere fact that contrasting claims have been made about the plausibility of a putative

cerebellar theory of autism. The source of the cerebellum-negative claim is, if not plainly consistent, thorough in its theoretical treatment of the cerebellum—ASD relationship, predominantly citing Courchesne (cited elsewhere in this thesis, [84–87]) and, for example, affirming as above that "[t]he most extensive and consistent anatomical and imaging evidence" in autism brain research "relate to the cerebellum [80, p. 20]," as well as to limbic and frontal cortex. Moreover, executive dysfunction is advanced as a plausible consequence of cerebellar dysfunction in ASD, and even more, the theoretical association is "very strong [80, p. 116]," particularly because of its competence to account for the developmental nature of the disorder. The primary critique, in fact, is that adult cerebellar injury does not present similarly to ASD-associated deficits, but the fundamental difference in etiology, despite the mutual implication of the same structure, between disorders of neural development affecting cerebellum ontogenetically and injury to the adult, relatively aplastic brain, establishes preliminary motivation to further characterize the structure—function relationship between cerebellum and ASD symptoms. Despite the centrality of this discrepancy to the apparent modest skepticism of the plausibility of a cerebellar theory, the observed correlation between cerebellarly mediated deficits in cognition and behavior, whether through injury, hereditary dysplasia, or other insult, is discussed; this relationship is discussed extensively in section 4.5.1. Thus, while a cerebellum-centric neural conception of autism has faced scrutiny relatively recently, ostensibly critical assessments acknowledge the evidence of significance, if not causality or necessity, of cerebellar dysfunction or dysplasia in association with ASD deficits is well-established.

Some of the most thorough evidence of a prominent cerebellar component in ASD pathophysiology comes from numerous translational studies. Knockout models of a gene (*PTEN*) associated with neuronal growth and survival, which conditionally targeted only Purkinje cells of cerebellum, resulted in ASD-like traits [88]. This, in addition to reinforcing the major role of cerebellum in ASD pathophysiology, relates it to neural circuit, and therefore connectivity, theories of ASD. Similarly, *Shank2*, a gene discussed above also in reference to neural circuit theories, also inactivated only in cerebellar Purkinje cells, likewise resulted in RRB-analogous behavior, although not ASD symptom analogies in the other core deficit domains [89]. These patterns have been repeated in other investigations based on animal models as well [90, 91]. Symptomatologically, cerebellar dysplasias are associated with ASD-like deficits across domains in the absence of ASD in both humans and in animal models as well [79].

Revisiting the most extensively discussed family of theories so far, neural circuit theories, as extensive evidence from animal models shows, are not constrained in implications to cerebrum. Functional connectivity differences along with excitation—inhibition imbalance, specifically, reduc-

tion, in posterolateral cerebellum and dorsolateral prefrontal cortex was associated with impaired listening comprehension among adolescent and adult subjects with ASD [92]. However, the broad implications of the excitation—inhibition ratio in the etiopathogenesis of ASD correspond to concomitant circumscription of its specificity and consistency; not only do different brain functional and anatomical divisions present differential alterations to the ratio, but patterns present heterogeneously between individuals diagnosed with the disorder as well [93]. Resolution of this apparent conundrum of heterogeneity, however, requires nothing more than consideration of the relevant factors in experimental design, although this does increase complexity. Recent efforts have done exactly this, observing rs-fcMRI in subject populations, and identifying genes of known functional significance to excitation—inhibition ratios in the same subject populations, and finding associations between the two in terms of ASD deficits [94]. Such an approach has all the functional and anatomical specificity that any other typical rs-fCMRI experimental design would while including the relevant genetic context in terms of its known implications on functional connectivity.

In addition to neural circuit and connectivity theories' relationship to the putative cerebellar theory, functional deficits in cognition in theory of mind, empathy, and executive function have been observed in a human medical case of bilateral cerebellar damage [95], relating this latter theory to the social motivation, metarepresenation, and weak central coherence theories of autism, furthering its significance as a fundamental pathophysiological mechanism of ASD deficits across symptom domains. Cerebellum also, relevant both to ASD's developmental nature and more specifically to neural circuit theories of autism, exhibits analogous neuroplastic flexibility and associated molecular mechanisms to as cerebrum [96]. Hemispheric specialization in patterns at least partially corresponding to those in ipsilateral cerebral cortex have been identified in cerebellum as well, e.g., left-language and right-spatial specialization [97]. Like cerebrum, then, cerebellum exhibits hierarchical functional organization [98]; functional lateralization and hemispheric specialization [97]; activity dependent structural and functional plasticity, along with underlying molecular mechanisms analogous to those subserving cerebral plasticity [96]; functional ubiquity, operating across cognitive—behavioral domains [99], both integrating and segregating information streams relevant to behavioral intention, execution, monitoring, and optimization; and inevitability of imputation to at least some significant aspects of the neuroanatomical and neurophysiological correlates of pervasive neurocognitive disorders irrespective of their (conjectured, where appropriate) provenience. However, cerebellum, especially cerebellar cortex, is of striking anatomical homogeneity, in contrast to the intrinsic laminar, cytoarchitechtonic, and biomolecular diversity of cerebrum and especially cerebral cortex. Just as some ASD-associated functional differences in cortex display lateralization

corresponding to, though not necessarily consistent with, the functional lateralization of the underlying cortical substrates in putatively typical cognition, cerebellum too presents an analogous functional scaffold for the investigation of differences in brain functional and anatomical lateralization associated with ASD. Cerebellum has been implicated in deficits in other neurodevelopmental disorders as well, for example, cerebellar dysfunction has been posited to underlie ADHD executive dysfunction as well [100].

Finally, yearly research output within neuroscience on the cerebellum has increased continuously for a few decades now, spurred by the number and significance of many novel findings which suggest no risk of saturation in the subfield as of yet; research output on the cerebellum is predicted to increase from the 310 articles published in 1980 and approximately 800 published per year in recent years to 891 per year by the end of 2028 [101]. Hence, research, especially on ASD, should discuss relevance of cerebellar mechanisms where possible given the potential for magnification novel findings at this time seem to facilitate.

Synchrony theory of autism

A *synchrony* theory of autism could account for the observed slower processing speed in addition to specific deficits. Evidence for a (a)synchronous explanation for ASD symptoms includes weaker interhemispheric synchronization in naturally sleeping toddlers observed via fcMRI. Notably, this method allowed correct identification of 21/29 ASD toddlers and 36/43 TD controls. The weaker synchronization was correlated with measures of expressive language ability (Mullen test), which the authors suggest might indicate excessive lateralization of language function in the cortex of the ASD toddlers [84].

Outstanding issues   Clearly, the proliferation of theories, rather than their paring down, suggests that a single theory encompassing all generally accepted aspects of the disorder is not likely to be forthcoming. However, their explanatory nature is of expected utility at the very least because the coherent nature of the disorder itself, even in full consideration of its heterogeneity, suggests that rigorous attempts to synthesize research results should yield analogously coherent theoretical explanations of the disorder; even if they are numerous and incomplete, they are still less numerous that the individual research results underlying them. Nevertheless, the extent of neurocognitive heterogeneity in what is classified as a neurodevelopmental disorder presents challenges for any synthetic theory of autism. ASD neurocognitive heterogeneity also proceeds across multiple domains. Among the more striking of these include IQ (which can be low, high, or within the typical range),

association with an identifiable direct genetic mechanism with somatic abnormalities (syndromic), or presentation with no clear differentiating genetic/somatic markers (non-syndromic, idiopathic) [102], and, most directly, symptom severity measures across the three core deficits that seem to vary, to at least a substantial extent, independently of one another [13]. Further complicating the matter is the fact that, in the case of syndromic ASD diagnoses, the underlying syndromes, most frequently fragile X syndrome, tuberous sclerosis, and Rett syndrome, can occur without the concomitant meeting of the ASD diagnostic criteria [14]. In light of this, the present dissertation seeks to assess whole-brain functional connectivity patterns associated with RRBs not as an attempt to explain the entirety of ASD, but to assess if the extent of heterogeneity even in this one symptomatological domain can be reduced inside the confines of rs-fcMRI. The rationale and context justifying this approach is given in the following section (1.3).

1.3   NEUROCOGNITIVE HETEROGENEITY AND ITS PROPOSED EXPLANATIONS

In addition to being heterogeneous, ASD has phenotypes that are "seemingly dissociable [103, p. 1433]." Both widespread methodological variability as well as the rapid pace of developments in neuroimaging, in combination with this heterogeneity of the disorder itself, makes ASD neuroimaging research, as a discrete field, particularly challenging [104]. Evaluations of the significance of the observed heterogeneity in the presentation of the disorder vary widely, from dismissing the viability of the disorder entirely, to reducing it to single mechanisms and attempting to explain all features in terms of those mechanisms. Heterogeneity in the disorder, then, also spurs the potential for heterogeneous interpretations of its significance.

Waterhouse [105, pp. 103–113], in her monograph on the topic, summarizes what she describes as "a modern 'phrenology' " of brain neurotransmitters, regions, and connections associated with specifically social deficits in ASD, and, in line with much popular and clinical and scientific thought, explicitly takes social deficits as the "core" of ASD in so doing. Included in her table are many of the results invoked by the above "theories of autism (section 1.2.2)." While Waterhouse asserts that the fragmentation in the evidence for ASD as a discrete, socially-mediated developmental disorder ultimately points towards the existence of multiple discrete disorders that are now aggregated into the current ASD, others coincidentally assert that a fundamental mechanism of disruption in the "social brain" actually tends to *resolve* the extant heterogeneity of the disorder [106]; under this paradigm, symptoms in the other core deficits naturally proceed form disrupted development of the "social brain" in specific patterns, arising from both genetic and environmental mechanisms.

26

Beyond the proliferation of disparate individual results, apparent contradictions have also been observed in individual studies. A longitudinal MRI study of subjects with idiopathic ASD, those with fragile x syndrome-associated ASD, and putatively typical subjects found that substantial enlargement of the caudate and modest reduction of volume of the amygdala in the fragile x subsample, while in the idiopathic ASD subsample, caudate enlargement was modest, but amygdala volume was substantially *larger* [107]. In a review of neuroimaging evidence bearing on ASD heterogeneity [27] makes several succinct observations:

- Social brain areas are particularly well characterized, and therefore, more likely to be invoked in explanations of ASD as a whole. However, correlations between specific symptom severity and structural or functional alterations across these brain regions are less numerous that simple association between social deficits, period, and alterations in the regions.

- Similarly, several particularly highly specific language areas have been associated with equally specific functions, these implicated in language deficits in ASD. Reduced or reversed asymmetry among typically highly lateralized brain regions was associated with language deficits, as well as changes in grey matter volumes in language areas. However, similar alterations were found in subjects with language impairment, but without ASD, and such differences were *not* observed in individuals with ASD but without language impairments [108], suggesting the differences are specific to language impairment, not to ASD.

- While associations between RRBs and both basal ganglia and frontal (i.e., motor and executive) structure and function have been documented, these too have presented directly contradictory results in the research, e.g., both positive [109] and negative [110, 111] correlations between caudate volume and RRB severity.

Worth noting additionally is the fact that the social category by far had the greatest number of individual citations of the three dealing with the core deficits—36 for social deficits, 19 for language deficits, and 14 for RRBs. Furthermore, additional subheadings related to sensory-, anxiety-, and attention-related features of ASD also relate these more frequently to social deficits: first, findings that explicitly correlate sensory abnormalities and social deficits [112], and second, findings and a proposal that the ASD construct is a socially impaired "version" of ADHD [113, 114]. Clearly, there is a, if not universal, clear predilection for accounting for the general features of the disorder in terms of primary social deficits, perhaps highlighted best by the latter assertion, in which ASD symptoms are substantially reproduced in another neurodevelopmental disorder, and it is specifically and exclusively the addition of social features that "transforms" that other disorder into ASD. This assertion,

though, is also itself complicated by an equally stark observation of the neurodevelopmental research literature: "Impaired social functioning has been well documented in individuals with [ADHD] [115, abstract (specifically, the first sentence)]." A distinct, but perhaps fundamentally related set of deficits, in that they are associated with an excessive and distressing preference for systemizing, is observed in borderline personality disorder, but recognizable variations of the other core deficits in ASD have not, to this point, been clearly associated with borderline personality disorder [28], reinforcing the view that ASD cannot be uniquely conceived in exclusively social terms, even if it can in *primarily* social terms.

Perhaps more significant than these difficulties in conceptualizing ASD in purely social terms is the tendency to conceptualize ASD RRB features, an ostensibly co-equal core deficit, in terms of other disorders, particularly obsessive compulsive disorder [116, 117] and Tourette's syndrome [118, 119]. Thus, the relevance of RRBs to a putative "core ASD phenotype" is subject to "double jeopardy" in terms of affording it theoretical significance: The disorder is presumptively and preemptively conceived in primarily, or even exclusively, social terms, whereas RRBs by comparison are, implicitly, at least, seen as to varying extents non-essential and even nonspecific. Of course, asserting ASD is fundamentally a disorder of RRBs or of language deficits would likely eventually run into analogous problems due to overlap with other disorders as in these very examples.

The simplest alternative hypothesis both to ASD's status as a heterogeneous disorder and one primarily associated with only one of its own three core diagnostic features is that it is in fact mulitple, distinct disorders. Some evidence that can be reasonably construed to support this possibility is the fact that there are clearly delineable clusters of comorbidity patterns among clinical patients with ASD diagnoses [120]. In fact, this possibility is especially attractive given the actually derived clusters from the clinical data. Individuals with ASD diagnoses in clinical records were assessed for their specific constellation of symptoms. Analysis of symptom clustering revealed that diagnosed individuals presented specific groups of symptoms that allowed their classification into one of three essentially exclusive groups, or "types" of ASD:

1. A high (77.5%) incidence of seizures and intellectual disability (60%)

2. A relatively high incidence (48.7%) of intellectual disability, along with high prevalence of autoimmune disorders, including asthma, and certain craniofacial abnormalities, especially ear and hearing problems

3. A relatively low (27.8%) incidence of intellectual disability, with comorbidities that are most frequently psychiatric disorders, with the exception of asthma and cardiac dysrhythmia; highest

incidence of the now deprecated Asperger's syndrome diagnosis

While three ASD "types" were identified, they do not correspond to the three discrete diagnoses in the DSM-IV, nor to the three severity categories in the DSM-5 (section 1.1.2). Moreover, while the authors do not explicitly assert the invalidity of the ASD diagnosis along any conceptual dimensions, the authors allow that substantially distinct phenotypes do apparently exist within the extant diagnosis, stating "[t]hese phenotypic distinctions may point to distinct etiologies with different genetic and environmental contributions [120, e55];" furthermore, with respect to both psychiatric and neurobiological aspects of the disorder "...analyzing individuals with ASD as a single group may have blurred the different etiologies responsible for this heterogeneous disease [sic] [120, e61]."

Overlapping, but distinct, "connectotypes" have been observed in ASD in association with divergent symptom presentation [121], both in part explaining, and recapitulating, the observed heterogeneity the cognitive and behavioral aspects of the disorder. In particular, subjects were distinguished as having equal, or directionally imbalanced, sociocommunicative- and RRB-domain deficits. Distinct, but not wholly isolable, patterns of connectivity were found between somatomotor, perisylvian, and visuoassociative cortical divisions such that somatomotor—perisylvian connectivity is reduced in the case of sociocommunicative predominance, whereas in equivalent extent of deficit severity, medial motor—anterior salience (ACC) circuitry was identified. Genes associated with these connectivity differences were too identified, resulting in a tripartite conception of ASD heterogeneity; such problematization is at this stage necessary given the proliferation of dimensions along which ASD may present heterogeneously, and efforts have been multiply made thereunto [46].

Some authors, however, feel no need to proffer any nuanced caveats; for example, the perspective article entitled "Time to give up on a single explanation for autism [122]" leaves little uncertainty as to the authors' conclusion regarding the nosological implications of ASD heterogeneity. Specifically, the paper notes the apparently independent mechanisms underlying each of the three core deficits in ASD based on twin studies. Nevertheless, the same paper notes that the ensemble of ASD symptoms is "highly recognizable" while still being represented among "richly heterogeneous [122, p. 1218]" individuals.

A similar position is held by Waterhouse [123]: The final chapter of her monograph *Rethinking Autism* includes a section entitled "Abandoning autism as a single disorder would eliminate three inferential problems in autism research [123, p. 414]." Among the specific benefits of so abandoning the disorder, she asserts, would be the resolution of apparent difficulties in relating the three core deficits to one another; avoiding having to explain and clinically treat the extensive list of frequent comorbidities observed in ASD diagnoses (e.g., epilepsy, intellectual disability, ADHD, etc.), which

29

tend to foster misunderstandings about the disorder and make specializing in clinical services directed towards it more difficult; the resolution of outstanding conflicts between certain evidence and certain theories of the disorder, and more generally, obviating any need for such synthetic theories of what is in any case a heterogeneous disorder in the first place; and ultimately, removing any need for any explicit discussion of what ASD is or is not, or which of its features are fundamental and which are not. She summarizes: "Given the totality of the existing research evidence, I believe the least speculative scientific position is that autism symptoms are just that, symptoms ... and not a single disorder or multiple disorders [123, p. 427]."

Certainly, eliminating the clinical diagnosis altogether would solve many extant issues in ASD research by rendering them moot. It would not, however, answer any of the unresolved questions actually underlying those issues. Ultimately, ASD is a recognized diagnosis with clearly articulated, if not always neatly conformed to, metes and bounds. While in certain respects it may be true that "the ever-increasing volume of research on [ASD] has, of late, been paralleled by an increasing opacity in the basic definition of the condition [124, p. 359]," such observations must be squared with those such as that "two key biological themes, namely synaptic non-plasticity and abnormal brain connectivity, link idiopathic and syndromic [ASD] [46, p. 23];" the extensiveness of the apparent explanatory divide made manifest by the fundamentally distinct conceptions of syndromic and non-syndromic disorder presentations is one whose bridging, in any manner or to any extent, has seemed to be an especially tall order. There is, too, additional substantial research on neurocognitive features of the disorder, as defined, and multiple such lines have just recently begun to collectively illuminate possibilities for the potential tailoring of treatment to discrete "neurosubtypes" within the disorder [125], clearly demonstrating the potential for ASD neurocognitive research to *resolve* issues with heterogeneity in the disorder, in contrast to simply compounding them. And, while Waterhouse's prescriptions are not wholly inconsistent with the literature, in fact making substantial use of it, the issue of heterogeneity within the disorder, and specifically, neurocognitive heterogeneity and its potential relationship with heterogeneity in clinical presentation and behavioral and cognitive aspects, has been the subject of scrutiny by those performing neuroscientific research on the disorder, with syntheses of results, including contradictory ones, cautiously summarized across the entire brain [126].

Consistent with these trends, and in an effort to generate results of the most clinical and theoretical use, this thesis proceeds with an "agnostic" view about the "true nature" of ASD, while still seeking to elucidate the potential neurocognitive implications of the hitherto least characterized core deficits: restrictive and repetitive behaviors (RRBs).

RRBs can be classified as belonging to repetitive motor behavior, insistence on sameness, and circumscribed interest domains [127], or, alternately, into restricted, stereotyped, ritualistic/sameness, and self-injurious classifications [128]. Symptom presentation can include motor behaviors such as flapping of the limbs and rocking of the body in addition to more abstracted patterns of behavior, such as persistent insistence on sameness (of environment, daily schedule, foods, etc.); the latter have been termed "higher-order" RRBs in contrast to the former "lower-order" or motor-centric presentation [47]. Whether two, three, or four classificatory subtypes are preferred, they all implicate overlapping but not entirely coterminous functional cortical and subcortical divisions [127] as summarized in section 1.4.3. RRBs can be identified in infants at least as young as 12 months [128]. Whereas there is significant between-core-deficit heterogeneity in the severity of symptoms, RRB has been associated sensory changes in ASD, often considered a hallmark, though not a diagnostic feature of primary significance to the disorder. For example, increased stereotypy has been associated with increased seeking of sensation-seeking behavior (colloquially, "stimming") using the repetitive behavior scale, revised (RBS-R) [129] to measure RRB severity [130]. While the mentioned lack of exclusive or even primary pharmacotherapeutic intervention in ASD treatment abides towards RRB symptoms, specific neurotransmitter systems, including serotonergic and adenosinergic transmission, have been found to have significance to RRBs in animal models [131]. Of the multiple implicated neurotransmitter systems in RRBs, dopaminergic transmission especially is associated with such behaviors, and alterations in dopamine receptor function [132, 133], transporter activity [134], and response to relevant psychopharmacological agents (in a mucine model) [135] have all been implicated in ASD-associated RRBs. Additionally, a putative "dopamine theory of autism" has been proposed in which dopaminergic system dysfunction in mesocorticolimbic pathway is associated with social deficits, whereas that of nigrostriatal pathway is so implicated in RRB deficits [136].

Additional primary motivation for the research of RRBs comes from the fact that they are associated with clinically significant measures of distress, and certain RRB manifestations in fact increase with stress level [137]. Correlations between RRB severity and task measures that might otherwise plausibly be identified as idiosyncratic and substantially of pure psychometric interest predicted RRB presentation in daily living in adolescent and young adult subjects with ASD [138]. Beyond specific relevance to ASD, RRBs are a common component of mental disorders generally, and are known to have a genetic basis distinct from ASD [139].

1.3.1 Designing a "theory-free" approach to ASD neurocognitive research

Many prior neurocognitive studies of ASD utilize a simple contrast between ASD and putatively typical subjects and identify significant effects at the group level; this method comports especially well to task-based fMRI methods in which task/no-task conditions form a binary contrast. However, given the previously discussed substantial heterogeneity within the disorder, even within the presentation of the individual core deficits, an experimental design that accounts for the full spectrum of heterogeneity can capture ASD-associated patterns of neurocognitive difference without the need for any *a priori* theory or model. An additional risk of subject differentiation via exclusively binary grouping is noted by Noriega: "An unfortunate consequence of this broad definition is the clear trend in research to focus on subjects on the 'mild' end of the spectrum. This trend, anecdotally known for some time, has now been well established in systematic fashion [2]. Inevitably, this bias is to the detriment of the more severe cases [124, p. 359]. " Even ordinal-scale measures of subject attributes overcome this challenge because they encapsulate severity. Noriega also notes, however, that symptom severity can make participation in neuroimaging research as subjects difficult for individuals who experience it; barring improved tolerability of neuroimaging apparati, extrapolation from observable variation in putatively quantifiable subject attributes nonetheless provides a better proxy for the plausible neurophysiology of more severe disorder forms than does the embiggening of observed effects between binarily grouped subjects. While formulating the analysis in this way does have the noted benefits with respect to analyzing heterogeneity in ASD and its neural bases, it must be noted that task-based activation studies in general are the source for many of the known cognitive functions of cortical areas as well as the areas previously implicated in ASD and RRBs, and hence, necessarily, such varied approaches together, and inseparably, form important bases from which various aspects of ASD neurocognition can be surmised.

Whole-brain connectivity analysis followed by modeling and testing of potential underlying brain networks allows the formulation of holistic, integrative hypotheses regarding aspects of ASD neurocognition without being constrained by preexisting theoretical models. Beyond the bare association of ASD symptom severity with changes in specific neurocognitive networks, a near certainty as discussed above, no assumptions are made with this approach about the specific nature of the networks, nor the way in which they vary with ASD symptoms. The comparison between this approach and the traditional two-subsample approach is depicted in figure 1.2.

Figure 1.2: Comparison of design matrices using behavioral measures within a group of participants who have ASD diagnoses (A) and traditional binary contrast utilizing a value of 0 for "controls" and 1 for "ASD diagnosis." The green arrows point to the "filled in" blocks representing a value of 1 in (B) rather than the continuous variation represented in the graded size of the blocks in (A).

(A)

Contrast (C)

Data (Y)

Design matrix (X)

All-ASD subject pool using a numerical variable (RBS-R CSS) as the independent variable

(B)

Contrast (C)

Design matrix (X)

Traditional design in which the independent variable is a binary classifier for ASD/cognitively typical
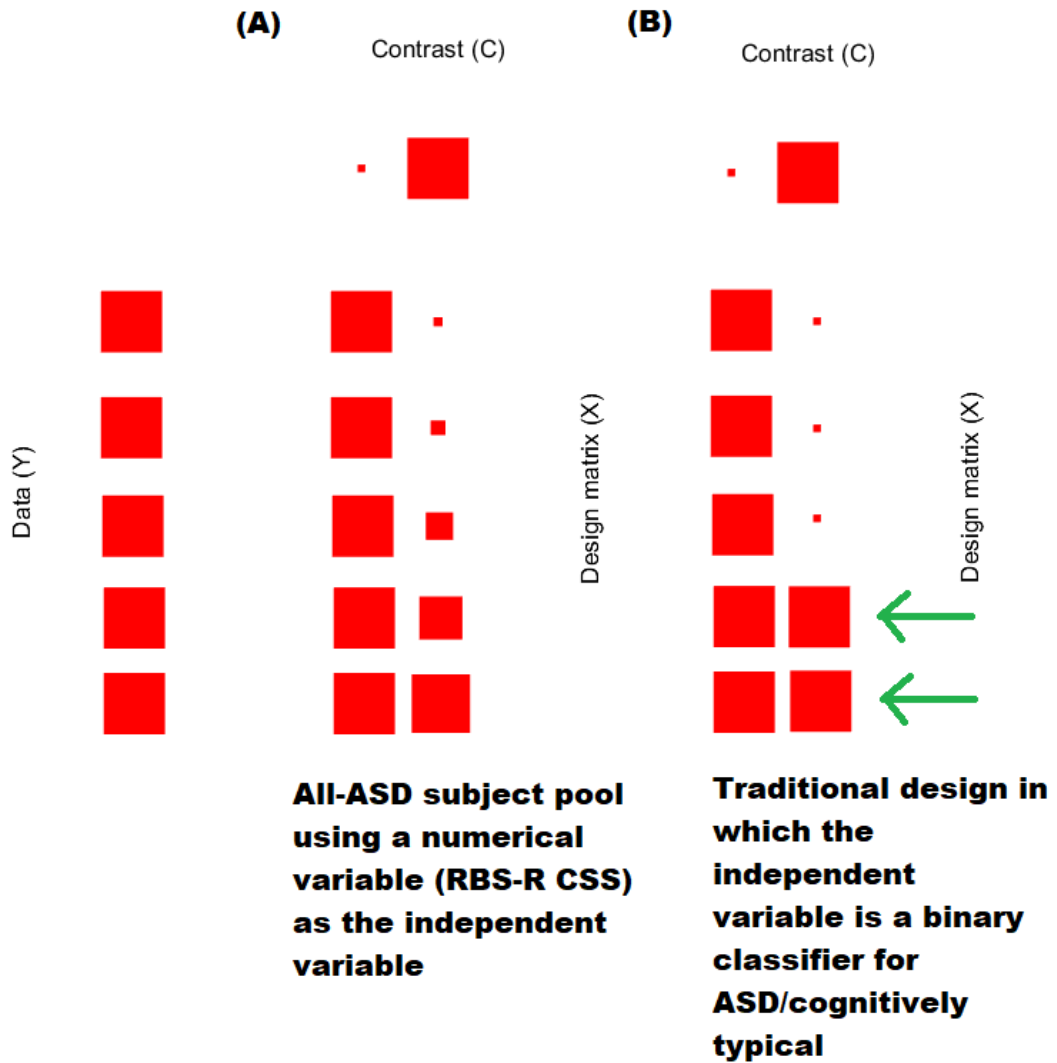
Table 1.4: Strengths and weaknesses of neuroimaging modalities [140].

Modality	Spatial res.	Temporal res.	Functional spec.	Anatomical spec.
fMRI	High	Low	Medium	High
M/EEG	Low	High	High	Very low
PET	Low	Very low	High	Low

1.4 FUNCTIONAL CONNECTIVITY AND NEUROCOGNITIVE NETWORKS

1.4.1 Functional brain imaging

Functional brain imaging has a long history that begins with the discovery of the scalp currents arising from brain activity detectable by superficial electrodes (electroencephalography; EEG). Further methodologies, comprising magnetoencephalography (MEG), positron emission tomography (PET), and nuclear magnetic resonance imaging (MRI) and its variations, followed thereafter. Each has been substantially utilized in ASD neurocognitive research. A brief summary of the methods themselves is presented in table 1.4.

All of these techniques can be used to image neurocognitive networks. fMRI, as the modality utilized in this thesis, will be explored in the most depth. The others will be briefly covered with respect to their impact on ASD neurocognitive research, and results from these modalities are included elsewhere in this chapter as well.

One of the most obvious clinical applications of the EEG is in epilepsy diagnosis, as spikes of up to 1000 uV can occur, in comparison to the 50 uV peak-to-peak measurement observed in normal physiology [141]. Additionally, its fine temporal resolution allows the discrimination of types of activity that fMRI simply cannot resolve; the order of the timescale they can discernibly image is on the order of one millisecond in the case of EEG, and two seconds, 2,000 times as coarse a scale, in the case of fMRI.

Subtler EEG patterns have been sought and identified in ASD clinical research. Comparison with clinically healthy controls of well-characterized auditory potentials has suggested differences in interhemispheric processing associated with ASD [142], perhaps relevant to observed language deficits [143, 144]. EEG measures have also correlated with differences in higher-order stimulus processing, in tasks which include components of novelty and error detection [85, 145].

While source-level analysis is ideal for studies of connectivity using electroencephalography, in clinical populations especially, a smaller number of electrodes and/or sensor-level analysis only may

be more practical. Sensor-level metrics continue to be used in clinical populations, including ASD and ADHD [24, 146].

EEG's primary advantage is its relatively high temporal resolution, which is sufficient for recording whole-brain oscillations. Dysfunctions in these oscillations are termed *oscillopathies* [147], and these, like functional connectivity disruptions, seem to be relevant to psychological disease states in general.

MEG is, for the most part, analogous to EEG; the primary difference is the orientation of the neurons within the cortical sheet that give rise to the largest part of the observed signal. MEG imaging of age-dependent differences in auditory potentials in subjects diagnosed with ASD suggest altered maturation of the brain compared with typical development [148].

PET is another major imaging modality, and the first, before fMRI, to create 3-dimensional functional reconstructions that directly localize activity in the brain in space. However, its fundamental mechanism involves the use of radiolabeled analogs of the molecules of interest (neurotransmitters, sugars, hormones, water, etc.) that expose subjects to potentially harmful radiation, and thus its use is limited in research applications. PET is further deprecated in comparison to fMRI for modern neurocognitive imaging in that it shares with MRI a very high installation cost [149], but also adds the additional preference for, although not requirement of, on-site cyclotrons to produce the necessary radioisotopes [150]. Nevertheless, the ASD neurocognitive imaging literature does present applications of PET.

PET imaging detected hypoperfusion among children with ASD and idiopathic intellectual disability using radiolabeled H_2O (water) in bilateral temporal lobe bounding areas of auditory association and multimodal regions of cortex, and these results were verified on a further sample of autistic adults [151]. More recently, and more specific to PET's differential utility, employment of a radiolabeled protein molecule of 18 kDa, two orders of magnitude heavier than glucose, and approximately three heavier than water, enabled detection of reduced expression of the protein translocator protein across multiple regions of cortex in young adult male subjects diagnosed with ASD [152]. Most notably, perhaps, PET in the future may more fully characterize the relationship between ASD-specific social deficits and cortical oxytocin expression, as some studies have begun to attempt to do [153, 154]. Oxytocin has been of significant interest, including as a therapeutic agent, regarding its association with ASD social deficits. However, research thus far has been complicated by the lack of useful PET-compatible human oxytocin receptor ligands [155].

fMRI theory

As fMRI is the focus of this thesis, the theory underpinning it will be briefly covered.

Magnetic resonance imaging, and more recently, functional magnetic resonance imaging, use the magnetic field generated by protons in tissue in order to construct a three-dimensional image of that tissue. The physics behind MRI operation are complex, and are reviewed briefly here. It is especially important to theoretically justify functional MRI experiments given the manifold assumptions required in their construction; a now infamous study [156] found neural activity in the brain of a dead salmon using commonly accepted statistical protocols to demonstrate the necessity of such caution. The following discussion of fMRI physics and fundamental statistical concepts refers principally to [157].

Physical basis of MR imaging Magnetic resonance imaging of tissue consists of the placing of the subject in a scanner which uses a strong magnetic field with strength B_0 to align protons (^{1}H nuclei, specifically ones attached to oxygen in water) in the same direction of the field. Protons have an angular frequency which is dependent on the strength of the applied magnetic field, the Larmor frequency, which determines what wavelength and frequency of electromagnetic radiation they are capable of absorbing and emitting, important for the next step.

Although the protons are aligned in the direction of B_0, their phases relative to one another are, by default, random. In order to align the phases, a strong radio frequency pulse of the appropriate frequency is applied, tipping the nuclei over so they precess in the xy-plane. After the phase-aligning pulse, a magnetic field with a spatial gradient is applied that varies in magnitude proportionally with distance. As the protons become out of phase with one another, there is some distance which must be traversed from one proton to the next one with the same phase for a given point in time. Thus, the phases are aligned helically, and the distance from one proton to the next with the same spin can be described as a "spatial period," similar to the inverse of the frequency of a typical wave.

The theoretical basis for image formation is that spin density varies in different types of tissue. Since water, which contains hydrogen atoms, is ubiquitous in human tissue, but in varying concentrations, different types of tissue have different proton density. The differences in proton density are used to create an image which is lighter or darker depending on the density, creating an image whose contrast correlates with the type of tissue represented.

MRI imaging protocols Two time constants describe the relaxation (return to equilibria) characteristics of an MR signal:

T1 (longitudinal relaxation constant) The longitudinal relaxation constant (or spin-lattice relaxation constant) signifies the amount of time it takes for protons to recover their thermodynamically equilibrious magnetization in the z-direction (parallel to the applied field), which had previously been disrupted by the radiofrequency pulse so that all nuclei were "tipped" orthogonally to the direction of the magnetic field.

T2 (transverse relaxation constant) The transverse relaxation constant (or spin-spin relaxation constant) describes the amount of time it takes for a loss of net magnetization in the transverse plane due to the phase relationship between protons tending towards random, after initially being aligned due to the RF pulse.

Correspondingly, there are two scanner parameters that can be adjusted that effect the dynamics of the signal generated:

TE (echo time) The echo time describes how soon after the pulse data collection is begun.

TR (repetition time) The repetition time describes how frequently the RF pulse is repeated.

In functional MRI, a parameter called $T2^*$ is defined by the adjustment of T2 for local disturbances in the magnetic field. These disturbances are caused by the magnetic differences between oxygenated and unoxygenated hemoglobin in red blood cells. Because cerebral blood flow is associated with neural activity, if $T2^*$ is emphasized, the signal and image will contain a correlate of neural activity. This correlate is called the BOLD (blood oxygen level dependent) signal, and forms the basis for functional MRI. As noted in the introduction to this chapter, careful theoretical considerations must be made when judging neuronal activity from a correlate so far removed from the actual physical basis (metabolism, action potentials, and neurotransmitter release and receptor binding). The same goes for finding neural correlates of cognition, and actually conscious information processing even moreso, as consciousness, let alone cognition in various abstraction, is even more profoundly phenomenologically distinct from the BOLD signal.

In task-based fMRI, presentation of stimuli and data collection can occur in "blocks" or "events." In blocked fMRI studies, separate stimuli are presented repeatedly in blocks, i.e., a given stimulus A is repeated several times over, and then a given stimulus B is repeated several times over. The strength of this method lies in the fact that a robust signal can be generated based on the assumption that the BOLD signal is additive (linearity), and hence, the total response to a given block is the sum of the individual responses to each iteration of the same stimulus. Event related fMRI experiments randomize the presentation of stimuli. Although lower in statistical power, randomization prevents

the acclimation and/or habituation to stimuli which may attenuate the BOLD response over time. While the BOLD signal is the MR signal correlate of blood flow, and hence, neural activity, some functional relationship between the BOLD signal and the actual extent of the change in blood flow must be established. The change in blood flow is referred to as the hemodynamic response, and the specific hemodynamic response underlying a, in this case, neural event is referred to as the hemodynamic response function (HRF). The current most common way to model the HRF in fMRI activation experiments is a linear time invariant (LTI) system, in which postulated neural activity in response to cognitive events represent an impulse to which the HRF directly corresponds.

Shortcomings of the task-based and activation-based approaches to fMRI research in autism spectrum disorder include, respectively, that they make strong, if implicit, assumptions about the specific relevance of the task, both to the brain areas of interest and in the proposed analogy of the task to natural behavior, and that they discount the manifoldly connected nature of the brain when analysis is constrained only to "relevant" brain regions. While such designs have and will continue to provide vast insight into the nature of human neurocognitive function, this thesis seeks to identify brain functional differences more innate to the brain itself, and thus uses techniques discussed in the next section. Nevertheless, this tried and tested approach has yielded countless of the insights that have guided the present research, demonstrating the importance of reciprocal contextualization of brain imaging research results.

1.4.2   Resting state functional connectivity

The standard approach to functional cognitive neuroimaging studies has been to measure changes between rest and task conditions and evaluate the implied association between the identified regions and the task being performed and/or between subjects drawn from a clinical population of interest and putatively typical controls. However, the experimental canon in neuroimaging has comprised measures of resting-state activity since essentially the inception of the field, with the discovery of a regular oscillation in human EEG in 1924 [158], the α-wave, that disappeared or was substantially attenuated when subjects were engaged in mental tasks, or even upon opening of the eyes [159]. In resting state functional connectivity inferred via fMRI, or rs-fcMRI, the measure usually taken as representing functional spatiotemporal relationships in the brain is the Pearson correlation between the time series of any two discrete regions, defined in various possible ways (voxels, anatomical structures, distributed functional networks, etc.). Other metrics, such as wavelet coherence, mutual information, dynamic time warping, and other measures [160] of relationships between two or more time series data, have seen employment varying from substantial to marginal. Beyond the metric

chosen, interpretation (see following subsection) is a primary methodological concern given the phenomenological separation of any particular metric from the underlying neurophysiological and, therefore, cognitive significance; section 3.7 in this thesis comprises its interpretation of the Pearson correlation values obtained in the connectivity analysis.

The proliferation of methods in general is of no surprise given resting state networks remain of methodological interest for many reasons. First, they are not dependent on tasks which may be difficult to reproduce and which may result in observed effects that are quite idiosyncratic to the specific task implementation. More importantly, the magnitude of the metabolic changes in brain activity between clinical and putatively typical subjects may be on the order of 1% [161]; hence, analyzing whole-brain activity, without specificity to any task, might enable the identification of an ensemble of changes which, in total, are more metabolically significant and therefore associated with correspondingly larger changes in the BOLD signal and any derived measures, such as functional connectivity.

Candidate neurocognitive networks active at rest have been called "endogenous" and "intrinsic" networks [162]. These networks may arise from a sort of neural homeostasis present at rest that differs in consistent ways in disease states [163]. Such differences may interact with task-related changes, resulting in the observed clinical symptoms in psychological disorders. Despite the rapid proliferation of resting-state studies, Greicius noted in the introduction to a 2008 paper that "fMRI has largely failed to fulfill its promise in the clinical realm [164, p. 424]." One such network with substantial empirical support is the default mode network (DMN), which has been substantially implicated in the social and communication deficits in ASD [165]. Multiple associations between ASD or particular of its features and aspects of DMN connectivity have been observed in rs-fcMRI, including decoupling of DMN structures [166] in accordance with long-range hypoconnectivity.

The traditional statistical approaches to rs-fcMRI analysis, both for studying disease states and typical patterns of connectivity, comprise seed-based approaches that utilize "seed" or "source" ROIs, which use anatomically defined volumes of the (typically normalized) brain as the functional target of analysis and calculate the connectivity between the functional/anatomical seed and other voxels in the brain, and voxel-based approaches, such as independent component analysis (ICA), which decomposes the voxel-to-voxel connectivity values into independent spatial components. In addition, several machine learning approaches have been successfully applied to rs-fcMRI data [167].

Each analytical approach has at least some advantages and drawbacks relative to the others. For example, independent component analysis (ICA) has the advantage of allowing whole-brain connectivity to be characterized without being constrained or biased by predefined anatomical volumes

39

corresponding to areas of known structural or functional significance, but the process, and hence, without interpretation, results, are more opaque than for ROI-based analyses where a clear correspondence can be made between the computed results and the neurology and cognitive neuroscience literature writ large. One manifestation of this concern is the fact that the components in ICA must be independent, which limits or abrogates the ability to find nodes that comprise portions of overlapping networks [168] or subnetworks.

Interpreting rs-fcMRI results

One important consideration is they very nature of rs-fcMRI: It identifies *functional* connections. Such connections are obviously of *a priori* interest because they indicate the manner in which disparate brain regions interact with each other, and yet exist both in the presence and absence of identifiable structural connections between the regions; in each of these cases, the precise implications of identified functional connections are subtly constrained. In the ideal case, functional connectivity results can be compared in the same data set with structure connectivity measures [169]. Likewise, hypotheses about the implications of altered rs-fc on behavior in clinical populations can only be directly tested when both resting-state and task-based imaging is performed on the same subject population under as nearly identical as possible circumstances [170].

1.4.3 Neurocognitive networks

A synthesis of the results of functional connectivity experiments requires assessment of the ensemble of connections at the level of a proposed network of brain regions subserving functionally specific cognitive processing; such networks are termed *neurocognitive networks*. The revelation that the brain comprises functionally distinct subunits provided one of the fundamental precepts underlying cognitive neuroscience. In 1861, French physician Paul Pierre Broca published a clinical case of a patient who had lost his speech faculties who upon autopsy was found to have lesions localized to a circumscribed area in the left frontal lobe. He concluded about this patient "[t]here is therefore every reason to believe that, in the present case, the lesion of the frontal lobe was the cause of the loss of speech [171] (translated)." His discovery of the now-eponymous Broca's area established a firm rationale to study the brain from the perspective of functional localization, and this paradigm has long been the dominant one, with clear shift toward reduced emphasis on localized activation alone occurring recently. However, combined with the already established nature of neurons as manifoldly interconnected with one another within cortex, this discovery simultaneously gave rise to a new problem in understanding the functioning of nervous systems: if there are functionally (and

cytoarchitechtonically) distinct "modules" in the brain, and yet neurons are densely interconnected with one another within and between regions, how, and to what extent, does the brain operate as a unified whole versus as a (mere) collection of "modules [172]?"

While cortex, and the rest of the brain, is certainly functionally segregated at the very least with respect to sensory and motor streams, there has always existed the notion in neurology and neuroscience that the entirety of the brain is involved (mass action) in at least some way in any major motor or cognitive activity, and that regions of brain are capable of adapting their functions as a consequence of damage to other areas (equipotentiality). Karl Lashley described the potential for the "diffusion of impulses through a fairly homogeneous matrix [173, p. 253]" of sensory information once it has left its associated primary cortex. Despite all the progress since 1931, Lashley's fundamental proposals were of accord with his own experimental observations, and the issues he raised, along with the caveats offered with them, remain remarkably prescient: "From the standpoint of an adequate cerebral physiology also, the classical concept of cerebral localization is of limited value, because of its static character and its failure to provide any answer to the question of how the specialized parts of the cortex interact to produce the integration evident in thought and behavior. **The problem here is one of the dynamic relations of the diverse parts of the cortex**, whether they be cells or cortical fields. The diversification of parts is a fact of fundamental importance, but it is only one of many which must be discovered before we can form any adequate conception of cerebral organization [173, p. 246] (emphasis added)."

Fundamentally, therefore, the notion of brain networks allowed the resolution of a long-standing debate over whether the brain was organized into functional modules, or acted as a unitary mass with all parts, at all times, acting in concert [172]. In the theory, brain networks consist of functionally distinct but interconnected regions at multiple scales, from microscopic columns of coactive neurons, to topographically organized sensory receptive fields or motor units, to higher level sensory cortex that integrates and segregates sensory information that is reciprocally connected with association cortex, which itself is reciprocally connected with other areas of association cortex, to the lobes of the cerebral hemispheres and finally to the entire cerebral cortex. The dense reciprocal projections between cortex and thalamus, limbic structures, and the basal ganglia show that networks are not restricted to neocortex alone. At the simplest level, functional networks comprise "interareal correlated activity [172, p. 289]." "Correlated" includes anticorrelation as well, allowing for functional reciprocal inhibition to undergird dynamic network behavior. As the vast majority of corticocortical connections between areas are in the form of excitatory synapses from cortical pyramidal cells, subcortical structures reciprocally connected with multiple cortical areas at once

could enable such mutual inhibition. Contrary to supervised machine learning models based on artificial neural networks, the real biological brain has no teacher, and so the manifold nature of cortical and subcortical-cortical connections allows for the different areas to guide the behavior of other areas through reentrant (also called recursive or reciprocal) connections and processing [172, 174]. Furthermore, biologically, processing can be parallel or serial, allowing for functional topology optimized for stimulus or behavior class. For example, visual input comprises a massively parallel stream of information beginning with the numerous photoreceptors in the retina, whereas, should that information stream contain visual data about a map that is being used to plan out a driving route, each step must be assimilated before the next, even while the photoreceptors themselves and even primary visual areas of cortex persist unhindered in transducing the sensory information to higher cortical areas for the relevant processing.

A further fundamental aspect of brain network behavior is metastability [174] (also section 1.5). Functionally, this characteristic is reflected in the balanced interplay between segregation and integration of information streams and the corresponding brain networks. Thus, the science of coordination dynamics is the most informative and biologically relevant quantitative framework in which to assess the behavior of real biological brain networks. An apt description in light of this view, in context referring to monkey local field potential data, can be found in "[t]he rapid transition from low to high coherence, and back again, is indicative of the relative coordination of these sites—their ability to partially synchronize their oscillatory activity without becoming locked into global synchronization [174, p. 27]." To suspend any uncertainty, the authors state: "We propose that a crucial aspect of cognitive function, which can both integrate and segregate the activities of multiple distributed areas, is large-scale relative coordination governed by way of metastable dynamics [174, p. 30]." Of interest to this study, one of the noted "outstanding questions [174, p. 34]" is whether or not errors in brain network coordination can lead to cognitive impairment or disease.

Evidence has been accumulating rapidly for a distributed network view of cognitive organization, and this has both been spurred by, and provides a motivation for further, advances and refinements in neuroimaging hardware and the analytical techniques used to understand the data it provides [175]. For example, node identification still frequently proceeds from a basis of cytoarchitectonic areas as identified by Brodmann and his contemporaries around 100 years ago. While the Brodmann scheme of cortical parcellations certainly has underlying neuroanatomical justification, convention likely also provides outsize influence in favor of its use in sophisticated functional connectivity studies. On the other hand, MRI is typically unable to differentiate cortical areas on the basis of their cytoarchitecture, and so there is a fundamental challenge in basing anatomical discrimination

in such a context on cytoarchitectonic properties. Advancements do continue, however, and other functional and anatomical atlases of brain ROIs with greater specificity and consistency across the entire brain are now used, such as those in this thesis (section 2.3.2).

With respect to ASD, the immensely distributed nature of social and emotional processing strongly implicates the significance of a neurocognitive network-based mechanism in the central deficits observed in ASD. For RRBs, too, motor behavior is dependent upon multiple functional divisions across cortical and subcortical structures and cerebellum and their reciprocal relationships. In turn, many outstanding questions invite further intensification of efforts in the area; differences associated with symptom-specific heterogeneity in connectivity, the developmental course of such heterogeneity, network classification according to neurotransmitter activity, and so on, are all avenues of promise for further research. In this study, heterogeneity in the RRB domain among subjects with an ASD diagnosis will be correlated with differences in functional connectivity in an effort to identify a putative brain network underlying this dimension of variability in ASD.

Brain networks in restrictive and repetitive behaviors

A putative "connectivity theory of autism," both as a developmental consequence of disruption in neural circuit formation and as a distinct explanatory framework, has substantial and increasing empirical support. The prevailing synthetic model aggregates connectivity patterns in ASD into a general scheme of increased local connectivity and decreased long-range (cortico-cortical) connectivity [86]. This simple theoretical scheme has significant explanatory power for various ASD cognitive deficits, but faces challenges. For example, instances of both long-range hyperconnectivity [176] and short-range hypoconnectivity [177] have been posited. Length-dependent connectivity variation determined via rs-fcMRI found decreased connectivity for both long- and short-range functional connections, but no pattern for medium-length connections [178]. Furthermore, intrinsic connectivity patterns in the grey matter in ASD, for example, are multifold and to some extent apparently idiosyncratic, as shown in table 1.5 [179].

ASD connectivity studies across neuroimaging modalities abound, but RRB-specific, and especially, RRB-specific within the diagnostic universe of ASD, connectivity studies are less numerous than those addressing social and communication domains. While neuroimaging research in animal models of ASD has become increasingly prevalent, as references in this thesis demonstrate, recent criticism has included that "there has been almost no exploration of how these findings pertain to RRB, or other abnormal behaviors, in such models [47, p. 153]." As discussed under the *neural circuit theories* heading in section 1.2.2, neural circuits, which comprise functional and anatomical

43

connections between multiple related regions, form a high plausibility candidate substrate in the pathophysiology of RRBs in ASD, and these subunits *have* been extensively and successfully researched in animal models of ASD RRBs. In RRBs specifically, cortico-basal ganglia neural circuits have been implicated in addition to interaction effects between basal ganglia and cerebellar networks mediated by mutual connectivity with multiple cortical, thalamic, and pontine nuclei regions. Given especially the functional ubiquity of basal ganglia across sensory, motor, and cognitive functions, it is not surprising that multiple subcortical nuclei would therefore be implicated in RRB manifestation; the manifold functional interconnectivity between brain regions, which does not require direct anatomical connectivity, would seem to suggest that a better question given cumulated evidence than "if" is "how" basal ganglia underlie relevant aspects of RRBs, especially in view of their motoric significance. Basal ganglia loops comprising cortico-subcortical connectivity subserve diverse limbic, associative, and motor function, with discrete, well-characterized basal ganglia circuits underlying each.

The default mode network (DMN) has also been implicated in ASD pathophysiology in general, and social-communication deficits [165] repeatedly, as well as in, though less frequently and comparitively more recently, RRB deficits. For example, DMN connectivity analyzed via ICA on fMRI data found the network to be more weakly connected in individuals with ASD, and the extent of the difference was associated with the severity of social and communication deficits [180].

While putative roles of DMN in RRBs in ASD are increasingly the subjects of neurocognitive research on the disorder, this proliferation has both raised and answered questions about the RRB—rest network functional relationship. Increased posterior cingulate—right parahippocampal gyrus rs-fcMRI has been associated with more severe RRB using the ADI-R measure [181], although an underlying functional network associated with RRBs beyond the DMN was not postulated from this result, and DMN connectivity across several ROIs has been identified in association with the compulsive behaviors in obsessive-compulsive disorder [182], increasing confidence as to its fundamental role in the class of behaviors.

Atypical striatal connectivity has been identified both with the disorder in comparison to putatively typical controls [183] and in specific association with RRBs [184, 185]. Specifically, corticostriatal hyperconnectivity has been observed between *a priori* chosen striatal seeds and frontoparietal and occipital cortex in association with higher RRB severity, measured as RBS-R score, as in the present study (and also using ABIDE datasets).

In cerebellum, "[t]he cerebellum and associated circuitry has begun to emerge from neuroimaging studies of RRB. Alterations to the cerebellum are also one of the most consistently reported patho-

logical findings in post-mortem studies in ASD [47, p. 165]." This latter result is to be of no surprise given the manifoldly extensive functional and anatomical reciprocity with supernumerary targets [186] when contrasted with most empirically employed functional brain parcels. The basal ganglia, however, are similarly so connected, and this creates the expected multifarious interactions between the anatomically discrete structures: In ultra-high field imaging in animal models of RRB, severity correlated with volumetric changes in cerebellar crus II, subthalamic nucleus, and striatum, together comprising important nodes in the indirect pathway [187]. Cerebellothalamocortical circuits have been broadly implicated in RRB manifestation as well.

At the RRB subcategory level, 12- and 24-month resting state scans of infants identified a negative ritualistic/sameness and visual—default mode network connectivity relationship, a positive stereotyped/restricted symptom extent and default mode—executive network connectivity, and two relationships between rs-fc and dorsal attention network connectivity: Stereotyped behavior was positively correlated with dorsal attention—subcortical connectivity, and restricted behavior severity was with dorsal attention—default mode connectivity [128].

An overview of multiple reviews and large-scale imaging studies[47, 127, 188] of resting-state functional and anatomical connectivity in RRBs in ASD and other neurodevelopmental disorders is given in table 1.6.

Beyond these incipient results, RRBs have even in recent history often been conceptualized in terms of their analogs in other disorders (in addition to OCD), such as Tourette's syndrome [118, 119] and Prader-Willi syndrome [47], whereas language, and to an even greater extent social deficits, have formed the bases for proposed unitary mechanisms underlying the whole of ASD pathophysiology (section 1.3). However, RRBs actually provide the set of symptoms most directly relevant to the cognitively-defined "hyper-systemizing" theory of autism, or, in slight variation, the "extreme male brain" theory of autism, as well as the adaptively-defined "assortative mating" theory of autism (section 1.2.2). This is because these theories conceive ASD as the manifestation of a preference *for* lawful, predictable, simple systems, rather than *against* complex ones, such as social interactions. Meticulous arrangement of objects, collection and organization of various objects (e.g., baseball cards), and a strong desire for uniformity in diet and routine all directly implicate such a preference *for* lawful systems. While apparently repetitive and purposeless motions, which are classified as RRBs, are of less clear significance, they nevertheless represent a sameness preference. By analogy, dance improvisation may be construed as purposeless, but, at least in contemporary Western forms, is not generally repetitive in a categorical sense as RRBs are. In fact, an article on the subject in *The Journal of Aesthetic and Art Criticism* warns that "...improvisation as a

form of performance runs the risk of falling into **habitual repetitive patterns** that may become stale for performers and viewers [189, p. 182] (emphasis added)." The significance is that dance improvisation is "successful" when it is *unpredictable*, not only for the audience, but specifically for the performer as well. RRBs, on the other hand, are "successful" precisely when they are predictable, whether through the satiation of a psychological compulsion, or via whatever intrinsic objective they satisfy. Hence, even stereotyped movements in isolation of other organized behavior satisfy the criteria for being the sorts of behaviors predicted by the aforementioned cognitive and adaptive theories of autism. As RRBs, unlike improvised dance, are not performed for an audience, this is also consistent with an at least apparent distaste for socializing: if easily predictable motor behavior is preferred, oneself is the most reliable source for it.

Because of this clear centrality to the relevant theories of autism, while also not contradicting that the other core deficit symptom categories are significant, combined with the correspondingly sparse research for RRBs compared to the other core deficits, they are chosen as the phenomenon of interest for seeking potential brain networks associated with ASD without making assumptions about the "true" nature of the disorder. While a composite measure of ASD symptom severity could also be used, assessment of the result would be less straightforward, and, additionally, repetitive behavior is marginalized in the ADOS-G as well, as discussed in chapter 2. Connectivity summarized here in prose and in tables 1.5 and 1.6 will provide a major facet of the context in which results are ultimately assessed.

Table 1.5: Differences in intrinsic connectivity in ASD

Measure	Anatomical cluster	BAs	Significance
Mean separation distance	Primary motor cortex, precentral gyrus, postcentral gyrus, somatosensory cortex, posterior parietal cortex (all left)	1, 2, 3, 4, 5, 7	Lower
	Anterior temporal lobe, middle temporal lobe (all left)	20, 21, 38	Lower
	Orbitofrontal cortex (left)	10, 11	Lower
	Temporoparietal junction (right)	39	Lower
	Inferior temporal lobe, somatosensory cortex, central gyrus, orbitofrontal cortex (all right)	10, 20, 37	Negatively correlated with ADI-R repetitive scores
	Temporoparietal junction (left and right)	39, 40	Negatively correlated with ADI-R repetitive scores
Radius function (within-path distances)	Anterior and medial temporal lobe (bilateral)	21, 22	Lower
	Dorsolateral prefrontal cortex (bilateral)	10, 11	Lower
	Somatosensory cortex, postcentral gyrus (bilateral)	1, 2, 3	Lower
	Posterior parietal cortex, temporoparietal junction (all left)	5, 7, 39	Lower
			Generally negatively correlated with ADI-R repetitive scores and social and communication deficits
Perimeter function	Temporal lobe (bilateral)	20, 21, 38	Higher
	Ventrolateral prefrontal cortex (bilateral)	10, 11	Higher

| Precentral gyrus (bilateral) | 4, 6 | Higher |
| | | Generally positively correlated with ADI-R repetitive scores and social and communication deficits |

Table 1.6: Differences in rs-fcMRI and DTI measures in RRBs in neurodevelopmental disorders. PWS, Prader–Willi syndrome; CBC, compulsive behavior checklist [190]; ADI-R, autism diagnostic interview, revised [191].

Region	Finding	Disorder	RRB inventory/direction of effect
Superior frontal gyrus	Decreased fractional anisotropy in SFG	ASD (children)	ADI-R↑ ⟺ FA↓
	Increased SFG—ACC resting state functional connectivity	ASD (children)	ADI-R↑ ⟺ FC↑
	Decreased SFG—PCC resting state functional connectivity	ASD (adolescents)	ADI-R↑ ⟺ FC↓
Middle frontal gyrus	Decreased fractional anisotropy in MFG	ASD (children)	ADI-R↑ ⟺ FA↓
	Increased MFG—caudate resting state functional connectivity	ASD (adults)	ADI-R↑ ⟺ FC↑
Inferior frontal gyrus	Decreased right IFG—ACC and right IFG—insula resting state functional connectivity	ASD (adults)	ADI-R↑ ⟺ FC↓
Superior temporal gyrus	Increased right STG—right ventral putamen resting state functional connectivity	ASD (children)	ADI-R↑ ⟺ FC↑
Anterior cingulate cortex/salience network	Decreased fractional anisotropy in ACC	ASD (children)	ADI-R↑ ⟺ FA↓
	Increased ACC salience network resting state functional connectivity	ASD (children)	ADI-R↑ ⟺ FC↑
	Decreased left ACC—right insula resting state functional connectivity	ASD (children and adults)	ADOS↑ ⟺ FC↓
	Decreased rostral ACC white matter integrity	ASD (adults)	ADI-R↑ ⟺ WM-INT↓

	Decreased salience network resting state functional connectivity	ASD (children)	ADI-R↑ ⟺ FC↓
Default mode network	Atypical default mode network resting state functional connectivity	ASD (adolescents, adults)	ADI-R↑ ⟺ FC↔
	Decreased left posterior cingulate cortex—right angular gyrus resting state functional connectivity	ASD (adolescents)	RBS-R↑ ⟺ FC↓
	Increased left posterior cingulate cortex—left STG (Wernicke's) resting state functional connectivity	ASD (adolescents)	RBS-R↑ ⟺ FC↑
Insula	Decreased right insula—left ACC resting state functional connectivity	ASD (children and adults)	ADOS↑ ⟺ FC↓
Caudate	Increased right caudate—right MFG resting state functional connectivity	ASD (adults)	ADI-R↑ ⟺ FC↑
	Decreased right caudate—mPFC resting state functional connectivity	PWS (adults)	CBC↑ ⟺ FC↓
Putamen	Increased right putamen—right STG resting state functional connectivity	ASD (children)	ADI-R↑ ⟺ FC↑
	Decreased right putamen—left globus pallidus and thalamus resting state functional connectivity	PWS (adults)	CBC↑ ⟺ FC↓
	Increased left putamen—right fusiform gyrus resting state functional connectivity	ASD (adolescents)	RBS-R↑ ⟺ FC↑
	Increased left putamen—primary motor and somatosensory cortex resting state functional connectivity	ASD (adolescents)	RBS-R↑ ⟺ FC↑
Globus pallidus	Decreased GP white matter fractional anisotropy	ASD (children)	ADI-R↑ ⟺ FA↓
	Increased right GP—left primary motor cortex resting state functional connectivity	ASD (adolescents)	RBS-R↑ ⟺ FC↑
Cerebellum	Decreased cerebellum fractional anisotropy	ASD (children)	ADI-R↑ ⟺ FA↓

	Increased superior/middle peduncle fractional anisotropy (low-order/motor)	ASD (young children)	ADI-R↑ $\iff$ FA↑
	Increased middle peduncle fractional anisotropy (high-order/ritual/sameness)	ASD (young children)	ADI-R↑ $\iff$ FA↑
White matter	Decreased forceps minor volume	ASD (adults)	ADI-R↑ $\iff$ WM-VOL↓

1.5   COMPLEXITY AND COORDINATION IN NEUROCOGNITIVE FUNCTION

The complex systems concept forms the basic theoretical framework from which the approaches in this thesis were developed and its results interpreted. A complex systems approach, rather than one of specific methods, methodology, or interpretation, is, to a substantial extent, one of a particular type abstraction. While a putative system certainly either does or does not operate complexly, the type abstraction of the interactions between its components is the practical challenge in a complex systems analysis. Rather than a formal definition, or an exhaustive treatise, generally accepted properties of complex systems given in [192] will be summarized. Complex systems typically:

- comprise constituent, hierarchically arranged subsystems that interact within and across multiple distinct scales in time and space

- are not explicitly contingent on their particular material substrate or on the precise nature of the physical interactions between their subsystems

- exhibit macroscopic patterns of behavior at yet larger scales than any of their subsystems, a property termed "emergence"

- dynamically shift between discrete modes or states such that they can be satisfactorily modeled with orders of magnitude fewer degrees of freedom than they formally possess in terms of their most basic subunits, even to the extent that their dynamical features can be successfully extrapolated beyond what direct casual observation reveals

This expansive description critically permits sundry natural phenomena to be conceptualized in complex systems terms, as has been increasingly done in the field of neurocognitive science and research on both putatively typical cognition and that defined or diagnosed as pathological. Moreover, not only mental disorders and their causes and symptoms, but their specific intensive milieu and all its idiosyncrasies, along with how they relate to other mental disorders and nonpsychological illnesses, and all of the above as they interface with environmentally relevant social interactions, institutional experiences with healthcare and education, natural histories, subjective experiences, and more, can be assimilated into a given complex systems model of a diagnostic category writ large. For example, it has been noted that "[h]eterogeneity is major feature of autistic disorder. This means that nonlinear, complex, dynamic relationships govern the disorder, since plenty of factors have been no[?] collectively, unpredictably implicated in its aetiology, pathogenesis, phenotypic expression and prognosis. Subsequently, principles from complex-dynamic systems theory could contribute to understand such a multidimentional disease [193, p. 2]. " This quotation should be considered while

noting that the "dynamical model" eventually formulated in this thesis is an abstraction of only a very small subset of phenomena that could be abstracted from the proffered list of nonlinear component systems, comprising substantially phenotypic expression, with further categorical overlap between the formulated model and above-listed possibilities being marginal or nominal. However, the point of merit is that substantial complexity of the stated kind is suited to meaningful analysis after drastic dimensional reduction without seriously compromising the elucidated behavior of the underlying "real world" system. Dynamical systems approaches can also be in terms of spatial, temporal, and spatiotemporal relationships in the brain, with a parcellation into a core—periphery spatial scheme proffering a hypothesized avenue for finding significant differences in dynamical behavior of brains of individuals with ASD [194]. Information theoretic measures, too, given their intrinsic nonlinearity, fall under the umbrella of complex systems approaches, and have recently and substantially been employed in neurocognitive ASD research [195], utilizing, as the present study, the ABIDE database and CONN functional connectivity toolbox. But, beyond these studies and their varying levels of analogy to the present thesis, more ambitious complex systems analytical approaches to ASD and its sociocultural context have begun appearing [196]. In the particular case cited, cognitive flexibility, related to executive function and underlying aspects of it, was evaluated in terms of its complex, time-dependent nonlinear relationship to the real sociocultural milieu in which individuals with ASD diagnoses find themselves, revealing, for example, that bilingualism may grant some protective effects against ASD-associated deficits in cognitive flexibility. These and other society-scale phenomena fall squarely within the theoretical purview, if not yet always the methodological scrutability, of the complex systems approach.

"Complexity" also can be conceived in the more common sense of "intricacy," and intricate systems tend to be complex, as many in nature so far studied have shown. Complexity, for example, is not just a property that the brain exhibits in its hierarchical organization and functioning, but one that is in fact desirable, in terms of the selective advantage it imparts on organisms possessing complex brains, and in terms of metabolic and computational efficiency. [197], for example, referencing [198], notes "a quantitative measure of complexity has been proposed as a measure of consciousness and brain binding (p. 13)." This is because increasing complexity is an intrinsic consequence of simultaneously increasing functional diversity and efficiency in a given domain with a fixed substrate, in this case, a fixed neuronal mass. Neural organization is a problem of optimization rather than maximization. Neurons possess certain common characteristics that enable their integration into functional subunits at dramatically different scales, and by this capacity, combined with manifoldly complex interactions across time, space, and between hierarchical levels of processing, the brain is

also said to be self-organizing, an intrinsic result of its complex dynamical behavior. That is, to put it succinctly—

> High values of complexity correspond to an optimal synthesis of functional specialization and functional integration within a system. This is clearly the case for systems like the brain—different areas and different neurons do different things (they are differentiated) at the same time they interact to give rise to a unified conscious scene and to unify behaviors (they are integrated) ([197, p. 13]).

Metastability, a property of complex dynamical systems, is the tendency to fall into regimes of various configurations of elements that lead to transiently stable states on, in this case, the biologically relevant timescales. Changes between such regimes are characterized by dynamic self-reorganization of the system subcomponent behaviors and the interactions between them in state space. This too, it has become increasingly clear in recent years and decades, is utterly fundamental to the functioning of the brain [199]. Metastability is a primary, and potentially *the* primary, nature of the behavior of the brain. Hence, identifiable transitions in dynamic behavior associated with repetitive behavior intensity in a hypothesized brain network identified via resting state functional connectivity analysis will be sought in a time-varying dynamical model of brain activation in various interconnected functional subnetworks in response to external stimuli in section 3.7; there is a long precedence of modeling the dynamical behavior and stable and transitional states of ensembles of neural masses analytically [200], of which functional ROIs and networks/subnetworks are a particular conceptual form.

1.5.1 Brain dynamics and ASD

The ultimate nature and purpose of brain networks is transaction of information [172]. Information processing in biological systems has been rigorously defined [201] and therefore lends itself to investigational techniques that assess brain dynamics in terms of underlying information processing activity. Information does not need to be complicated to undergo complex processing, and this fact is taken advantage of in section 3.7 in which a dynamical model is constructed based on the results (chapter 3) of the brain connectivity analysis that explicitly includes the connectivity values (Pearson correlations) between every pair of significantly connected nodes in the functional network subunits by constructing parameters from a simple linear combination of every possible path within and between functional network subunits and using them as coefficients for the model variables in the dynamical rate equations. Stimulus input to the network, however, is initially modeled as a sine wave, or even,

in the preliminary assessment of the model's qualitative behavior, as an arbitrarily varied integer constant within each model realization representing a fixed stimulus drive. Additionally, rest, used as the "stimulus" in the present study, is likewise a simple stimulus. Resting state brain activity can be construed as "noise-driven fluctuations around a state of equilibrium, which corresponds to a stable fixed point [202, p. 2]" in the dynamic landscape of brain activity. Background "noise" prevents the total entrenchment of any stable state at rest by proffering continuous perturbation. The sinusoidal stimulus function in the dynamical model in section 3.7 likewise provides continuously varying, if predictably so, perturbation. In order to more faithfully capture the notion of "noise driven fluctuations," however, the sinusoidal model stimulus input is augmented by stochastic influences modeled in the form of a random walk. Because complex dynamics form the very heart of the brain's function as a biological system, they are inescapably imputed in disease states, and it should be possible to capture such a dynamic relationship via quantitative modeling based on empirical results, if such results are of true significance to the disorder (and the experimental data is of sufficient quality and quantity, and the chosen model form is biologically appropriate).

Given the recency of the (actually applied) neurodynamic approach to ASD research, the landscape of research results is still relatively sparsely populated; neurodynamics in ASD was "understudied [203, p. 2] in 2016. However, work that has been done so far shows the promise of the approach and the motivation to broaden its deployment; it is especially suited to a systems-level account of the ASD neurocognitive phenotype, and is also synergistic with the growth in collaborative neuroimaging databases, which, if they include resting state data, also allows such approaches to be extended to lower functioning individuals with ASD [204].

Nascent though the application of the approach to ASD research may seem (as may the application of even the most orthodox research methods to the neuroscience of ASD given the vicissitudes of research on a subject of exuberant interest), robust results have been obtained. Using an energy-landscape quantitative method on resting-state fMRI data, the brains of subjects with high-functioning ASD were found to exhibit fewer state transitions than the brains of TD controls [203]. The intermediate state between transitions was less stable in participants diagnosed with ASD, resulting in more frequent return to the prior state. Furthermore, IQ in the TD group was positively correlated with the frequency of transitions, while it was correlated instead with greater stability in individuals with ASD. This suggests that there may in fact be a unique ASD "cognitive style" that could perhaps impart benefits in addition to imposing costs in a manner that comports with the adaptive theory of ASD. The method employed creates an "energy landscape" of different brain states based on an analogy to the concept of physical potential energy. Complex systems ap-

proaches are replete with such quantitative abstractions that may elucidate patterns of function of biological, neurocognitive, psychological, and sociocultural relevance. Information theory generally is applicable to biological systems as processors of and responders to inputs from the environment, and complex systems theory generally is applicable to information theory. An information theoretic metric, paradigmatically a class of fundamentally dynamical, fundamentally complex metrics, information gain, also termed relative entropy, calculated at the sensor level for resting-state MEG data found that the brain activity of subjects diagnosed with ASD in response to stochastic inputs encapsulated greater information gain than for TD controls, suggesting that, at rest, the ASD brain is "noisier," which the authors go through great pains to emphasize might reflect a cognitive quality of withdrawal into a personal inner world [202]. Another explicit information metric, active information storage, was calculated for source-level MEG data from subjects with ASD and TD controls, with results showing that the brains of individuals with ASD showed activity patterns that were some combination of less predictable and less dynamically rich than those of TD controls [205]. While findings so far have been mixed, as has often been the case with any modality employed in ASD research, even those repeatedly so, graph theoretic models have indicated generally lower modularity of brain networks with less apparent segregation, consistent with the results of other methods of connectivity analysis in neuroimaging [204]. The characterization of brain network dynamics lends itself to cutting-edge analytical techniques as well, such as machine learning algorithms for pattern classification [204].

The present study will employ traditional analysis of the dynamical trajectories in systems of differential equations of variables abstracted from neurocognitively-functionally and behaviorally relevant constructs, such as repetitive behavior and cognitive executive control of compulsive motor activity. This approach constitutes one to the matter of fMRI's ponderous rate of data polling in comparison with the timescales of known physiological mechanisms, electrophysiological oscillations and neuronal impulse discharge, of neural activity. The relevance of the timescale of brain activity underlying fMRI has become of increasing interest recently, with techniques such as sliding window analysis [206, 207] assessing changes in the time course of functional connectivity measures within a resting state scan session, rather than evaluating time series correlations between operationalized brain functional parcels across the entire scan duration, thus assigning each such functional or anatomical division a single, unisolable time series. The conceptual appeal of the elected method here is that the modeled system is ostensibly independent of temporal scale entirely, although in actual fact this would require that the functional connectivity measure used, the Pearson correlation between activation time series in subject fMRI data, itself arises out mechanisms infinitely temporally

decomposable, when in fact, contrariwise to this postulation, the temporal dynamics underlying rs-fcMRI measures are known to have underlying neurophysiological mechanisms with which they share the correspondence to the actual timescales along which such data is collected [208].

CHAPTER 2

METHODS

2.1 SUBJECTS

Data were acquired from the publicly available ABIDE II dataset ([209], `http://fcon_1000.`
`projects.nitrc.org/indi/abide/abide_I.html`) provided by Katholieke Universiteit Leuven
(KUL) [210]. 28 male subjects (22 right-handed, 6 left-handed) aged 18 to 35 years with diag-
noses of autism spectrum disorder were selected from a clinical sample for inclusion in the dataset
at KUL. One participant was excluded from the current analysis for not having complete behavioral
assessments.

The inclusion criteria used by KUL were a DSM-IV-TR diagnosis of ASD, aged in the above
range, and male sex. No control subjects were included. Measures or estimates for IQ, Repetitive
Behavior Scale, Revised (RBS-R) (self-reported, Dutch version), Autism Diagnostic Observation
Schedule—Generic (ADOS-G), and Social Responsiveness Scale, Adult (Dutch version), were col-
lected, and subjects were screened for comorbid psychological conditions. Potential subjects were
excluded based on comorbidity of depression or anxiety, or contraindications for MRI scanning.

2.1.1 Behavioral assessment

Analysis was performed directly with the behavioral data, which were also used in the fMRI connec-
tivity experimental design matrix, as described below. The ADOS-G and RBS-R inventories provide
the measures used for analysis.

Autism Diagnostic Observation Schedule—General

The ADOS-G provides a diagnostic assessment tool for establishing an ASD diagnosis. The DSM 5
provides the current diagnostic criteria for ASD, but the ADOS-G provides a systematic, standard-
ized tool that can be used by clinicians and in research. Scores for the communication, social, and
stereotyped behavior domains, as well as the total (or composite scale) score, are provided for each
subject in the dataset. The social subscale score of the ADOS-G inventory were used to identify
possible correlations between RRBs and social deficits, and the communication ADOS-G subscale

was likewise used for RRB-language deficit association assessment.

Repetitive Behavior Scale—Revised

The RBS-R provides a behavioral inventory specific to repetitive and stereotypical behavior, the primary ASD deficit of theoretical interest in this analysis. Subjects were administered the RBS-R questionnaire by the KUL researchers. Scores were provided for the stereotyped, self-injurious, compulsive, ritualistic, sameness, and restricted subscales, as well as for the composite scale. Measures from version 6 of the test were used in the present analysis. Scores for one subject are missing in the dataset, so this subject was excluded from analysis.

2.2 MRI SCANNING AND IMAGE PROCESSING

Scan acquisition was by a 3.0 T Philips scanner with a 32-channel phased-array head coil at KUL. Anatomical scans were performed first followed by functional scans. Task-related scans followed resting state scans, but these data are not used in this analysis. Subjects were told to relax, fixate on a white cross on black background, and to think of nothing in particular.

Anatomical scans used a 3D turbo field echo sequence with T1 = 900 ms, TE = 4.6 ms, TR = 9.4 ms, 182 axial slices, a slice thickness of 1.2 mm, a 250 mm × 250 mm FoV, 208 × 207 acquisition matrix, and a slice in-place resolution of 1.2 mm × 1.2 mm. Functional scans used an echo planar sequence with TE = 30 ms, TR = 2500 ms, 45 axial slices, a slice thickness of 2.7 mm, an FoV of 200 mm × 200 mm, 80 × 78 acquisition matrix, and a slice in-place resolution of 2.5 mm × 2.56 mm. 162 measurements were acquired with a total scan time of 420 s.

2.3 DATA ANALYSIS

2.3.1 Regression of behavioral assessments

Subject ADOS-G, social and communication subscale scores, and RBS-R composite scale scores (RBS-R CSSs) were analyzed using ordinary least squares regression in R in order to assess the extent to which behavioral measures of one of the core deficits of autism might correlate with measures of another of the core deficits. Since the present analysis is concerned specifically with RRBs, given their relative paucity of rsfc-MRI analysis compared to the other core deficits, both ADOS-G social and communication subscale scores will be regressed on RBS-R CSSs to determine if repetitive behaviors are behaviorally correlated with the other core deficits within this subject data.

2.3.2 fMRI data analysis

The `CONN` connectivity toolbox was used in the `MATLAB` environment to analyze brain functional connectivity. The metric used was the bivariate Pearson correlation.

A schematic representation of the rs-fcMRI experimental pipeline and results analysis is shown in figure 2.1. A summary of the steps taken in the ROI-to-ROI connectivity analysis in `CONN` is shown in figure 2.2. A summary of the steps taken in the seed-to-voxel connectivity analysis in `CONN` is shown in figure 2.3.

Preprocessing

Processing on the raw dataset as provided consisted only of excluding the most extreme instances of subject movement from the sample, as reported in the ABIDE II KUL dataset summary information, so the data were processed using standard MRI preprocessing procedures for the purposes of the present analysis. Preprocessing was performed in `CONN`, which utilizes `SPM` functions to do so, and consisted of functional realignment and unwarp, slice-timing correction, outlier identification, direct segmentation and normalization, and functional smoothing, indirect segmentation and normalization, and functional/anatomical coregistration. Realignment and unwarp consisted of coregistering and resampling all scans to the first scan of a session via b-spline interpolation. Next, motion distortion was estimated and corrected via the derivatives of the deformation field and resampling of the functional data to match the deformation field. Slice-timing correction accounted for temporal misalignment between slices in functional image scans. Segmentation and normalization was performed to normalize subject scans to standard MNI space. Functional smoothing was performed with an 8 mm FWHM Gaussian kernel to increase SNR in the bold data, the default setting in `CONN`. Inter-modality coregistration was then performed to co-register functional and anatomical subject data. `CONN`'s default denoising pipeline was used. This pipeline consists of linear regression to estimate BOLD signal confounds and the application of a temporal bandpass filter to the data. Signal components outside of the interval $0.008 \leq f(\text{Hz}) \leq 0.09$, f the frequency in cycles per second, are filtered, as these arise primarily due to non-BOLD physiological sources, or from subject motion or other sources of noise. Linear regression then estimates and removes white matter, CSF, and subject motion signal components.

Connectivity measures

Whole-brain ROI-to-ROI, and seed-to-voxel, connectivity measures associated with subject RBS-R CSS were calculated in accordance with the procedures given in [211] using default settings except

where noted.

ROI-to-ROI connectivity Anatomical ROIs were defined using `CONN`'s combination of the FSL Harvard-Oxford atlas for bilateral cortical (91 ROIs) and subcortical (15 ROIs) areas; the AAL atlas for cerebellar areas (26 ROIs), provided with `CONN`, was excluded in the initial whole-brain connectivity analysis. Anatomical ROIs used are described in `conn/rois/atlas.info` in the `CONN` toolbox. These ROIs are defined anatomically in MNI152 space. 32 network ROIs are defined "from `CONN`'s ICA analyses of HCP dataset (497 subjects)," as described in `conn/rois/networks.info`. Brainstem ROIs (comprising a single anatomically defined ROI) were also excluded, and connectivity between the remaining 137 mapped ROIs was calculated. Subject RBS-R composite scale score was used in this design as a predictive variable to identify pairs of ROIs with connection strengths significantly correlated with RRB severity.

Network-level thresholding ROI connectivity data was performed to identify ROIs that were significantly connected within the entire calculated ROI network and exclude connections to ROIs not more significantly connected to the rest of the network than would be predicted by chance ($p < 0.05$). A strict uncorrected threshold for connection significance was used in order to identify only those ROIs of the most plausible significance to RRB severity given the numerosity of statistical comparisons inherently performed. The ROI pairs with significant RBS-R CSS-correlated connectivity values were used as seeds in the subsequent analysis to identify which connections show the strongest subject RBS-R CSS effects.

Seed-to-voxel connectivity Seed-to-voxel connectivity maps were calculated using ROIs identified empirically in the previous step. The default significance threshold for random-field theory parametric statistics in `CONN` was used to characterize connections of potential significance to RRBs. Clusters to which the chosen seeds demonstrated significant RBS-R CSS-correlated connectivity were recorded along with their MNI coordinates and size in voxels.

Next, two *a priori* seeds (bilateral nucleus accumbens) were used to assess the level of correspondence with prior literature results for RRB-associated connectivity and confirm the potential significance, or lack thereof, of seed-based connectivity results calculated using ROIs identified in the above-described exploratory search as seeds. Two additional *a priori* seeds (bilateral hippocampi) were chosen to identify and characterize potential effects arising specifically within the default mode network due to their dense connections within it.

Connectivity values were extracted for connections identified as significant in the previous step for each subject based on the value of the Pearson correlation coefficient between the chosen seed and the peak voxel of the most significantly connected cluster. Summary subject-level data were represented graphically to qualitatively assess trends in the data via methods in [212, 213].

In addition to individual subject RBS-R CSSs, subjects were parcellated into high- and low-RRB severity categories using a binary variable based on a literature threshold of "high" RRB trait presence [184], corresponding to an RBS-R CSS score of 22. Again, trends in the data associated with this parcellation scheme were qualitatively assessed.

Regression testing of RRB and connectivity relationships

While qualitative assessment of cortical surface projections did identify several patterns of connectivity that seemed to be plausibly related to RRB severity or category, none was definite enough to form the basis for a model of the data.

The most salient trend identified in the graphical representation of subject- and group-level data were an apparent qualitative shift occurring at or near the previously discussed threshold for "high" RRB severity. The subjects in the "high" RRB category always shared the same sign for their connectivity values for a given connection with all other members of their category. This was not true for the "low" RRB severity subgroup. In fact, the trend within the "high" RRB group was observed to no longer hold by the inclusion of the "low" RRB subject with the highest RBS-R CSS score into the putative "high" RRB group. Hence, a candidate regression analysis approach was devised and developed in order to determine if this trend in the data could be quantitatively verified relative to analogously identified patterns arising due to statistical chance. The candidate regression comprised a (log transformed) linear probability least-squares regression utilizing a statistic calculated as the product of all connectivity values for a given subject for each connection in order to ensure the salience of the sign of the connectivity value, and not just its magnitude, in determining the regression equation's viability. That is, the sign of a given connectivity value, if inconsistent with the sign of the subgroup average connectivity value, would lead to an entirely erroneous prediction by delivering a negative probability estimate. The statistic was thus the pure interaction term between all candidate regressors (Pearson correlations between pairs of ROIs whose connectivity is significantly associated with subject RBS-R CSS). As interaction term significance implies the interdependence between underlying variance of the dependent variable and multiple independent variable observations simultaneously, and the ROI pairs identified certainly function interdependently in the context

of the brain, this was chosen as the most constraining straightforward test of underlying ensemble significance of observed connectivity, both in terms of the risk of regression overspecification, which is minimized in light of such constraint, and in terms of the risk of identifying spurious correlations, which is likewise maximally mitigated.

Because of mediation effects (see [214]) due to the correlation between the response variable (RRB severity category) and the method of deriving the regressor (beginning with subject RBS-R CSSs in ROI-level exploratory analysis), further mitigation of Type II risk was achieved by implementing a structurally identical model using separate values for these same measures that were identified via identical computational steps, but which were statistically independent from the values in the original model. The independent regression model realization was constructed in order to test the hypothesis that the original regression equation's predictive capacity was the result of genuine RRB-functional connectivity associations, versus the alternative that its predictive capacity arose from the hyperabundance of possible permutations intrinsic to data of the present capacity and the volume of empirical search computations, that is, by chance alone due to multiple comparisons effects. The model was evaluated in light of the results of hypothesis testing of its statistical validity using methods in [215].

To control for the effects the specific regression equation form might have, additional variations using standard linear and power regression equation forms were analyzed for fit for both independent model derivations, and compared between the real empirical and randomized data realizations. Step-wise analysis [216] of all five identified significant connections was performed using sequential replacement to compare the empirically and *a priori* identified connections in terms of their predictive power, and to identify which connections independently had the most and least predictive power for subject RRB classification.

Internal model validity was then evaluated, and distinct regression equation forms compared, using leave-one-out cross-validation according to the method in [217].

Figure 2.1: Schematic of connectivity analysis. Based on the hypothesis regarding ASD RRB-associated brain connectivity, RBS-R CSSs were used to identify connections in whole-brain ROI-based analysis. Significant ROIs identified in this step were then used as seeds for seed-based metrics, as were *a priori* seeds chosen based on existing knowledge regarding RRBs in ASD. Subject-level connectivity values were exported for each significant connection identified in the seed-based analysis. Regression testing was performed (i) using only the empirically identified connections, (ii) using both the empirical and *a priori* seeds, and (iii) based on spurious reassignment of RBS-R CSSs. The empirical and spurious models, and well as the empirical and full models, were compared to assess the plausibility of the association between the identified connections and RRB severity.
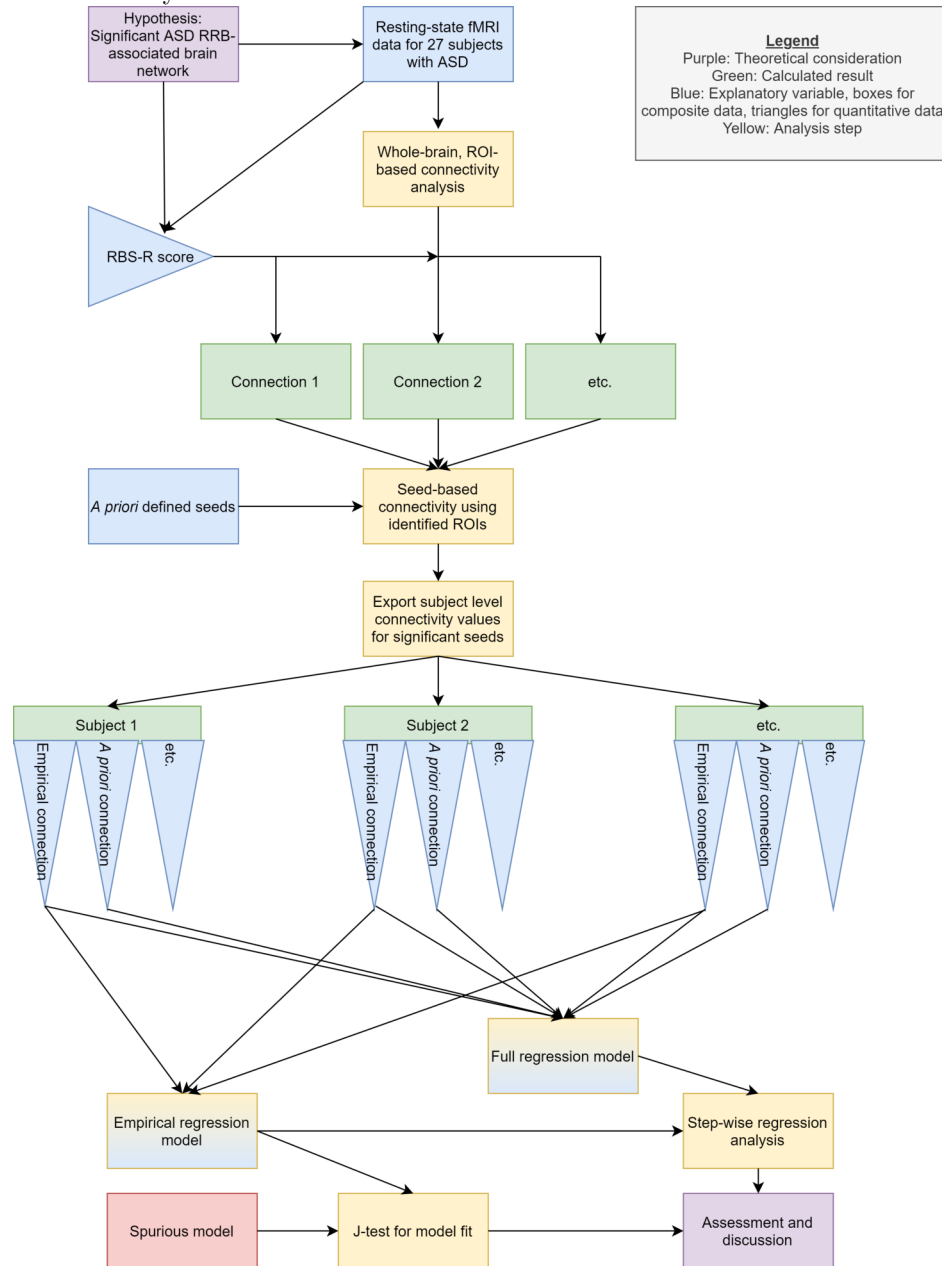
Figure 2.2: Summary of ROI-to-ROI connectivity methods. (a) Subject RBS-R CSSs as a 2nd-level covariate. (b) Selection of the subject effects. (c) Roi-to-ROI connection diagram of significant results. (d) Names and statistics for significant ROIs.
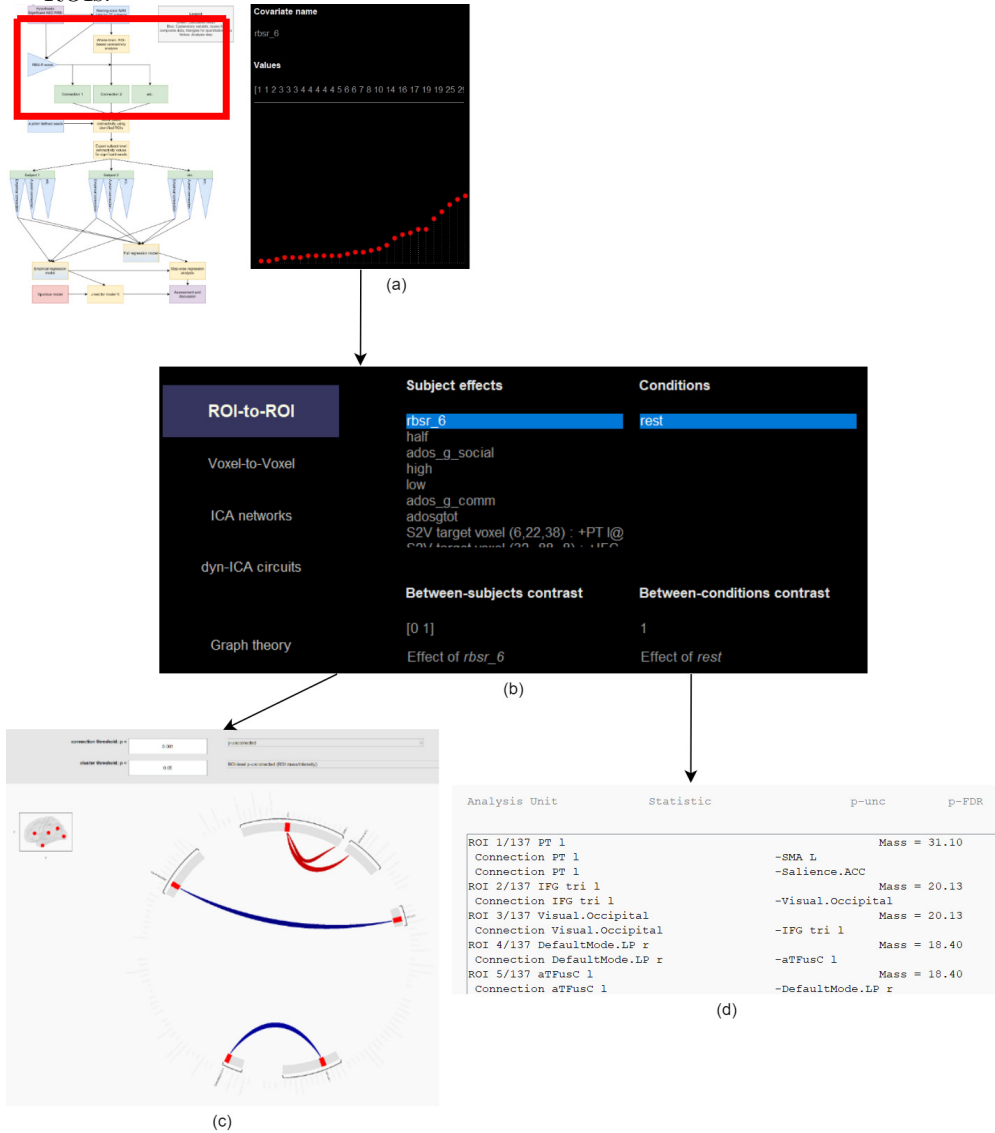
Figure 2.3: Summary of seed-to-voxel connectivity methods. (a) Subject RBS-R CSSs as a 2nd-level covariate. (b) Selection of the subject effects and seed ROI. (c) Identification of significant cluster coordinates. (d) Input of the identified coordinates in MNI space. (e) Display of subject-level connectivity values from the seed to the selected voxel in the cluster. (f) csv-export of subject-level data.
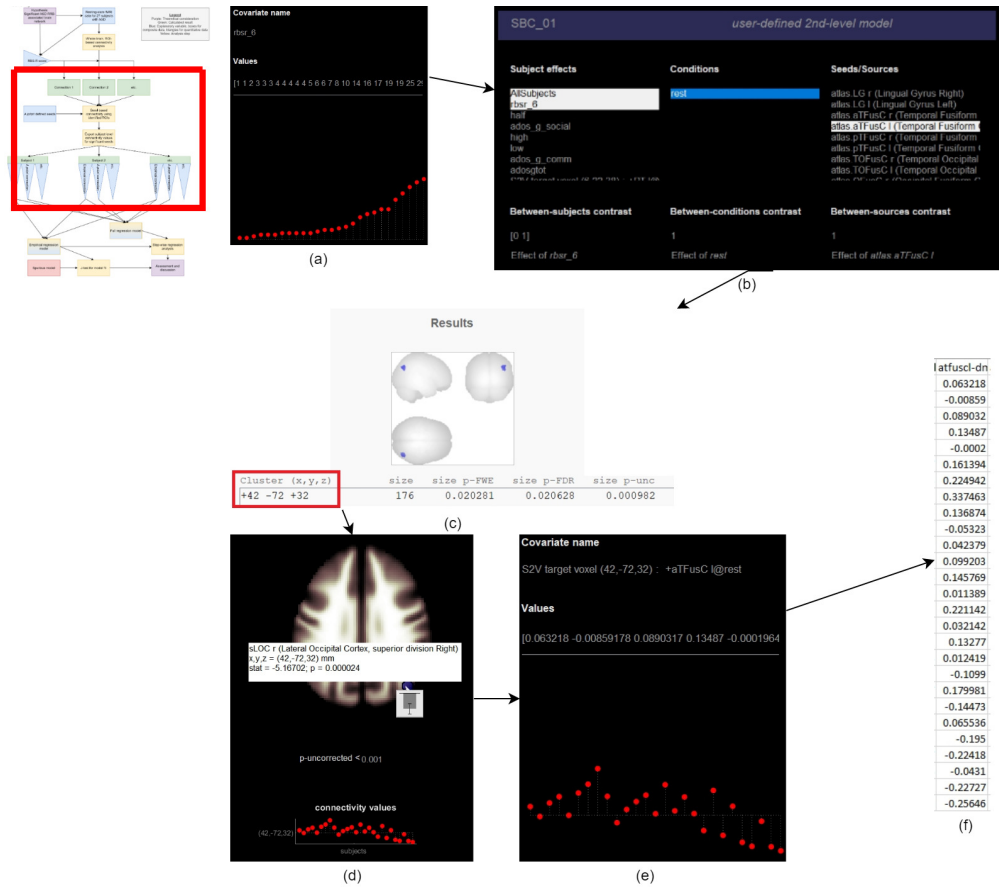
2.4 QUALITATIVE CONNECTIVITY PATTERN ASSESSMENT AND HYPO-THETICAL NETWORK DELINEATION

Using the identified ROIs from either the ROI- or seed-level connectivity analyses, seed-to-whole-brain connectivity was explored seeking connections with large effects sizes, plausible functional significance to ASD RRB manifestation in light of prior literature, and functional overlap with the putative network of until-then identified ROIs. All ROIs identified were used as seeds in turn, with the prior restriction to cerebral ROIs removed. When a seed chosen in this way exhibited connectivity with large RBS-R CSS effects sizes to other ROIs, those ROIs too were then used as seeds. This sequence was performed iteratively with those ROIs most frequently identified forming the functional "core" of the putative functional network, and peripheral ROIs being evaluated in terms of connectivity to the core regions. This process resulted in the identification of a densely functionally connected cerebellar hub, which formed the core of the putative network, and from which multiple additional ROIs were identified as significantly connected to either the core seed itself, or to ROIs which were themselves significantly connected to the core.

In constructing a simple graph-theoretic representation of the putative network, cerebellum and anterior cingulate cortex were identified and placed as functional network hubs that mediated transmission between sensory, default mode, salience, executive, motor, and reward functional network subdivisions. Subject connectivity (Pearson correlation) values between each network edge we used to calculate parameter values in the dynamical model whose description follows.

2.5 DYNAMICAL MODELING OF THE PUTATIVE BRAIN NETWORK

Based only on the identified functional connections between ROIs within putative neurocognitive network functional subdivisions of conjectured significance to the generation, maintenance, or suppression of restrictive and repetitive behaviors in ASD in the connectivity analysis and qualitative network assessment steps, a three-dimensional system of differential equations will be constructed to assess how modulations in a stimulus input function, x, to sensory areas of the brain may in turn modulate the functional activation, y, of connected executive and salience subnetwork regions in the computed network, and how these in turn modulate repetitive behavior, z, in this case abstracted as functional activation in parts of the motor subnetwork with relatively direct anatomical routes to descending motor pathways. For simplicity, the change in the intensity of the time-varying stimulus function will be modeled either as a sinusoid, allowing the manipulation of the initial intensity, periodicity, and amplitude peaks to affect the dynamical behavior of downstream network subunits,

in order to effect analytically scrutable spatiotemporal dynamics while attaining threshold physiological plausibility in that the time-varying stimulus signal is functionally realized by changes in activation in sensory regions of cortex, or, for initial model behavior characterization, as taking a null value, construing model stimulus input as a constant input or drive to the sensory functional network subdivision. Dynamic stimulus input will then be considered in terms of model behavioral regimes induced.

The model will be explored in terms of its *a priori* utility for realizing dynamic, spontaneous shifts into new patterns of time-dependent behavior based on simple manipulation of its parameters, but, necessarily, it will only be regarded as plausibly significant in the real case of RRBs in ASD if it can successfully generate such dynamical regimes based only on the actual connectivity values for connections between the identified brain regions, without the introduction or fine-tuning of extraneous parameters.

To achieve this, changes in cortical activation in response to environmental stimuli will be modeled as the product of the initial sensory subnetwork's activation and the product of the Pearson correlations of all connections between the sensory subnetwork node, the relevant executive or salience network nodes, and finally, the motor subnetwork nodes, representing behavioral output. Additionally, changes in within-motor-cortex reinforcement activation will be realized via coupling parameters, again the corresponding Pearson correlations and their products between the relevant nodes, intrinsic to the motor subnetwork and independent of contemporaneous stimulus- or executive-network-mediated cortical activity, representing motor behavior *not* in response to the environment, or, that is, intrinsic, repetitive motor behavior, a proxy for restrictive and repetitive motor behaviors. These interactions in sum will be abstracted from the several nodes per subnetwork into three discrete model parameters. The derivation of these parameters is defined in section 3.7, and described and illustrated in more detail in A.2.

Only if the dynamical model so-derived exhibits salient qualitative reorganization of time-dependent behavior (course of activation extent within the subnetwork regions) using none but the true subject connection values and group-level averages, and using exactly all of the connection values within and between each of the relevant subnetworks, can it be said that it plausibly represents dynamic relationships between brain function connectivity, and only if these patterns can be quantitatively (statistically) correlated with relevant subject behavioral measures can it be said that it plausibly represents such dynamic relationships as are relevant to RRB manifestation among those diagnosed with ASD; in the absence of these observations, irrelevance of the model will be taken as most probable. The functional—neurophysiologically plausibility of the dynamical model

will thus be assessed via multiple avenues relevant to establishing confidence in its demonstration of these two properties:

- The dynamical behavior of the simplest implementation of the model will be observed in response to arbitrary manipulation (not based on any subject data) of its parameter values to determine whether or not it can demonstrate even trivially distinct spatiotemporal patterns (e.g., figures 3.29 and 3.31).

- Empirical (subject-derived) parameter values will be substituted into the aforementioned simple model implementation to determine if its dynamical behavior varies with measures of RRBs in ways consistent with its conception, that is, if it can produce abstract output with both a statistically significant and theoretically intelligible relationship to the upstream behavior-measure and brain-connectivity input it is attempting to operationalize in time (e.g., figures 3.36, 3.37, and 3.38).

- Any statistically significant relationships found in the preceding manner will be assessed for whether or not they also appear when the dynamical model form is substituted with an analogous, but neurocognitively naïve alternate form that utilizes all of the same underlying brain connectivity data to calculate its parameters, that is, it uses the same parameters but the system of differential equations is simplified to ignore certain hypotheses about the between-subnetwork functional relationships relevant to RRB manifestation (e.g., table 3.19, figure 3.46).

- General model behavior under more dynamic stimulus input conditions will be qualitatively assessed (e.g., figure 3.52).

- Based on the preceding qualitative assessment, dynamic stimulus input will be incorporated into a extension of the base model that adds a reactive, nonlinear component to the modeled cortical activation. Statistical significance and theoretical intelligibility of the extended model's output will be assessed as above (e.g., figure 3.64, table 3.22).

- In addition to the dynamic stimulus and nonlinear reactivity components incorporated so far, a stochastic component will be added to the value of the stimulus function at each step and multiple randomized iterations will be computed of this inclusive dynamical model. Again, model statistical robustness to increased

69

complexity, and model neurocognitive and behavioral plausibility and theoretical intelligibility, will be assessed (e.g., figure 3.75, table 3.25).

- The putative relationship between the extensive dynamical model and ASD symptoms, including but not limited to those in the RRB domain, will be assessed synthetically, to generate preliminary conclusions and further hypotheses (table 3.27).

In addition to the results of the dynamic modeling analysis in section 3.7, relevant code examples and output data tables are given in A.2.

CHAPTER 3

RESULTS

3.1   ASSESSMENT OF BEHAVIORAL DATA

Mean subject age was 23.57 years at the time of scan with a minimum of 18 and a maximum of 35. The quartile cutoffs were 19.5, 24, and 25. The standard deviation was 4.85. The two highest ages were outliers in the dataset, but as age is not a target of analysis, this was tolerated. Mean subject RBS-R CSS was 11.89 with a minimum of 1 and a maximum of 38. The quartile cutoffs were 4, 6, and 19. The standard deviation was 11.38. There were no outliers in the RBS-R CSS data. Mean subject ADOS-G total score was 8.21 with a minimum of 2 and a maximum of 16. The quartile cutoffs were 6, 8, and 10. The standard deviation was 3.60. There were no outliers in the ADOS-G total data.

Subject ADOS-G, social subscale scores versus RBS-R composite scores are displayed in figure 3.1, and regression statistics are summarized in table 3.1. For both scales, a higher score indicates a greater presence of ASD traits. Ordinary least-squares regression finds a significant intercept and a small and statistically insignificant negative coefficient of the RBS-R composite score regressor.

Regression of ADOS-G communication subscale score on RBS-R composite scale score yielded a statistically significant small, negative relationship between the variables. Subject values are plotted in figure 3.2 and the model is summarized in table 3.2.

These results indicate that there does not appear to be a substantial correlation between the measures for the different core ASD deficits for a subject provided in the KUL dataset, but that there is plausibly a relationship between the severity of the communication and repetitive behavior deficits, albeit one that suggests an inverse relationship.

Figure 3.1: Subject ADOS-G social score plotted as the dependent variable versus subject RBS-R composite scale score.

ADOS-G social subscale
score vs. RBS-R composite score
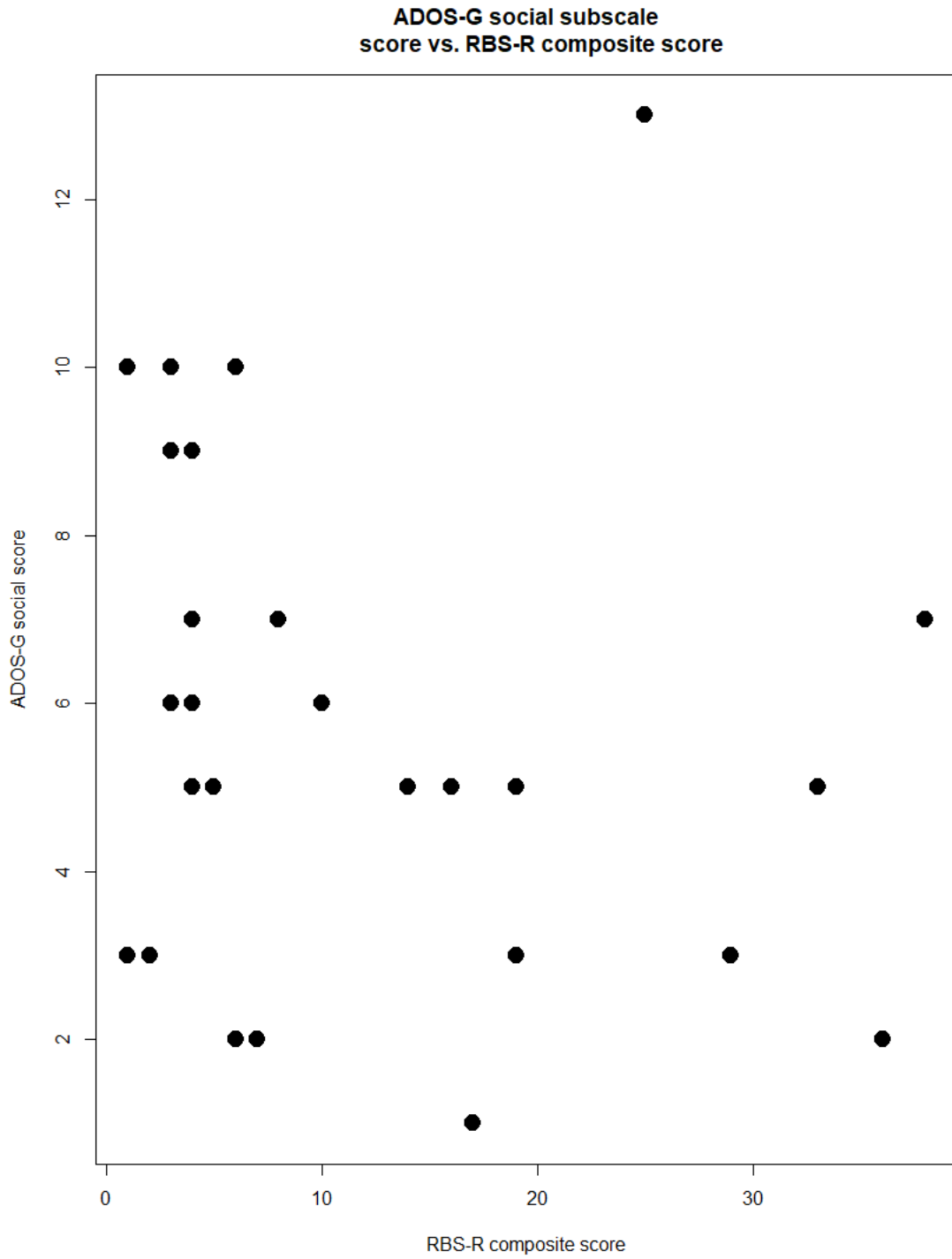
Table 3.1: OLS regression model for ADOS-G social score on RBS-R composite score. Multiple $R^2 = 0.03422$. The coefficient of RBS-R composite score is statistically insignificant and the model explains a negligible portion of the observed relationship.

	Estimate	Std. error	t-value	$\Pr(>|t|)$
Intercept	6.35609	0.84290	7.541	6.79e-08***
rbsrtot	-0.04864	0.05169	-0.941	0.356

Figure 3.2: Subject ADOS-G communication score plotted as the dependent variable versus subject RBS-R composite scale score.

ADOS-G communication subscale
score vs. RBS-R composite score
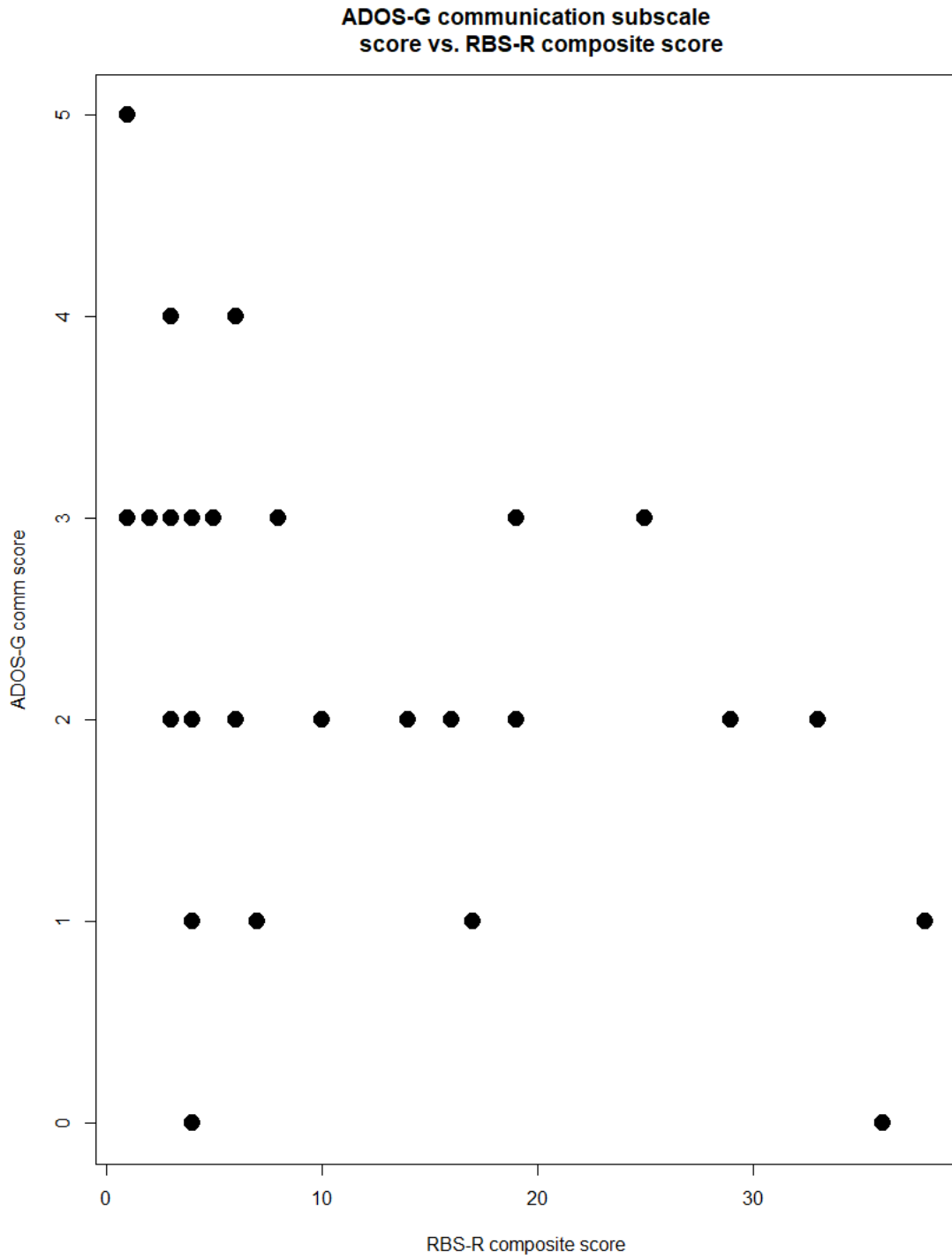
Table 3.2: OLS regression model for ADOS-G communication score on RBS-R composite score. Multiple $R^2 = 0.1855$. The coefficient of RBS-R composite score is significant and negative at $p < 0.05$.

	Estimate	Std. error	t-value	$\Pr(> |t|)$
Intercept	2.82317	0.30292	9.320	1.3e-09***
rbsrtot	-0.04432	0.01857	-2.386	0.0249*

3.2   ROI-TO-ROI CONNECTIVITY RESULTS

Subject data were analyzed to find connections that were significantly correlated with subject RBS-R composite scale score. Connectivity values are summarized in table 3.3 and figure 3.4. Significant connections are diagrammed in figure 3.3 and ROI locations and connections are represented in a glass brain in figure 3.5.

Significant positive connectivity values were found between the left planum temporale and both the left supplementary motor area ($T(25) = 4.01$, $p = 0.000482$) and the salience network, anterior cingulate cortex ($T(25) = 3.88$, $p = 0.000682$). Significant negative connectivity values were found between the left pars triangularis of the inferior frontal gyrus and the visual occipital network ($T(25) = -4.49$, $p = 0.000141$), and between the right lateral parietal default mode network and the left anterior division of temporal fusiform cortex ($T(25) = -4.29$, $p = 0.000235$). When including cerebellar ROIs in the connectivity analysis, connectivity between right posterior division of temporal fusiform cortex and vermis 10 was significantly associated with RBS-R CSS, but this result did not survive cluster-level thresholding; however, as the qualitative network generation procedure (section 3.6) is contingent on sufficient functional connection overlap between the final set of component ROIs, and as said functional connections will actually be used to generate parameter values for an analytically disconnected model system of differential equations representing the time course of brain activity rather than as entities explicitly conjectured to independently comprise functional and anatomical units of isolable pathophysiological centrality in ASD RRB manifestation, effects sizes, rather than particular explicit threshold values of specific statistics, will be the salient quantity in that procedure, and this observation was therefore recorded.

Table 3.3: Pearson correlation coefficient values for connections significantly associated with subject RBS-R composite score, connection threshold 0.001, cluster threshold 0.05, uncorrected p-values.

ROI	Connection	T(25)	p	Mass
L planum temporale			0.018781	31.10
	L supplementary motor	4.01	0.000482	
	Salience network, anterior cingulate	3.88	0.000682	
L pars triangularis			0.031518	20.13
	Visual network, occipital	-4.49	0.000141	
R DMN, lateral parietal			0.037730	18.40
	L anterior temporal fusiform	-4.29	0.000235	

Figure 3.3: Connections for ROI-to-ROI connectivity significantly associated with subject RBS-R composite score. Significant ROIs, clockwise beginning from 12 o'clock: left planum temporale; left supplementary motor area; salience anterior cingulate cortex; left pars triangularis of inferior frontal gyrus; left anterior division of temporal fusiform cortex; right default mode network, lateral parietal; visual occipital cortex.

Figure 3.4: Connectivity values for RBS-R composite score-associated functional connectivity, connection threshold 0.001, cluster threshold 0.05, uncorrected. Two transcortical (one interhemispheric and one from the frontal to occipital lobes) connections display a significant negative correlation between their strength and RBS-R CSS. The left planum temporale, in the superior temporal gyrus, displays significantly positively correlated connection strengths to frontal areas. ROI labels: aTFuscC L: left anterior division of temporal fusiform cortex; DefaultMode.LP R: right default mode network, lateral parietal; IFG tri L: left pars triangularis of inferior frontal gyrus; PT L: left planum temporale; Salience.ACC: salience anterior cingulate cortex; SMA L: left supplementary motor area; Visual.occipital: visual occipital cortex.
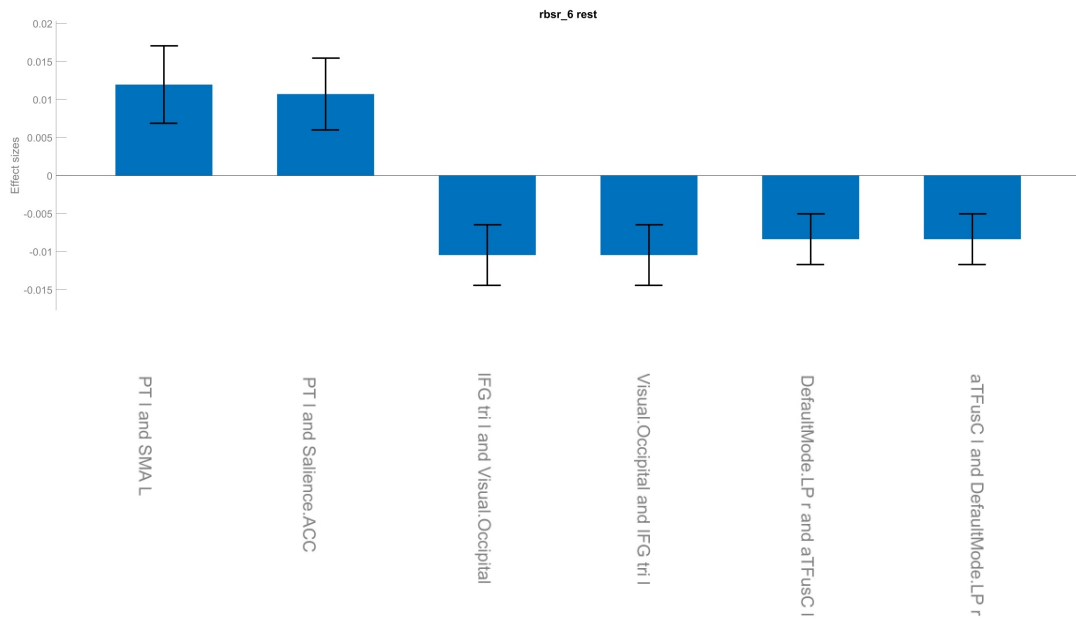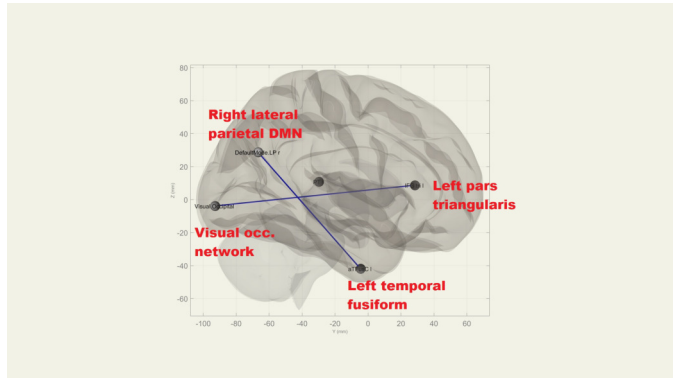
(a) Lateral (right)
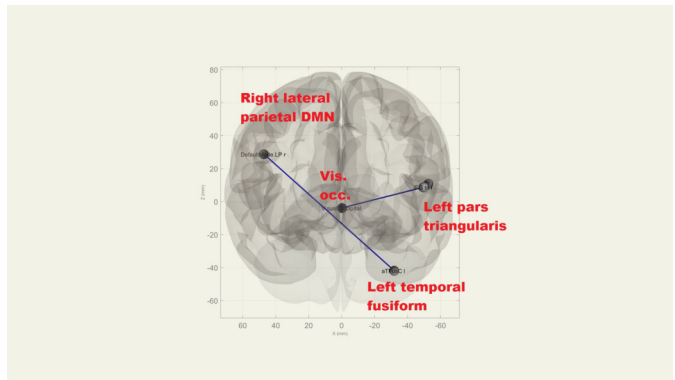
(b) Anterior
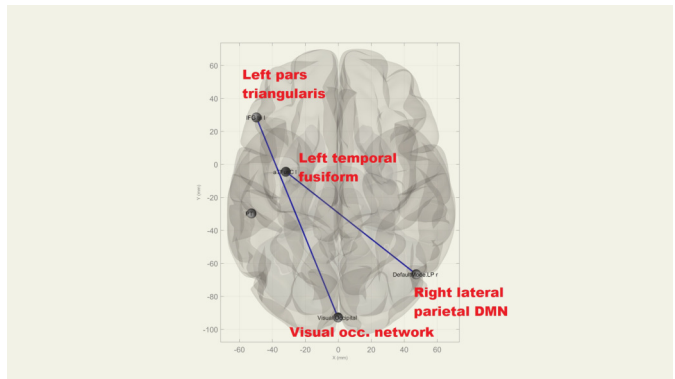
(c) Superior

Figure 3.5: Glass brain representation of significantly connected ROIs associated with RBS-R composite scale score. Note the long range of the two connections with a significant negative correlation with RBS-R CSS: the left pars triangularis—visual occipital connection spans most of the posterior-anterior axis of the cerebral hemispheres, and the right DMN—left temporal fusiform connection prominently crosses the midline, as well as a significant portion of the superior-inferior axis.

3.3 SEED-TO-VOXEL CONNECTIVITY RESULTS

Seed-to-voxel connectivity maps were constructed from the significant ROIs found in the empirical whole-brain ROI-based connectivity analysis. Additionally, seeds in each of the hippocampi and nucleus accumbens were chosen *a priori* based on the intrinsic dense connection to the default mode network and prior literature results implicating them in RRBs, respectively.

The left planum temporale seed displayed significant positively RRB-correlated connectivity to anterior cingulate cortex and left and right paracingulate gyri, consistent with the connection to the salience network, ACC portion found in the ROI-level analysis. However, no significant results were identified for the corresponding salience.ACC seed. Statistics are summarized in table 3.4. A cortical surface projection of the identified cluster is shown in figure 3.6.

The left pars triangularis seed displayed significant negatively RRB-correlated connectivity to a cluster comprising parts of right inferior lateral occipital cortex, the right occipital pole, and right occipital fusiform gyrus. This is consistent with the ROI-based search. In this case, however, significant negatively RRB-correlated connectivity was found in bidirectional tests, with the seed placed in the visual occipital network ROI likewise yielding significant results. However, subject-level analysis did find important differences in the connectivity patterns depending on which ROI was used as the seed. These differences are demonstrated in section 3.4. Statistics are summarized in table 3.4. A cortical surface projection of the identified cluster using the pars triangularis seed is shown in figure 3.7.

The left temporal fusiform seed displayed significant negatively RRB-correlated connectivity to the right superior lateral occipital cortex, an ROI largely within the right lateral parietal default mode network ROI. Statistics are summarized in table 3.4, and a cortical surface projection of the identified cluster is shown in figure 3.8. This connection is consistent with that identified in the ROI-level analysis. However, no significant connections were found from the right lateral parietal DMN seed, the paired ROI in the ROI-level analysis.

In addition to the seeds chosen based on the empirical ROI-based analysis results, two seeds were chosen *a priori* based on prior literature results of RRB-associated connectivity. The seeds chosen were in left and right nucleus accumbens. Significant RRB-correlated connections were identified in a similar manner to above. A significant positively RRB-correlated connection was identified from left nucleus accumbens to left Brodmann area 6, comprising parts of left pars opercularis, and precentral and middle frontal gyri, regions adjacent to left pars triangularis. No such connections were identified from the right nucleus accumbens seed. Statistical results are summarized in table

3.4, and a cortical surface projection of the significant cluster is shown in figure 3.9.

Because of the widespread connectivity of hippocampus to DMN structures due to the prominent memory-associated functions within DMN [218] bilateral hippocampus was chosen as a control to ascertain the extent to which connectivity strength correlations are broadly distributed across DMN-associated ROIs. Left and right hippocampal seeds were analyzed independently. No significant RRB-correlated connections were found from either hippocampal seed.

Figure 3.6: Cortical surface projection of clusters with significant RRB-correlated connections to left planum temporale using default random field theory parametric statistics settings (voxel $p < 0.001$, cluster size $p - \mathrm{FDR} < 0.05$). Consistent with ROI-level analysis, connection strength to portions of cingulate cortex are significantly positively correlated with RBS-R CSS.
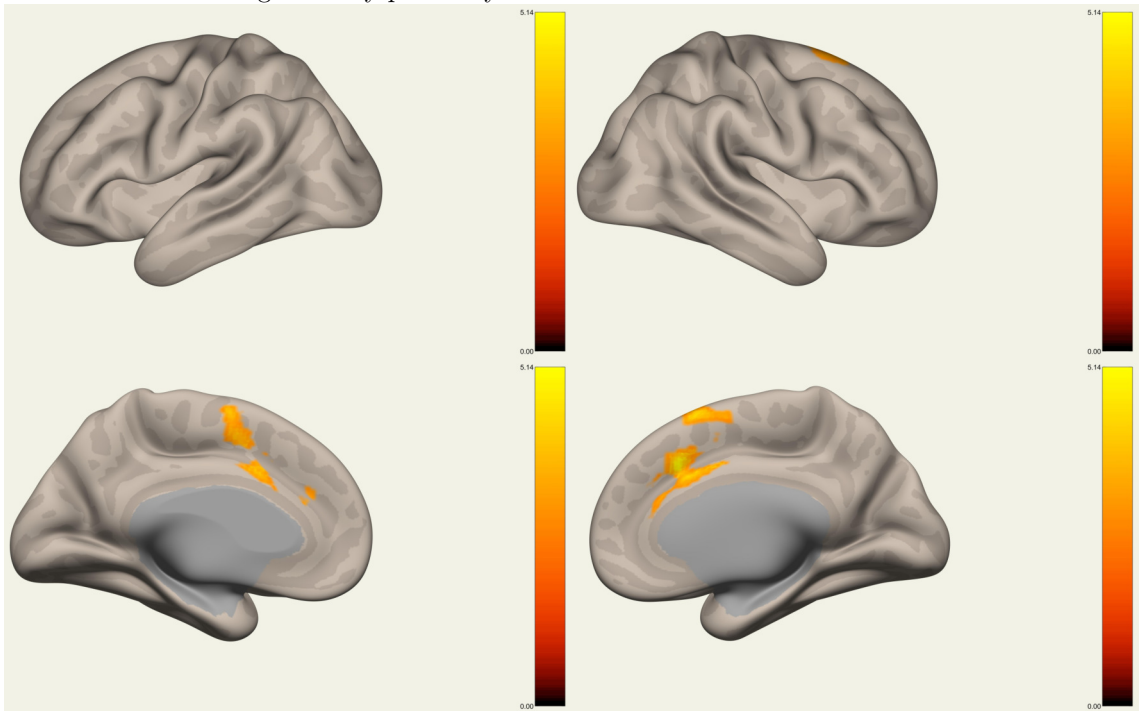
Figure 3.7: Cortical surface projection of clusters with significant RRB-correlated connection to left pars triangularis using default random field theory parametric statistics settings (voxel $p < 0.001$, cluster size $p - \mathrm{FDR} < 0.05$). Because of the lower voxel threshold used to visualize the cortical surface projection, bilateral occipital cortex connectivity appears as negatively RRB-correlated. The negative RBS-R CSS correlation in connection strength is consistent with the ROI-level analysis.
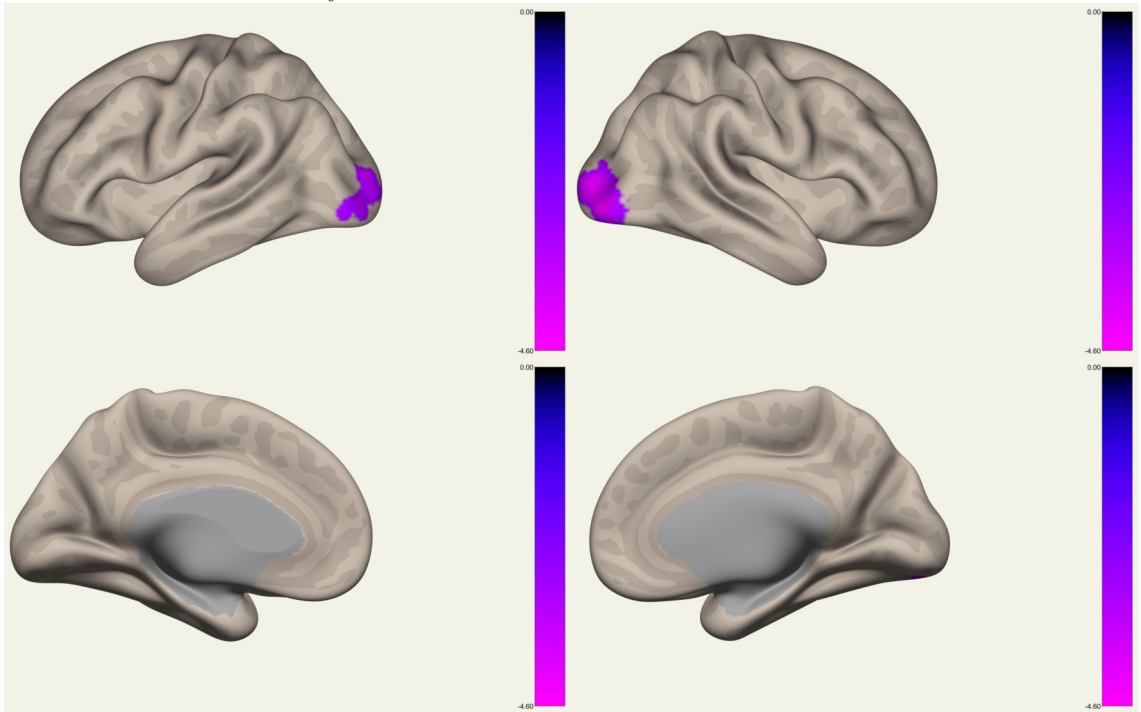
Figure 3.8: Cortical surface projection of clusters with significant RRB-correlated connection to left anterior temporal fusiform cortex using default random field theory parametric statistics settings (voxel $p < 0.001$, cluster size $p - \mathrm{FDR} < 0.05$). The right lateral parietal default mode connection demonstrates significant negative correlation with RBS-R CSS.
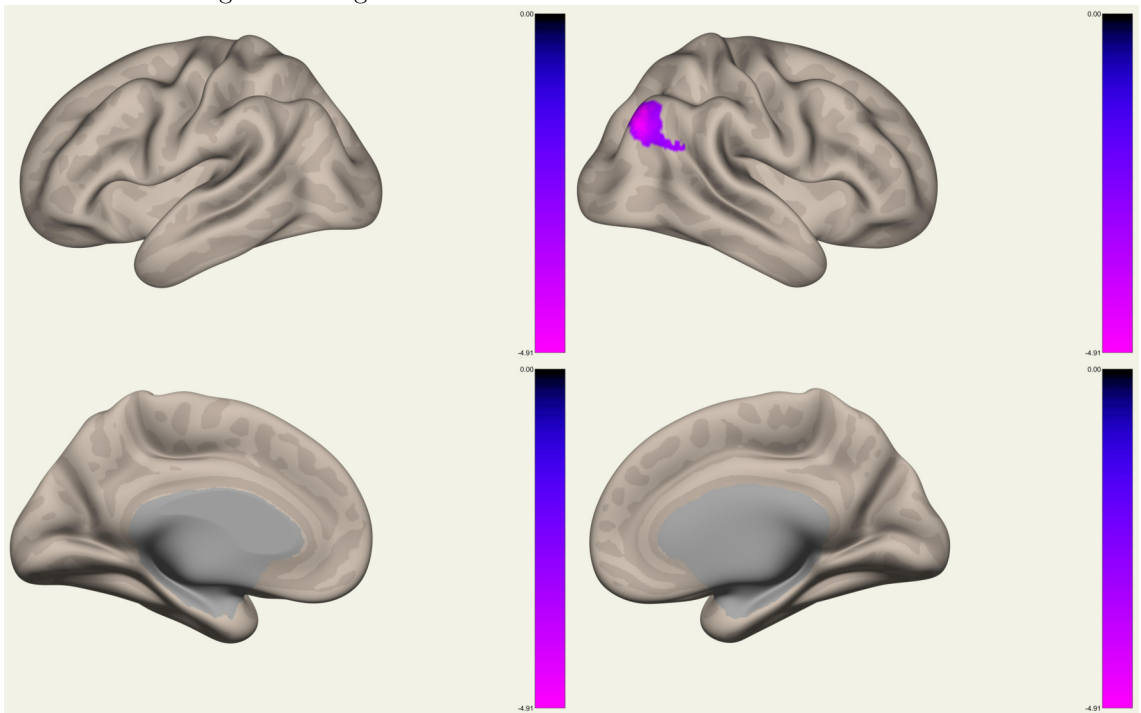
Figure 3.9: Cortical surface projection of clusters with significant RRB-correlated connection to left nucleus accumbens using default random field theory parametric statistics settings (voxel $p < 0.001$, cluster size $p - \mathrm{FDR} < 0.05$). This seed, chosen *a priori* based on results in the literature, displays statistically significant, positively RBS-R CSS-correlated connectivity to regions of ipsilateral frontal lobe, confirming the plausibility of the empirically derived seeds used to this point to identify putatively RRB-associated connections and networks.
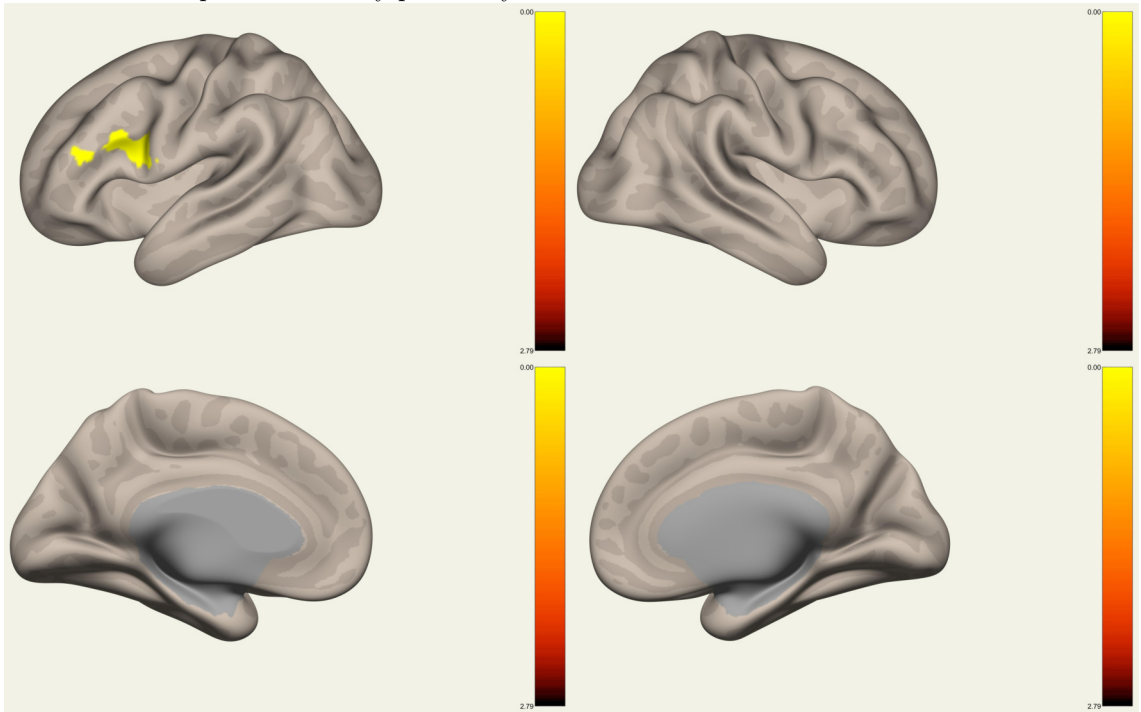
Table 3.4: Seed-to-voxel connectivity statistical summary. Clusters with significantly RBS-R CSS-correlated connectivity to the selected seeds are identified by their MNI coordinates and size in voxels, voxel $p < 0.001$ uncorrected, cluster $p < 0.05$ FWE-corrected. Seeds from which no significant connectivity correlations were identified have dashes for all entries. Note that the p-value for the *a priori* left nucleus accumbens seed is bound by the p-values for the empirically derived seeds, suggesting it is plausible to consider the potential for a real effect (see section 3.5) of RBS-R CSSs on the connection strengths.

Seed	Cluster coordinates	Size (voxels)	p-FWE
L planum temporale	(6, 22, 38)	207	0.010732
L Supplementary motor cortex	—	—	—
Salience network, anterior cingulate	—	—	—
L pars triangularis	(32, -88, 8)	323	0.000883
Visual occipital network	(-54, 34, 4)	220	0.008410
Right lateral parietal DMN	—	—	—
L anterior temporal fusiform cortex	(42, -72, 32)	176	0.020281
L nucleus accumbens	(-48, 0, 18)	256	0.001894
R nucleus accumbens	—	—	—
L hippocampus	—	—	—
R hippocampus	—	—	—

3.4   ANALYSIS OF GROUP- AND SUBJECT-LEVEL CONNECTIVITY DATA

Using a cutoff value of 22 for RBS-R composite scale score, as in [184], separates the highest 5 subject scores (the "high" RRB group) from the other 22 subjects (the "low" RRB group). Taking the significant seeds with RRB-associated connectivity identified in section 3.3 and summarized in table 3.4, cortical surface projections were created for the entire subject pool and the high-RRB category subjects (figure 3.10). Then, the entire-pool connectivity was compared on the cortical surface to the *contrast* between entire-pool and high-RRB category connectivity (figure 3.11).

Connectivity from each seed was then individually compared between low-RRB category and high-RRB category subjects to determine if the baseline putative network including the identified seeds overlapped significantly in terms of connected ROIs (figure 3.12). For these qualitative representations of connectivity and network differences between groups, uncorrected p-values were used for both voxel- and cluster-level thresholds, with the voxel threshold set between $p < 0.01$ and $p < 0.05$ to generate figures with roughly equal total significant connectivity due to the differences in sample sizes between low- and high-RRB category groups. The heatmap scale was [-10 20] for all figures.

Individual subject connectivity values from each significant seed to the voxel coordinates identified within the most significant cluster identified in table 3.4 were then extracted and are summarized in figure 3.13.
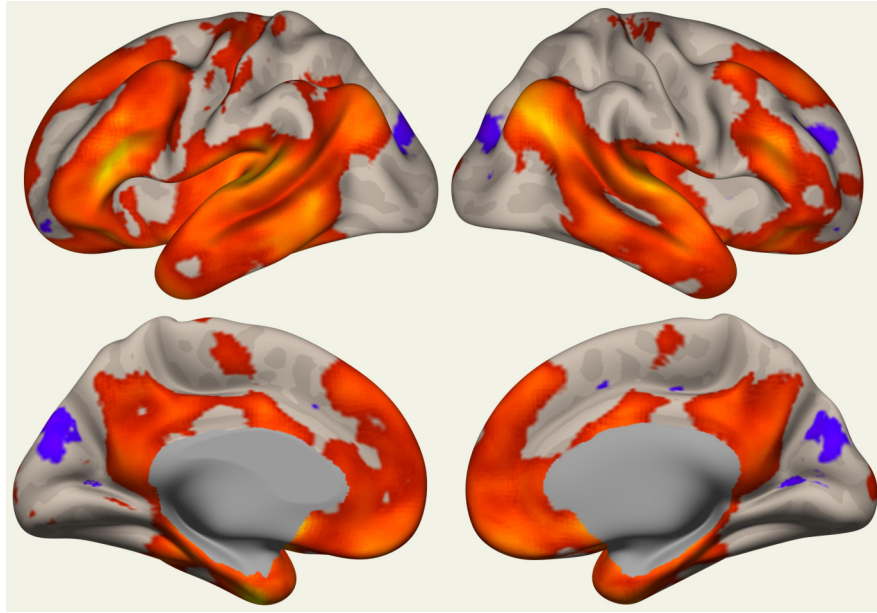
(a) All subjects
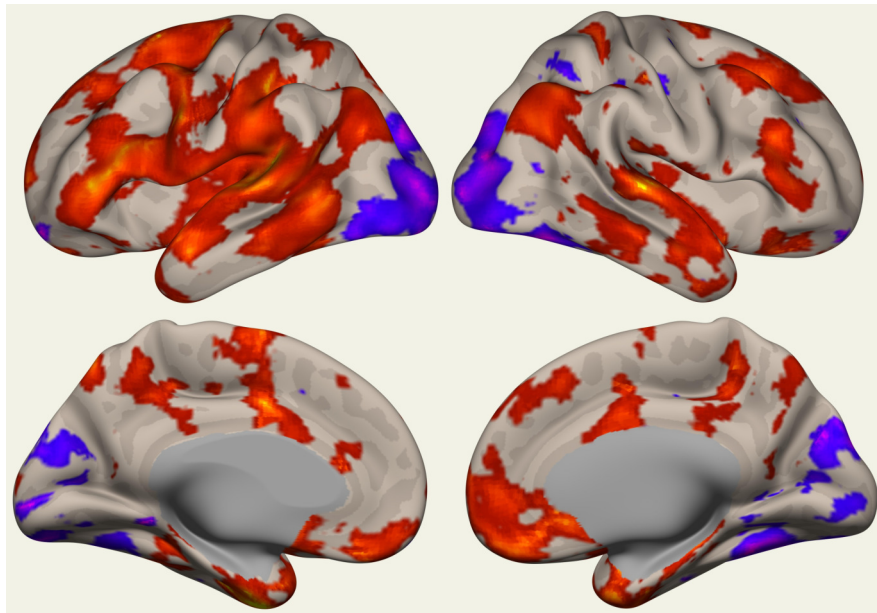
(b) High-RRB category subjects

Figure 3.10: Cortical surface projection of clusters with significant connectivity to the significant seeds/ROIs identified in table 3.4, separated into (a) the average across all subjects and (b) for high-RRB subject. There is significant negative connectivity to visual cortex in (b) compared with the lack of significant connectivity to that ROI in (a). This is consistent with the connectivity values from IFG to visual cortex. Both projections show significant positive connectivity to portions of left and right angular and supramarginal gyri, corroborating the overall significance of these ROIs as they comprise the lateral parietal DMN network ROI.
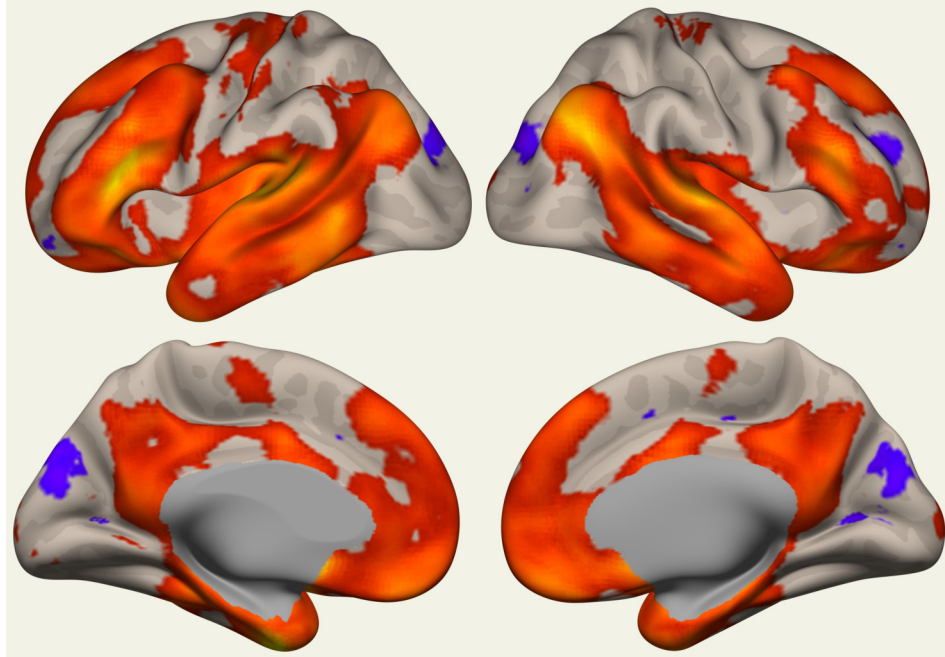
(a) All subjects
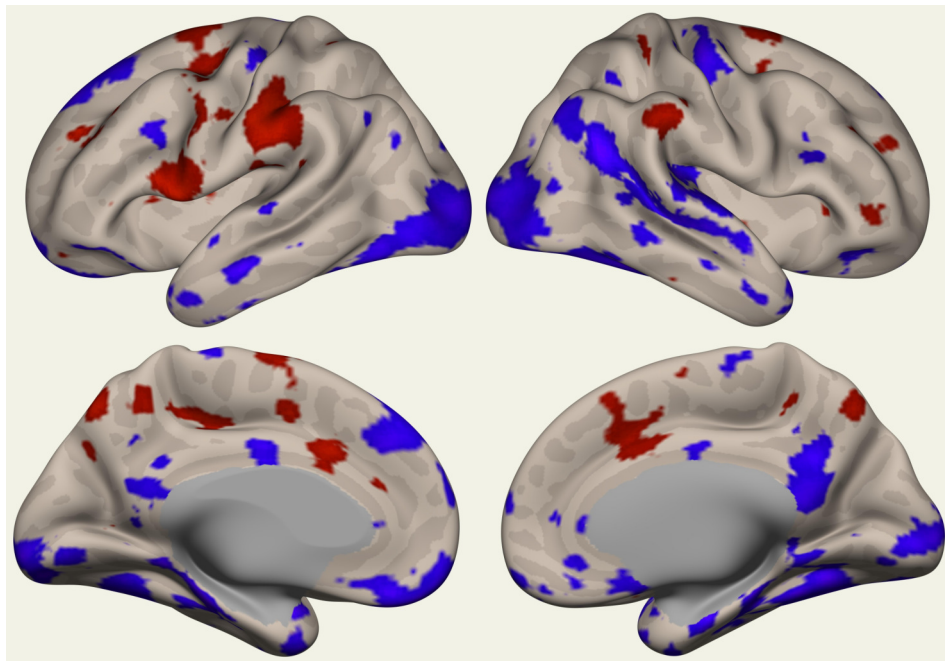
(b) Contrast between all subjects and high-RRB category subjects

Figure 3.11: Cortical surface projection of clusters with significant connectivity to the significant seeds/ROIs identified in table 3.4, separated into (a) the average across all subjects and (b) the contrast between all subjects and high-RRB subjects. (b) shows the major connections identified in table 3.4, with endpoints from the seeds located at L PT (+), cingulate cortex (+) L IFG (-), visual cortex (-), R LP DMN(-), and L SMA (+).

(a) L planum temporale

(b) L pars triangularis

(c) L anterior temporal fusiform cortex

(d) Nucleus accumbens
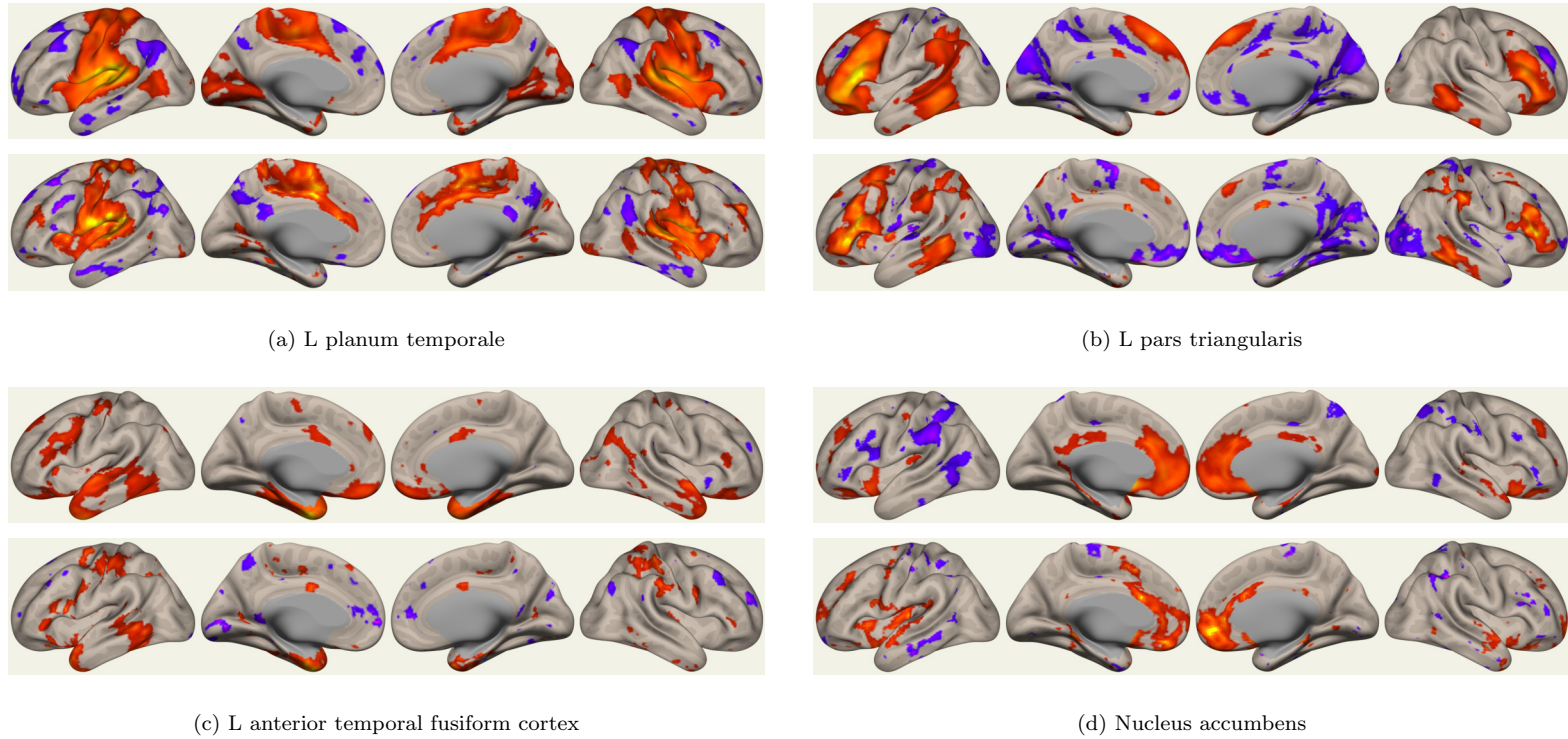
Figure 3.12: Connectivity from significant seeds identified in table 3.4, excluding visual and LP DMN given connectivity overlap with that depicted, for low- (top row in each pair) and high-RRB category subjects, thresholded qualitatively to show roughly equivalent total connectivity for each group given subsample size difference.

Figure 3.13: Plot of each individual subject's connectivity values from the significant seeds to the central voxel in each cluster identified in table 3.4. Subjects are arranged in rank-order of ascending RBS-R composite scale score. The 5 highest RBS-R CSS subjects fall into the "high-RRB" category, and always have the same connectivity value sign for a given connection as all other members in the category. This trend no longer holds upon extending the category by one subject, as the subject with the sixth highest RBS-R CSS demonstrates an opposed sign for the left anterior temporal fusiform—right lateral parietal DMN and left nucleus accumbens—frontal lobe connections.
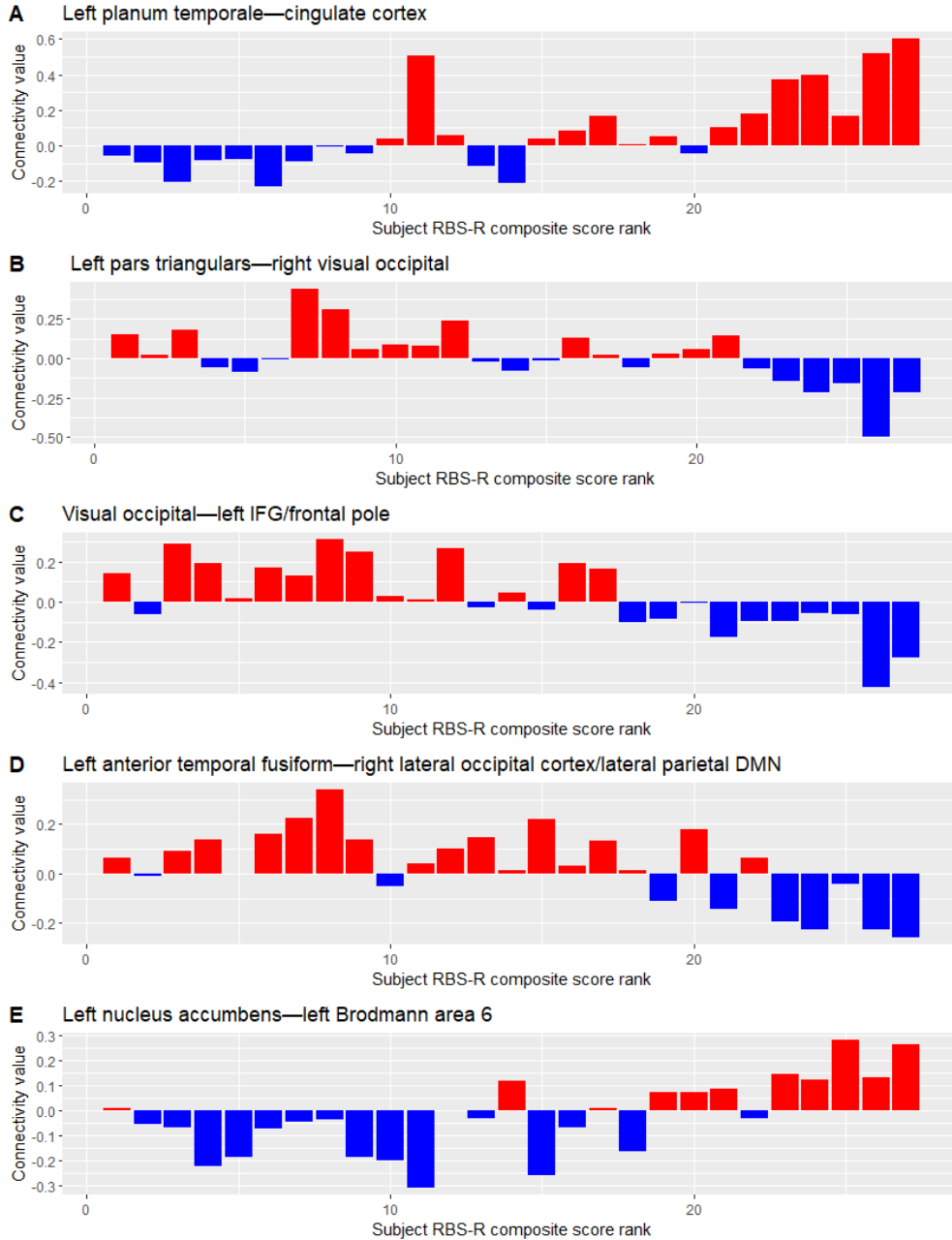
3.5   REGRESSION ANALYSIS OF FUNCTIONAL CONNECTIVITY RESULTS

The FWE-corrected p-values calculated for cluster size provided in table 3.4 adjust for the many comparisons that occur between the chosen seed location and all other voxels in the brain (cerebrum, in this case). However, as four of the five seeds with significant connectivity correlations to RBS-R CSS were identified empirically, this adjustment undercorrects for the true number of comparisons performed to arrive at the results. Considering the combined 137 anatomical and network ROIs, a total of

$$\frac{n(n-1)}{2} = \frac{137(137-1)}{2} = 9,316 \tag{3.1}$$

comparisons were performed to identify the initial 7 seeds of which four demonstrated connectivity significantly correlated with subject RBS-R CSS. While the p-FWE $= 0.001894$ value calculated for the left nucleus accumbens seed survives correction for the fact that three other *a priori* seeds were tested and found to have no significant connectivity, using the ROI-level results obtained in section 3.2 as seeds in section 3.3, while more precisely characterizing their connectivity patterns, does not increase confidence in the estimates, which are insignificant at the ROI level after correction for multiple comparisons.

As discussed in the previous section, and shown in figure 3.13, "high" RRB presence seems to correlate significantly with both the magnitude and sign of the calculated Pearson correlations for all five significant ROIs. To ascertain whether the connectivity pattern (figure 3.11) putatively associated with high-RRB trait presence represents a real effect, log-transformed linear probability models (that is, functionally, power regression probability models) of subject categorization based on the identified seeds/ROIs will be constructed, initially excluding the *a priori* seeds to specifically determine if the putative empirically derived RRB-connectivity association is of overall significance or an artifact of the large number of comparisons made to derive it.

In order to capture the postulated qualitative transition in the sign (correlation vs. anticorrelation) of the connectivity values that occurs between the low- and high-RRB conditions, a regression statistic will be computed by finding the product of the four significant empirically derived connectivity values for each subject, that is, a pure interaction effect term based on subject FC; note therefore that the model will include only one regressor and no other interaction effects, and is thus first-order, rather than including any explicit polynomial regressors. This also ensures the regressor is not biased towards any particular connection.

The initial interaction-term-only regression regresses RRB category, a binary variable, on a statistic derived from the four significant empirical connectivity values. To test hypotheses about

the actual relationship between RRB severity category and connectivity patterns, the statistical comparison used must be independent of subject RBS-R CSS, because RRB categorization is not independent from RBS-R CSS, the variable with which significant connectivity correlations were originally identified. Thus, a second regression will be constructed using the same subjects along with their corresponding rsfMRI data, and the same distribution of RBS-R CSSs, but which is independent of the actual subject RBS-R CSSs. This will be achieved by reassigning each of the actual RBS-R CSSs in the dataset to a random subject. Beyond this random reassignment, construction of the second model is exactly identical to construction of the first: (1) whole-brain ROI-level results will be used to identify ROIs that may potentially function as seeds that can more fully characterize any connectivity patterns present in the data, then (2) seed-based connectivity values will be tabulated from the seeds so identified, then (3) subject-level connectivity values will be extracted for each significant connection, then (4) subjects will be segregated into low- and high-RRB groups (based on the randomly reassigned RRB CSSs), and finally, (5) the connectivity values found in step (3) will be used to construct a statistic that will be used as a regressor in a power-regression probability model (log—log transformed variables used for ordinary least squares regression of a binary dependent variable) that attempts to classify subjects according to the parcellation performed in step (4).

This process ensures that regression tests are independent from the self-correlations inherent in the regression derivations. Additionally, because the same numerical RBS-R CSSs are used, the data structure is identical in both models, and therefore any significant test results cannot be due to the structure of the underlying data either.

ROI-level connectivity, analogous to that summarized in table 3.3 and figures 3.3 and 3.4, is shown in figure 3.14 for the spurious model. The quantity and strength of significant connections is similar to that found in the original analysis with correctly-matched subject RBS-R CSS data. Seeds for seed-to-voxel connectivity measures were chosen from among the depicted ROIs, and subject-level values were extracted for the four most significant connections and used to construct the regressor.

The regression results from both the real and randomly reassigned data are summarized in table 3.5. The regression coefficient and regression as a whole are statistically significant for the empirical ($p = 0.00196$), but not for the spurious ($p = 0.1722$) version. The multiple R^2 was 0.3236 for the empirical and 0.0732 for the spurious regression. A Davidson-MacKinnon J-test found that the addition of the fitted values from the other regression as a regressor significantly improved the spurious regression, but did not significantly improve the empirical one ($p = 0.002405$).

This regression form verifies that the *interaction* component of the empirical network predicts RRB category significantly better than if there were no real effects. However, to ascertain if the

Figure 3.14: Connections associated with randomly reassigned RBS-R CSSs. Note qualitatively, the number and strength of connection correlations does not seem substantially distinct from that for the actual data depicted in figure 3.3.
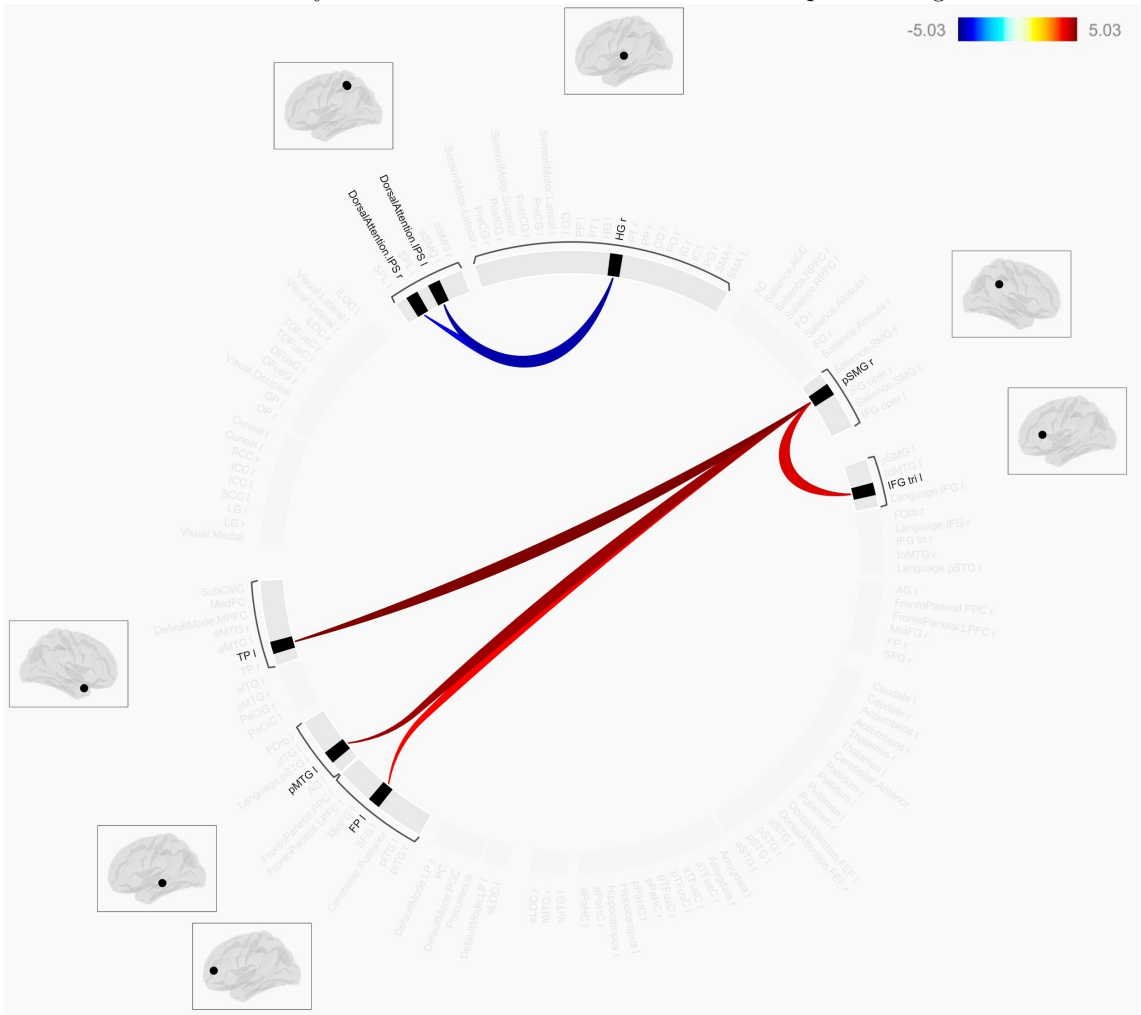
Table 3.5: Classification model of "high" (value = 1) versus "low" (value = -1) RBS-R CSS and empirically derived connectivity. (A) The proposed model based on subject classification and calculated connectivity values to central cluster voxels. (B) The model resulting from the identical method except for random reassignment of subject RBS-R CSSs. Random reassignment of scores was followed by repeating the procedure used in sections 3.2, 3.3, and 3.4 verbatim, ensuring that H_0 (no true relationship) is true in this case. (C) Davidson-MacKinnon J-test of the non-nested models, showing that actual equivalence of the models would result in the calculated improvement of the spurious model that results from the addition of the fitted results from the experimental model as regressors is expected with $p = 0.002405$.

(A) Connectivity derived from subject RBS-R CSS

	Estimate	Std. error	t-value	$Pr(> |t|)$
Intercept	-0.7553	0.1329	-5.685	6.4e-06***
I(ptl.cing * ifgl.occr * visocc.ifgl * atfuscl.dmnlpr)	-89.7425	25.9465	-3.459	0.00196**

$R^2 = 0.3236$, $p = 0.001958$

(B) Connectivity derived from randomly reassigned (spurious) RBS-R CSSs

	Estimate	Std. error	t-value	$Pr(> |t|)$
Intercept	-0.4893	0.1798	-2.721	0.0117*
I(random1 * random2 * random3 * random4)	-34.4508	24.5113	-1.406	0.1722

$R^2 = 0.07323$, $p = 0.1722$

(C) Davidson-MacKinnon J-test of the models

Model 1: hi $\sim$ I(ptl.cing * ifgl.occr * visocc.ifgl * atfuscl.dmnlpr)

Model 2: hi $\sim$ I(random1 * random2 * random3 * random4)

	Estimate	Std. error	t-value	$Pr(> |t|)$
M1 + fitted(M2)	0.82838	0.59916	1.3826	0.179529
M2 + fitted(M1)	0.96673	0.28501	3.3919	0.002405**

full power model, with its concomitantly greater degrees of freedom, erases this advantage, the process was repeated while allowing the exponent of each individual connection to vary. Results are summarized in table 3.6. As with the interaction-only regression, a Davidson-MacKinnon J-test identifies that the empirical regression's predictions would significantly improve the spurious regression if added as regressors, but the reverse is not true. Additionally, three of the individual regressors in the empirical version, but none in the spurious one, are significant.

In order to ensure that the form of the regression equation alone is not responsible for the observed differences, despite the fact that it is taken to be the most physiologically plausible simple form, a linear regression where each regressor was term with its own coefficient was constructed for the empirical and spurious cases. The empirical regression explained more of the variation ($R^2 = 0.6896$ versus 0.5546) and was more significant overall ($p = 2.214 \times 10^{-5}$ versus 0.0009723), however, a J-test between the models found the predictions of each significantly improved the other, but with greater confidence for the predictions of the empirical model ($p = 0.0001385$) versus those of the spurious model ($p = 0.0286510$). Thus, the empirically-derived regression equation in this case, despite not being taken as equally physiologically plausible to the power-regression and interaction-only forms, is still superior in the proportion of variance explained and the confidence that the model represents real effects. These observations are treated synthetically in section 3.7.5.

3.5.1 Comparison between empirical and *a priori* ROIs

Step-wise analysis of individual regressors in the full power-regression model, including the left nucleus accumbens—left BA6 connection identified *a priori*, was performed to rank the regressors from most to least independent predictive power of subject RRB classification. Results are summarized in table 3.7. Of note is the fact that the first regressor included is for the connection between L temporal fusiform cortex—R angular gyrus, but this connection does not appear in any iteration again until the last. This implies that this connection contains the most information about subject RRB classification independently, but also that the information it contains is substantially reproduced in the other connections. This is consistent with the fact that, in the unrestricted regression, the estimate for this connection is the least significant. Additionally, the L nucleus accumbens—L BA6 connection is the second to be included in the stepwise analysis, and it remains in all subsequent iterations, further pointing to the significance of this *a priori* seed.

Table 3.6: Classification regression equation utilizing the maximum available number of DoF using the log-transformed data. Note no spurious regressor is significant, and three empirical regressors are. A J-test identifies the empirical model as a significant improvement ($p = 2.221 \times 10^{-5}$).

(A) Connectivity derived from subject RBS-R CSS

	Estimate	Std. error	t-value	$\Pr(> |t|)$
Intercept	0.16979	0.05375	3.159	0.00455**
logptl	0.78670	0.33628	2.339	0.02880*
logifgl	-1.10030	0.39918	-2.756	0.01152*
logvisocc	0.69340	0.48964	1.416	0.17074
logatfuscl	-1.10032	0.52910	-2.080	0.04942*

$R^2 = 0.7223$, $p = 6.775\text{e-}06$

(B) Connectivity derived from randomly reassigned (spurious) RBS-R CSSs

	Estimate	Std. error	t-value	$\Pr(> |t|)$
Intercept	0.44649	0.09789	4.561	0.000153***
lograndom1	0.56559	0.36675	1.542	0.137295
lograndom2	0.27751	0.22394	1.239	0.228322
lograndom3	0.11948	0.29623	0.403	0.690592
lograndom4	0.22889	0.29955	0.764	0.452926

$R^2 = 0.4568$, $p = 0.007313$

(C) Davidson-MacKinnon J-test of the models

Model 1: loghi $\sim$ logptl + logifgl + logvisocc + logatfuscl

Model 2: loghi $\sim$ lograndom1 + lograndom2 + lograndom3 + lograndom4

	Estimate	Std. error	t-value	$\Pr(> |t|)$
M1 + fitted(M2)	0.31339	0.23409	1.3388	0.195
M2 + fitted(M1)	0.94560	0.17435	5.4235	2.221e-05***

Table 3.7: (A) A regression equation analogous to that in table 3.6 is first constructed. (B) Then, sequential replacement of the regressors is performed to compare their predictive ability. The iteration (number of regressors) is listed along with the combination of regressors (connections) that maximize model performance.

(A) Full power-regression

	Estimate	Std. error	t-value	$\Pr(>|t|)$
Intercept	0.18808	0.04342	4.331	0.000294***
logptl	0.89620	0.27152	3.301	0.003404**
logifgl	-1.12158	0.32036	-3.501	0.002127**
logvisocc	0.77782	0.39358	1.976	0.061406.
logatfuscl	-0.48354	0.45731	-1.057	0.302356
logaccl	1.07519	0.29629	3.629	0.001572**

$R^2 = 0.8293$, $p = 2.035\text{e-}07$

(B) Step-wise sequential replacement of the power regression regressors

5 Variables (and intercept)

Forced in: NONE

Forced out: NONE

logptl	logifgl	logvisocc	logatfuscl	logaccl
			*	
*				*
*	*			*
*	*	*		*
*	*	*	*	*

3.5.2 Cross-validation of statistical analysis results

The p-values of the individual coefficients and whole regression equations using true subject data establishes a significant correlation between these variables of interest, and the J-test between the true-data and randomized-data regression variants establishes that the extent of the observed correlations are extremely unlikely to have occurred by chance alone given the several orders of magnitude between the test p-values between the two model derivations. Though the regression analysis was performed to reinforce within-sample result validity rather than to model or predict associations between brain and RRBs more broadly, the former goal still can be more substantially achieved concomitant with the ability of the regressions to actually predict subject RRB categorization in terms of statistical correlation. However, this requires validation against data not included in the model derivations. In order to effect such an analysis, leave-one-out cross-validation was conducted for the true-data regression equations according to [217]. Analysis results are summarized in table 3.8.

Important observations are that the interaction-term-only regression equation, consistent with the significant constraints imposed by the regressor derivation, can explain only just over 20% of the variance within the left-out observations, and likewise has a very substantial RMSE of 0.97 given that the entire range of the independent variable is 2 being that it is a contrast variable taking values of either -1 or 1. Since the original intent of this regression equation form construction was to *minimize* explanatory power while still including all empirical connectivity data in at least some form, these results are not unsurprising, but do provide further impetus for actual physiological and functional analysis of the connectivity patterns associated with RRB severity in the present data.

Next, the stepwise iteration results likewise confirm that the addition of regressors in successive iterations improves fit only incrementally with each step. This is consistent with the already noted fact that the fusiform gyrus—LP DMN connection encapsulates information substantially redundant with the remaining connections in the power regression model class; between the first and last step, R^2 less than doubles, whereas it *more* than doubles between the interaction-only and first iteration stepwise models. By the Pearson correlation (and therefore R^2 measure, however, statistical significance (if only statistical) would appear incontrovertible; in addition to the significant correlations found with subject RRB-severity subgroup across regression equations for almost all of the conditions using traditional statistical tests, note also the last stepwise iteration does in fact account for a large percentage (73%) of the variance of the left-out observations with an RMSE of approximately one-fifth the interaction-only model. This remains consistent with the numerous degrees of freedom available in the underlying 5-connection model, but does reinforce the conclusion that a network

of real functional significance might underlie RRB severity, motivating the effort to characterize a potential form of such network in the next section, given the lack of such an association in the spurious regression derivation. Additional assessment in the form of leave-one-out cross validation and nonparametric statistical tests of the regression predictions clarifies the relationship between RRBs and observed connectivity in this subject sample, but only by affirming further alternative approaches before even seeking to validate results with external sample data.

Both cross-validation and unrestricted regression predictions are plotted in figures 3.15, 3.16, and 3.17, and in tables 3.9 and 3.10. A summary of both the cross-validation and final power regression values predicted are shown in tables 3.11 and 3.12. An eclectic set of tests was performed given the inherent eclecticism in the model derivation and selection process, as dramatically different precise model outputs in the essential form of power-regression probability model predictions are being tested both against other model outputs and against binary behavioral data. To assess whether the regression models were perhaps more closely correlated with one another than any were with the actual subject RBS-R severity subgroup category data, a suspicion the method confirmed, an omnibus Hoeffding's D test was performed across the subject behavioral data and regression predictions in accordance with [219]. The three tests performed pairwise with cross-validation testing output and full regression predictions comprised the Pearson test, tau star test [220], and Kallenberg test [221]. Note that the latter two test forms assess observation rank and assume non-atomic variables, that is, variables like the subject RRB-severity category subgroups which are represented with binary contrast in this data, though algorithms for each do account for rank ties. Because of extensive self-correlations in the regression derivation procedure despite independent validation against structurally and procedurally identical models of known insignificance, testing within the data set itself faces substantial limits. Test results on either side of the standard α threshold $p < 0.05$ across both nonparametric tests, and categorical insignificance in the Hoeffding's D test results, combined with the ubiquity of subthreshold results from the Pearson correlation test, along with the nature of the dependent variable (a categorical contrast), all indicate the utility and necessity of other means of result validation. Thence, a putative fully interconnected functional network will be constructed based on subject connectivity data, and then used to model time-dependent interactions between the component ROIs and subnetworks within the putative RRB-associated brain network.

Table 3.8: Root-mean-squared error, R^2, and mean absolute error for (A) the interaction-term-only regression (table 3.5), (B) the step-wise regressions (table 3.7). The lack of improvement in CV predictions in the step 5 model is consistent with the high independent predictive ability, but also substantial overlap with information in other connections, of the DMN—fusiform connection.

(A) Interaction-term-only model

	RMSE	R^2	MAE
Interaction model	0.973959	0.2092279	0.5839706

(B) Step-wise regression models

	RMSE	R^2 LOOCV (full model)	MAE
Step I	0.313359	0.4635955 (0.5485105)	0.2459801
Step II	0.2653374	0.6153522 (0.6978974)	0.2238443
Step III	0.2247882	0.7272578 (0.7959384)	0.1876212
Step IV	0.2198303	0.7391625 (0.8202430)	0.1772213
Step V	0.2260756	0.7258793 (0.8293294)	0.1785765

ID	RRB	Cmp	SI	SII	SIII	SIV	SV
1	-1	-0.7379	0.1196	0.135	0.0413	0.0575	0.0709
2	-1	-0.745	0.2726	-0.0066	0.0373	-0.0548	-0.0281
3	-1	-0.6549	0.0673	-0.214	-0.2461	-0.1986	-0.1538
4	-1	-0.7571	-0.0238	-0.2931	-0.1303	-0.036	-0.0266
5	-1	-0.7451	0.254	-0.2092	-0.0323	-0.038	0.0084
6	-1	-0.7514	-0.0761	-0.269	-0.1204	-0.0704	-0.0765
7	-1	-0.6358	-0.202	0.011	-0.2935	-0.4231	-0.4824
8	-1	-0.7169	-0.4378	0.1303	-0.0908	-0.0219	-0.1254
9	-1	-0.7358	-0.0277	-0.1631	-0.1361	-0.0515	-0.0394
10	-1	-0.7446	0.3766	-0.0714	-0.0982	-0.1427	-0.0755
11	-1	-0.7469	0.1627	0.3636	0.1393	0.1376	0.1272
12	-1	-0.7802	0.0469	0.2696	0.0713	0.1612	0.1648
13	-1	-0.7442	-0.0453	-0.0084	0.0768	0.0256	-0.0239
14	-1	-0.7458	0.2286	0.0569	0.2468	0.267	0.292
15	-1	-0.7455	-0.1944	-0.1963	-0.1109	-0.1859	-0.2946
16	-1	-0.7515	0.1842	0.2034	0.0904	0.1654	0.1964
17	-1	-0.7534	-0.0196	0.4063	0.3319	0.489	0.4606
18	-1	-0.7451	0.2264	-0.0508	0.0563	-0.0333	-0.0265
19	-1	-0.7461	0.5246	0.3568	0.3065	0.2454	0.3065
20	-1	-0.7452	-0.1127	0.2384	0.1987	0.1612	0.096
21	-1	-0.7792	0.6285	0.4366	0.2804	0.1296	0.2206
22	-1	-0.7519	0.1149	0.3649	0.3741	0.3457	0.3102
23	1	-0.7282	0.6422	0.7001	0.6838	0.7242	0.7572
24	1	-0.7179	0.718	0.6982	0.7599	0.852	0.9089
25	1	-0.8209	0.3021	0.628	0.6678	0.7212	0.6651
26	1	4.7043	0.7264	0.8154	1.4004	1.3175	1.244
27	1	-0.0561	0.8104	1.0631	1.0295	0.9733	0.9944

Table 3.9: Calculated predictions of subject RRB severity category, that is, estimates of the probability a subject would belong to a given class RRB-severity category group on the stepwise and composite (interaction term) regressions developed when observations are excluded one at a time. Final power regression prediction values are given in table 3.10.

LOOCV prediction results, all power regression model
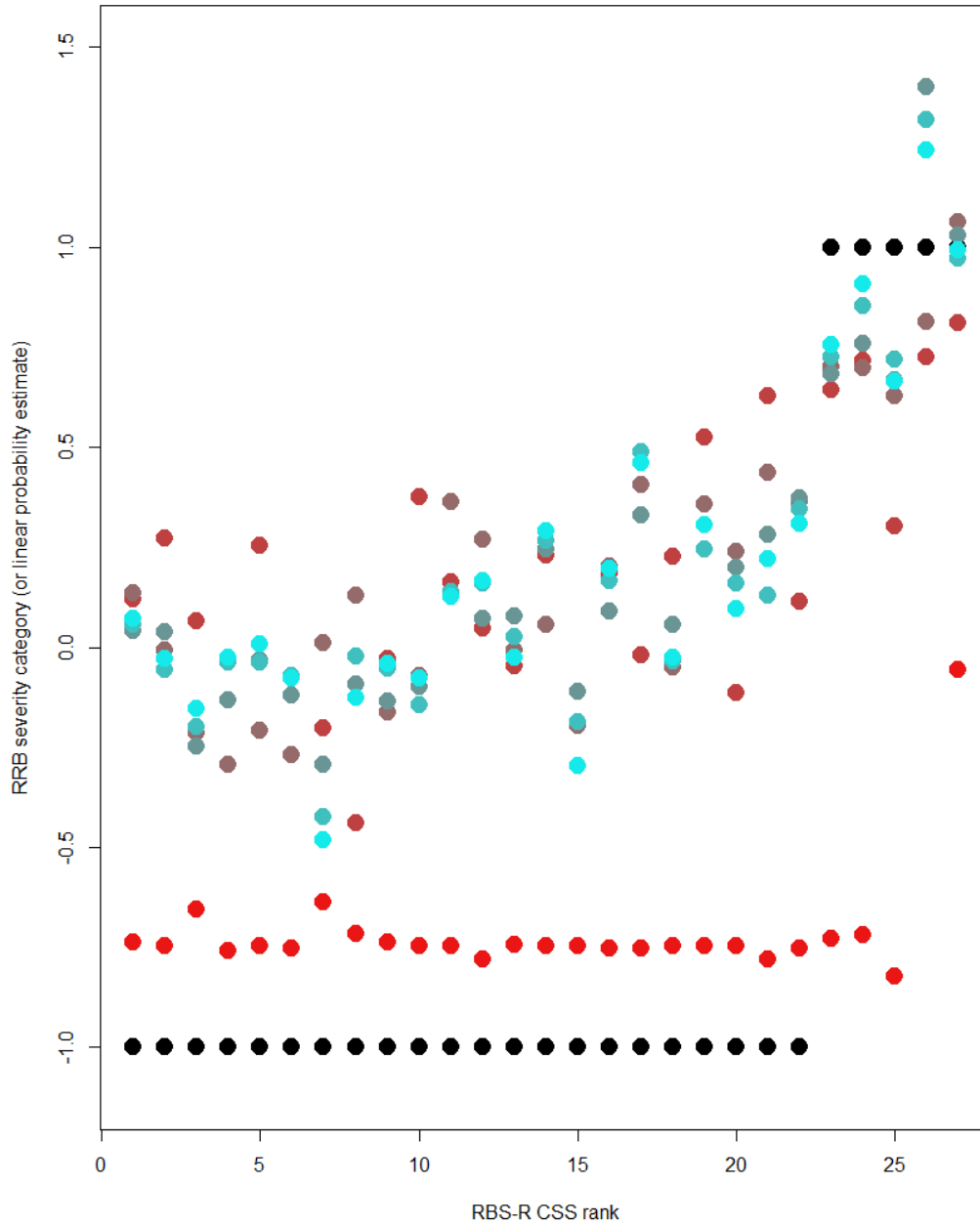
Figure 3.15: Graph of the leave-one-out cross-validation predicted values of the composite, and all five stepwise regression iterations, color mapped from red to cyan, of subject RBS-R severity category.
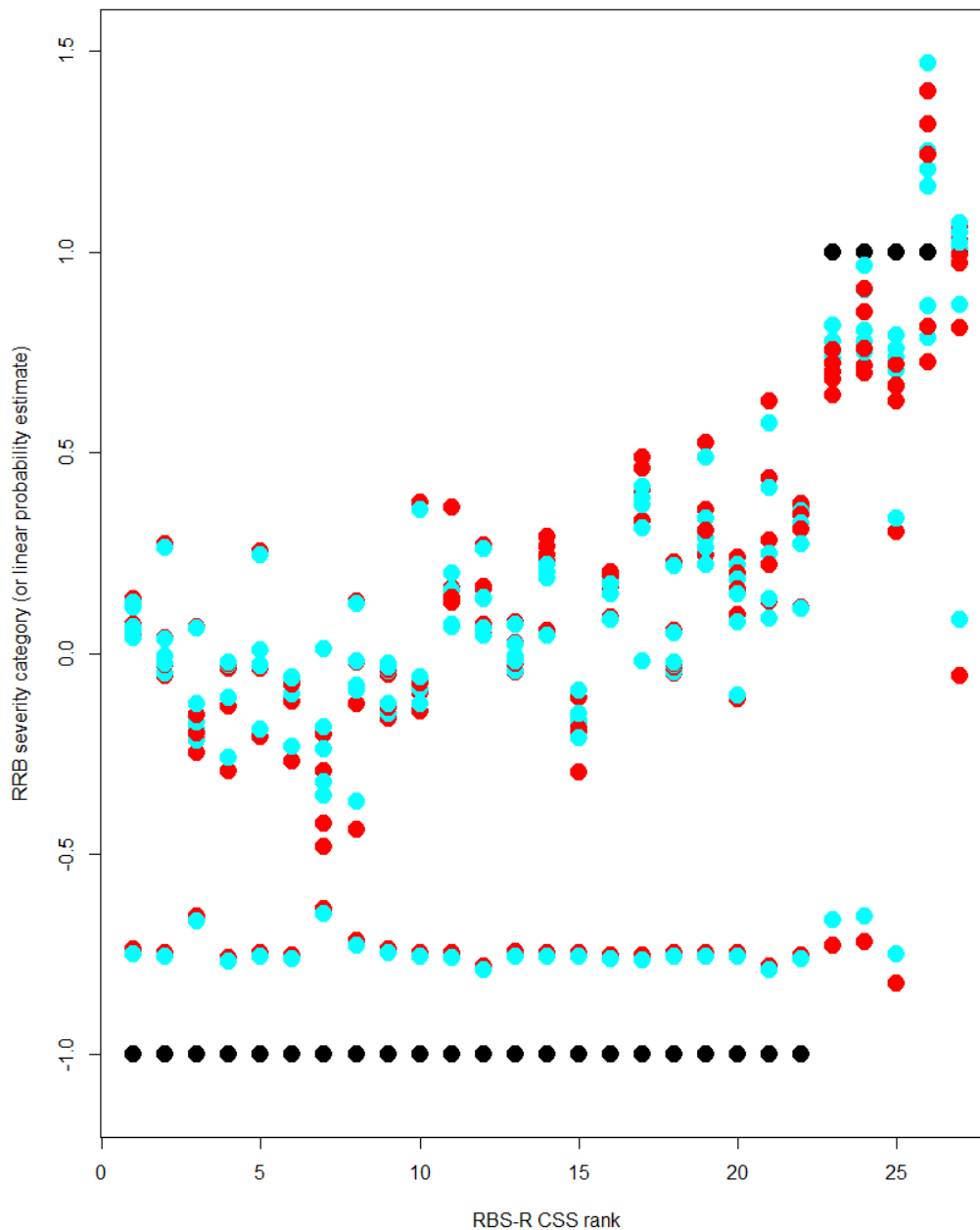
Figure 3.16: Graph of the leave-one-out cross-validation predicted values of the composite, and all five stepwise regression iterations, red, and final power regression model predicted values of the composite, and all five stepwise regression step models, cyan, of subject RBS-R severity category. Contrast this with figure 3.15; all of the predicted values plotted in figure 3.15, that is, those generated in the LOOCV calculation, are red in this graph. Final power regression, or essentially, log-transformed variable linear probability estimate, predictions are cyan, for ease of comparison of the difference in predictive ability between the full-power power regression and that in estimating an excluded element.
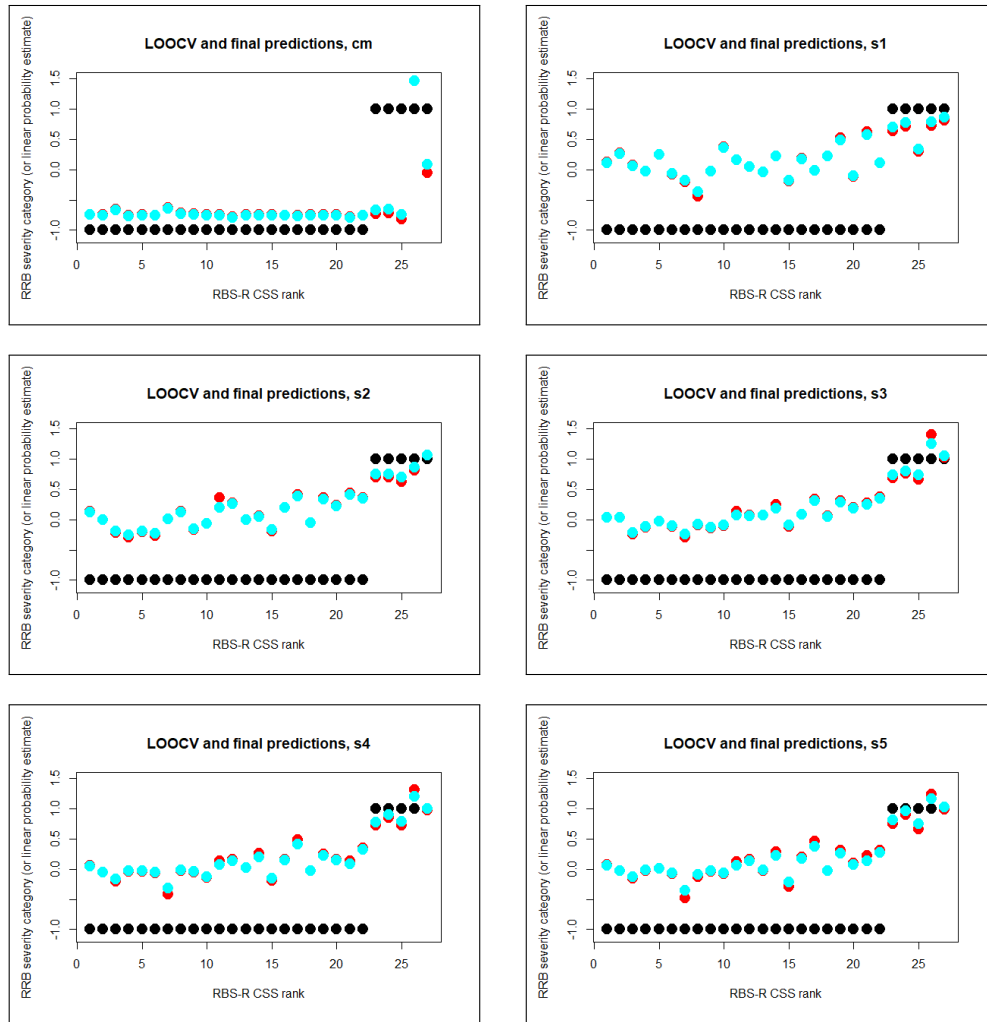
Figure 3.17: Direct within-model comparison of LOOCV predictions (red) and those based on the full data set (cyan), for the composite (or interaction) and all five stepwise regression iterations.

ID	RRB	Cmp	SI	SII	SIII	SIV	SV
1	-1	-0.7483	0.1149	0.1273	0.0383	0.0531	0.0653
2	-1	-0.7552	0.2622	-0.0062	0.0350	-0.0482	-0.0243
3	-1	-0.6677	0.0643	-0.1891	-0.2170	-0.1718	-0.1257
4	-1	-0.7670	-0.0224	-0.2594	-0.1093	-0.0282	-0.0208
5	-1	-0.7553	0.2444	-0.1906	-0.0276	-0.0325	0.0069
6	-1	-0.7614	-0.0711	-0.2334	-0.1000	-0.0574	-0.0623
7	-1	-0.6493	-0.1833	0.0103	-0.2386	-0.3203	-0.3533
8	-1	-0.7279	-0.3685	0.1250	-0.0793	-0.0184	-0.0908
9	-1	-0.7462	-0.0262	-0.1493	-0.1243	-0.0443	-0.0338
10	-1	-0.7548	0.3592	-0.0646	-0.0887	-0.1272	-0.0595
11	-1	-0.7570	0.1566	0.2002	0.0720	0.0710	0.0656
12	-1	-0.7894	0.0447	0.2590	0.0628	0.1350	0.1379
13	-1	-0.7545	-0.0426	-0.0078	0.0705	0.0231	-0.0205
14	-1	-0.7560	0.2201	0.0459	0.1885	0.2034	0.2206
15	-1	-0.7557	-0.1768	-0.1657	-0.0923	-0.1497	-0.2118
16	-1	-0.7615	0.1773	0.1952	0.0844	0.1488	0.1738
17	-1	-0.7633	-0.0185	0.3869	0.3122	0.4159	0.3699
18	-1	-0.7553	0.2180	-0.0472	0.0512	-0.0285	-0.0227
19	-1	-0.7563	0.4893	0.3369	0.2879	0.2214	0.2640
20	-1	-0.7554	-0.1046	0.2208	0.1834	0.1470	0.0770
21	-1	-0.7884	0.5734	0.4112	0.2488	0.0864	0.1352
22	-1	-0.7619	0.1103	0.3467	0.3554	0.3259	0.2732
23	1	-0.6638	0.7010	0.7497	0.7356	0.7761	0.8177
24	1	-0.6541	0.7788	0.7492	0.8052	0.9060	0.9654
25	1	-0.7486	0.3368	0.7038	0.7383	0.7920	0.7579
26	1	1.4702	0.7872	0.8656	1.2529	1.2066	1.1646
27	1	0.0853	0.8683	1.0723	1.0475	1.0075	1.0234

Table 3.10: Calculated predictions of subject RRB severity category, that is, estimates of the probability a subject would belong to a given RRB-severity category group based on the stepwise and composite (interaction term) regression forms developed when all observations are included.

	RRB	Cmp	SIc	SIIc	SIIIc	SIVc	SVc	Cmp	SI	SII	SIII	SIV	SV
RRB	N/A	1	0.264	0.164	0.164	0.164	0.164	1	0.264	0.164	0.164	0.164	0.164
Cmpc	1	N/A	0.247	0.158	0.268	0.311	0.033	0	0.247	0.158	0.268	0.311	0.033
S1c	0.264	0.247	N/A	0.003	0.001	0.003	0	0.247	0	0.003	0.001	0.003	0
S2c	0.164	0.158	0.003	N/A	0	0	0	0.158	0.003	0	0	0	0
S3c	0.164	0.268	0.001	0	N/A	0	0	0.268	0.001	0	0	0	0
S4c	0.164	0.311	0.003	0	0	N/A	0	0.311	0.003	0	0	0	0
S5c	0.164	0.033	0	0	0	0	N/A	0.033	0	0	0	0	0
Cmp	1	0	0.247	0.158	0.268	0.311	0.033	N/A	0.247	0.158	0.268	0.311	0.033
S1	0.264	0.247	0	0.003	0.001	0.003	0	0.247	N/A	0.003	0.001	0.003	0
S2	0.164	0.158	0.003	0	0	0	0	0.158	0.003	N/A	0	0	0
S3	0.164	0.268	0.001	0	0	0	0	0.268	0.001	0	N/A	0	0
S4	0.164	0.311	0.003	0	0	0	0	0.311	0.003	0	0	N/A	0
S5	0.164	0.033	0	0	0	0	0	0.033	0	0	0	0	N/A

Table 3.11: Matrix of $p-$values from Hoeffding's D statistic. The purpose of employing a test based on this statistic here is to determine if the low-high transition in RRB subject category is associated with a corresponding clear shift in the predicted values between closer to -1 and closer to 1 as well. Additionally, if the modeled values were poor at capturing the transition itself due to excessive linearity, this would be compounded by the fact the various predictions would still likely correlate with one another, exactly as seen here, due to the very same relatively uniform fluctuations. These data suggest that the modeled RRB severity category does not track the actual data closely, although as table 3.12 shows below, the "classical" correlation is still strong.

Cmp	SI	SII	SIII	SIV	SV
Tau-star (CV)	0.055167	0.000577	0.000197	0.000197	0.000181
Tau-star (FM)	0.001659	0.000577	0.000197	0.000197	0.000197
Kallenberg (CV)	0.078892	0.001800	0.000700	0.001000	0.000900
Kallenberg (FM)	0.007499	0.002500	0.001300	0.000800	0.000500
Pearson (CV)	0.016444	0.0000925	0.00000128	1.61E-08	9.18E-09
Pearson (FM)	0.001958	0.00000998	5.91E-08	4.12E-10	8.34E-11

Table 3.12: Multiple statistical tests with the potential to provide further novel information about the cross-validation process, and more importantly, the ultimate relationship of the observed correlation between the behavioral measure RBS-R CSS and the brain connectivity patterns identified in the subject population. As expected, despite the dual transformations of the data being correlated, Pearson correlation (last two rows) suggests significance of both every cross-validation derived prediction of RRB severity category and every final regression prediction. In general, these statistics show much greater significance of the regression predictions overall, but notably, both the Tau-star and Kallenberg test identify an insignificant relationship between the cross-validation derived, but not final regression model, predictions of subject RRB-severity category subgroup with the composite (or interaction-effect only) model form. While none of the individual regressions, and least of all the composite regression, were formulated to actually capture extra-sample associations in the population between RRB severity and brain connectivity (the dynamical model developed later does this), the specific insignificance of only the values derived during the cross-validation step demonstrates that at least that model form does demonstrate a high liability for a lack of generalizability. Of course, this is not the case with the regression forms that were much freer to vary, albeit even in those cases, the correlations were stronger between the predictions of the various regressions with one another (table 3.11) than between any set of predictions and the actual subject data.

3.5.3 Summary of regression analysis

Importantly, both the empirical and spurious regression equations were equally prone to overfitting their underlying data, in that the true RBS-R CSSs were used indirectly to predict the true RRB-severity category in the empirical realization, and the randomly reassigned RBS-R CSSs were used indirectly to predict the RRB-severity category associated with the randomly assigned score. Therefore, if there were no significant relationship between RRB severity and the empirically determined brain connectivity pattern, each analogous regression pair would be equally good at fitting its own data. The fact that each empirical (true-value) regression was both significant when considered in isolation, and a significantly better predictor of its own underlying data than the spurious model, allows the rejection of the statistical hypothesis that there is no relationship between RRB-severity category and brain connectivity.

While regression on individual connections actually tends to increase regression significance and fit, this is the expected result given the ROI search and connection identification process; the interaction-term-only regression was chosen for its ability to discern the presence of the postulated strong relationship between high RRB severity categorization and predictability of the overall connectivity pattern, should discrete patterns be discernible, while minimizing the total number of degrees of freedom.

Further pointing to the real significance of the identified suite of connections, none of the individual regressor estimates was significant in table 3.6 for the randomized data regression, while three of the empirical regression coefficients were significant for the empirical model. Additionally, the empirical regression was once again a statistically significant improvement over the randomized data regression.

Step-wise testing of the four empirical and one *a priori* seed verified that the *a priori* seed seemed to be of comparable or better ability in predicting subject RRB classification independently, being the second term to be included in the regression iteration. The single best predictor, however, was the L fusiform—R default mode/angular gyrus connection.

Leave-one-out cross-validation suggested several properties of the ensemble of connectivity patterns and, therefore, the putative network which in part comprises them:

- The interaction-term-only regression yields large prediction errors and a relatively low proportion of variance in the excluded observations and therefore the connections seem likely to constitute parts of functionally distinct subnetworks rather than a monolithic brain network with a single pattern of functional connectivity changes associated with RRB severity.

- Stepwise iteration revealed the step I regression equation substantially improved upon the predictive power of the interaction-term-only model suggesting that individual connectivity values do, conversely, vary relatively predictably with subject RRB-severity category.

- Likewise, the final (5-connection) iteration explained a substantial portion of the variance in the excluded observations with an RMSE not significantly larger than a tenth of the overall parameter space of the independent variable, which suggests the identified empirical and *a priori* connections do potentially substantially underlie a putative functional network whose behavior is altered in the presence of severe RRBs.

A putative whole-brain functional network will thence be specified via search of the largest effect sizes of putatively within-network connections starting with the so-far identified ROIs in terms of connection topology consistent with these observed features:

- Altered primary sensory, specifically visual, functional connectivity

- Altered DMN—sensory association functional connectivity

- Altered anterior cingulate salience network—sensory and association functional connectivity

- Involvement of both primary and supplementary motor cortex in the generation of motor RRBs

- Significant influence of striatal reward reinforcement on putative motor cortex activation

- Alterations to frontal executive influence on frontal motor areas

3.6 SYNTHESIS OF FUNCTIONAL CONNECTIVITY DATA INTO HYPOTHET-ICAL NETWORK

The connections, and the network they putatively form, identified and assessed via regression testing in the previous section, establish confidence in the behavior-neurocognition relationship in the present subject data between RRBs and brain connectivity. While the relationship appears to be one of clear statistical significance, the actual form of the dynamic relationship that mediates the functional, neurocognitive, behavioral, and symptomatological aspects of ASD RRBs remains unestablished in light of this result alone.

To competently generate hypotheses of potential behavioral significance to the experience of RRBs in ASD, both by those with the disorder and those with whom they interact, as well as to potential future clinical developments when considered in full view of all the available evidence on ASD RRBs, such a dynamic relationship must at least be postulated and demonstrated to be

successful at dynamically mediating, at the very least, the relationship between abstracted measures in the neurocognitive and behavioral domains. Before attempting to construct such a model in analytical form, an initially qualitative assessment of the functional relationship between the nodes of the putative network will be undertaken. Those ROIs which were removed in the network-level and multiple-comparisons-associated thresholding in previous steps will be considered here, as they can potentially be of modeling utility by providing edges between nodes in the network that allow access between ROIs with known functional relationships without taking a circuitous route through functionally unspecific areas of cortex, and, ideally, in the identification of functional hubs densely connected to distributed network functional subunits. As well, ROIs in cerebellum and the brain stem will be tested for connectivity to the seed ROIs already identified. As calculations in the dynamical modeling step will use actual subject-level connectivity values for all included connections, significance levels for the individual connections are not meaningful, but rather the functional-topological layout represented by the chosen connections, and therefore the calculated significance of the model's output, determines the plausibility of the chosen connections in the aggregate; the success of the model in abstracting RRBs in terms of dynamic brain behavior thus determines their aggregate significance. While both the explicit model form and functional connectivity values are of intrinsic importance to the model behavior, the model form specifically can construe the functional connectivity values in ways that result in arbitrary correlation between model abstract numerical output and subject RBS-R CSS, or any other set of values. Hence, simplicity and functional and neurophysiological plausibility will be the objects of chief pursuit.

The initial ROIs and nodes are represented in figure 3.18. The relationship between functional network subcomponents may be more easily visualized by splitting the network into negatives- and positively-RRB associated connections, as shown in figures 3.19 and 3.20.

Proceeding in this manner, and further investigating seeds of potential significance as nodes in the inclusive network as those to which the already-identified ROI seeds displayed significant connectivity when thresholded as above, reveals the extremely dense connections between combined left cerebellar area 8 and vermis area 10, and the majority of salience/executive and motor nodes in those respective functional subnetworks. Hence, a topological arrangement of the nodes and connections will be constructed as in figure 3.21. Specific connections from which the model was constructed are given in table 3.13. Note that anterior cingulate, a substantial part of the salience detection network, provides another, though less profusely connected, node that can potentially accommodate the dynamic mediation of activity between subnetwork subcomponent ROIs. This arrangement of nodes and their connections will be used in the model construction carried out in section 3.7, which

asserts the functional significance of both ACC and cerebellum as trans-network hubs that mediate communication between motor/reward and sensory/integration/executive subnetworks. Representation of putative hub connectivity on the cortical surface is provided by figures 3.6.1, 3.6.1, 3.6.1, and 3.6.1, with commentary given in figure 3.26.

The functional divisions within the network mirror aspects of those in [127], with salience, executive control (cognitive control), attention (here, sensory input, as most identified sensory areas are association), and reward (reward processing) functional network subdivisions being here suggested. In the former case, network functional topology was derived from task-based contrasts across a large number of fMRI activation studies primarily. Known behavior of the salience network implicates it in mediation via reciprocal inhibition, or, in other words, functional selection between, default mode and executive networks [222]. While no direct anterior cingulate—prefrontal connection was identified as significantly associated with RRB severity herein, the shortest path between the functional components via cerebellum results in the expected behavior via interaction effects: In the absence of other influences (physiologically unrealistic, but consistent with the interpretation of Pearson correlation and valid in the context of simultaneous functionally specific interdependence across all functional subdivisions in the network as will be modeled), increased anterior cingulate activation results in decreased DMN activation, and vice-versa (and also in both directions absent other information because Pearson correlations are undirected).

3.6.1   Interpretation and significance of network topology

Although amygdala in the proposed functional network topology is otherwise to the cerebellum functionally disconnected from the rest of the network, its established significance both in ASD pathophysiology, along multiple dimensions, and in the early history of neuroanatomical and neurophysiological research into the disorder, merits its mention. Decreased amygdalocortical effective connectivity involving medial prefrontal cortex has been associated with social deficits in ASD [39]. Considering the proxy effect on motor subnetwork activation in the absence of other effects, the sign of the interaction effect (product of the Pearson correlations) between amygdala and either supplementary motor area or precentral gyrus, would be positive, implying (weak) functional coactivation. Likewise, the signs of the interactions between amygdala and anterior cingulate, and between amygdala and DMN, would be positive and negative respectively, which presents a functionally plausible picture in which amygdalar activation results in suppression of default network activity, activation of the salience network, and, plausibly, eliciting of motoric response. While not actually realized given the resting state cognitive condition for the subjects, the network functional topology as explicated is

consisted with such functional behavior. As time-dependent activity within component subnetworks is to be modeled, it is this type of functional relationship that is of initial interest. Cerebellum, however, is the central (functionally, and not just in the diagram) feature of the functional network arrangement.

While relatively few uncontestably "motor" ROIs were identified in the network extension search analysis, consistent, perhaps, with the fact that substantially motor cortex would have little practical importance, and indeed, would be according to the typical subject instructions deliberately suppressed, alterations in motorically engaged brain connections and function have recently emerged as mechanisms potentially fundamental to ASD pathophysiology [223]. This postulated mechanism explicitly includes alterations in corticocerebellar motor circuits, involved in coordination, motor planning, and cognitive control of motor function, which comprise an important, though far from exclusive, functionally significant role of cerebellum [223]. Cerebellum—inferior parietal lobule connectivity was identified as functionally associated with RRB severity as well, as is the case here with respect to labeled "DMN" functional subunit which consists essentially of portions of right inferior parietal lobule and is herein implicated in RRB-severity-associated connectivity with the putative cerebellar hub. Cerebellum itself, though with profuse functional connectivity to other divisions of cerebrum, and with therefore concomitant functional roles, does nevertheless display aspects of topographic functional organization with respect to spatioanatomical distribution of skeletal muscle, as does primary motor cortex. In fact, somatomototopic functional organization along primary somatosensory and motor cortex is represented in a corresponding somatomototopic map in contralateral anterior lobe of cerebellum, affirming the significance of the motor functional division of cerebellum [224]. Retinotopic functional maps, too, have been identified within cerebellar cortex. Finally, discharge of neurons in cerebellum of the bat, to whom auditory stimuli are of particular importance, has been identified via single-unit recordings [225], establishing a cerebellar role in all primary non-chemoceptive senses at least in addition to cerebellum's unisolable functional interconnection with association cortex and basal cerebral nuclei. Yet further evidence for cerebellum's diverse role comes in the specificity of cerebellar dysplasias in different regions of cerebellum and their associated cognitive deficits which imply a spatial organization that likewise includes functional maps of frontal (lobules VI and VII of the posterior lobe) and limbic (posterior vermis) cortical areas [226]. These features, in sum, correspond closely to cerebellum's functional connectivity with neocortex: Closed-loop functional connections between cerebellar output nuclei and cortex-wide functional divisions are arranged spatially within those nuclei and allow reciprocal influence between cerebellum and neocortex [227]. This all despite a general conception over two centuries of functional

114

neuroanatomy that cerebellum was primarily, or indeed, exclusively, motor, too must be added to direct implication in various cognitive processes known now for decades, for example, selective attention [228]. The observed interconnection between the putative cerebellar hub and salience, default mode, limbic, and sensory association cortex clearly provides avenues along which such a cerebellar role may proceed. The repeated implication of cerebellum in ASD pathophysiology across diverse experimental paradigms is the most salient functional significance here, and this agreed-upon role tends to render as plausible one significant aspect of the network topology: the dense cerebrocerebellar connectivity. Four decades have passed since an anatomical association between vermal volume and ASD was identified [87], although hypoplasia was observed in lobules VI and VII contrary to the functional connectivity in cerebellum X identified herein. The finding, though, as stated, was anatomical, but, as the generative process underlying the hypothesized network arrangement was constructed in terms of postulated target regions, starting with the ROIs identified in the functional connectivity analysis step, no assertion whatsoever is made that the hypothesized network is wholly or even remotely substantially a significant component of any putative RRB-associated brain network in any estimable proportion, but only that it does encapsulate and mediate *a* specific, identifiable functional role. Therefore, it is asserted that the network will, in light of the functional relationships between the regions known and the connectivity values identified for the connections, underlie dynamical behavioral that can be modeled and assessed for at least statistical plausibility in RRB pathophysiology.

Summary of cerebellar significance to the network and its modeled dynamical behavior merits nuance, beginning even with its general structure and function. Succinct and thorough summaries of cerebellar anatomy informing the relevant discussion in this thesis include [229, 230], though note these sources are approximately two decades old. Of the most direct relevance to this thesis, cerebellar functional connectivity and significance in cognition, including executive control, attention, and motoric behavior, relevant to this RRBs in ASD, have been recently and thoroughly summarized in [231], the latter extensively consulted for the proceeding discussion. At the most fundamental level, the general functional scheme of cerebellum is one of motoric and somatotopic representation in anterior lobe and cognitive representation in posterior lobe, with complete topographic maps for each present. [232]. Thus, interpretation can be within the universe of the posited putative functional RRB-associated network that includes cerebellum, functional significance in actual brains given the same connectivity patterns to and from cerebellum, correspondence to prior results, and so on. As a first-pass assessment of the bald feasibility of integration into known results, several confirmatory observations are made: Cerebellum has significant functional connectivity to networks

significant in the resting state, these comprising at least the default mode network, salience network, and frontal-control (executive) networks [233]. As noted, motor cortex and mototopic representation in cerebellum is also precisely characterized and renders the two cerebellar connections to putative motor cortex of at least threshold plausibility. Hence, already, then, the only unaccounted-for cerebellar functional connection in the hypothesized network is that to fusiform cortex. Interestingly, but of unclear, if any in particular, significance, the presently observed increased cerebellum—fusiform cortex connectivity in association with RBS-R CSS is consistent with likewise increased connectivity between the structures in posttraumatic stress disorder [234]. In any case, variations in the connectivity values between the structures have been significantly associated with neurocognitive disease states.

While an inferential assessment when Pearson correlation of BOLD time series is the underlying measure, in the hypothesized network with the high-RRB connectivity values, cerebellar functional inhibition of motor cortex is not inconsistent with the popular conception of its role in motor regulation which is, if not necessarily its primary one, nevertheless, a significant one. However, while output of cerebellar cortex to deep cerebellar nuclei is inhibitory, deep cerebellar efferents to thalamus, and hence, to various downstream cortical areas via functional connections, are excitatory [235]. Therefore, only the general observation of significant functional connectivity, and not its valence, can be said to reflect *a* cerebellar—motor functional relationship, not one with direct relationship to known anatomical tracts and synaptic functions in the various structures along them. Additionally, as illustrated below (table 3.21), the mirror symmetry of the connectivity value correlation signs on either side of cerebellum reflect similar, but not identical, results of transduction of sensory and executive input to motor areas in both low- and high-RRB subcategory subjects.

A broader incorporation of functional roles implicating potential "ground-truth" significance of the putative cerebellar hub can be had in terms of segregation of cerebral and cerebellar structures in terms of functional-computational terms. The scheme relevant here is that in which basal ganglia, in this network represented only by nucleus accumbens, participate in reinforcement learning, cerebral cortex participates in unsupervised learning, and cerebellum in supervised learning [236]. This conception suggests that basal ganglia promote actions that conform to those that were in the past successful in bringing desirable results, that cerebrum performs especially computations on substantially incomplete or fragmented information, or information of an unfamiliar nature, and that cerebellum actively assesses the results of undertaken actions and adjusts them on the fly in order to bring them in conformity with intent (and outcomes also so). Therefore, the form of the dynamical model shall reflect this by modeling cerebral areas as the primary agent of perturbation

on the network, while reward and intrinsic reinforcement circuitry promotes gratifying behavior, here an abstracted representation of repetitive motor behavior, and cerebellum, as its connection topology suggests, mediates between these influences in terms ultimately determined by its suite of functional connectivity.

Though supervised learning as a computationally-defined functional role is consistent with cerebellum's anatomy and dynamic *in vivo* behavior, this influence on behavior includes action more highly abstracted from "merely" refining motor behavior in real time, as discussed above. A proposed mechanism by which cerebellum performs its functions across cognitive domains and cortical functional areas despite a manifest uniformity across its cortex is a "cerebellar transform," "transform" in the sense of an algorithmic computational process that operates on information input and modifies it for the purpose of returning the information in useful and actionable forms to the originating cortical area [237]. This proposal squares the functional diversity with the anatomical uniformity of cerebellum, and functional research on the structure confirms its plausibility across cognitive domains. For example, cerebellum is proposed to participate in a functional loop in which planned actions, intended outcomes, and anticipated rewards, all are integrated with the actual results of behaviors inferred through primary sensory and sensory association areas, all mutually updated in light of these sensory streams, and hence their specific influence on the "action selection" role of cerebellum, and hence dynamic cerebellar function, are also both continually updated [238]. This, too, comports to the functional connections identified in the hypothetical network, as relevant cortical areas (and amygdala, which may be conceived as attaching affective valence to results of behaviors) are all functionally connected to cerebellum. An additional consistent observation is decreased functional connectivity between salience and default mode networks in undiagnosed relatives of individuals with ADHD diagnoses [239]; this is consistent with the high-RRB functional network in which, mediated by cerebellum, DMN and anterior cingulate salience components are weakly inversely connected through their shortest path of functional connections. Also directly related, while implicating distinct cerebellar divisions (VIIb and VIIIa), the dorsal attention network, overlapping in the hypothetical network with the lateral parietal network, is functionally connected to cerebellum in visual working memory and attention tasks [240]. Also observed in ADHD has been increased cerebellum—default mode, frontoparietal, dorsal attention, and visual (in the network, fusiform cortex) network connectivity (consistent with the hypothesized network), and increased cerebellar-DMN—connectivity to salience network (inconsistent with the hypothesized network in high-RRB) [241]. While the patterns are not entirely coterminous, they implicate all of the same functional networks, and more (4) are of the same than opposite (1) valence. This again substan-

tiates the extensive role of cerebellum in a wide range of disorders (and therefore, their symptoms across cognitive domains) of a neurodevelopmental nature, an even more significant fact given other common features across neurodevelopmental disorder symptoms.

Cerebellar connectivity in the hypothetical network functionally both modulates and transduces signals between subnetworks, establishing a path through which signals from any ROI can affect that time course of activity in any other ROI. This includes, given the proposed network is not a full enumeration of functionally significant ASD RRB-associated brain divisions (as that enumeration would simply be the entire brain) and modeled activity must be transmitted along available paths, communication between sensory, association, default mode, and salience and attention cortical divisions, and subcortical structures, in the model, nucleus accumbens and amygdala, though the latter is not incorporated into the first-approximation dynamical model in this thesis given its sparse connectivity to the rest of the network. While not extensively incorporated into the model in terms of ROI proportion, basal ganglia *are* of relative functional prominence in the model developed and evaluated. Functional significance of striatal connectivity identified in the present network arrangement extends beyond the identification of the single included ROI (nucleus accumbens), not only because it is of central importance to the modeled network behavior (in the next section), but because basal ganglia, like cerebellum, and to an extent shared only *by* cerebellum, present ubiquitous anatomical and functional alterations in ASD, across deficit categories, symptom severity, age, gender, and most other relevant factors. While the hypothetical functional network constructed in this section includes nucleus accumbens functional connectivity only to putative motor cortex, it is modulated dynamically across SMA by PT in the functional model, the most directly association cortex—striatum functional relationship in the model, of note since striatum—PT connectivity, consistent with an observed pattern of general corticostriatal hyperconnectivity, especially involving association cortex, observed in children diagnosed with ASD via rs-fcMRI [183]. Specifically, corticostriatal connectivity, when disrupted in mucine knockout models, is associated with substantial and deleterious manifestation of RRB analogs [242]. Given that the cerebellar hub putatively transduces all signals from the sensory periphery and control networks to motor cortex and limbic and basal gangliar structures, the two in the model can be accurately conceived as contributing to a competitive equilibrium based on modeled stimulus input and its propagation via network edges. The specific hypothesized nature of cerebellar influence on subcortical, as well as motor function, can be particularized in terms of anatomically and physiologically specific aspects of cerebellar function. This is a point of theoretical significance given that synthetic view of RRBs with accumulating evidence is that functionally dysconnectivity between posterior cerebellar (neocerebellar) and basal

gangliar control circuits [243]. Cerebellum's centrality to modulation of (modeled, eventually, in this thesis) cortical activity is its fundamental significance to the hypothetical functional network, and its manner of effecting this role will be briefly reviewed.

Cytoarchitechtonically, cerebellum engenders highly stereotyped circuit arrangements, with only a few types of neurons in repetitive arrangements subserving its diverse functions. This architecture is thought to specifically endow cerebellum with its massively parallel processing power [96]; while both cerebrum and cerebellum exhibit ubiquity of function, cerebrum accomplishes its ends specifically through structural heterogeneity, whereas cerebellum does so through structural homogeneity. It appears cerebellum performs the same general processing steps on all inputs, and its functional generality therefore seems to rest in part on the contemporaneity of, and comparisons between, its various input streams, i.e., most simply, between intended and actual results of actions, although "actions" must be construed to comprise a hyperdiversity of cognitive regimes. Through repeated comparison of cerebral afferent streams, including both sensory and association streams relevant to the intentions and outcomes of behaviors, cerebellum refines cognitive processing in the same manner it refines motor execution, both in real time, and through time [100], a role for which cerebral processing speed is too slow relative to the perception of the consequences of actions, and the incorporation of those consequences into a continually updated activity plan [238]. The actual dynamical operation of cerebellum in performing these distributed functions has been conceptualized for some time (1982) as that of an adaptive linear filter that optimizes the final (motor) output of intentional actions, regardless of the actual nature of the intent (so independent of cognitive domain) by means of the optimization of the transfer function between the initial cortical output with volitional intent and the final signal sent to the peripheral nervous system [244]. Note that this function cannot be subsumed by cerebrum with equivalent efficacy; it is the massive parallelism of cerebellum that engenders it with sufficient bandwidth and latency to effect its transfer function. The signal transduced by cerebellum has been conceptualized both as representing likely sensory feedback from an action (forward model) and as representing the course of motor behavior required to effect a desired result [245]. Corroborating this processing behavior and its consequences is that weaker corticoneocerebellar connectivity has been found to correlate with slower processing speed in schizophrenia [246]. The conception of cerebellum as mediating between executive and motor subnetwork function coheres the functional framework of cerebellum elaborated in the dynamical model. Nearest the observed pattern in cerebellar functional connectivity associated herein with RRBs is that weaker functional connectivity was also observed between cerebellum and executive cortical areas in obsessive compulsive disorder [247].

From this, cerebellum can be comfortably asserted to subserve executive function generally [248, 249], and its deficits in ASD specifically [81], but beyond this, for the purposes of the present network model, executive function must be operationally defined; the term "executive function" has been criticized as underspecific [238], but consistent with the resolution proffered in the cited case, it is taken here simply to encompass the various cognitive mechanisms that regulate behavior. The word "regulate" in this case becomes key, and it is taken to mean "to attenuate excessive influences and potentiate beneficial influences." Thus, as will be seen, "executive function" is that contrary to "intrinsic reinforcement function." This specific generalized conception of executive function is not wholly inconsistent with alternative schemes positing discrete domains of executive function, such as set shifting, response inhibition, and working memory (implicated in the executive dysfunction hypothesis [250]), and it also is compatible with such a scheme as "implicates a broader influence of [executive function] on the ASD phenotype. These include impacts of [executive function differences] on social cognition (16, 17), mental health (18), disability (19, 20), and lifelong functioning outcomes (21). [250, p. 2]."

Figure 3.18: Schematic representation of all the relevant ROIs and connections in the putative RRB-associated network, including those that were removed due to network-level thresholding or multiple comparisons corrections in the ROI- and seed-level connectivity calculations. These are included because they increase the chances of finding an arrangement of network nodes that can be straightforwardly dynamically modeled. Network and cognitive-behavioral functional domains are given along the axes.
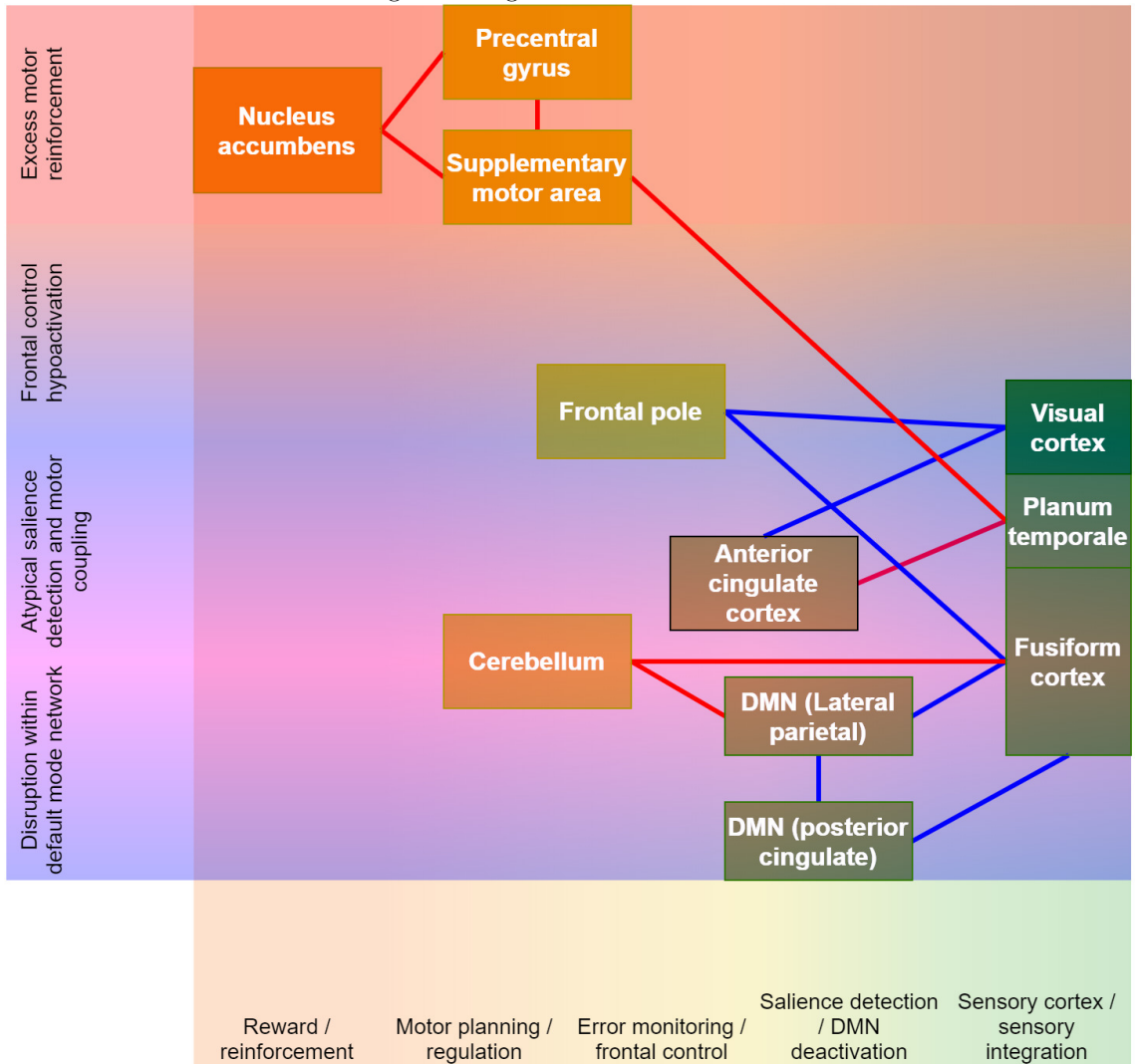
Figure 3.19: Schematic representation of all the negatively RRB-connectivity correlated connections, representing default mode, sensory, salience, and sensory areas.
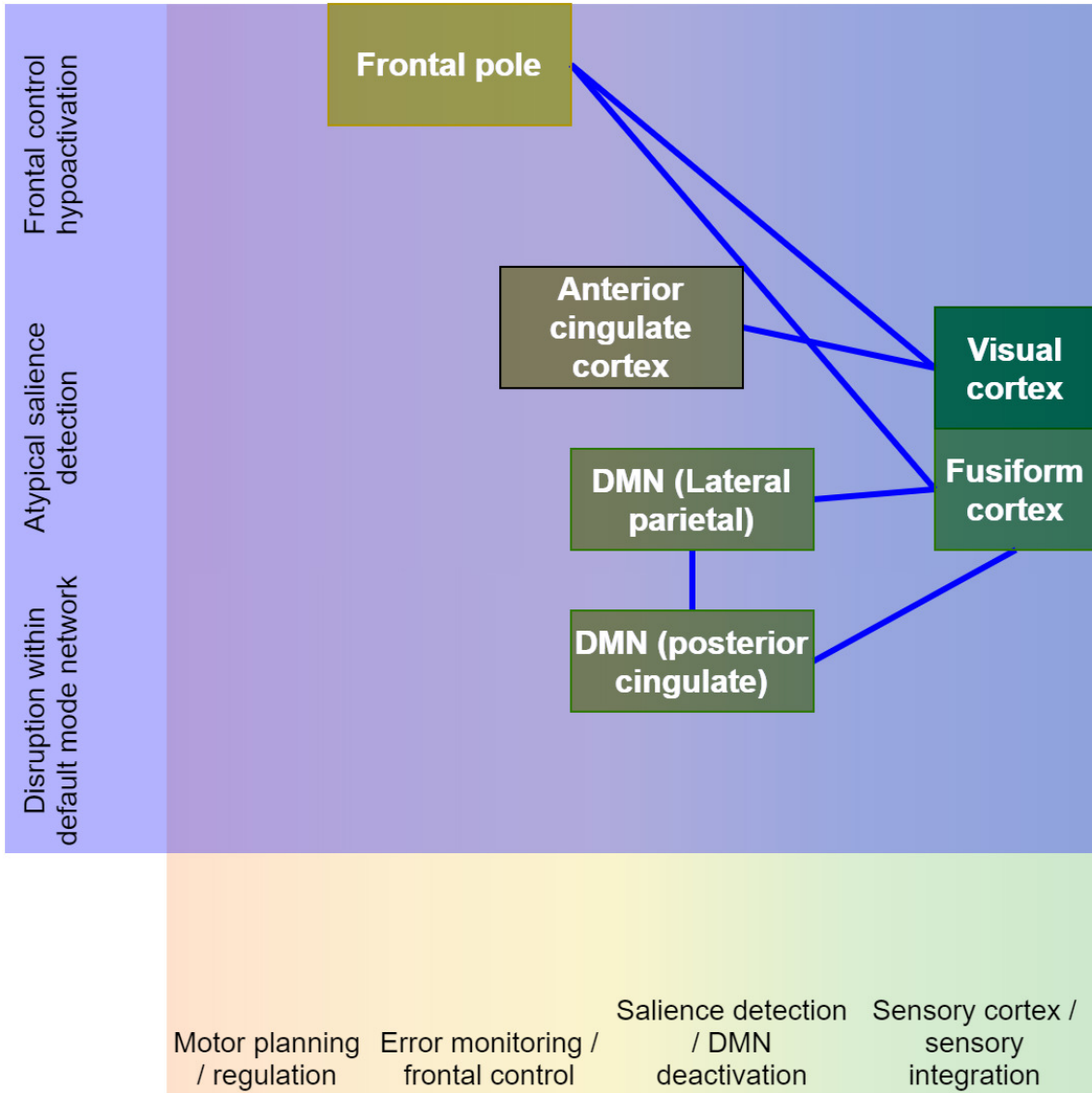
Figure 3.20: Schematic representation of all the positively RRB-connectivity correlated connections, representing especially motor and reward regions of the brain, and other ROIs connected to them as nodes.
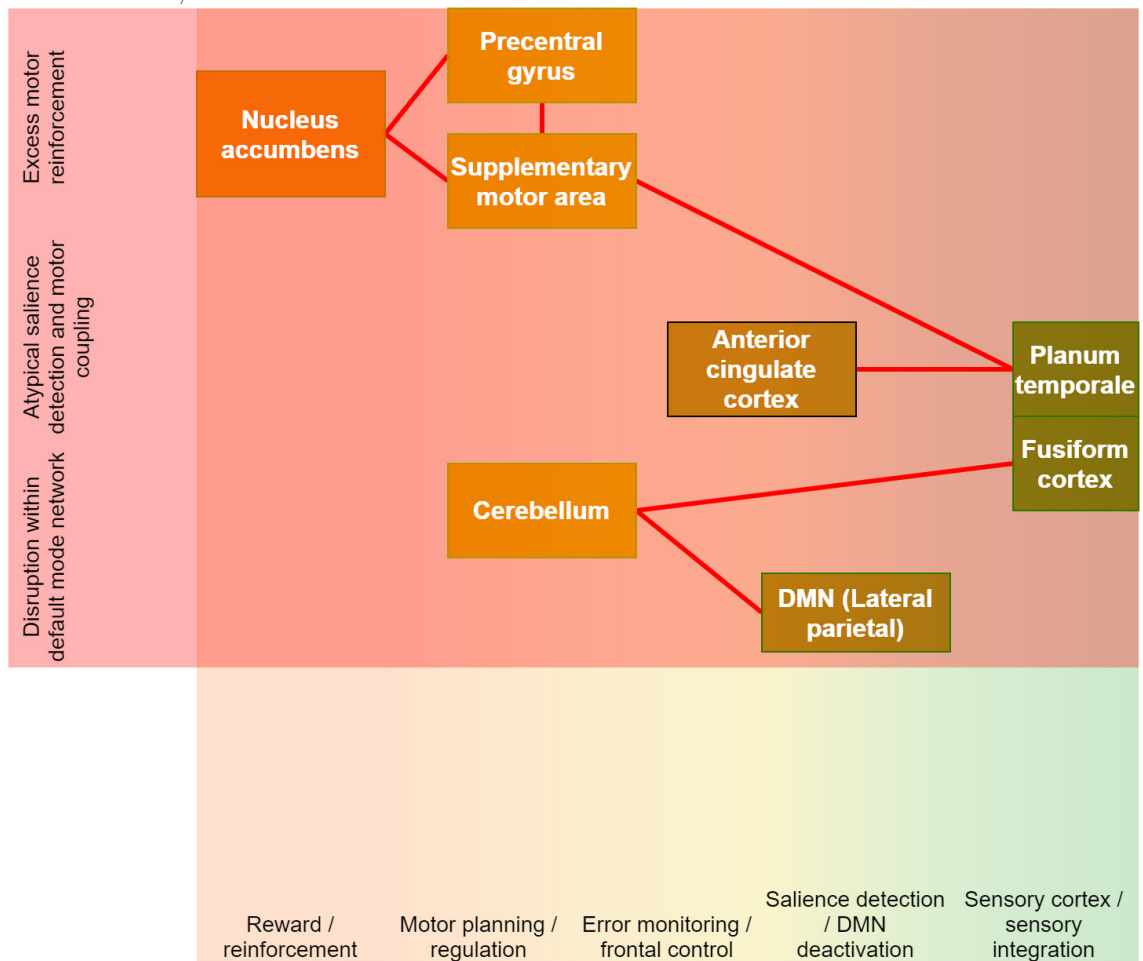
Figure 3.21: Schematic representation of a hypothetical functional network topology in which cerebellum, as the most densely connected single node, serves a mediating role between sensory, executive, salience, motor, and reward areas. This is consistent with its dense anatomical connectivity to disparate areas of cortex. Anterior cingulate cortex provides an "alternative pathway" for mediation between the subnetworks, albeit much less direct from the perspective of most pairs of topologically distant nodes.
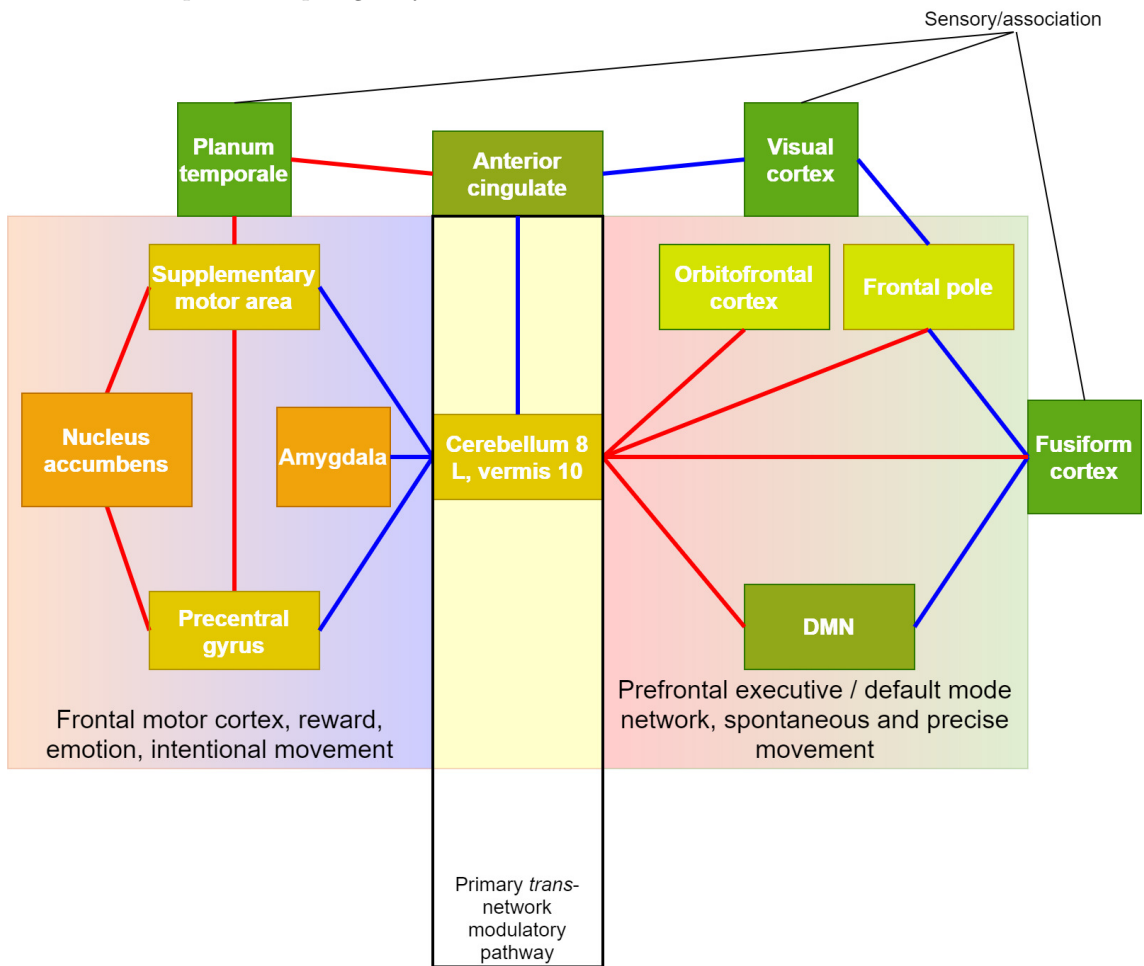
Table 3.13: ROI coordinates in hypothetical network from network seeds. Target voxels were chosen as the voxel within the target ROI with largest effect sizes from the indicated seed.

Seed	Target	Coordinates
+AC@rest	R occipital	(40, -74, 24)
+Accumbens l@rest	L precentral	(-50, 0, 18)
+Accumbens l@rest	L supplementary motor	(-12, 8, 52)
+aTFusC l@rest	R frontal pole	(12, 56, -12)
+aTFusC l@rest	R DMN LP	(42, -72, 32)
+0.5*Cereb8 l@rest +0.5*Ver10@rest	Anterior cingulate	(8, 12, 36)
+0.5*Cereb8 l@rest +0.5*Ver10@rest	L frontal pole	(-24, 44, 26)
+0.5*Cereb8 l@rest +0.5*Ver10@rest	R frontal pole	(42, 34, -16)
+0.5*Cereb8 l@rest +0.5*Ver10@rest	R fusiform	(40, -30, -20)
+0.5*Cereb8 l@rest +0.5*Ver10@rest	Orbitofrontal	(34, 28, -20)
+0.5*Cereb8 l@rest +0.5*Ver10@rest	L precentral	(-54,-2, 16)
+0.5*Cereb8 l@rest +0.5*Ver10@rest	R precentral	(58, -2, 32)
+0.5*Cereb8 l@rest +0.5*Ver10@rest	L supplementary motor	(-10, -2, 58)
+0.5*Cereb8 l@rest +0.5*Ver10@rest	R supplementary motor	(10,-8,64)
+0.5*Cereb8 r@rest +0.5*Ver10@rest	L fusiform	(-40, -46, -24)
+DefaultMode.LP r@rest	L cerebellum	(-24, -62, -46)
+PT l@rest	Anterior cingulate	(62, 2, 34)
+PT l@rest	L supplementary motor	(-24, 4, 48)
+pTFusC r@rest	R frontal pole	(30, 64, -4)
+SMA L@rest	L precentral	(-62, -4, 24)
+Visual.Occipital@rest	L frontal pole	(-50, 38, 4)
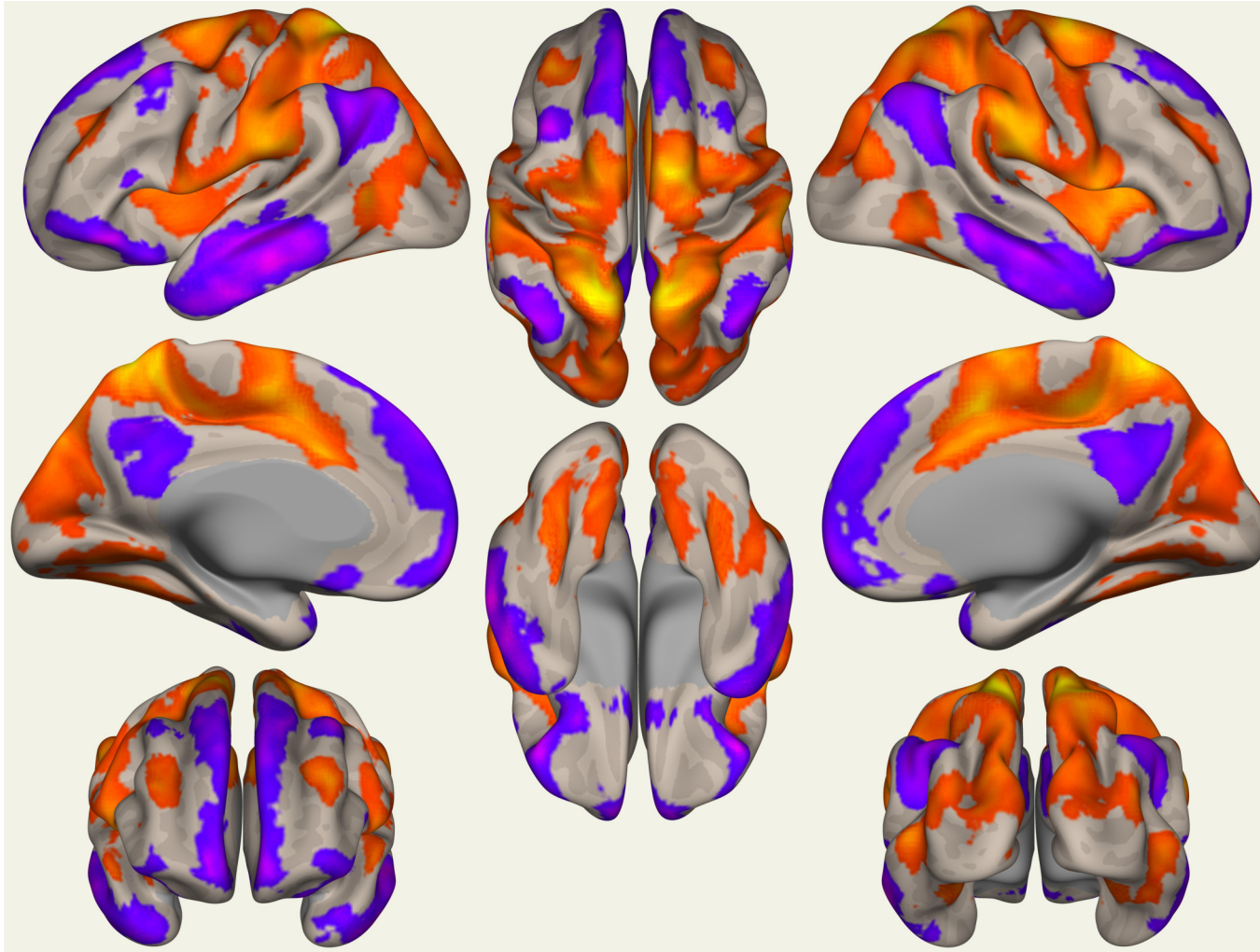
Figure 3.22: Results of seed-to-voxel connectivity using bilateral cerebellum XIII and vermis X as seeds to ROIs within the formalized putative functional network.
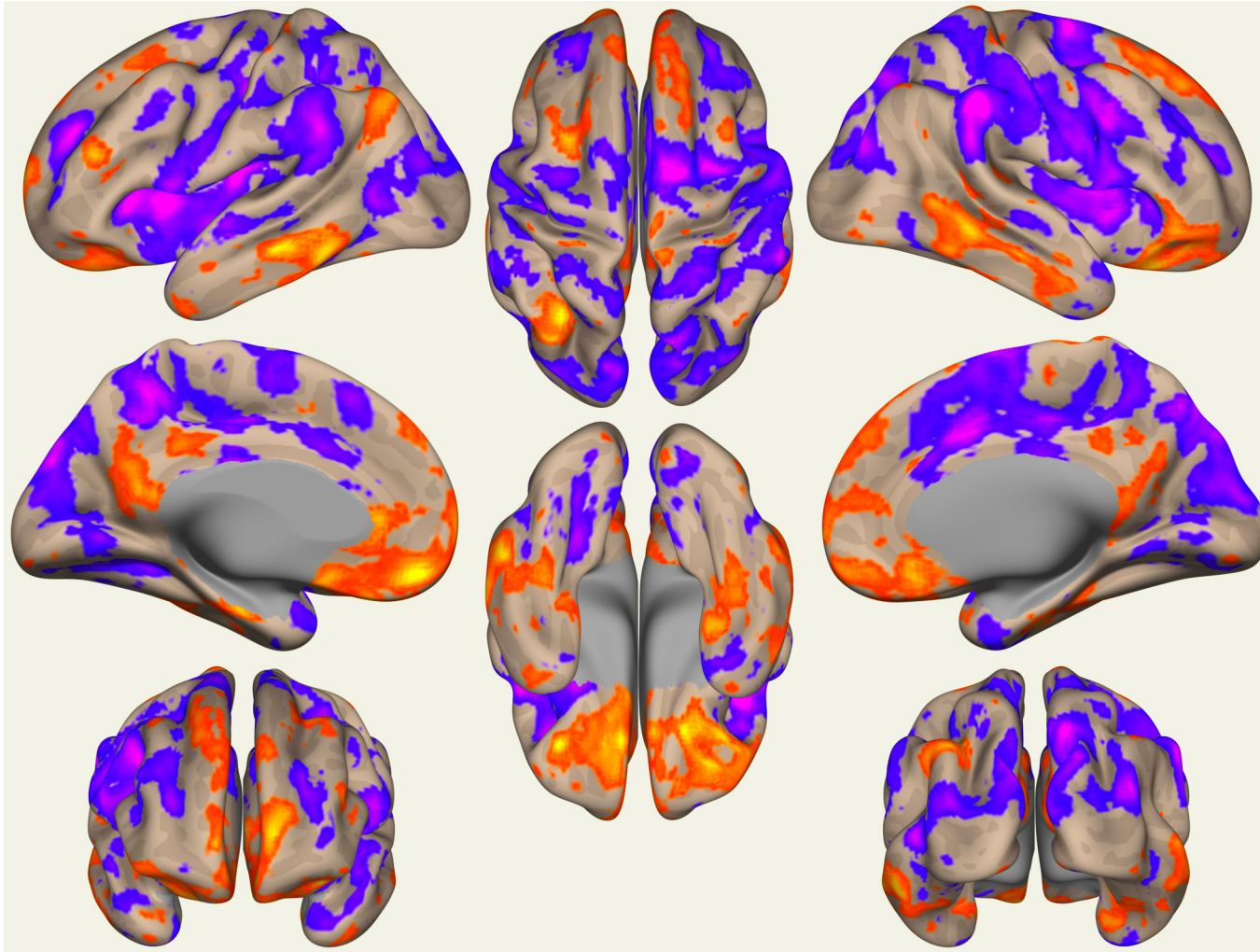
Figure 3.23: Results of seed-to-voxel connectivity using bilateral cerebellum XIII and vermis X as seeds to ROIs within the formalized putative functional network, high-RRB subject correlation compared to entire subject pool.
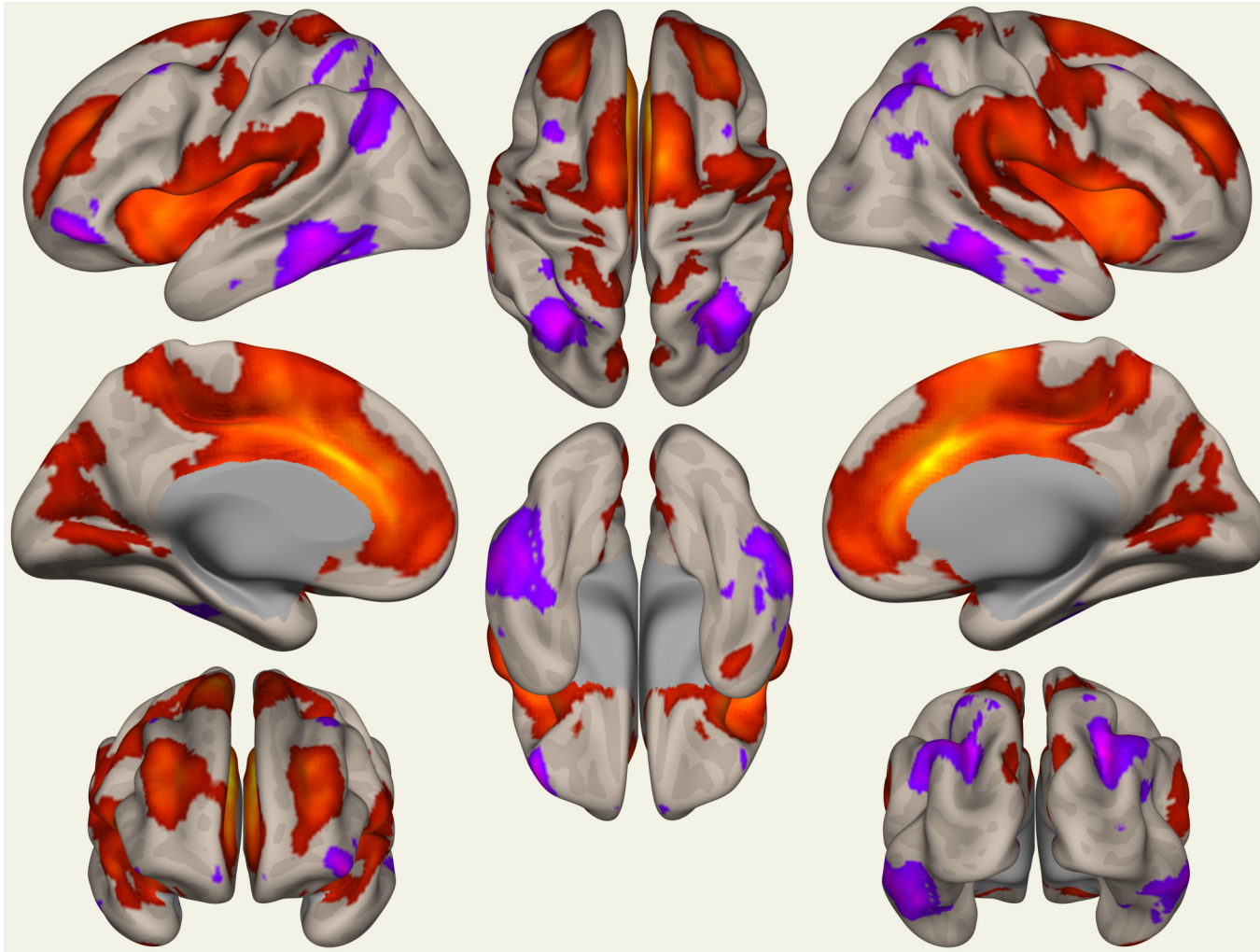
Figure 3.24: Results of seed-to-voxel connectivity using anterior cingulate cortex network and anatomical ROIs as seeds to ROIs within the formalized putative functional network.
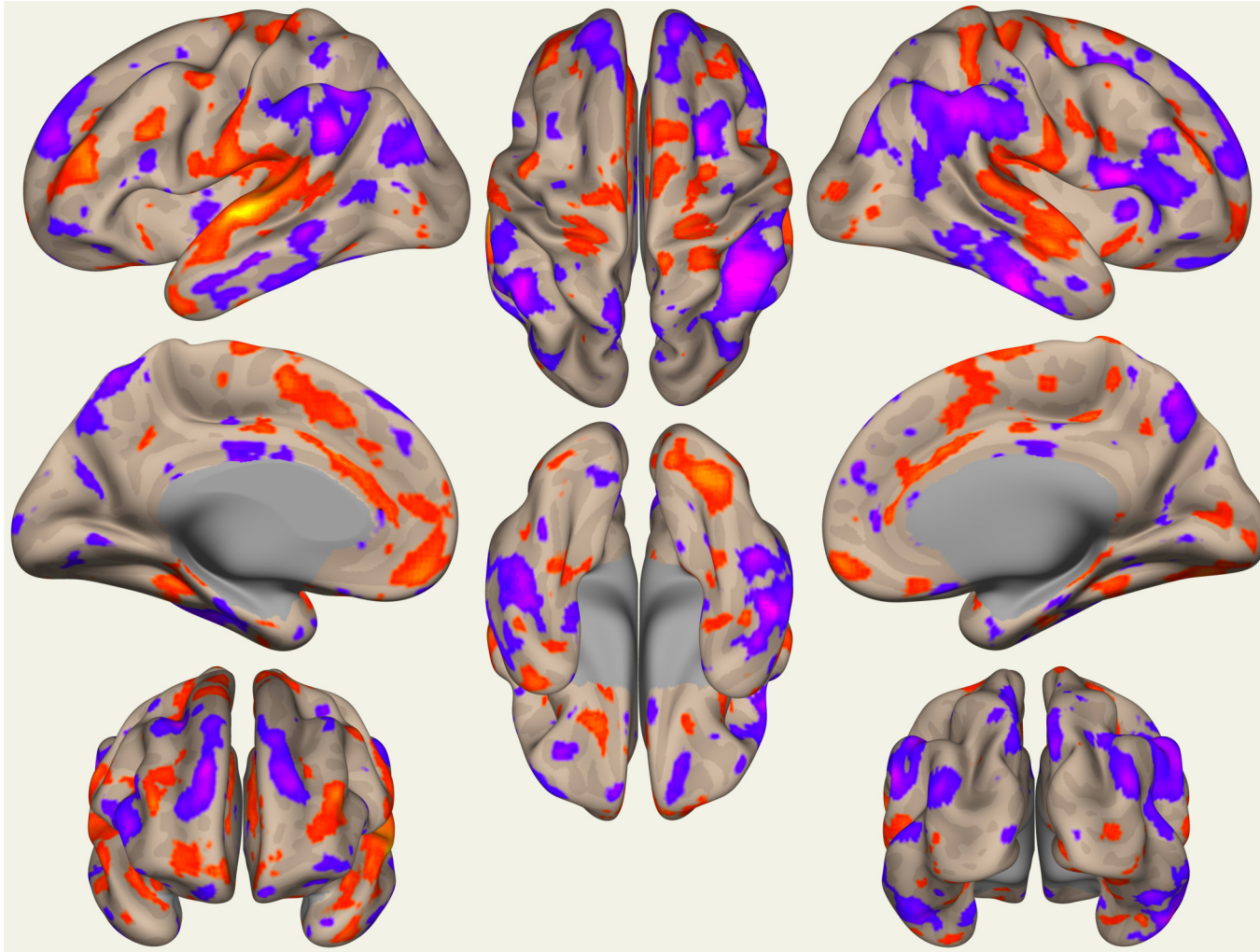
Figure 3.25: Results of seed-to-voxel connectivity using anterior cingulate cortex network and anatomical ROIs as seeds to ROIs within the formalized putative functional network, high-RRB subject correlation compared to entire subject pool.

Figure 3.6.1 shows clear, prominent motor and somatosensory cortex connectivity with cerebellum (XIII L and R and vermis X) in the pooled subject connectivity data. Negative prefrontal connectivity with cerebellum is also exhibited, including portions of frontopolar cortex and orbitofrontal cortex, connections identified as positively correlated with high RRB trait measures. In this vein, lateral parietal DMN—cerebellum connectivity, the former represented roughly by the location of the angular gyri and parts of supramarginal gyri, is positively associated with high RRB trait measure and RBS-R CSS, and is clearly negative on average across the subject sample as a whole, although its putative overall significance is supported given the well-delineated FC relationship for the whole sample across the ROI. Likewise, connectivity opposite that of the "high-RRB pattern" is observable across the cortical surface from cerebellar hub, including to anterior cingulate and superior temporal gyri, and primary and supplementary motor cortex.

Figure 3.6.1, showing the high-RRB subject subgroup data, largely explicitly depicts patterns opposite those immediately above. There are positive connectivity associations of the cerebellar hub with frontopolar and orbitofrontal cortex, as well as with apparent portions of fusiform gyrus, and negative associations with substantial portions of motor cortex, along with lateralized effects on lateral parietal DMN connectivity. Cerebellar hub—whole brain connectivity analysis identified a p-FWE and p-FDR significant ($p < 0.05$) voxel cluster comprising parts of right lateral occipital cortex using default settings for random field theory parametric statistics.

Figure 3.6.1 most clearly indicates a spatial dependence of anterior cingulate functional connectivity, with adjacent portions of cortex showing strong positive connectivity associations. Extension of this spatial pattern to planum temporale, or else independent planum temporale connectivity, is evident. Notably, this is concordant with the high-RRB connectivity pattern, rather than an inversion of it. Hence, anterior cingulate and planum temporale apparently exhibit at least weak positive connectivity across the subject pool (this is consistent with the data tables beginning with A.2; a very weak positive association across the subject pool) Some isolated, weak negative connectivity between the anterior cingulate hub and orbitofrontal cortex is observed as well, consistent with extrapolated connectivity via intermediate nodes in network diagram in figure 3.6, another pattern consistent between the whole subject population and the high-RRB subgroup subjects, although the high-RRB subject subgroup evinces mixed patterns of sporadic connectivity from anterior cingulate to orbitofrontal cortex. Connectivity to visual cortex is not apparent in the cortical surface projection.

Figure 3.6.1 does manifest the major connectivity association distinctive of the "high-RRB" pattern: positive connectivity association of anterior cingulate cortex with planum temporale. Additionally, in both the whole sample and the high-RRB subgroup, apparent functional antagonism manifests between lateral parietal default mode network, a significant node in the network, and anterior cingulate. Interestingly, and unaccounted for, the whole subject sample exhibits apparent positive anterior cingulate—middle frontal gyrus connectivity, but this connectivity is negatively associated with RRB severity. As anterior cingulate and middle frontal gyrus both are substantially implicated in attention, but with middle frontal gyrus apparently subserving switching endogenous and exogenous attentional control [251], such a putative dysconnectivity pattern is not inconsistent with an implicit inward focus in RRB manifestation in ASD.

Figure 3.26: Summary of functional connectivity patterns from figures 3.6.1, 3.6.1, 3.6.1, and 3.6.1 associated with putative network hub cerebellum VIII/vermis X and anterior cingulate cortex function and relation to ASD RRB manifestation.

3.7 DYNAMICAL MODELING OF PUTATIVE FUNCTIONAL NETWORK

The identification of a statistically significant ensemble of functional brain connections that differs between low- and high-RRB subject subgroups within subjects with ASD diagnoses clearly suggests that altered functional brain connectivity is a highly plausible pathophysiological mechanism for some of the behavioral and cognitive aspects of RRB presentation in ASD. Additionally, the fact that the interaction-term-only regression was robustly significant in comparison with the chance-model demonstrates the likelihood of relationships between not only the ROI nodes, in the form of functional connections, but between and across the connections as well, forming a qualitative network, as demonstrated in section 3.6. However, the relatively poor cross-validation results for the interaction-term-only model (section 3.5.2) do merit an attempt to give the network an explicit form that can be tested for actually physiologically plausible behavior.

Additionally, because the elucidation of a coherent, orderly topological arrangement of the network components in the form of the ROI arrangement given in figure 3.18 allows for greater ease in the analytical manipulation of the underlying data than regression modeling on the subject-level connectivity values, a model will be designed that attempts to capture the functional implications of the topological arrangement and its postulated significance. In order to do so, the consideration of the wholly integrative and wholly interactive nature of the brain as a fundamentally complex and dynamical system must be given due precedence in the model design. Hence, a three-dimensional dynamical model will be constructed that can predict changes in the activation level within the node ROIs based on such a change in any of the other nodes, duly constrained by the graph-theoretic collection of nodes and vertices in the hypothetical network, and will be formulated in terms of the three time derivatives of the activation level in the three major subnetworks: sensory (in terms of stimulus input), executive/salience, and motor/reward. Full implementation will proceed through three discrete realizations of the model with functional extension occurring in each so as to accommodate additional dynamical spatiotemporal regimes. The methods used are substantially described in [192].

The model will initially take the form of a linear system described by

$$\dot{x} = -\omega \sin(\omega t)$$
$$\dot{y} = cx - \delta y \qquad\qquad (3.2)$$
$$\dot{z} = r|z| + sz - fy$$

131

where

$$x = \text{time-varying stimulus function}$$

$$\omega = \text{stimulus function angular frequency, 0 for static drive}$$

$$y = \text{executive network activation}$$

$$z = \text{motor-reinforcement network activation}$$

$$c = \text{stimulus amplitude, or, equivalently, executive network stimulus sensitivity}$$

$$\delta = \text{damping parameter of executive network (time decay of activation)}$$

$$r = \text{functional reward motor reinforcement}$$

$$s = \text{functional intrinsic motor reinforcement}$$

$$f = \text{functional executive control.}$$

ω, c, and δ are exogenous parameters; r, s, and f will be empirically derived from RRB-severity category subgroup average values for the relevant connections, and for individual subject values for the same connections in the subject-level model implementation. An additional exogenous parameter j in the model script in `MATLAB` represents the stimulus function initial conditions. In the first model realization, ω will be held at 0 so that the trajectories of model output can be trivially evaluated in terms of their spatiotemporal dynamics via inspection of phase portraits associated with parameter sets of interest. As a first assessment, an additional value `mact` will be used to expediently modulate whole-motor-network activity in the *a priori* assessment of the model's dynamical utility and clarity in putatively abstracting and representing RRB-associated functional network behavior in terms of differential brain activation across functionally specific subnetworks.

Fundamentally, the variable z represents the time-dependent fraction of activation in motor cortex due to putative reward (striatal) reinforcement and intrinsic (within motor cortex) reinforcement within the motor subnetwork *in excess of* motoric cortical activity initiated by executive, salience, and attention, including default mode, subnetwork influence. In this way, the sum of the two self-reinforcing (with positive values of r and s) motoric influences putatively represents motor cortex lability while at rest, and, in naturalistic extrapolation, movements of repetitive and compulsive behavioral valence, i.e., RRB-like behaviors. Because motor cortical, and other brain activation is to be abstracted from functional connectivity (Pearson correlation) values and a simple numerical stimulus input drive, no cogent metric encapsulating "total motor cortex activation" can be attributed to the model's output. Therefore, the sources of motor cortex drive of putatively distinctly intentional valence will be subtracted from those of putatively reinforcing valence to yield an abstracted measure of "excess motor activity," or that which is the dominant component, i.e., when

the calculated difference is positive, of modeled motor cortical activity.

3.7.1 Dynamical model interpretation and application

The sign of the fy in equation 3.2 indicates that the proxy of interest for RRB-associated motor behavior, $\dot{z}$, is the proportion of motor cortical activation independent and in excess of executive and salience network-mediated effects. That is, rather than overall or absolute motor cortical activation, only such activation as is caused by intrinsic (between motor areas) and reward (arising via nucleus accumbens connectivity) reinforcement, less that which arises due to sensory, salience, and executive subnetwork influences, is encapsulated in $\dot{z}$; the postulated relevance is that repetitive motor behavior arises from other than executively mediated motor activation, and hence, the components must be separable to make predictions of proposed functional validity to RRBs. Especially given the lack of straightforward behavioral and environmental relevance of the precipitating fMRI environment, the model form importantly does not seek to model "activity, period" within the motor cortex; there is no plausible neurophysiological—RRB *behavioral* mechanism to be identified via subject behavior while being scanned in a resting state. Indeed, "[o]nly a single study has reported findings of individuals actively engaging in RRB (skin picking in PWS) during neuroimaging (Klabunde et al., 2015) [47, p. 156]." Rather, the Pearson correlation values between functionally distinct ROIs and the putative subnetworks comprising them are taken to indicate, as discussed in the Background, the *intrinsic* network connectivity that might underlie severe RRB presentation. Similarly, the absolute value is taken of the z factor in the rz term in $\dot{z}$ to represent the conjectured reward-reinforcement of repetitive motor behavior; this represents a putative desired "baseline" of (putatively repetitive) motor activity represented by the always-additive effect of this term: Motor cortical activation results in reward-reinforcement (further increase in activation), and sub-baseline motor cortical activation results in reward-driven increase towards baseline activation. Contrast with the term sz in which intrinsic (between-motor) reinforcement *is* dependent on the sign of modeled motor activation, that is, whether it is above or below baseline. The physiological plausibility of the specific model form is validated at the end of this section, after the results of the testing of the model with arbitrary and group- and subject-derived parameter values.

The first analytical step in assessing model performance is establishing its potential to generate biologically plausible and varied dynamical behavior of straightforward cognitive and behavioral interpretation in RRBs in autism. Preliminary viability will be determined by assignment of arbitrary parameter values in an attempt to generate various regimes of dynamical behavior. This is achieved in figures 3.29 and 3.31. Next, the analytical forms of the functionally-derived parameters will be

determined based on the hypothesized network defined in section 3.6, also shown in figure 3.33. Particularly, based on the node labels show in figure 3.33, the connectivity values summarized in tables 3.14 and 3.15 will be used to calculate the functional parameters as shown in equations 3.3 and 3.4. Doing so produces the parameter values summarized in table 3.16.

Next, model behavior must be evaluated in light of the calculated connectivity values for RRB-severity category groups and individual subjects. The posited canonical behavior of the dynamical model with respect to RRB severity using empirically derived parameter values is demonstrated in figure 3.36. Demonstration that perturbations of the model dynamical behavior in the form of increases in the magnitude of the stimulus input produces regimes of trajectories of executive, salience, and motor-reinforcement subnetworks of the brain that are of clear and straightforward relevance to RRBs in ASD, and in an exactly predictable manner, are given in figures 3.37 and 3.38. Subject-level model behavior is given in figures 3.39, 3.40, and 3.41, and in table 3.17.

The preliminary stage of validation of the model to this point will be established by comparison of its utility to two naïve formulations of the same general system type, but which explicitly do not include the postulated functional relationship between the putative network and RRB severity. Identical analysis as above results in ostensibly variable dynamic behavior of the model across subjects (figures 3.43 and 3.44), but its explicit form makes any correlation with subject RBS-R CSS as observed in the original model form impossible (figure 3.42 and table 3.18). However, restricting the same naïve form of the model to only quadrant I (positive values of y and z only) does allow such correlations, and indeed, there is a significant relationship between model output in this case and subject RBS-R CSS. However, to five significant figures, the predictions of the original model significantly improve the restricted naïve model predictions, but the latter does not significantly improve the former. These results are summarized in figures 3.45 and 3.46, and in table 3.19.

Potential avenues for further testing and development of the model are investigated via modulation and perturbation of modeled dynamical behaviors in the form of increasing complexity of the stimulus input and incorporation of nonlinear reactivity of the excess motor activation in order to constrain model spatiotemporal trajectories and prevent unbounded end behavior. Variation of the stimulus function through time is introduced and explained in figure 3.49. Modeling of putative "mid-RRB" behavior in the model is effected by averaging parameter values for the high- and low-RRB subject subgroups to qualitatively assess the model's capacity to generate interprable interpolations of behaviorally relevant abstractions. Then, the three regimes (true high- and low-RRB derived parameters and the averaged parameters) are analyzed with respect to various modeled stim-

ulus conditions, shown in figure 3.50. After assessment of interpolative capacity, the extrapolative analogy is similarly conducted and summarized in figure 3.52. As a final analysis of the potential utility of the linear implementation of the dynamical model, individual network hub connectivity is modulated based on the variations in functional connectivity between the high- and low-RRB subject subgroups. Varying stimulus conditions are again applied, and the resulting dynamical behavior is shown in figure 3.54. Next, nonlinear reactivity of modeled brain function is introduced in the model extension given in equation 3.11 and illustrated beginning in figure 3.57, followed by statistical analysis. This is followed by introduction of a stochastic component per the model extension given in equation 3.12, likewise followed by similar graphical depictions of dynamical behavior allow qualitative assessment of spatiotemporal patterns, and explicit statistical analysis.

3.7.2 Initial analysis of dynamical model behavior

The dynamical behavior of the initial base model form will be assessed in three contexts:

1. Arbitrary assignment of trivial parameter values to investigate general dynamical behavior

2. Empirical parameter values determined by RRB-severity category subgroup connectivity values

3. Empirical parameter values determined by individual subject connectivity values

Additionally, a naïve formulation of the base model that ignores the postulated physiological—functional significance of the subnetworks to RRBs and instead calculates only total abstracted activation predictions is tested using subject-level data and compared with the hypothesized physiologically—functionally valid model form used in this section until that point.

Arbitrary assignment of trivial parameter values

Arbitrary parameter value assignment using trivial values (typically integers or round decimal values) was used to identify dynamical patterns that emerge based on the model form. In figure 3.29, slight variations of two gross patterns are depicted: substantial executive/salience subnetwork influence, and substantial motor-reinforcement subnetwork influence. In figure 3.31, two more substantial variations of model parameters are used to depict unstable dynamical behavior with clear bifurcations based on initial conditions due to more asymmetry between executive/salience, intrinsic-motor, and reward-motor subnetworks. For these and all other phase portraits, graph parameters and interpretation is given in 3.7.2. Each aggregation of phase portraits is followed by the parameter values assigned. Stimulus function angular frequency is set to zero in these calculations, effectively yielding a constant stimulus drive at the initial value of x.

135

Parameter values chosen are listed on the following page after the figures in the form of the raw MATLAB code assigning the parameter values. Increasing r is expected to increase motor-reinforcement activation across the entire coordinate space. Increasing s will likewise increase $\dot{z}$ when z is positive but decrease it when it is negative. Increasing f will decrease excess (that is, reinforcement) motor activation on the right half ($y > 0$) of the graph (quadrants I and IV) and decrease it on the left half (quadrants II and III).

These patterns are confirmed in the phase portraits in figures 3.29 and 3.31. 3.29(a) shows a sign change in the $\dot{z}$ component of the vectors approximately along the diagonal of the graph, showing a balance between sensory/salience/executive control and motor-reinforcement effects. Increasing f as in 3.29(b) results in the dividing line being rotated so that it is along the vertical (z) axis. In 3.29(c), with high r, $\dot{z}$ is large and positive everywhere except when y is large and z is small. In 3.29(d), it is instead s that is large, again resulting in division in the sign of $\dot{z}$, this time along the horizontal (y) axis; this results from the fact that the sign of z in the first place is now the most substantial component determining the sign and magnitude of $\dot{z}$.

More extreme patterns are demonstrated in figure 3.31. 3.31(a) shows high reward- and intrinsic-motor reinforcement (r and s, respectively), with somewhat increased f. The large intrinsic reinforcement parameter results in the large negative values of $\dot{z}$ in quadrant IV, but large positive values everywhere else; this shows the interaction between the reward and intrinsic components of motor reinforcement with meaningful, but less substantial sensory/executive/salience control (f). 3.31(b) shows a vertical bifurcation as in 3.29(b), except f is increased even more substantially, resulting in larger absolute values for $\dot{z}$ and the "fingerprint" pattern caused by the predominance of the executive (f) parameter over the model's dynamics in time. 3.31(c) shows constant positive stimulus input (setting $\omega = 1$ results in no change to the initial value over time). Under these conditions, executive influence is increased even though f is not altered from 3.31(a). 3.31(d) shows that high reward-reinforcement (r) results in a "buffering" effect wherein the potential for sensory/executive/salience influences to tamp down relative reinforcement-motor activation is limited, preventing the deep groove represented by negative $\dot{z}$ shown in the dynamics of 3.31(c).

Note on phase portraits: In all phase portraits representing the dynamical behavior of the model, the horizontal axis is y, the vertical axis is z, and vectors representing $\dot{y}$ and $\dot{z}$, where shown, point in the appropriate direction for each combination of initial conditions in y and z and are color mapped with low values of $\dot{z}$ cyan (#00ffff) and high ones red (#ff0000). Until section 3.7.5, when vector fields are absent, the plotted phase trajectories will be color mapped according to the same scheme. The scale/bounds of the axes are arbitrary and unitless, but each axis can be considered to correspond to putative baseline activity within the relevant subnetworks. To most simply represent general dynamical tendencies, graphs with neither phase trajectories nor vectors, but instead color mapping of the coordinate grid itself according to the scheme above, are shown as adjunct representations to the phase portraits in the subject-level and model modulation analyses. Revision of the color mapping parameters for the nonlinear model extension in section 3.7.5 is described in figure 3.7.5.

Figure 3.27: Explanation of phase portrait representations of dynamical model behavior in arbitrary, and group- and subject-level diagrams.
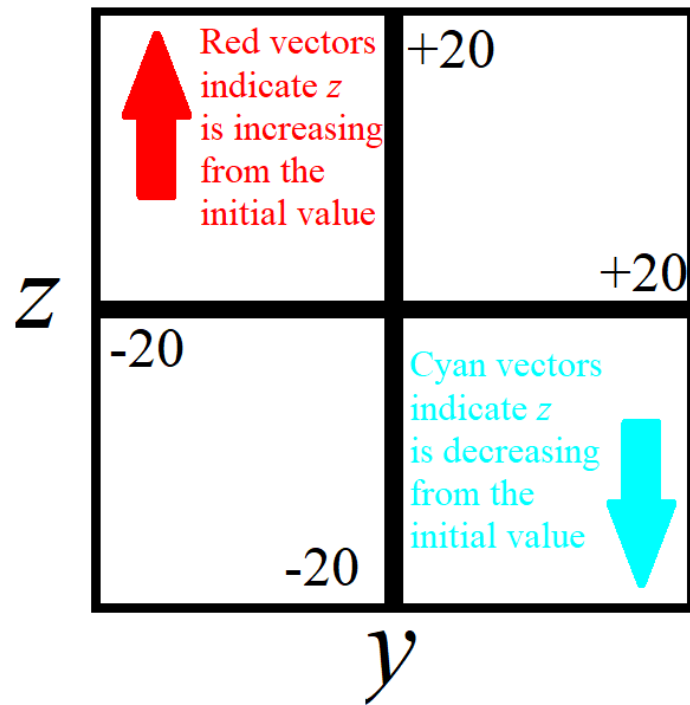
Figure 3.28: Phase portraits depict dynamical behavior of the model within the arbitrary bounds of -20 to +20 of relative modeled cumulative cortical activation for the horizontal (y) and vertical (z) axes, representing executive network and excess motor reinforcement network activity, respectively.

(a) BALANCE

(b) EXECUTIVESUPREMACY

(c) MOTORCRUSH

(d) INTRINSICDOMINANCE
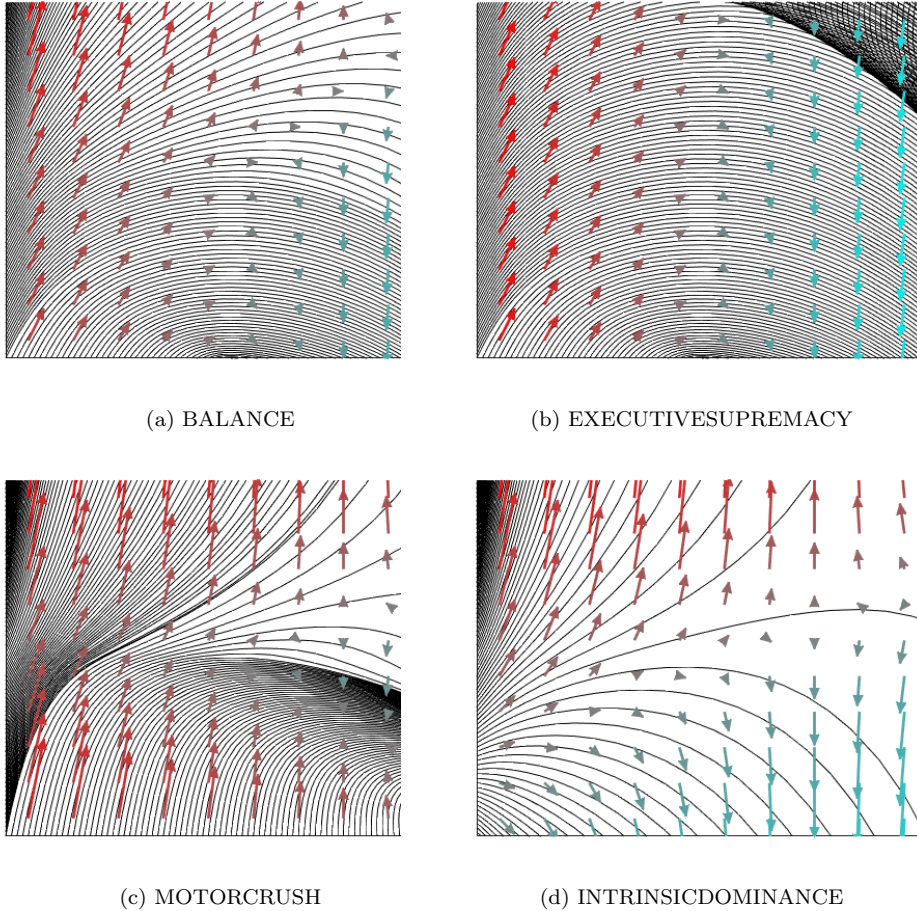
Figure 3.29: Representative dynamical behaviors of the model. See figure 3.28 for a schematic summary of these and other phase portrait representations in this section. (a) Gentle oscillations in y and z with modest stimulus input and balanced reinforcement and executive inhibition. (b) Motor reinforcement one-tenth of that in (a), leading to a bifurcation in behavior between negative y values (executive reinforces motor) and positive ones (executive damps motor). (c) Motor reward reinforcement is quadruple that in (a), leading to rapid escalation of exuberant motor reinforcement with slight changes in initial motor activity. (d) Similar to (c), except intrinsic (within-subnetwork) reinforcement, rather than reward reinforcement, dominates the trajectory of z. See figure 3.30 for the parameters used.

```
BALANCE

r = 1; %motor reinforcement strength

s = 1; %intrinsic reward strength

EXECUTIVESUPREMACY

r = 0.1; %motor reinforcement strength

s = 0.1; %intrinsic reward strength

MOTORCRUSH

r = 4; %motor reinforcement strength

s = 1; %intrinsic reward strength

INTRINSICDOMINANCE

r = 1; %motor reinforcement strength

s = 4; %intrinsic reward strength

Common

c = 1 %executive network sensitivity (parameter)

n = 0.05 %stimulus-negative decay of executive activation

f = 2 %executive control

w = 0; %stimulus function angular frequency

mact = 0.1 %motoric activation

j = 0.5 %stimulus initial condition
```

Figure 3.30: Representative arbitrary parameter values

(a) VOLATILE

(b) EXECUTED

(c) DRIVEN

(d) DRIVING
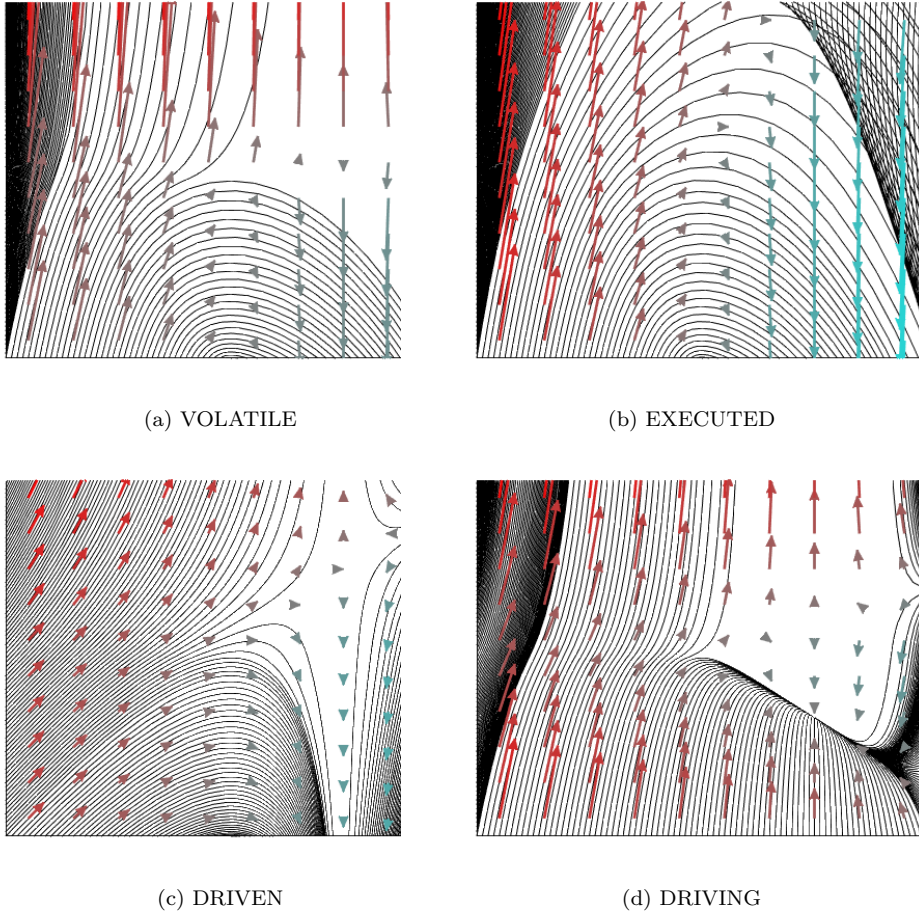
Figure 3.31: Dynamic reorientation and emergent patterns in the dynamical model with more substantial alterations of the model parameters. (a) All parameter strengths are influenced, with intrinsic and reward motor reinforcement both dominating executive inhibition of motor activity. There is a critical threshold of motor activity clearly visible where executive effects become trivial. (b) The reverse, intense dominance of executive network influences. The trajectory of z is determined almost entirely by the value of y. (c) Constant strong stimulus drive, rather than the cognitive/motor reciprocal influences, become apparent with this set of parameters, as the term `mact` is multiplied by the entirety of $\dot{z}$, reducing motor significance wholesale in this realization of the model. (d) Driving stimulus influence can avert suprathreshold runaway motor activity to an extent in comparison with figures 3.29 (c), but forceful motor reward reinforcement does still overcome it outside of the "valley" of stable and small $\dot{z}$ in quadrant IV of the phase portrait. See figure 3.32 for the parameters used.

```
VOLATILE

r = 4; %motor reinforcement strength

f = 2

s = 4; %intrinsic reward strength

mact = 0.25 %motoric activation

EXECUTED

r = 1; %motor reinforcement strength

f = 6

s = 1; %intrinsic reward strength

mact = 0.1 %motoric activation

DRIVEN

r = 1; %motor reinforcement strength sn

f = 2

s = 1; %intrinsic reward strength st

mact = 0.05 %motoric activation

DRIVING

c = 1 %executive network sensitivity (parameter)

n = 0.05 %stimulus-negative decay of executive activation

r = 4; %motor reinforcement strength sn

f = 2

s = 1; %intrinsic reward strength st

mact = 0.1 %motoric activation

Common

c = 1 %executive network sensitivity (parameter)

n = 0.05 %stimulus-negative decay of executive activation

j = 0.5 %stimulus initial condition

w = 0; %stimulus function angular frequency
```

Figure 3.32: Potentiated arbitrary parameter values

RRB-severity category subgroup derived parameters

Connectivity values for low- and high-RRB severity category subgroups for the relevant connections are given in tables 3.14 and 3.15. The connection labeling scheme is depicted in figure 3.33. The connectivity values are used to calculate parameter values according to equations 3.3 and 3.4. Calculated parameter values are given in table 3.16. The dynamics of the model with low- and high-RRB connectivity derived empirical parameters and a default set of exogenous parameters is given in figure 3.36. Model dynamical behavior for the subgroups under different modeled stimulus conditions is given in figures 3.37 and 3.38.

Salient observations are:

1. There is a pattern of changes between the empirical parameter values for the two groups that reflects possible aspects of the underlying network behavior associated with high-RRB severity.

2. 73.3% of initial conditions tested predicted increased reinforcement- and reward-motor activation, $\dot{z}$, using the high-RRB parameters versus 36.7% for the low.

3. There are clearly distinct dynamical patterns between the subgroup models consistent with expectation.

4. There are clearly distinct changes associated with varying stimulus drive conditions between the subgroup models consistent with expectation.

Figure 3.33: Node labels as used in tables 3.14 and 3.15 showing connectivity values between the nodes for low- and high-RRB subjects for use in calculating the functionally-derived model parameters.
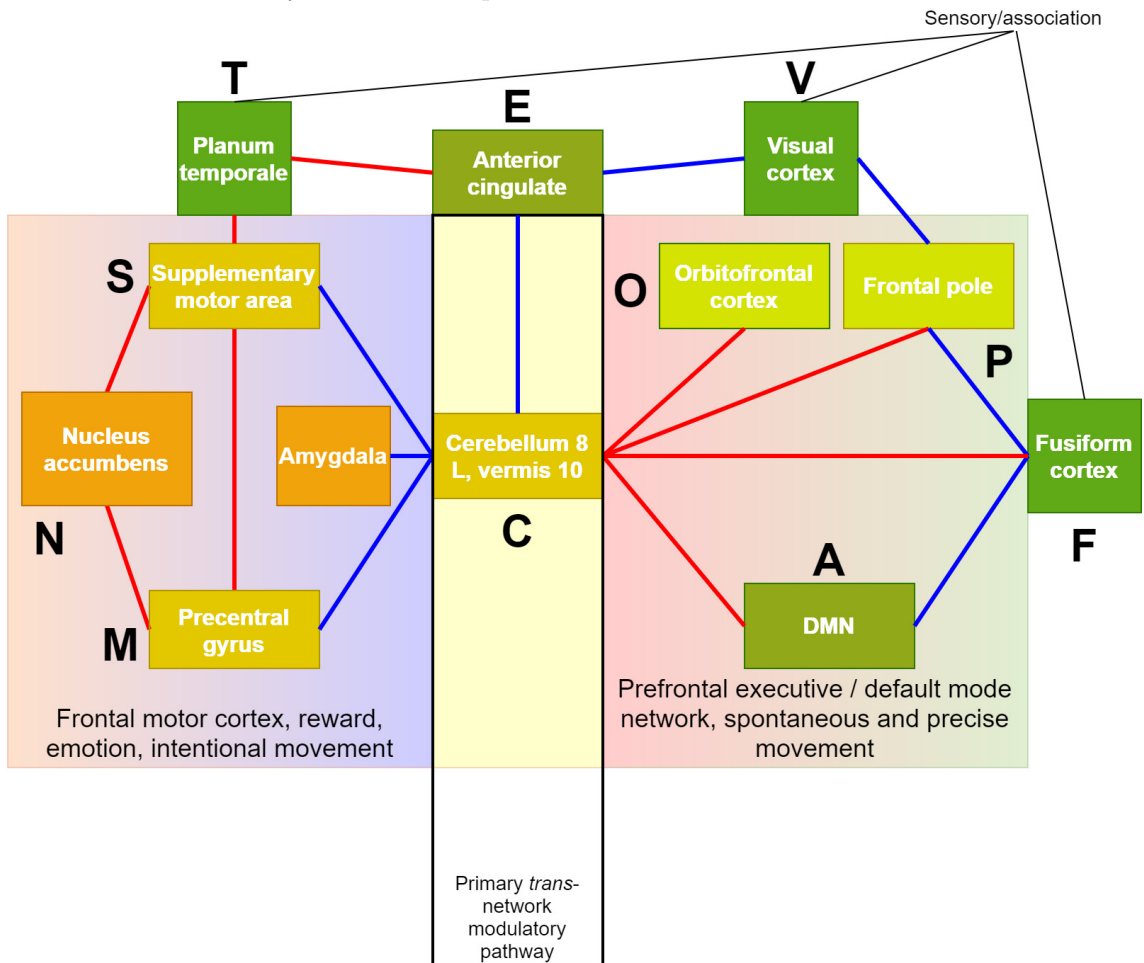
Table 3.14: Connectivity values from low-RRB subjects identified by the labels defined in figure 3.33 (connections in tables 3.4 and 3.13, "R" = right hemisphere), truncated to three decimal places, to calculate the functionally derived parameters in the model summarized in equation 3.2 according to the definitions in equations 3.3 and 3.4.

	F	FR	P	PR	A	V	VR	O	E	C	T	S	M	MR	N	
F	x	-	-	-	0.080	-	-	-	-	0.026	-	-	-	-	-	F
FR	-	x	-	-0.021	-	-	-	-	-	-0.118	-	-	-	-	-	FR
P	-	-	x	-	-	0.065	-	-	-	0.070	-	-	-	-	-	P
PR	0.107	-0.021	-	x	-	-	-	-	-	-0.141	-	-	-	-	-	PR
A	0.080	-	-	-	x	-	-	-	-	-0.191	-	-	-	-	-	A
V	-	-	0.065	-	-	x	-	-	-	-	-	-	-	-	-	V
VR	-	-	-	-	-	-	x	-	-0.028	-	-	-	-	-	-	VR
O	-	-	-	-	-	-	-	x	-	-0.095	-	-	-	-	-	O
E	-	-	-	-	-	-	-0.028	-	x	-	0.073	-	-	-	-	E
C	0.026	-0.118	0.070	-0.141	-0.191	-	-	-0.095	-	x	-	0.118	0.127	0.082	-	C
T	-	-	-	-	-	-	-	-	0.073	-	x	0.237	-	-	-	T
S	-	-	-	-	-	-	-	-	-	0.118	0.237	x	0.174	-	-0.069	S
M	-	-	-	-	-	-	-	-	-	0.127	-	0.174	x	-	-0.051	M
MR	-	-	-	-	-	-	-	-	-	0.082	-	-	-	x	-	MR
N	-	-	-	-	-	-	-	-	-	-	-	-0.069	-0.051	-	x	N
	F	FR	P	PR	A	V	VR	O	E	C	T	S	M	MR	N	

Table 3.15: Connectivity values from high-RRB subjects identified by the labels defined in figure 3.33 (connections in tables 3.4 and 3.13), truncated to three decimal places, to calculate the functionally derived parameters in the model summarized in equation 3.2 according to the definitions in equations 3.3 and 3.4.

	F	FR	P	PR	A	V	VR	O	E	C	T	S	M	MR	N	
F	x	-	-	-	-0.189	-	-	-	-	0.122	-	-	-	-	-	F
FR	-	x	-	-0.246	-	-	-	-	-	-	-	-	-	-	-	FR
P	-	-	x	-	-	-0.225	-	-	-	-0.107	-	-	-	-	-	P
PR	-0.162	-0.246	-	x	-	-	-	-	-	-0.021	-	-	-	-	-	PR
A	-0.189	-	-	-	x	-	-	-	-	0.010	-	-	-	-	-	A
V	-	-	-0.225	-	-	x	-	-	-	-	-	-	-	-	-	V
VR	-	-	-	-	-	-	x	-	-0.241	-	-	-	-	-	-	VR
O	-	-	-	-	-	-	-	x	-	0.054	-	-	-	-	-	O
E	-	-	-	-	-	-	-0.241	-	x	-	0.424	-	-	-	-	E
C	0.122	0.160	-0.107	-0.021	0.010	-	-	0.054	-	x	-	-0.026	-0.049	-0.066	-	C
T	-	-	-	-	-	-	-	-	0.424	-	x	0.526	-	-	-	T
S	-	-	-	-	-	-	-	-	-	-0.026	0.526	x	0.510	-	0.180	S
M	-	-	-	-	-	-	-	-	-	-0.049	-	0.510	x	-	0.226	M
MR	-	-	-	-	-	-	-	-	-	-0.066	-	-	-	x	-	MR
N	-	-	-	-	-	-	-	-	-	-	-	0.180	0.226	-	x	N
	F	FR	P	PR	A	V	VR	O	E	C	T	S	M	MR	N	

Figure 3.34: Connectivity-based formula for calculating the value of the empirical dynamical model parameters r and s, or the motor reward and intrinsic motor reinforcement parameters. The terms and the interactions within them follow every path possible from and between putative motor areas, counting all possible interaction along the network edges between the relevant nodes within the motor/reward subunit once. The variable names comprise the two node ends according to the lettering scheme in figure 3.33, with subscripts representing the second node forming the functional connection.

$$r \approx S_N + N_M + S_N M_S + N_M M_S$$

$$s \approx M_S$$

$$(3.3)$$

Figure 3.35: Connectivity-based formula for calculating the value of the empirical dynamical model parameter f, or the executive network influence parameter. The terms and the interactions within them follow every path possible from sensory areas (here, V, VR, F, FR, O, T) to motor areas, including through interactions between motor areas, counting every possible interaction along the network edges between the relevant nodes once, except those passing between cerebellum and anterior cingulate cortex, taken in this formulation to be functionally separable modulatory hubs between subnetworks. The variable names comprise the two node ends according to the lettering scheme in figure 3.33, with subscripts representing the second node forming the functional connection.

$f \approx$

from sensory to frontal pole via cerebellum to motor/reward:

$(PR_F + PR_{FR})C_{PR}S_C + P_V C_P S_C + (PR_F + PR_{FR})C_{PR}M_C + P_V C_P M_C$

$+(PR_F + PR_{FR})C_{PR}MR_C + P_V C_P MR_C + (PR_F + PR_{FR})C_{PR}S_C M_S$

$+P_V C_P S_C M_S + (PR_F + PR_{FR})C_{PR}M_C M_S + P_V C_P M_C M_S$

$+(PR_F + PR_{FR})C_{PR}S_C S_N N_M + P_V C_P S_C S_N N_M$

$+(PR_F + PR_{FR})C_{PR}M_C N_M S_N + P_V C_P M_C N_M S_N$

from sensory (fusiform) to default mode via cerebellum to motor/reward:

$+A_F C_A S_C + A_F C_A M_C + A_F C_A MR_C + A_F C_A S_C M_S + A_F C_A M_C M_S$

$+A_F C_A S_C S_N N_M + A_F C_A M_C N_M S_N$

from sensory (fusiform) via cerebellum to motor/reward:

$+C_F S_C + C_F M_C + C_F MR_C + C_F S_C M_S + C_F M_C M_S + C_F S_C S_N N_M$

$+C_F M_C N_M S_N + C_{FR}S_C + C_{FR}M_C + C_{FR}MR_C + C_{FR}S_C M_S + C_{FR}M_C M_S$

$+C_{FR}S_C S_N N_M + C_{FR}M_C N_M S_N$

from sensory (visual) via anterior cingulate to planum temporale:

$+E_{VR}T_E S_T + E_{VR}T_E S_T M_S + E_{VR}T_E S_T S_N N_M M_S$

from sensory (orbitofrontal) via cerebellum to motor/reward:

$+C_O S_C + C_O M_C + C_O M_{RC} + C_O S_C M_S + C_O M_C M_S + C_O S_C S_N N_M$

$+C_O M_C N_M S_N$

from sensory (planum temporale) to supplementary motor:

$+S_T + S_T M_S + S_T S_N N_M$

(3.4)

Table 3.16: The calculated values for the empirical parameters r, s, and f, the motor reinforcement, intrinsic motor, and executive and salience network influence, for low- and high-RRB category subjects.

	Low-RRB average	High-RRB average
r	-0.1413	0.6150
s	0.1748	0.5106
f	0.2003	0.6667

(a) Low-RRB-derived empirical parameters

(b) High-RRB-derived empirical parameters
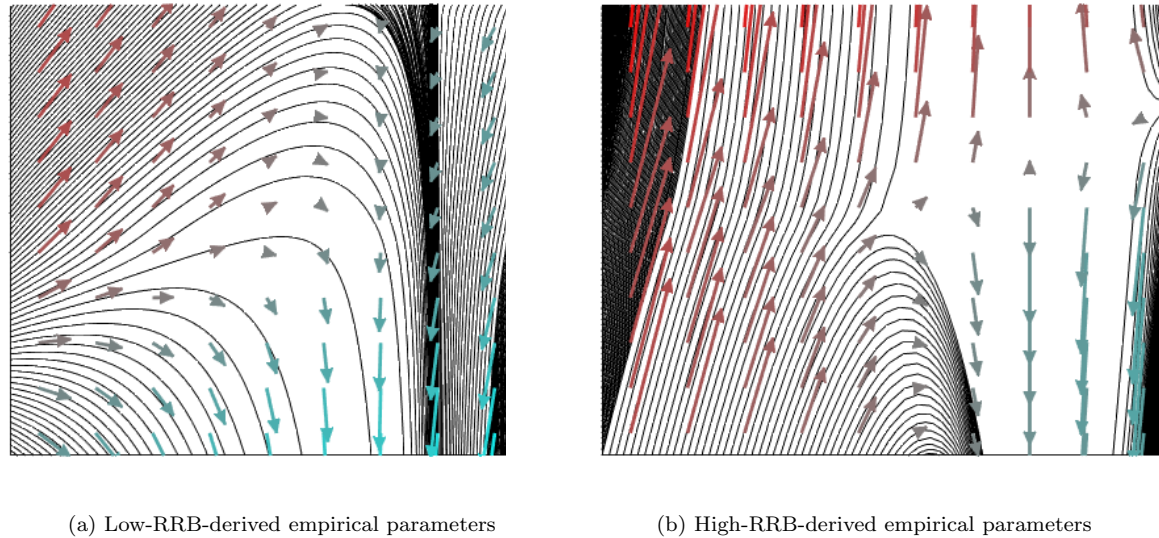
Figure 3.36: Phase portrait of the dynamical model, equation 3.2, using parameter values for r, s, and f according to equations 3.3 and 3.4. The arbitrary parameters are set at "default" values, with $c = 1$, $\delta = 0.1$, $w = 0$, $j = 0.5$, and no scaling of motor activity (`mact` used to demonstrate intrinsic model dynamics in figures 3.29 and 3.31). Using values for the relative influence of motor reward, intrinsic motor, and executive influences derived from connectivity averages in the low- and high-RRB subgroups based on summing all possible interactions across the three relevant subnetworks through the cerebellar or cingulate hubs, a clear pattern is evident between the dynamical behavior of the two models. While there is strong motor reward reinforcement in the high-RRB model ($r = 0.6150$) this effect is actually reversed in the low-RRB group. Potentially a relevant indicator of the nature of cognitive control mechanisms in RRB presentations, coupling between executive and motor subnetworks is actually stronger in the high-RRB subject subgroup. While this greater executive control may serve to balance intrinsically and reward-driven motor behavior, the actual trajectories through the z direction show the bifurcated behavior evident in 3.31 (d). As in that case, motor reinforcement can cause runaway activation of the motor network. While 3.31 (d) uses simple arbitrary values for the functional parameters ($r = 4$, $s = 1$, $f = 2$), the functional parameters in (b) in this figure were obtained empirically using only, and all of, the underlying connectivity data for the proposed subnetworks for the high-RRB group. The similar dynamic behavior of the two phase portraits suggests the physiological plausibility of the dynamical model by showing it can successfully account for the behavior of the putative real brain network by many fewer parameters than are represented by the actual Pearson correlation values used to construct them.
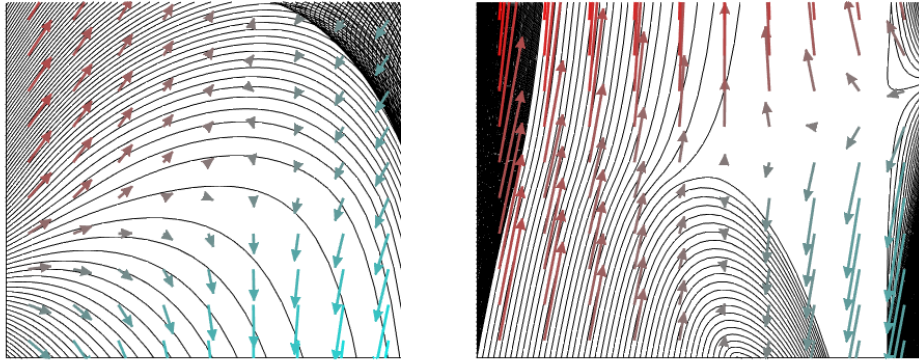
(a) Low-RRB model with more static stimulus (b) High-RRB model with increased stimulus
drive   drive
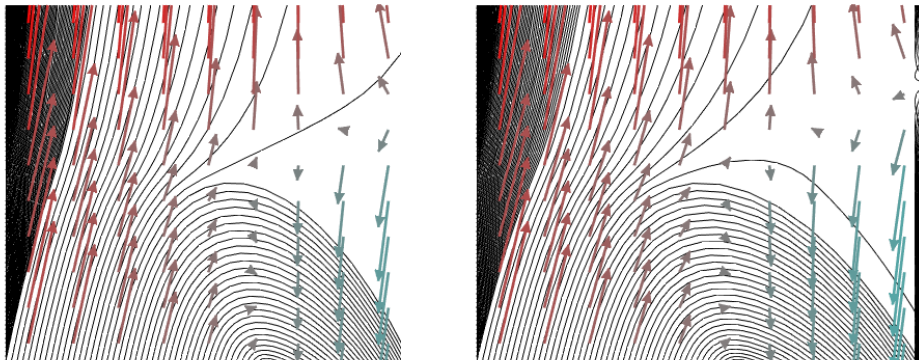
(c) Increased stimulus amplitude compared to   (d) Even greater stimulus magnitude
(a) and (b) in the High-RRB model

Figure 3.37: Manipulation of static stimulus amplitude in the empirical dynamical model. As would be predicted in clinical ASD, high-RRB severity is associated with a less robust modeled responsive to external stimulus drive in the terms of alterations to ostensible prepotent activity patterns (represented by excess reinforcement activation in motor areas in the model). While increasing stimulus magnitude does tend to fill the unstable void in the phase portrait trajectories by moderating motor reinforcement to an extent, even with much greater stimulus input amplitude, the bifurcation between phase trajectories in the high-RRB derived model is still evident.
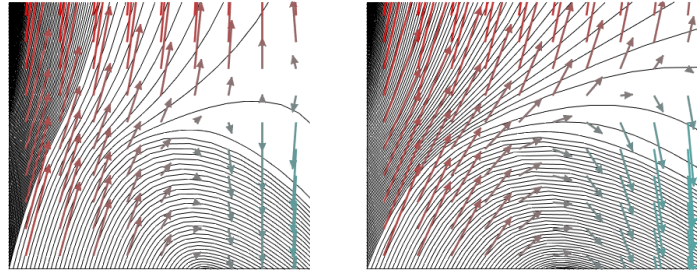
(a) High-RRB, double the stimulus magnitude as in 3.37 (c)

(b) High-RRB, quintuple the stimulus magnitude as in 3.37 (c)

(c) High-RRB, ten time the stimulus magnitude as in 3.37 (c)
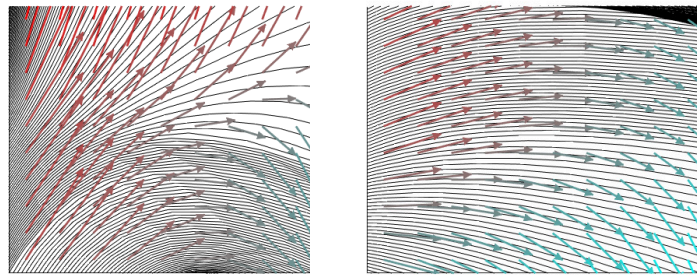
(d) Low-RRB, ten times the stimulus magnitude as in 3.37 (c)
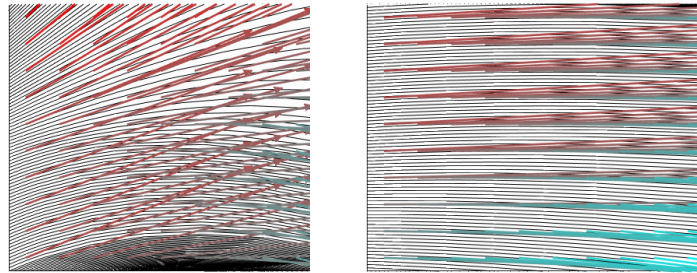
(e) High-RRB, 100 times the stimulus magnitude as in 3.37 (c)

(f) Low-RRB, 100 times the stimulus magnitude as in 3.37 (c)

Figure 3.38: Variation of stimulus drive magnitude across two orders of magnitude shows more substantial perturbations in the realization of the model using the high-RRB empirical dynamical coefficients. (a), (b), (c), and (e) represent the high-RRB case, (d) and (f), low. The motor-reward feedback loop reinforces extreme motor reinforcement and creates instability in trajectories in the phase portrait in the high-RRB cases. Again, apparent recovery of low-RRB cognitive dynamic behavior is possible with increased stimulus drive, but even at extreme stimulus amplitudes, 200 times higher than the default value of $j = 0.5$, the low-RRB phase portrait maintains regularly patterned trajectories, while the high-RRB case shows more abrupt transitions in the direction vectors in the yz plane representing, respectively, executive network activation and motor reinforcement.

Individual subject-level derived parameters

Subject-level connectivity statistics were extracted for the connections require to calculate the empirical parameter values for model 3.2 according to equations 3.3 and 3.4.

Phase portraits for all subjects are shown in figure 3.39. Color maps using the same scale showing the $\dot{z}$ component at each combination of initial conditions, with low values in cool colors and high values in hot colors, are shown in figure 3.40 for each subject. The values indicated by the color map can be averaged for the ith subject according to

$$\bar{z}_i = \sum_{j=y_{\min}}^{y_{\max}} \sum_{k=z_{\min}}^{z_{\max}} \frac{r_i|k| + s_i k - f_i j}{jk} \tag{3.5}$$

where the bounds of summation correspond to the coordinate boundaries represented by the color map plots. Because the proxy measure $\bar{z}_i$ is scale-free, it can be more simply expressed as

$$\hat{z}_i = \sum_{j=y_{\min}}^{y_{\max}} \sum_{k=z_{\min}}^{z_{\max}} r_i|k| + s_i k - f_i j. \tag{3.6}$$

Given the unaltered value of f and the symmetrical bounds over which this statistic is calculated, the statistic captures specifically intrinsic and reward reinforcement strength on motor cortex activation. f significantly affects modeled neural dynamics as the phase portraits have shown so far, and $\hat{z}$ isolates the hypothesized cognitive mechanism driving RRB-like motoric behavior.

The value of $\hat{z}$ across all of the depicted initial conditions for each subject is plotted versus subject RBS-R CSS in figure 3.41. Regression analysis using RBS-R as the independent variable and summed (or effectively, averaged) $\dot{z}$ components is given in table 3.17. The proposed form of the relationship between the variable of interest is thus

$$\text{R} = \alpha \hat{z} + \beta + \epsilon \tag{3.7}$$

where R is RBS-R CSS, α is the regression coefficient, β is the intercept, and ϵ is the error term.

These results demonstrate that, at the subject level, the dynamical model successfully predicts over half of the variance in the original subject RBS-R CSS with a p-value for the regressor coefficient of 2.81×10^{-6}. Hence, the dynamical model, which takes only three empirical parameters as inputs, is successful at predicting RRB intensity (as RBS-R CSS) at the subject level.

153
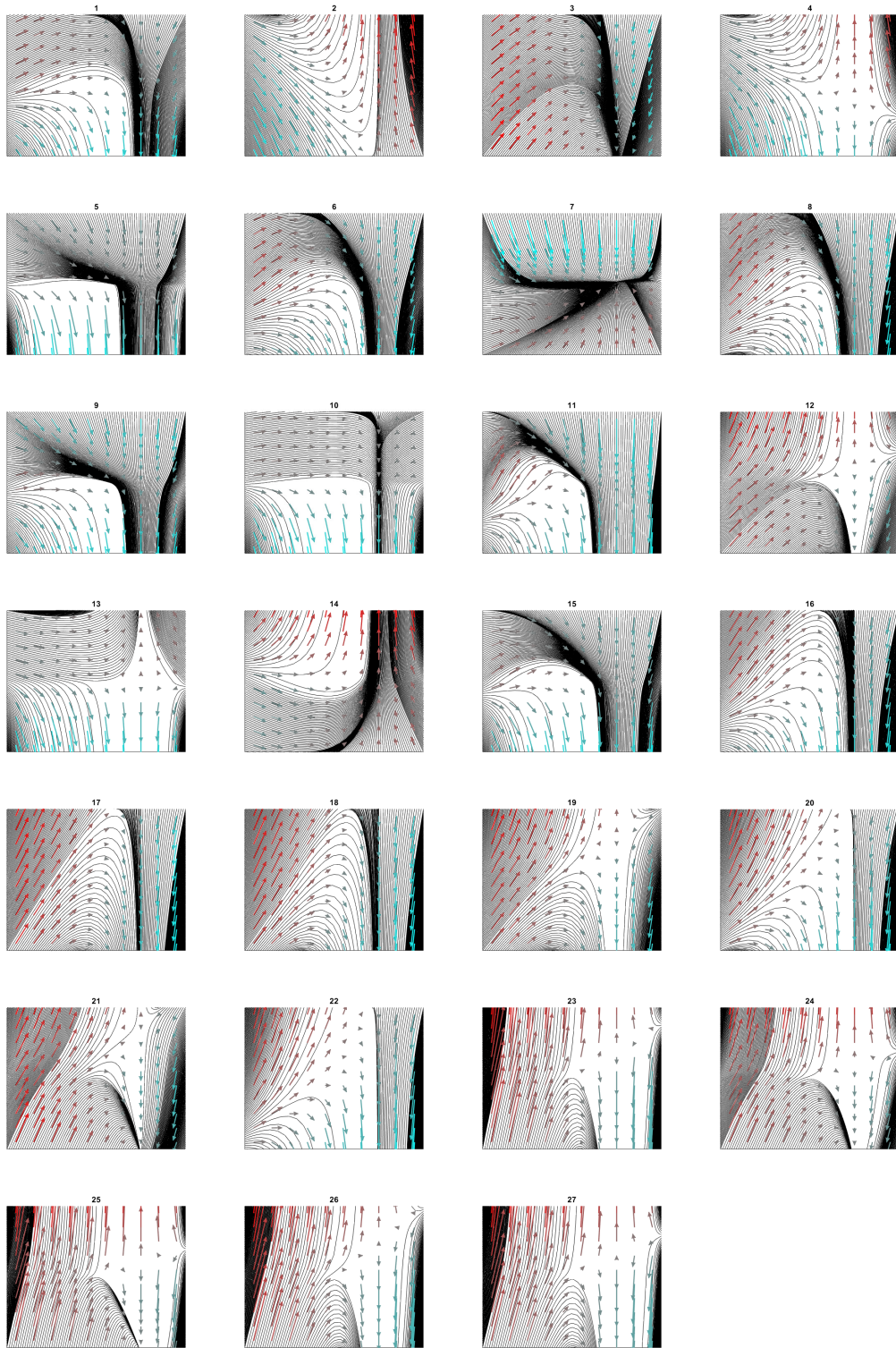
Figure 3.39: Subject-level phase portraits.
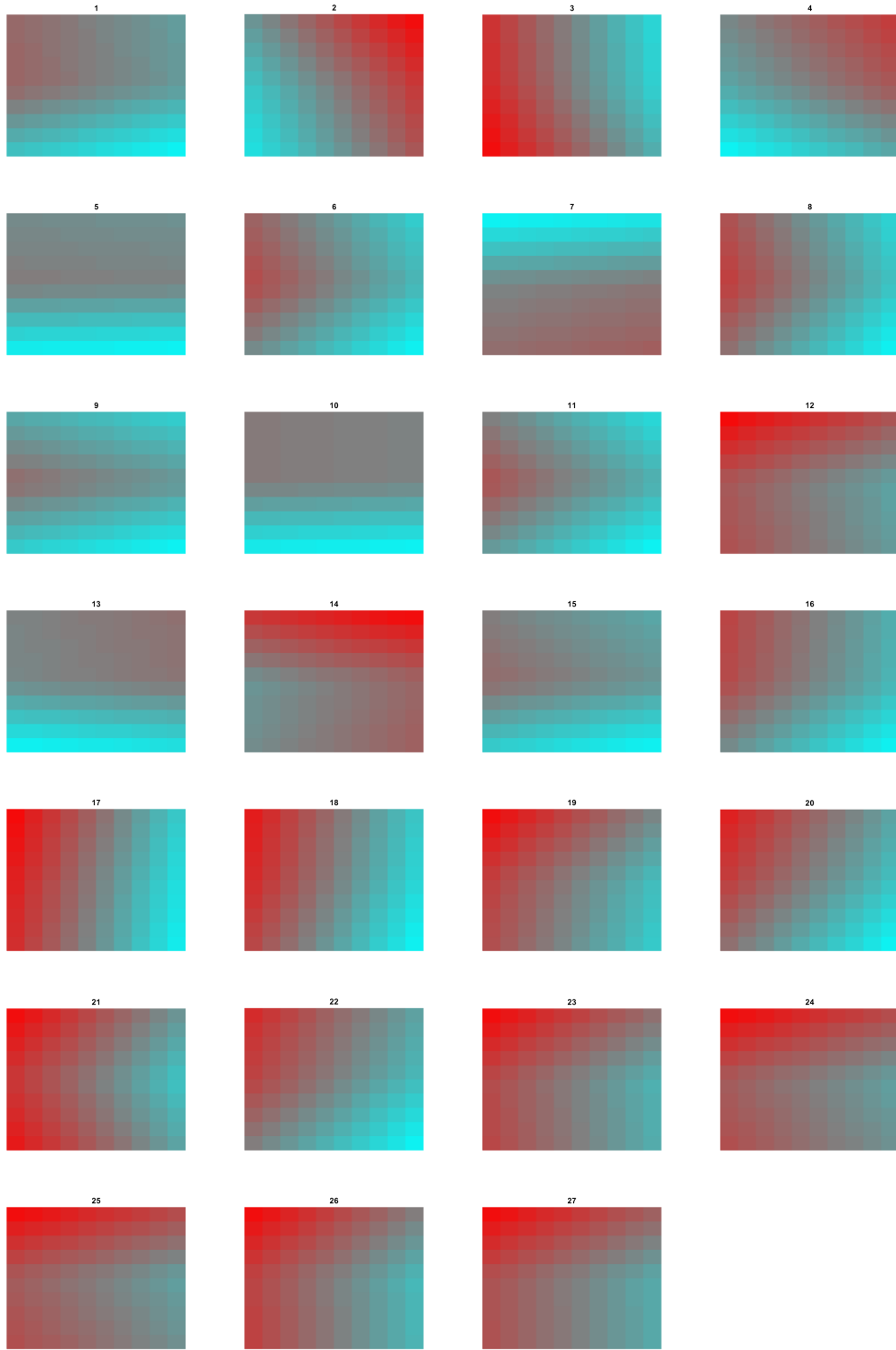
Figure 3.40: Subject-level dynamic color maps of $\bar{z}_0$.
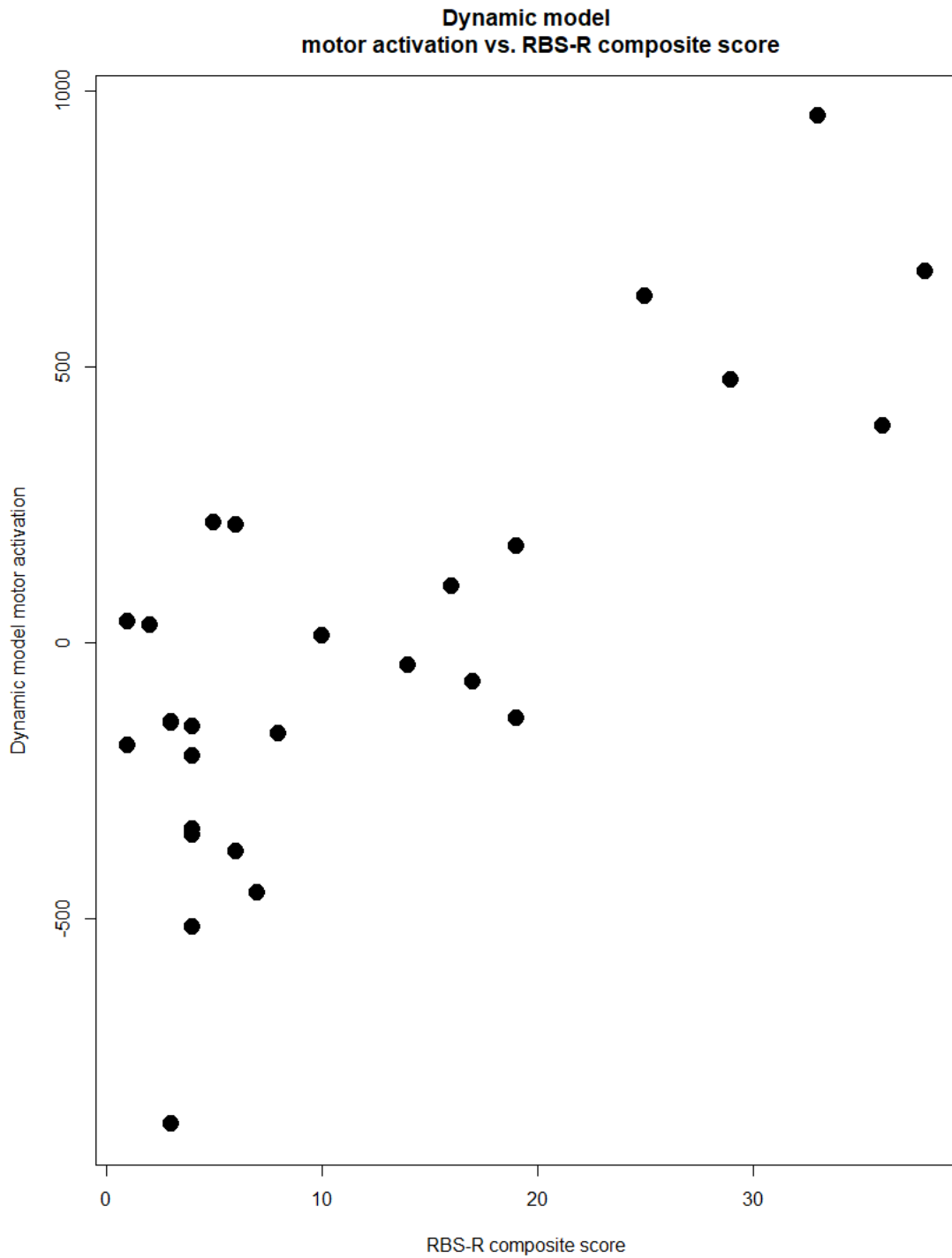
Figure 3.41: Graph of subject-level dynamical model prediction of excess motor reinforcement averaged across initial condition vs. subject RBS-R CSS. A putative linear relationship would suggest that the model accurately captures RRB intensity, and hence the putative network does; in the absence of the real significance of the full network in figure 3.21 to RRB intensity, the variables would be unrelated.

Table 3.17: OLS regression model for subject-level dynamical model prediction of motor reinforcement averaged across initial conditions on subject RBS-R CSS. Multiple $R^2 = 0.591$. Any significant regression coefficient, as well as the total variance explained, indicates the plausibility of the proposed network's subserving the dynamical process giving rise to RRBs, as determined by the model form and empirical model parameters arising from subject-level connectivity values.

	Estimate	Std. error	t-value	$\Pr(>|t|)$
Intercept	-326.351	72.595	-4.495	0.000138***
rbsrtot	26.756	4.451	6.011	2.81e-06***

3.7.3   Initial assessments of model validity

In order to establish preliminary model validity and plausibility, a naïve formulation of the base model form was constructed as follows:

$$\dot{x} = -\omega \sin(\omega t)$$
$$\dot{y} = cx - \delta y \tag{3.8}$$
$$\dot{z} = rz + s + fy$$

The differences between this naïve model and the conjectured physiologically and functionally valid model given in equation 3.2 is that the z factor in the rz term in $\dot{z}$ is now the verbatim, rather than absolute value of z, and the fy term is positive, hence yielding a value of z in the model that instead represents the total modeled motor cortical activation, rather than that due exclusively to, and in excess of, intrinsic- and reward-reinforcement influences. For this assessment, ω is again held at 0.

First, regression modeling as in the previous section at the subject level is not possible; given that symmetrical bounds were used for each axis (i.e., in equation 3.6, $j = k$), all three terms in $\dot{z}$ will cancel out when calculating $\hat{\dot{z}}_i$, modifying equation 3.7 to

$$R = \beta + \epsilon, \tag{3.9}$$

which yields no relationship and an $R^2 = 0$, as shown in figure 3.42 and the regression analysis summary in table 3.18; only rounding-error values for $\hat{\dot{z}}_i$ result. This trivial result does, however, show that the model form, and not the *mere* use of the subject connectivity values to calculate the empirical model parameters, results in the observed correlation between the model output chosen as the regressor in equation 3.6 and subject RBS-R CSS.

While the naïve model form cannot make predictions to be tested for correlations with subject RBS-R CSS in the same way as the postulated dynamical model, it can still demonstrate varying patterns of dynamical behavior: Compare figure 3.41 with figure 3.42, and figure 3.39 with figure 3.43. Note, however, that the dynamical behavior as represented by the subject color maps is indeed always symmetrical across some line that divides the phase space exactly in half. Hence, the initial dynamical model form is confirmed as of plausible physiological and functional significance given naïve application of the same empirical model parameters alone cannot elicit the desired, or any, given the analytical form of the chose regressor, behavior or correlation with subject RBS-R CSS. A potentially meaningful qualitative observation can however be made regarding dynamical

behavior even in the naïve-form model: Figure 3.43 shows, as in several priorly observed metrics (connectivity value sign, regression model significance with binary contrast, separability in figure 3.41 between the low- and high-groups into non-overlapping regions, discrete dynamical regimes in the postulated relevant form of the model based on parameters derived from subgroup membership) a consistent regime of dynamical behavior for the high-RRB (subplots 23-27) subjects that does not continue in the very next subject (22) phase portrait. Hence, while the naïve-form model cannot produce output in terms of predicted motor-reinforcement activation, the parameter values alone still substantially enforce identifiably distinct regimes of dynamical behavior. Nevertheless, the comparison summarized in table 3.18 show that it is the specific form of the dynamical model, and not the use of calculated subject connectivity values to derive parameters alone, that yields the observed correlation between model output and subject RBS CSS.

Beyond a minimal demonstration of the significance of the specific model system to its correlation with a behavioral measure itself correlated with the functional connectivity values used to derive the model parameters, the superior predictive ability, at least in the form of greater linear correlation, of the chosen model system in contrast to a putative alternative that can also produce output that can be regressed on, should be demonstrable if the model is to be accorded preliminary behavioral and neurophysiological plausibility. The naïve model formulation can be modified such that summation across the coordinate plane still does return variable results by subject if the analysis is restricted so that $\hat{z}_i$ is calculated only for quadrant I. Explicitly, this model form alters equation 3.6 to

$$\hat{z}_i = \sum_{j=0}^{y_{\max}} \sum_{k=0}^{z_{\max}} r_i k + s_i k + f_i j; \tag{3.10}$$

the differences are the absolute value is no longer taken of z, as in the naïve form so far used, $f_i j$ is added, again as in the naïve form so far used, and the bounds are restricted to quadrant I (non-negative j and k) only. By so doing, it can be assessed if the previously observed correlation in figure 3.41 and table 3.17 is actually due to the positive motor-reward-reinforcement in below-baseline motor activation and the calculation of specifically motor activation *not* due to stimulus/executive/salience network effects, and furthermore above and beyond them, or again, *only* the per-subject derived parameter values. The scatter plot of this variation is shown in figure 3.45. Model summaries for the original model with the postulated form, the naïve form restricted to quadrant I, and a J-test between them is summarized in table 3.19. While the quadrant-I-only naïve model is in fact of overall significance, the model as originally postulated improves its predictions significantly according to the J-test to five decimal places, while it itself does not significantly improve the model as originally postulated. Moreover, in this case, unlike in the original dynamical

model-based regression, the 5 "high-"RRB subjects are unisolable within the coordinate plane from the "low-"RRB subjects (there is overlap between these and "low-"RRB subjects on the vertical axis), breaking the above-mentioned repeatedly observed pattern of such separability. This separability is shown in figure 3.46. This further reduces the maximum plausibility of this "improved' naïve model form in terms of the postulated network dynamical behavior it was contrived to encapsulate. Leave-one-out cross-validation was performed on both the original and naïve quadrant I models. Summary statistics are given in table 3.20. As leave-one-out cross validation can both inform regarding aspects relevant to the potential for generalization of tested models, and also aid in making comparisons between models, the within-model difference in output between the left-out estimates and the fill model predictions was compared, as shown in figure 3.47 , as were summary statistical differences between models; the original model explains approximately five times as much of the observed variance in the RBS-R CSSs than the naïve model, and both the root-mean-squared and mean-absolute errors associated with estimating the excluded observations were notably lesser in the original model.

These attributes of the original dynamical model form, as first conceived, verify it is not *merely* the empirical derivation of the model parameters, nor the existence of specific (non-zero) variation between the subjects in terms of model prediction based on those parameters, that result in the model significance initially observed in table 3.17. Rather, it appears that the chosen model form does in fact plausibly represent, at an absolute minimum in terms of statistical significance of the relevant behavioral measure used in this study, specific functional properties of the putative brain network that correlate with RRB severity in the form of subject RBS-R CSS.
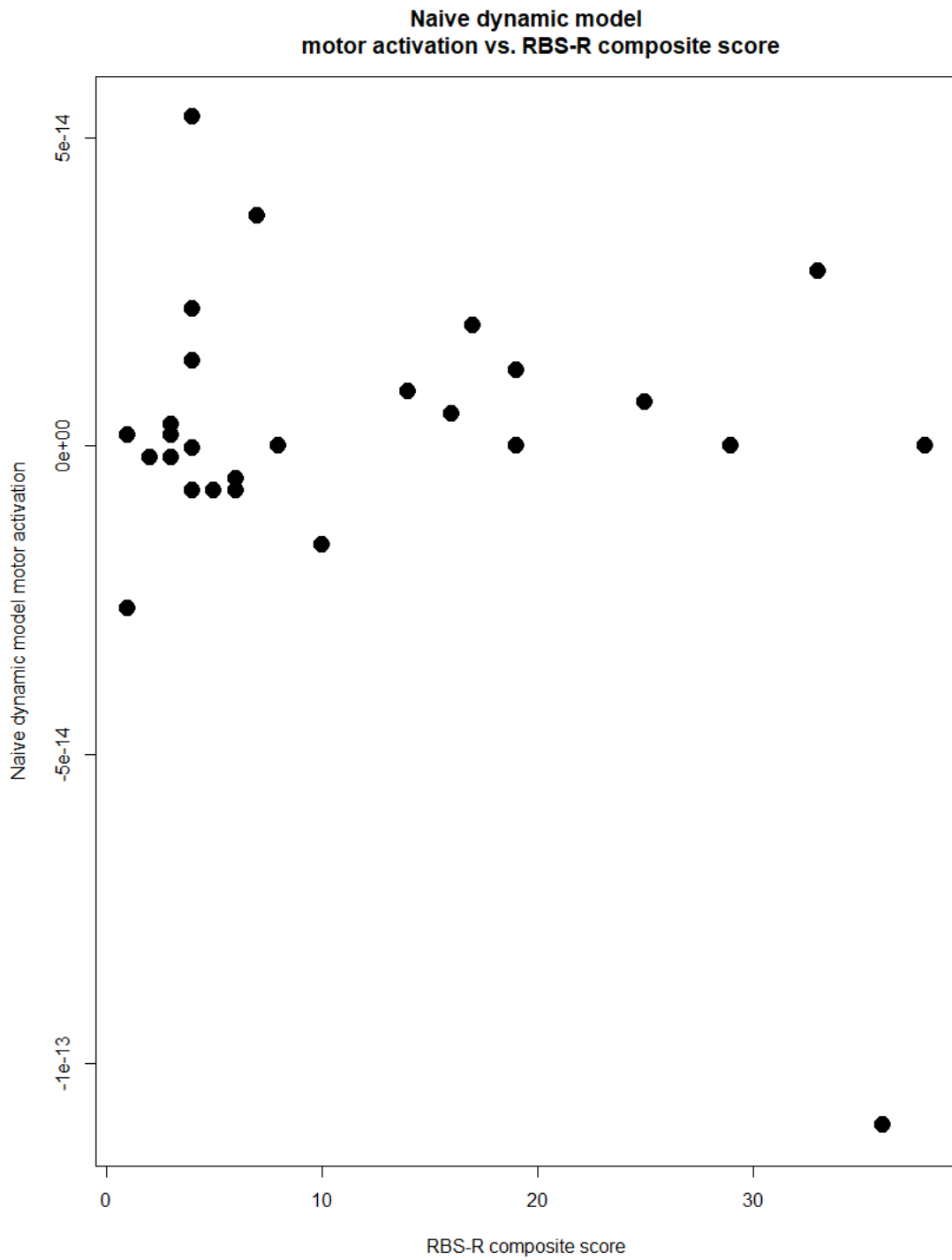
Figure 3.42: Graph of subject-level naïve dynamical model prediction of motor activation averaged across initial condition vs. subject RBS-R CSS. Compare the clear lack of correlation (variation in the independent variable is due only to rounding errors in computation) with that shown in figure 3.41.

Table 3.18: OLS regression model for (A) subject-level dynamical model and (B) naïve dynamical model prediction of motor reinforcement (hypothesized model) and absolute activation (naïve form) averaged across initial conditions on subject RBS-R CSS; the intercept and RBS-R CSS coefficient are both significant in (A) and both insignificant in (B). Again, the model in (B) strictly has a zero-correlation. (C) Davidson-MacKinnon J-test of the models reveals a significant p-value to six decimal places for the improvement of (A)'s predictions of (B)'s model fit, and an insignificant one (over 0.5 one-sided, consistent with the true lack of any correlation) for the improvement of (B)'s predictions of (A)'s model fit.

(A) Regression model from dynamical model

	Estimate	Std. error	t-value	$\Pr(> |t|)$
Intercept	-326.351	72.595	-4.495	0.000138***
rbsrtot	26.756	4.451	6.011	2.81e-06***

$R^2 = 0.591$, $p = 2.809\text{e-}06$

(B) Regression model from naïve dynamical model form

	Estimate	Std. error	t-value	$\Pr(> |t|)$
Intercept	8.820e-15	7.595e-15	1.161	0.256
rbsrtot	-6.404e-16	4.657e-16	-1.375	0.181

$R^2 = 0.07032$, $p = 0.1813$

(C) J-test of the models

Model 1: rbsrtot $\sim$ subject

Model 2: rbsrtot $\sim$ naive

	Estimate	Std. error	t-value	$\Pr(> |t|)$
M1 + fitted(M2)	0.34186	0.50144	0.6818	0.5019
M2 + fitted(M1)	0.97247	0.17296	5.6225	8.68e-06***
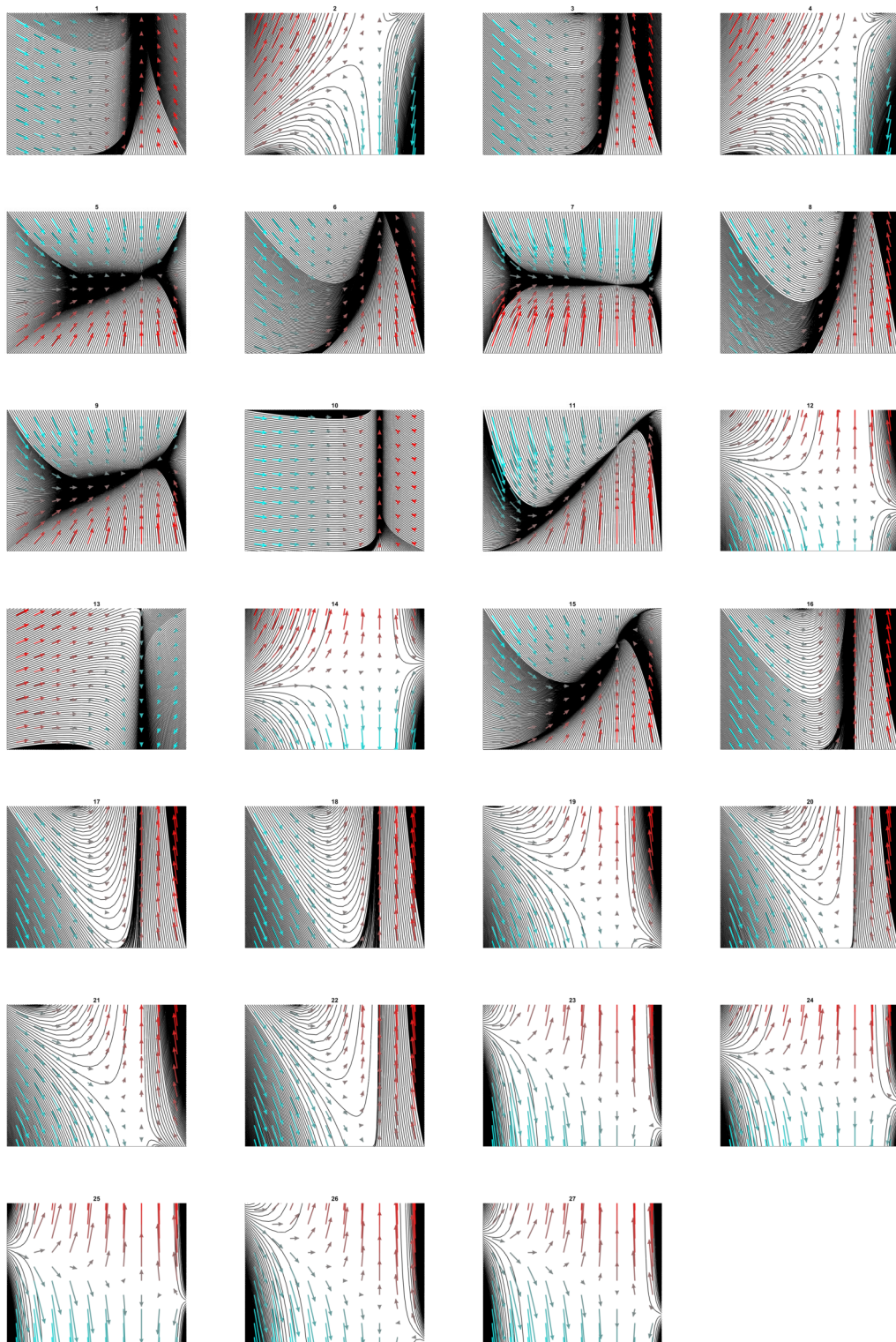
Figure 3.43: Subject-level naïve-model phase portraits.
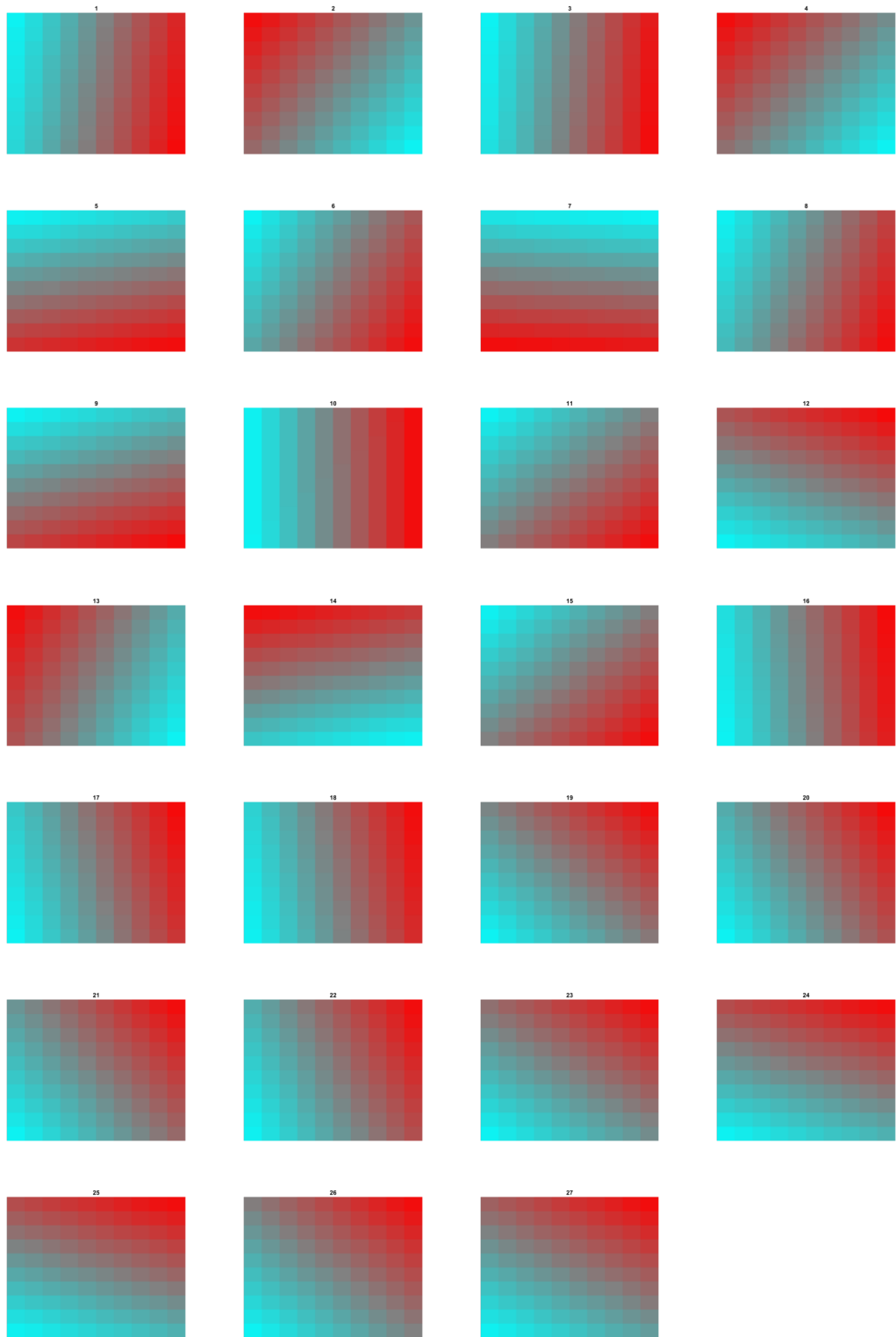
Figure 3.44: Subject-level naïve dynamic color maps.
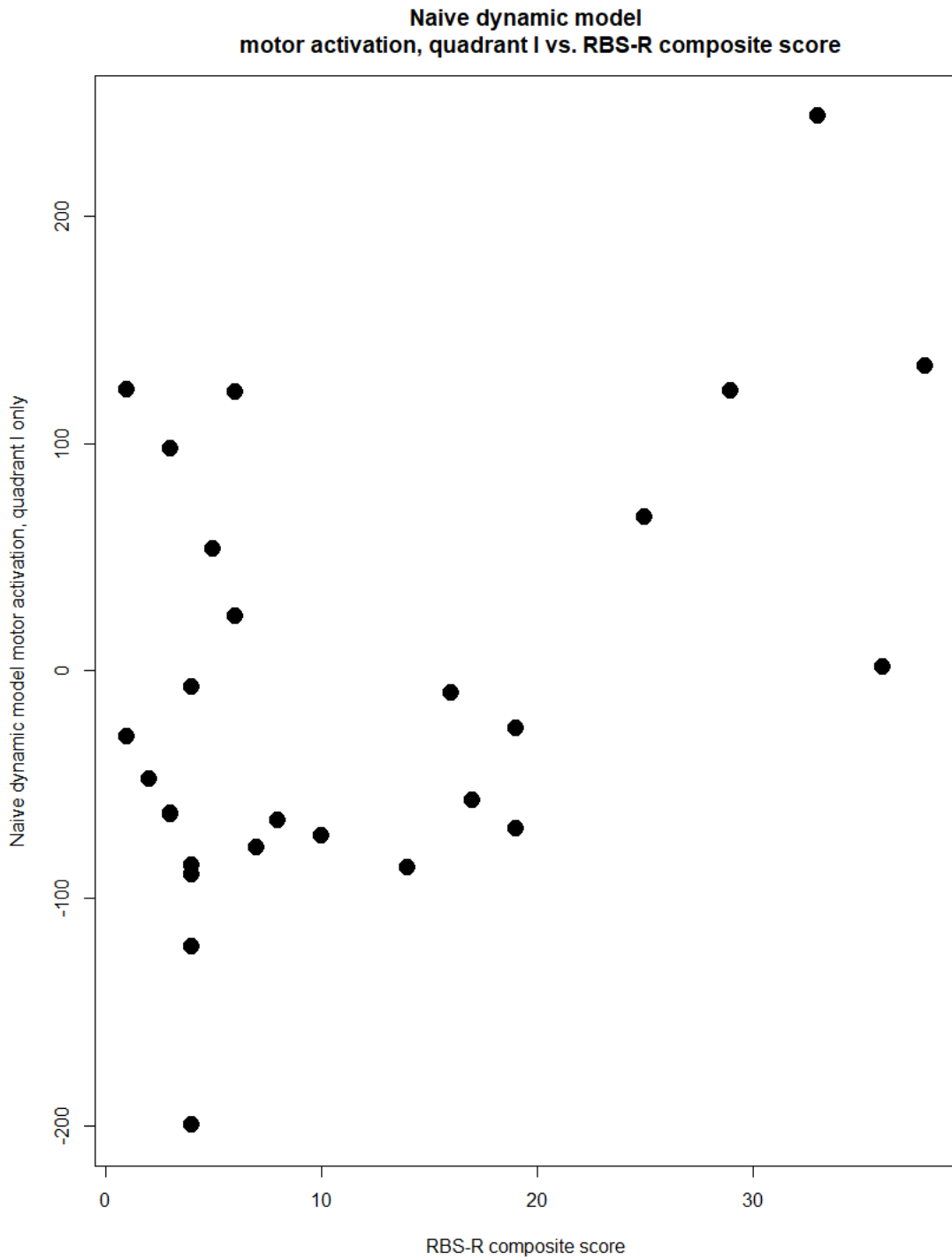
Figure 3.45: Graph of subject-level naïve dynamical model prediction of motor activation across initial condition, but restricted to quadrant I, vs. subject RBS-R CSS. Here, the is some apparent correlation, which will be tested versus that in figure 3.41.

Table 3.19: OLS regression model for (A) subject-level dynamical model and (B) naïve dynamical model prediction, restricted to quadrant I of motor reinforcement (hypothesized model) and absolute activation (naïve form) summed across initial conditions on subject RBS-R CSS; the intercept and RBS-R CSS coefficient are both significant in (A) and both significant in (B). (C) Davidson-MacKinnon J-test of the models reveals a significant p-value to five decimal places for the improvement of (A)'s predictions of (B)'s model fit, and an insignificant one (0.3101) for the improvement of (B)'s predictions of (A)'s model fit.

(A) Regression model from dynamical model

	Estimate	Std. error	t-value	$\Pr(> |t|)$
Intercept	-326.351	72.595	-4.495	0.000138***
rbsrtot	26.756	4.451	6.011	2.81e-06***

$R^2 = 0.591$, $p = 2.809\text{e-}06$

(B) Regression model from naïve dynamical model form restricted to quadrant I

	Estimate	Std. error	t-value	$\Pr(> |t|)$
Intercept	-54.909	24.935	-2.202	0.0371*
rbsrtot	4.074	1.529	2.665	0.0133*

$R^2 = 0.2212$, $p = 0.0133$

(C) J-test of the models

Model 1: rbsrtot $\sim$ subject

Model 2: rbsrtot $\sim$ positive

	Estimate	Std. error	t-value	$\Pr(> |t|)$
M1 + fitted(M2)	-0.41174	0.39706	-1.0370	0.3101
M2 + fitted(M1)	1.18377	0.24291	4.8734	5.731e-05***

Comparison between original dynamical and naive quadrant I models

Original dynamical model/naïve quadrant I model output

RBS-R composite score

Legend:
- Original, low-RRB
- Original, high-RRB
- Naïve, low-RRB
- Naïve, high-RRB
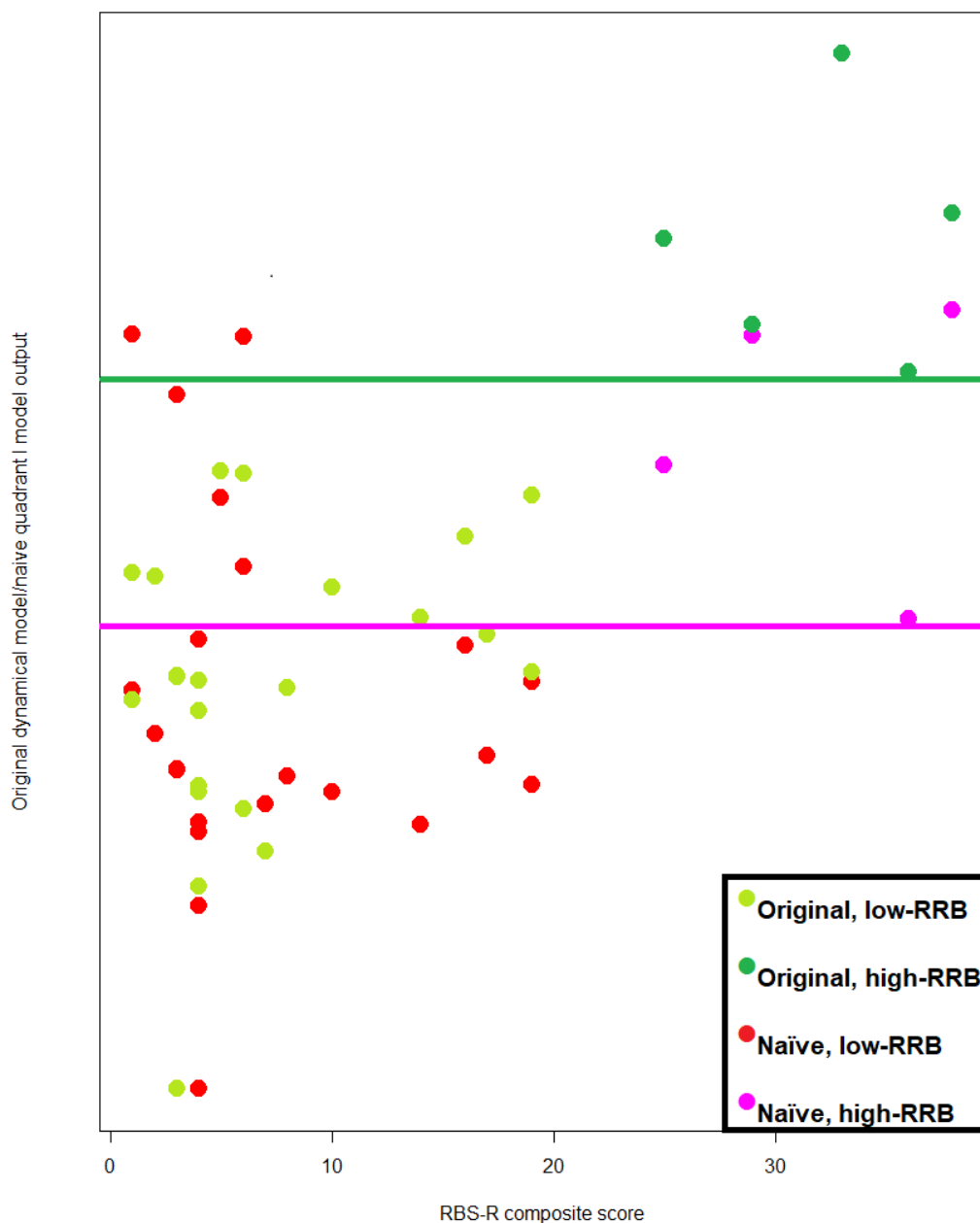
Figure 3.46: Graph of subject-level original form vs. naïve dynamical model prediction, superimposed *sans* vertical scale; points plotted are identical as in figs. 3.41 and 3.45. The horizontal lines indicate the lowest (on the vertical axis) high-RRB subject prediction. For the original model, there is no overlap in model prediction values ($\hat{z}$) between high- and low-RRB category subjects, whereas for the naïve quadrant I model, there is overlap among several (five) low-RRB category subjects along the vertical axis, in fact covering approximately the same vertical range of all except the third-highest subject CSS.

Table 3.20: Root-mean-squared error, R^2, and mean absolute error for (A) the original dynamical model, (B) the naïve model restricted quadrant I. The original model explains approximately five times the variance in the excluded subjects than the naïve quadrant I model does. A graph of both final model predictions and leave-one-out cross-validation predictions corresponding to this statistical summary is provided in figure 3.47.

(A) Original dynamical model

RMSE	R^2	MAE
7.756117	0.5209921	6.187472

(B) Naïve quadrant I model

RMSE	R^2	MAE
10.6957	0.1018719	8.865538
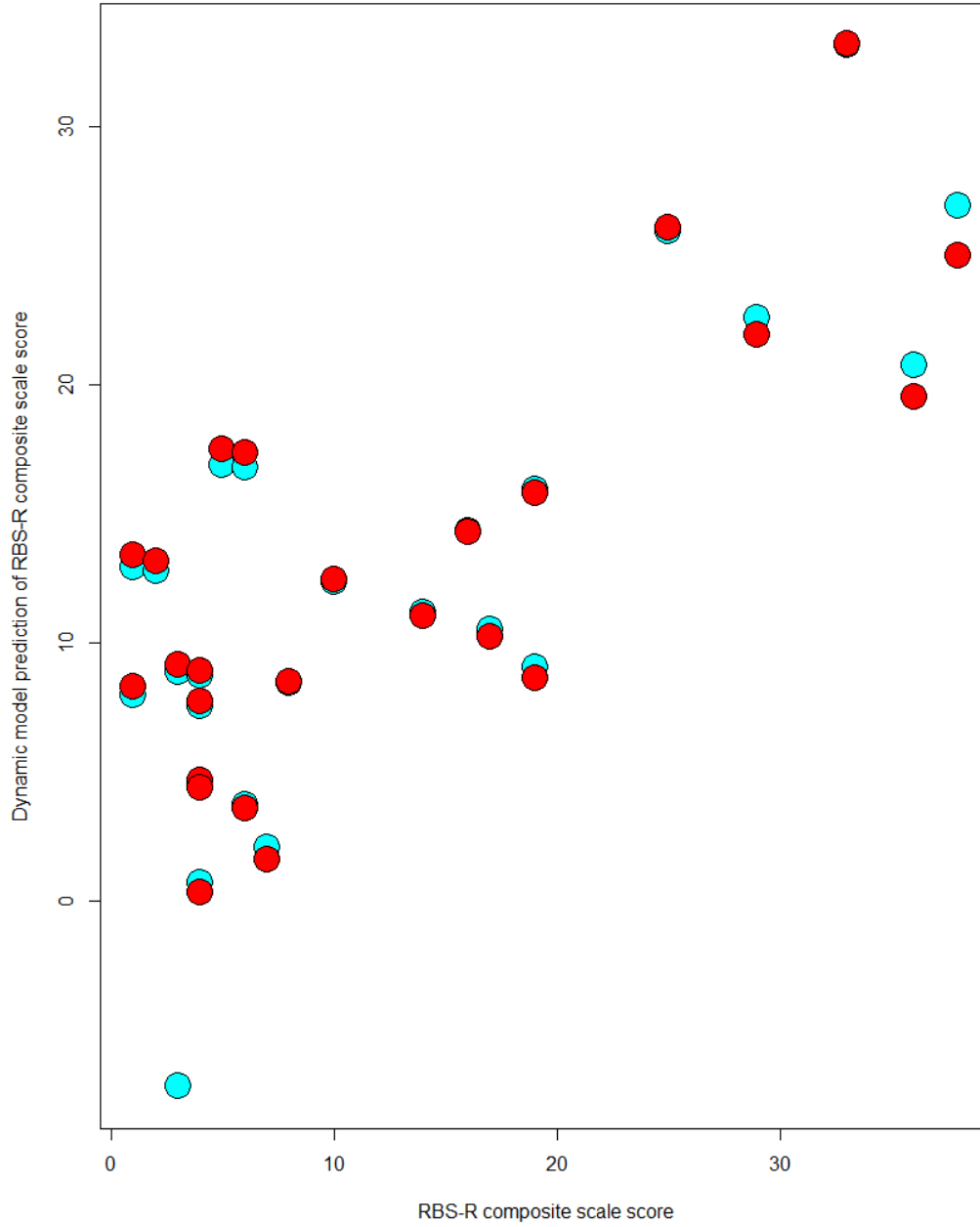
Figure 3.47: Graph of both the leave-one-out cross-validation step values predicted for subject RBS-R CSS, and those predicted by the final dynamical form after the cross-validation step. The subtle differences in the predictions do demonstrate that even the highly significant correlation observed between the model output and the chosen behavioral measures is well removed from a perfect one.

3.7.4 Subnetwork-behavior and stimulus-input dependent model dynamics

In considering three observations—(i) the orderly symmetry in connectivity correlations with RRB severity category on either side of the hypothetical network, with both cerebellum and anterior cingulate cortex showing opposite polarity between network halves; (ii) the repeatedly invoked interdependence between any brain structure and any other in terms of reciprocal functional influences; and (iii) the clear distinctiveness in empirically derived dynamical model parameters between the low- and high-RRB subgroups—along with the particular applicability of a complex systems approach to assessing the relationship between them, model characteristics will now be evaluated under conditions other than arbitrary value imputation and empirical parameter assignment.

The first and most straightforward question regards the extent to which individual ROIs in the hypothetical network influence overall behavior. A trivial way of addressing this is to create hybrid parameter values that use true subject functional connectivity values, but not consistently according to subject RRB severity category. Given the centrality between distinct subnetworks of the putative cerebellar and cingulate network hubs, the demonstrated functional significance of the structures to ASD-associated cognitive and behavioral domains, and the ease of altering major portions of the "canonical" low- and high-RRB network variants by changing all connectivity values between one or both of the hubs and all connected ROIs and observing the effects on dynamic model parameters, the two distinct network variants were modified in this way. The resulting parameter values for f, a putative measure executive—motor coupling and the relative executive influence on motor cortical activation, were calculated. Results are given in table 3.21. While no particularly profound results were observed in this calculation the notable alteration in the low-RRB subject subgroup-derived value of parameter f, at least in the abstract, suggests a "theory of cerebellar involvement in," if not "the cerebellar theory of the origin of" RRBs in ASD. The results do suggest a method of assessing the behavior of the dynamical model under biologically plausible conditions based on hybridization (interpolation) or extrapolation of model parameters from the calculated connectivity values. Such an analysis might also generate hypotheses for further testing of the methodological approach in this thesis on similar data.

Preliminary validation of model plausibility and validity primarily establishes a rationale for assessment of its applicability to extrinsic functional imaging data. Ideally, this would be done with multiple and/or large analogous fMRI datasets. As the model is not itself a statistical tool, but rather is posited to capture important aspects of RRB symptom manifestation in ASD, generation of potential research questions in terms of the model behavior and postulated utility and relevance should be undertaken following the preliminary statistical validation. To this end, assessment of

170

model behavior under three novel applications of the present imaging data will be performed. All of these conditions will involve dynamically varying stimulus input, as opposed to the static stimulus drive that has been applied to the model so far, although the later condition will be one of those assessed in each case. While static stimulus input facilitates ease of assessment and interpretation of model behavior, the original model form given in equation 3.2 includes parameters for stimulus dynamic behavior. Modification of previously discussed phase portraits by addition of stimulus time variation is depicted in 3.49.

As described, the first modulation of the model implementation itself will be in terms of interpolation of parameter values intermediate between those calculated for the high- and low-RRB subject subgroups, as is done in the middle column of phase portraits in figure 3.50, with the left and right columns comprising low- and high-RRB subgroup models, respectively. As with all implementations in this section, dynamic stimulus input of varying magnitudes is applied to the modeled brain activity. Qualitative hybridity of dynamical behavior between the subject subgroup derived model realizations is observed in the interpolated "mid-RRB" realizations across stimulus magnitudes. Perhaps of more direct significance, though, to the relationship between RRB symptom manifestation associated with ASD and the dynamical model, is the even more clear difference between the true empirical-value models under intense and dynamic stimulus conditions than under conditions of lesser, static stimulus drive. In comparing the bottom left and bottom right figures, the diversity of phase trajectories in terms of the evenness of coverage of phase space is categorically distinct. The low-RRB derived model realization covers the majority of the plotted phase space fairly evenly, with no particularly evident contrast between regions in the color mapping of the trajectories; while a distinct chromatic distribution is evident, it is less vibrant, and thus activation changes are more consistent between subnetworks. The high-RRB phase portrait is distinct on every one of these points under intense dynamic stimulus input. Despite the large magnitude swings in the actual quantitative input to the modeled sensory, executive, and salience subnetworks, clear, distinct, stereotyped trajectories emerge, with sharp contrast between the dominate subnetwork activation component per correspondence of the trajectories with the color mapped activation values. Much less of the total phase space is evenly covered by phase trajectories. Of additional note in this regard is the fact the bottom center phase portrait is inverted with respect to its densest areas of coverage relative to the high-RRB (bottom right) portrait. A last preliminary qualitative observation is that the middle two rows show the clearest gradation between the phase portraits for the low-, "mid-," and high-RRB models. In both of the middle two rows, the low-RRB phase portraits is continuous along the upper boundary with a narrow gap along the lower one, the 'mid-'RRB por-

traits have modest discontinuities along both the upper and lower boundaries with some trajectories being driven somewhat into the bifurcation gap, and the high-RRB realizations have clear gaps at the upper and lower boundaries with little more than incidental veering of phase trajectories into the divide between the two contiguous agglomerations of trajectories.

The second modulation of model implementation entails a five-step gradation in network hub (cerebellum and anterior cingulate cortex) connectivity, with results given in figure 3.52. The middle column represents true high-RRB subject subgroup parameter values, with the "high-RRB-ness" of network hub connectivity values increasing from left to right. This formulation tests to what extent the central network hubs affect modeled brain dynamic behavior. As the role of motor cortex and striatal reward circuitry is fundamental to the model, assessment of the most central functional and anatomical divisions is the salient objective regarding potential real physiological significance of the model. As increasingly "high-RRB" character of network hub connectivity results in decreasing executive subnetwork influence (reduced f), the coordinate space color maps on the bottom row correspondingly depict a rotation about the origin of the relative positions of the executive-dominated and reinforcement-dominated divisions. With exaggerated executive influence (less "high-RRB" character of the hub connections), the separation in the coordinate color map is primarily along the horizontal (y or executive activity) axis, as shown on the bottom far left, whereas the bottom far right, with negligible executive influence on motoric activity, shows dominance of the vertical, or reinforcement axis, in the color mapped activation values across initial conditions. As well in this collection of plots, the diminished influence of equivalent stimulus input can be seen from the left to right as the modeled executive/salience response to powerful stimulus diminishes. Especially in the fourth row, the relatively broad ripples in the left half of phase space in the far-left graph transition smoothly to the "seashell" like pattern in the correspondingly flattened trajectories on the left half of the phase space of the graph on the far right of the fourth row. For the same reason, the reduced executive influence, which tamps down the trajectories that would otherwise fill the gap along the bottom edge of the fourth-row portrait on the far left, allows the bridging between the two separate contiguous collections of trajectories progressively towards the right, with another rippled pattern opposed to the "seashell," demonstrating modest dynamism when perturbed by tempestuous stimulus input.

Lastly, under conditions of extreme amplitude dynamic stimulus input, behavior is modeled for two contrasting network functional connectivity patterns—either low- or high-RRB connectivity values for connections within motor, executive, and sensory subnetworks, and variation of connectivity values across the cerebellar and cingulate hubs across a spectrum of values within each of those

conditions. Plots are given in figure 3.54. The first pattern is one that has already been manifested in the previous model modulations by maintaining high-RRB associated functional connectivity values for all connections not to or from the central hubs, but modulating the connectivity values to and from the hubs along a five-step gradation. That is, the leftmost column, for the top two rows, depicts high-RRB functional connectivity between motor and sensory areas, but exaggerated low-RRB functional connectivity across network hubs, with the rightmost column therefore depicting, in the top two rows, high-RRB motor and sensory connectivity, with exaggerated high-RRB functional connectivity values across hubs. Similarly, the bottom two rows effect the same pattern, except with low-RRB connectivity values left for sensory and motor connections within subnetwork, and an inversion of the order of the hub functional connectivity pattern. Cursory appraisal of qualitative patterns exhibited by this extrapolation of modeled brain dynamical behavior associated with RRBs reveals that, consistent with the inversion in the order of the subject-subgroup associated network hub functional connectivity values between the top rows (high-RRB connectivity values outside hub connections) and the bottom rows (low-RRB connectivity values outside hub connections), qualitative similarities between phase trajectories are observed between opposite-end figures of the top and bottom rows. Specifically, columns 1 and 5, 2 and 4, and 3 correspond in qualitative aspects of their dynamical behavior.

But while qualitative patterns in phase trajectories correspond in this way, important differences are noted when taking into account the coordinate-wise colormaps of values of $\dot{z}$ across initial conditions. The top left plots demonstrate reinforcement dominance in the upper left quadrant of their coordinate planes, indicating below-baseline (perhaps lesser than intrinsic tonic neuronal activity) executive activation contributes to reinforcement motor dominance of modeled brain dynamic behavior regardless of the actual level of motor activation, consistent with the model formulation in which negative executive network activity values actually contribute to reinforcement motoric behavior. The top right plots show that intrinsic, rather than reward, reinforcement motoric activity predominates, and executive activation level has negligible effects on the time course of modeled functional brain activity. This is consistent with the diminished value of the parameter f in the upper right compared to upper left plots. For the low-RRB sensory and motor connectivity model, from left to right along the bottom, executive control is actually increasing, resulting in a coordinate activation plot on the bottom right with an arrangement perpendicular to that of the plot in the top right, that is, clear executive dominance, consistent with the lesser magnitudes of the other parameters in the low-RRB connectivity-derived parameter values. However, the distribution of the color map in coordinate space for the top left and bottom left plots actually appears *similar* despite the top left's

depicting exaggerated executive influence in modeled high-RRB brain activity and the bottom left's depicting diminished executive network influence on motor cortex of otherwise low-RRB-associated network behavior. Thus, the "high-RRB, augmented executive" and "low-RRB, diminished executive" patterns present analogous regimes of dynamical behavior, whereas the "high-RRB, diminished executive" and "low-RRB, augmented executive" realizations present with distinctly orthogonal patterns of cortical influence relative to the same distribution of initial conditions. To formulate the most behaviorally and neurophysiologically plausible model-based hypotheses for statistical testing, a nonlinear term will be introduced into the expression for $\dot{z}$ in the next section, such that model output from behaviors across transitional and dynamic equilibrium states can constitute the input data for the calculation of spatiotemporal metrics associated with modeled brain behavior of conceptual significance, to the end that they can be evaluated in terms of statistical significance.

Table 3.21: Considering the functional network fully developed from figure 3.33 and used to derive empirical parameter values for the dynamical model described by the system in equation 3.2, the relative influence of connectivity values between network hubs (cerebellum and anterior cingulate) and components in either primary subnetwork, or within the sensory periphery, can be evaluated by substituting connectivity values between the hubs and other nodes into the functional network representing either low- or high-RRB severity category subject subgroups. Doing so yields the values calculated below, along with the following summary observations: within the low-RRB functional network, substituting cingulate cortex connectivity values from the high-RRB network decreases executive—motor coupling, substituting cerebellum connectivity values from the high-RRB network realization increases executive—motor coupling, and the net effect of substituting the high-RRB connectivity values for both hubs is a negligible decrease in executive—motor coupling. In the case of beginning with the high-RRB network connectivity values, substitution of the connectivity values associated with either hub from the low-RRB network results in tighter executive—motor coupling, with complete substitution of the hub connectivity values resulting in the summation of both connectivity. With respect to the network hubs, given the symmetrical, mirrored correlation signs with RBS-R CSS on either side of each, one conceivable result would have been no apparent influences of network hub connectivity pattern inversions. However, instead, the low-RRB network demonstrates resistance to functional alteration with the substitution of all connectivity values across hubs, as cingulate and cerebellar connectivity value substitutions exhibit opposing effects, but the high-RRB network behavior is notably altered, with increased effective executive control over motor activation upon complete substitution of hub connectivity values from the low-RRB network connectivity values. To test high-RRB network functional lability, hub connectivity values equal one-quarter and twice the actual high-RRB network values were substituted, with the exaggerated high-RRB hub connectivity resulting in dramatically reduced executive—motor coupling, and the strongly attenuated connectivity values increasing it. Notably, then, both moderating intrinsic hub connectivity, and substituting the low-RRB hub connectivity values, tighten executive—motor coupling in the otherwise high-RRB functional network. The final row illustrates the mirror symmetry of cerebellar functional connectivity in the derived network.

Primary	Cingulate	Cerebellar	f
Low	Low	Low	0.2003
Low	High	Low	0.1724
Low	Low	High	0.2278
Low	High	High	0.1998
High	High	High	0.6667
High	Low	High	0.7477
High	High	Low	0.6833
High	Low	Low	0.7642
High	$0.25\times$ High	$0.25\times$ High	0.8073
High	$2\times$ High	$2\times$ High	0.2167
High	$-1\times$ High	$-1\times$ High	0.6667

Figure 3.48: Comparison between the high-RRB associated network schematic, as first demonstrated in figure 3.21, and the same functional arrangement but with connectivity values between cerebellum or cingulate cortex and other nodes substituted with those from the low-RRB functional network realization, resulting in a hybrid network. The direct relevance to the dynamical modeling, as summarized in table 3.21, is that the calculate value for f, or executive control of motoric activation, is increased due to the substitution from 0.6667 to 0.7642, providing one potential hypothesis for the combined role of cerebellum and anterior cingulate cortex in the network.
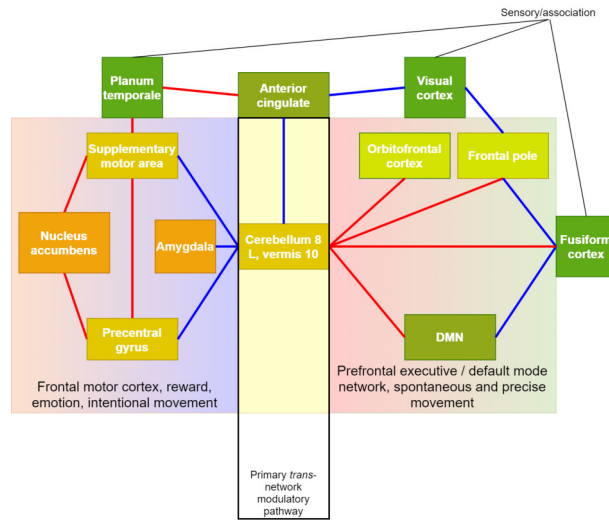
(a) High-RRB network
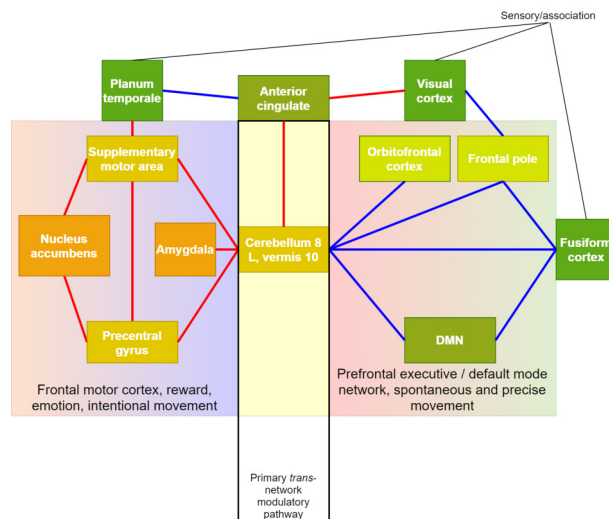
(b) High-RRB network with low-RRB connectivity values between ACC or cerebellum and other nodes substituted

(a) Low-RRB, static stimulus

(b) High-RRB, static stimulus

(c) Low-RRB, stimulus frequency 0.25

(d) High-RRB, stimulus frequency 0.25

(e) Low-RRB, stimulus frequency 0.5

(f) High-RRB, stimulus frequency 0.5
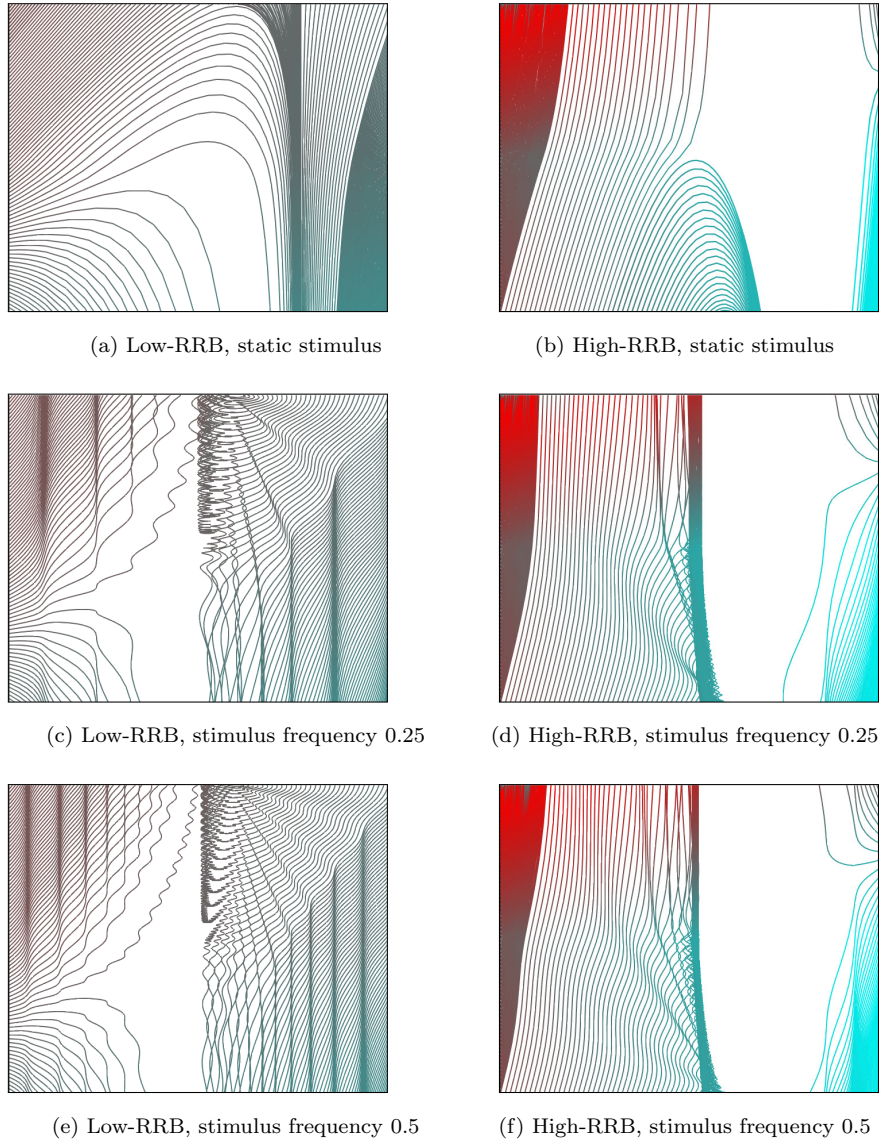
Figure 3.49: Beginning with the same data as in figure 3.36, color mapping the phase trajectories, and removing the color-mapped state vectors, the perturbations of trajectories due to a dynamically varying stimulus, as conceived in the generic model formulation in equation 3.2, can be clearly represented. The second row takes the original phase portraits and introduces periodicity into the stimulus function (x) value that varies the value of the stimulus function at each discrete time step according to a frequency of 0.25 per one time step. The third row increases the frequency to 0.5. Of note, the greater magnitude across parameters and associated tighter coupling between subnetwork behavior is reflected in the high-RRB phase portraits as more distributed undulations within the grouped phase trajectories, compared with the low-RRB models with tight ripples in individual phase trajectories.
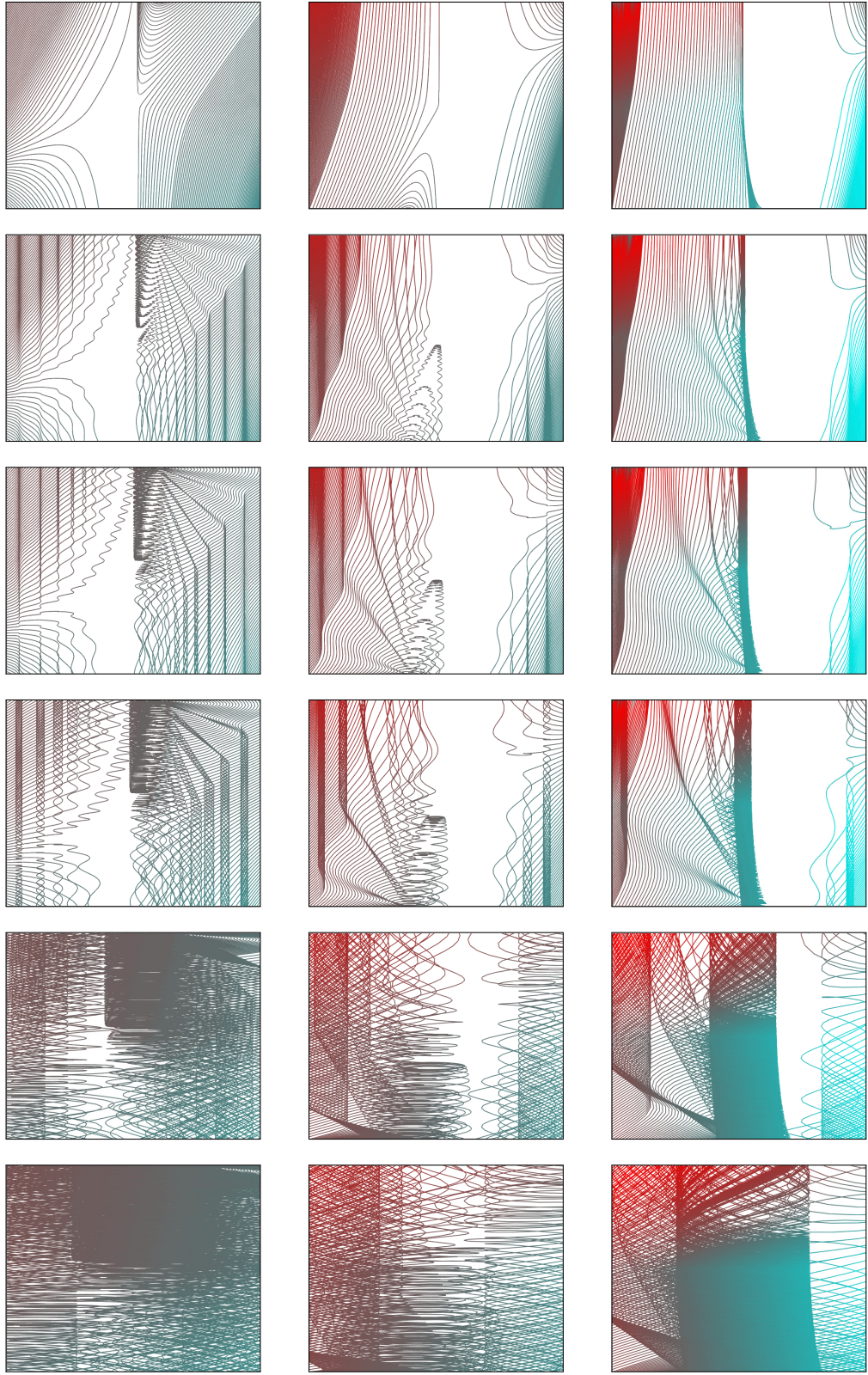
Figure 3.50: Left to right: low-, averaged, high-RRB empirical parameters.

Color-mapped phase portraits are grouped into columns by RRB-severity category empirical parameter values, and into rows by stimulus function (x) magnitude. From left to right the columns contain graphs for empirical parameter values for the low-RRB subject subgroup, averaged parameter values between the two subgroups, and the high-RRB subject subgroup. From top to bottom the stimulus magnitude (c) values are 0, 1, 2, 4, 16, and 32, with stimulus angular frequency ω remaining fixed at π. Parameter values used, in each case for the left, middle, and right columns, corresponding to low-, simulated mid-, and high-RRB severity-associated functional brain network behavior, were $f = \{0.2003, 0.4335, 0.6667\}$, $r = \{-0.1413, 0.2369, 0.6150\}$, $s = \{0.1748, 0.3427, 0.5106\}$. Clear intermediacy of phase trajectories between the low- and high-RRB dynamical model realizations is evident in the middle column portraits.

Figure 3.51: Description of figure 3.50 on the previous page.
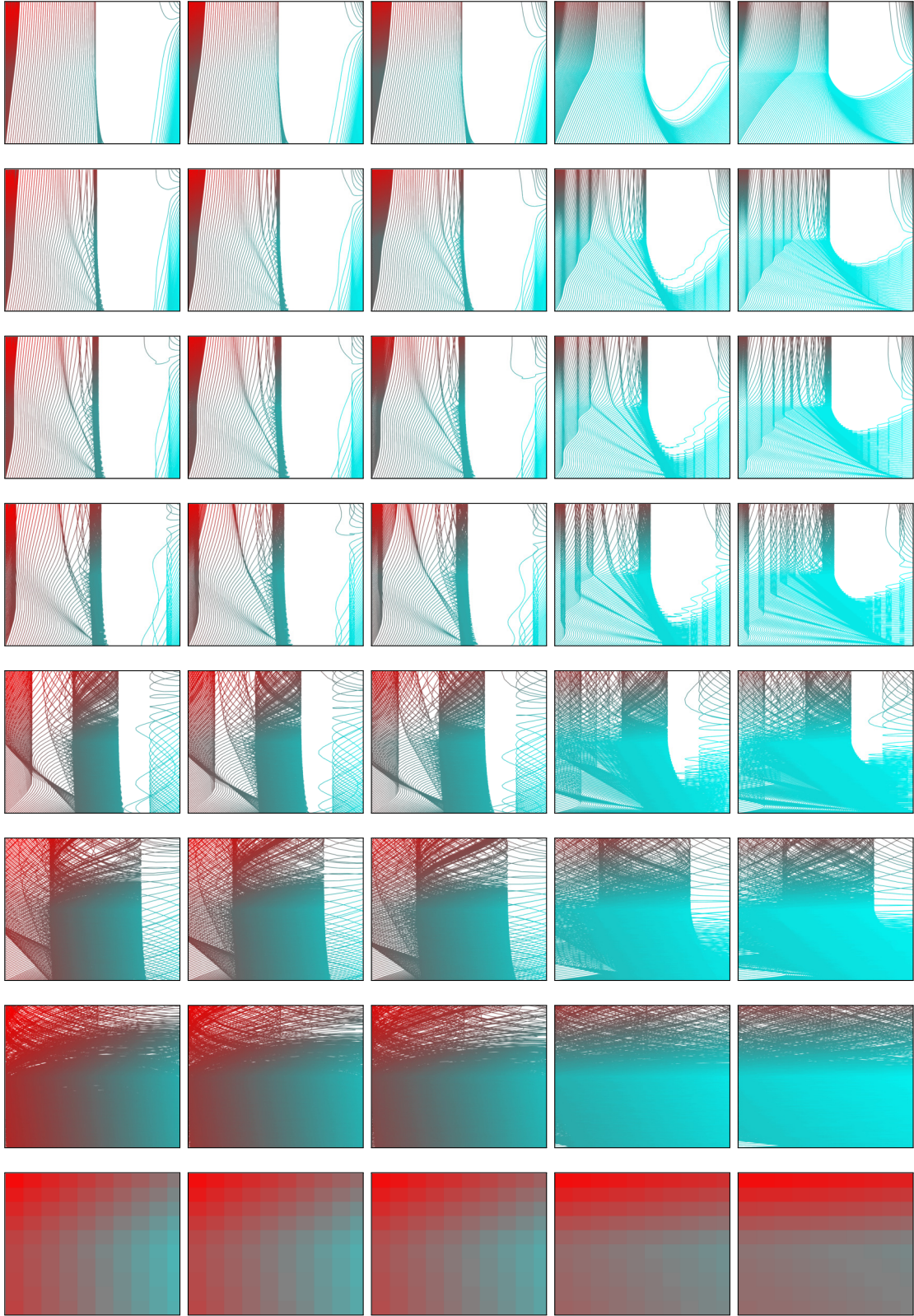
Figure 3.52: Left to right: increasing high-RRB-like hub connectivity.

Color-mapped phase portraits are grouped into columns based on connectivity values to the primary trans-network hubs, cerebellum and anterior cingulate cortex. The columns contain portraits corresponding to functional connectivity values between the hubs and other network structures that are attenuated to the left of the center column and potentiated to the right of the center column. Adjacent to the middle column, values for f are substituted from the two penultimate rows in table 3.21. For the outer two columns, a value of unity was assigned for f for the far left, and a value of 0.1084, or half that of the adjacent column, was assigned. As Pearson correlation values with magnitudes dramatically greater than one quickly appear if connectivity values are simply blanket scaled upward, and it is the ensemble, or emergent, behavior of the dynamical model that is of interest, the far left and right column values of f were chosen based on extreme bounds distant from, but not categorically differing in magnitude, the actual high-RRB-associated functional network connectivity values. The final row is a color mapped coordinate plot of the distribution of $\hat{z}$ in initial conditions generated according to equation 3.6. From top to bottom the stimulus magnitude (c) values for the first six rows are 0, 1, 2, 4, 16, 32, and 64.

Figure 3.53: Description of figure 3.52 on the previous page.
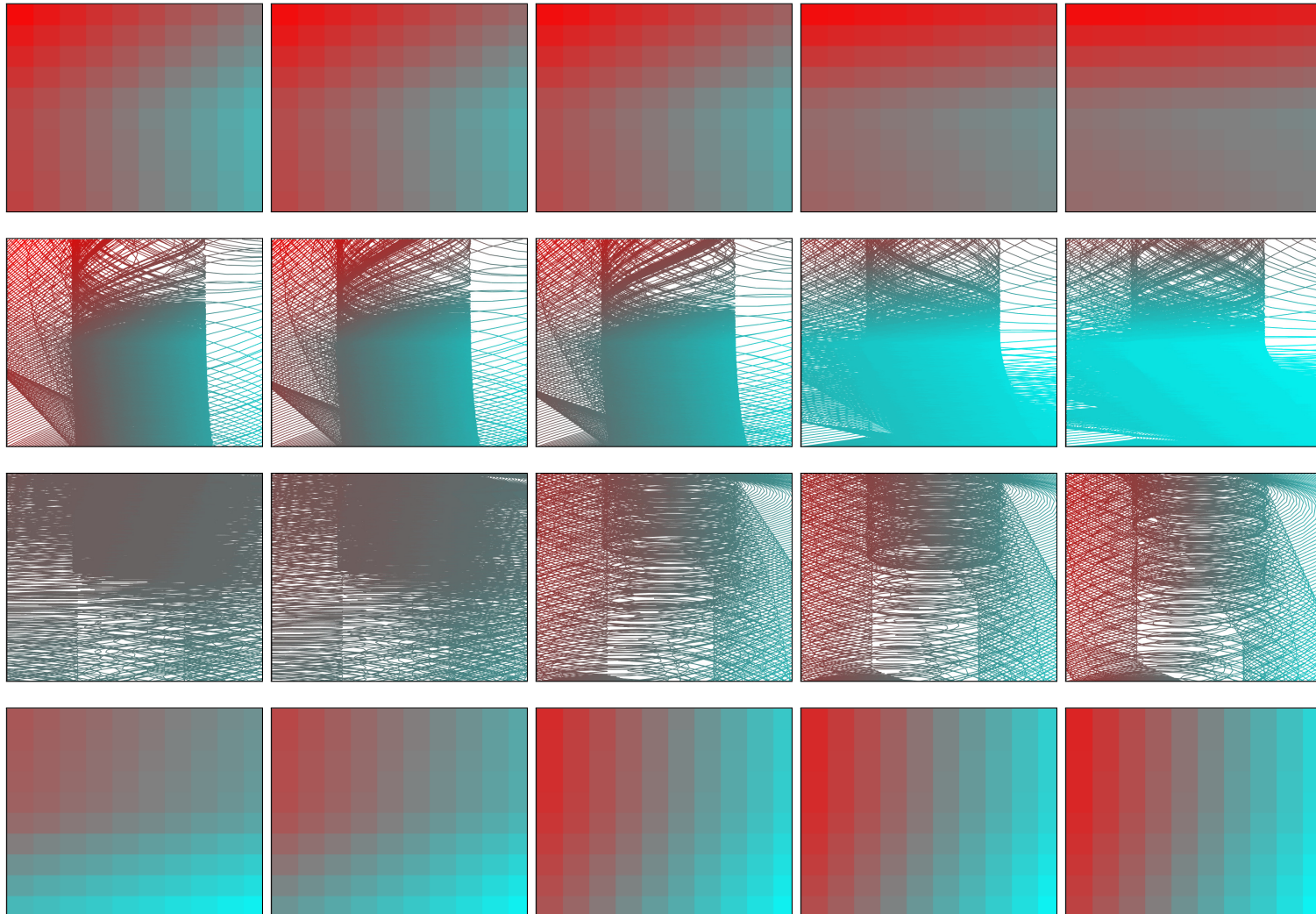
Figure 3.54: Comparison of low- and high-RRB hub-modulation dynamics.

The top row of color maps matches that from the bottom row of figure 3.52, and the second row of phase portraits matches that from the sixth row of figure 3.52 The third and fourth rows are analogous representations using the low-RRB subgroup derived connectivity values for sensory and motor reinforcement connections. Values of parameter f for the top two rows are $\{1, 0.8073, 0.6667, 0.2167, 0.1084\}$, corresponding to attenuated high-RRB network hub connectivity character to the right, and potentiated high-RRB network hub connectivity character to the left. Given the lesser coupling between nodes in the low-RRB, rather than independently calculating parameter values for the bottom to rows, the values $\{0.1084, 0.2167, 0.6667, 0.8073, 1\}$ were used, creating contrast pattern in which exaggerated primary behavior is exhibited for each network from left to right. For the top two rows, intrinsic and reward reinforcement effects dominate in the rightmost column, with a clear division along the horizontal axis of the color mapped coordinate values. For the bottom two rows, executive influence dominates. Thus, the dynamics in each case exaggerate the original empirically derived parameter value network behavior; greater moderation of excess motor activation is seen in the modified low-RRB phase portrait and coordinate color map, and greater dominance of the same excess motor activation is seen in the modified high-RRB network. In fact, the vertical cylinder-like grouping of phase trajectories in each portrait in the far right demonstrates opposite behaviors in some respects: The grouping is of dense trajectories with negative values of $\dot{z}$ in quadrants III and IV in the modified high-RRB network portrait, while it is instead sparse (and vertically divided in terms of the sign of $\dot{z}$ in the modified low-RRB network portrait. The trajectories are primarily horizontal in the latter portrait, and closer to 45-degrees in the former. Similarly, in the far-left portraits, quadrants I and II have sparse, and III and IV dense, trajectory groupings in the modified high-RRB portrait, whereas for the modified low-RRB network portrait, quadrants I and II have dense, and III and IV sparse, trajectory groupings. The sign of $\dot{z}$ is also largely exchanged, with mostly positive values in quadrants I and II and negative ones in III and IV in the modified high-RRB network portrait, and mostly negative values in quadrants I and II and positive ones in III and IV in the modified low-RRB network portrait. However, by another measure, dispersion of trajectories in phase space increases to the right for the upper portraits, and the left for the lower ones. Note that the approximate true value for the low-RRB network f parameter corresponds to the second column from the left, while the middle column corresponds to the exact value of f for the high-RRB network.

Figure 3.55: Description of figure 3.54 on the previous page.

3.7.5 Model extension: nonlinear dynamics

While the model described in equation 3.2 exhibits dynamical behavior plausibly relevant to that corresponding within the brain during execution of RRBs, insofar as model output correlates with subject RBS-R CSS, its linearity limits its ability to expediently generate nontrivial long-term eqilibrium states or those of posited behavioral or neurocognitive relevance. Even in the case of dynamic stimulus input, the magnitude of z eventually increases without bound. Therefore, an extension of the model, which will take the form

$$\dot{x} = -\omega \sin(\omega t)$$
$$\dot{y} = cx - \delta y \qquad (3.11)$$
$$\dot{z} = r|z| + sz - fy - \frac{\phi z^3}{|z|},$$

where ϕ is a damping term, or, conceivably, a term representing neural accommodation and attenuation of reinforcement motor circuit excitability due to recurrent excessive activation. Practically, this term reduces all influences on z as its magnitude increases. In all model realizations incorporating the nonlinear term, $\phi = 0.075$, as this value tends to constrain phase trajectories to the axis bounds of $[-2020]$ used so far along with the empirically derived parameter values and dynamic stimulus input similar to that in the preceding section.

This extension of the model allows meaningful interpretation of the time course of dynamic equilibrium states in the modeled output from the already time-inhomogeneous (when the stimulus function is dynamic rather than fixed drive) model. In the simplest formulation, that in equation 3.2 with $\omega = 0$, model system is both linear and homogeneous. Dynamic stimulus input and modeled neural circuit plasticity yield a nonlinear and inhomogeneous system that readily produces output that can be evaluated analogously to the output generated in previous model realizations.

In section 3.7.4, dynamic stimulus input led to oscillations in y, and concomitant effects on the time course of z, with apparently meaningful qualitative correlations with the set of empirical parameters chosen, in those cases ones interpolated or extrapolated from subject group-level values. In this section, stimulus input will be modeled similarly, with $\omega = \pi$, $j = 1$, and $c = 32$, except where noted. These and ϕ will be held fixed so that model behavior and output can be evaluated and compared under conditions of group- and subject-level parameter value assignment, as well as assignment of extrapolated and interpolated parameter values similar to those used in section 3.7.4.

Figure 3.7.5 introduces the phase portrait representation used in this section. Figure 3.57 compares the current and prior phase portrait representations. Figures 3.58 3.59 are time series and phase portrait representations, respectively, of actual subject subgroup and interpolated, as in table

3.21, parameterizations of the nonlinear inhomogeneous model form. Figure 3.60 modulates network hub connectivity values in a manner similar to figure 3.54. Figures 3.62, 3.64, 3.65, and 3.66 comprise subject individual phase portraits and time series, as well as aggregated time series und the conditions of dynamic and static stimulus input.

Statistical test results are summarized in tables 3.22, 3.23, and 3.24, and in figures 3.67, 3.68, and 3.69, using both dynamical model output and prior model formulations for comparison, conducting J tests and leave-one-out cross-validation analysis to assess relative model performance. In this case, the two best single regressors for predicting subject RBS-R CSS were both from the nonlinear dynamical model variation, although they were not significantly better than the previously tested $\hat{z}$ regressor, despite one, the temporal correlation in z, showing insignificant J test results near the threshold value with $p = 0.06$. Stepwise regression of subject RBS-R severity category, however, identified the nonlinear dynamic model output as superior in terms of predictive power qualitatively, as summarized in table 3.24.

The continued statistical significance, and even the improvement thereof, of the dynamical model output with increasing complexity prompted further assessment of model behavior including the nonlinear reactivity component effected in this section along with an additional stochastic component added at each time step to the stimulus function, such that homeostatic circadian, infradian, or ultradian rhythms can be conceived to comprise the sinusoidal component, and the environment to comprise the stochastic component of modeled stimulus input. This extension is realized in section 3.7.6.

Nonlinear model dynamic phase portrait and time series representations: In figures 3.57, 3.59, 3.60, and 3.64, phase portraits are shown in which trajectories are color mapped to t, with a gradient from green ($\approx$"screamin green," #40ff40) to magenta (pure, #ff00ff) corresponding to increasing t. `ode45` in `MATLAB` with 100 time steps, broken into segments automatically or deliberately in the case of some graphic representations, was used to produce the trajectories as well as the raw coordinate data depicted in these portraits, and both linear trajectories and overlayed scatterplots of the discrete data are color coded so that $t = 0$ maps to green, whether continuously along trajectories or discretely sample-wise, and $t = 100$ maps to magenta. In this way color-mapped phase portraits can be used for, in addition to portraying the derivative, $\dot{z}$,of z, of interest given that modeling *change* in neurocognitive activity that might be associated with RRB manifestation is the aim in developing the dynamical model, representing the value of both y and z as plotted along the horizontal and vertical axes of the phase portraits, respectively, while also directly depicting the time course of model dynamical behavior. Now that color-mapped phase portraits in $\dot{z}$ on the yz axis have been extensively used, this intuitive alteration allows simultaneous spatiotemporal representation of model behavior at the group, synthesized, and subject levels, maintaining the visual relationship between y and z in the coordinate plane as in preceding phase portraits and implicitly representing the time series behavior of both variables. Figure 3.57 on the proceeding page contrasts information in the z-mapped and t-mapped phase portraits, representing the linear inhomogeneous and nonlinear inhomogeneous model manifestations, respectively. The cyan—red $\dot{z}$-mapping emphasizes excess motoric reinforcement, hitherto the primary metric of interest. The green—magenta t-mapping scheme is, as can be seen, useful for representing dynamic equilibrium regimes given variable stimulus input. Compare the linear model dynamics in the inner two rows, in which phase trajectories in the z direction are unbounded, rendering the portraits a window only into the ephemeral coordinate plane-bounded portion of the overall ensemble of time-dependent phase trajectories. The addition of the damping term effortlessly introduces practicable discrete equilibrium regimes the behaviors of which are themselves assessed and statistically tested in this section. Explicit plots of z versus t (figs. 3.58, 3.60, 3.62, 3.65, 3.66) are also utilized, color mapped based on either actual subject subgroup or RBS-R CSS rank, or the alterations to the executive control parameter f network hub connectivity modulation evoked relative to the group-derived parameter values in section 3.7.4; in each case blue (medium blue, #0000C0) corresponds to low-RRB subject subgroup membership or network hub connectivity patterns (f increased relative to subgroup-derived value), and yellow (aureolin, #fdee00) corresponds to the high-RRB subject subgroup membership or hub connectivity pattern (f decreased).

Figure 3.56: Summary of behavior of the dynamical model when extended to accommodate nonlinear behavior.
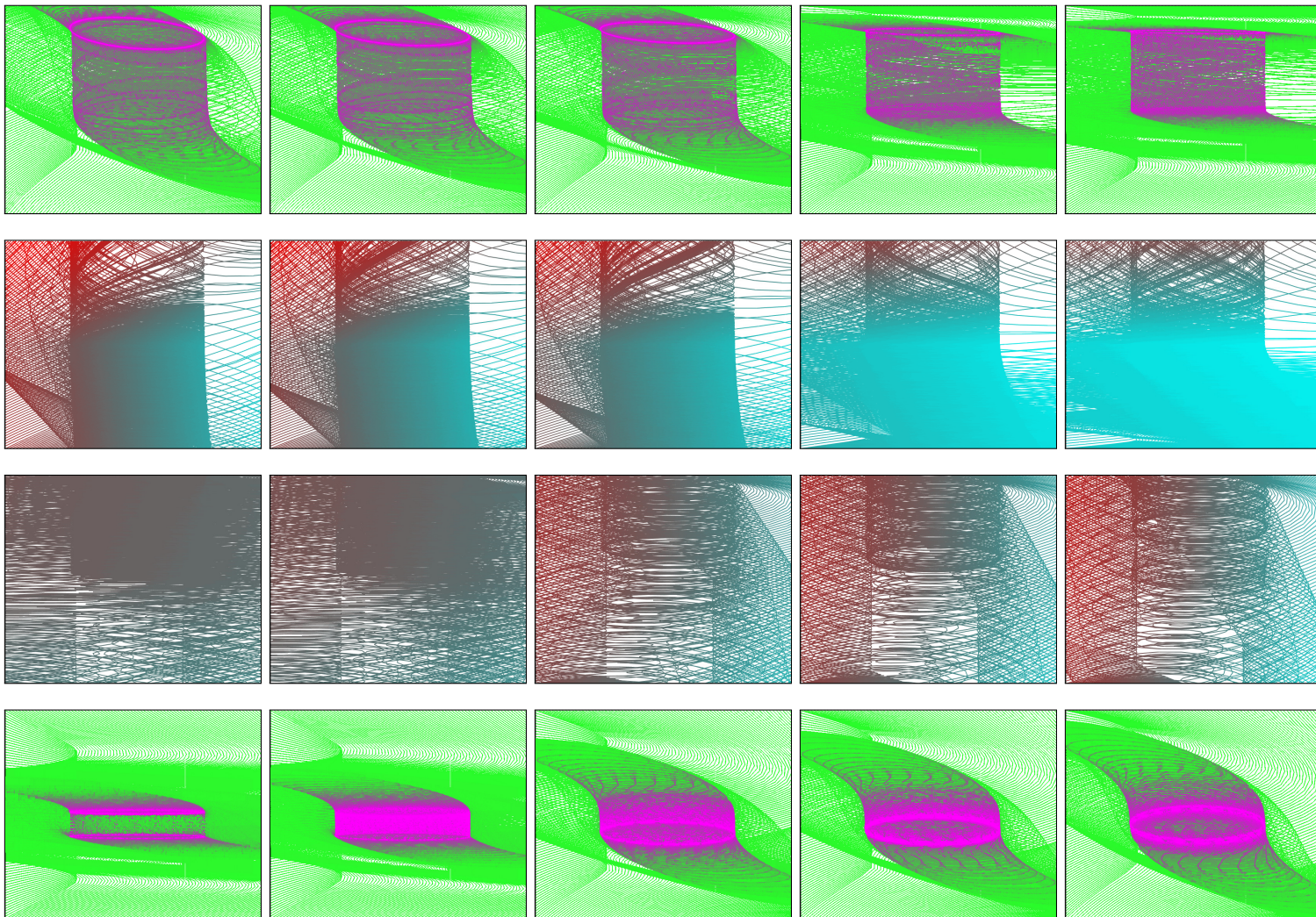
Figure 3.57: Contrast figs. 3.55, 3.60

(a) Low-RRB-derived parameters

(b) Interpolated parameters; 2/3 low-, 1/3 high-

(c) Interpolated parameters; 2/3 high-, 1/3 low-

(d) High-RRB-derived parameters
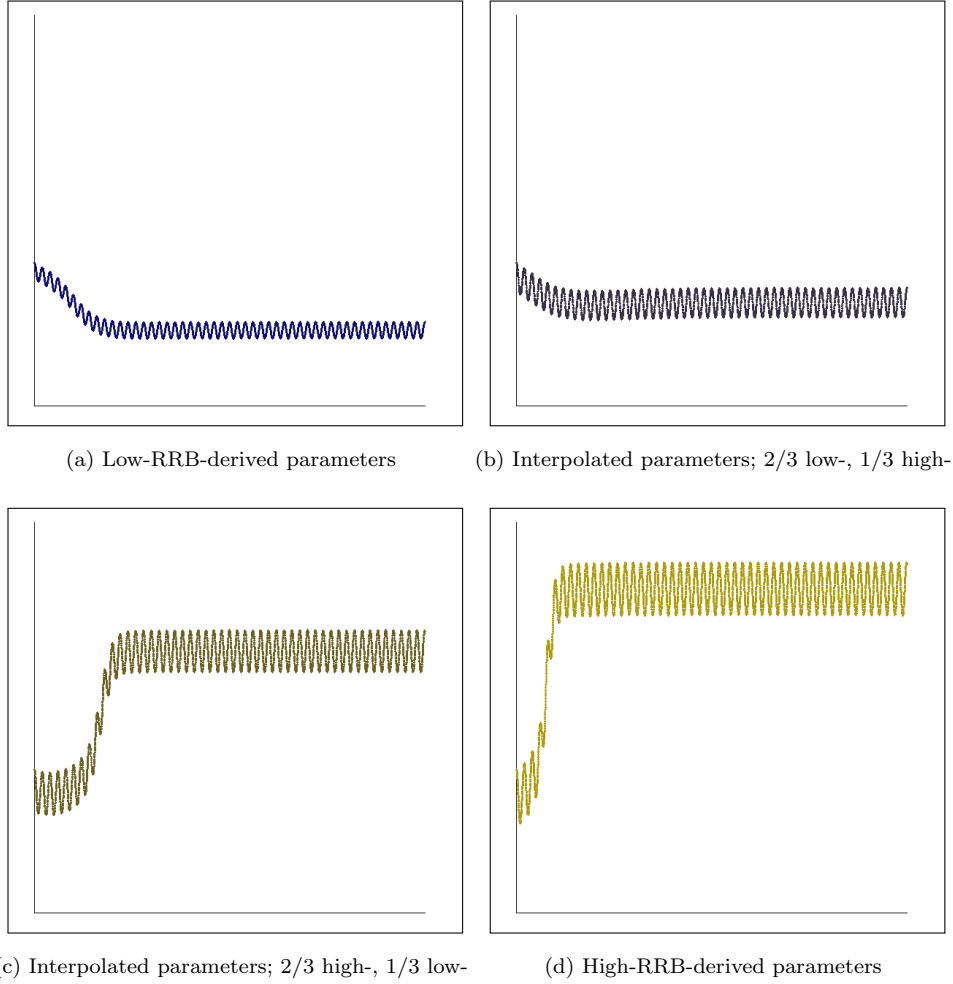
Figure 3.58: Time series plot of z with model output taken from the extension of the model with the nonlinear term $-\frac{\phi z^3}{|z|}$ appended to $\dot{z}$. This nonlinear term, along with the time inhomogeneity added in the prior section in the form of a positive ω, results in dynamic equilibrium behavior, represented by the oscillations around a fixed z value past a certain t. Color mapping is blue for low-RRB graph character and yellow for high.

(a) Low-RRB-derived parameters

(b) Interpolated parameters; 2/3 low-, 1/3 high-

(c) Interpolated parameters; 2/3 high-, 1/3 low-

(d) High-RRB-derived parameters
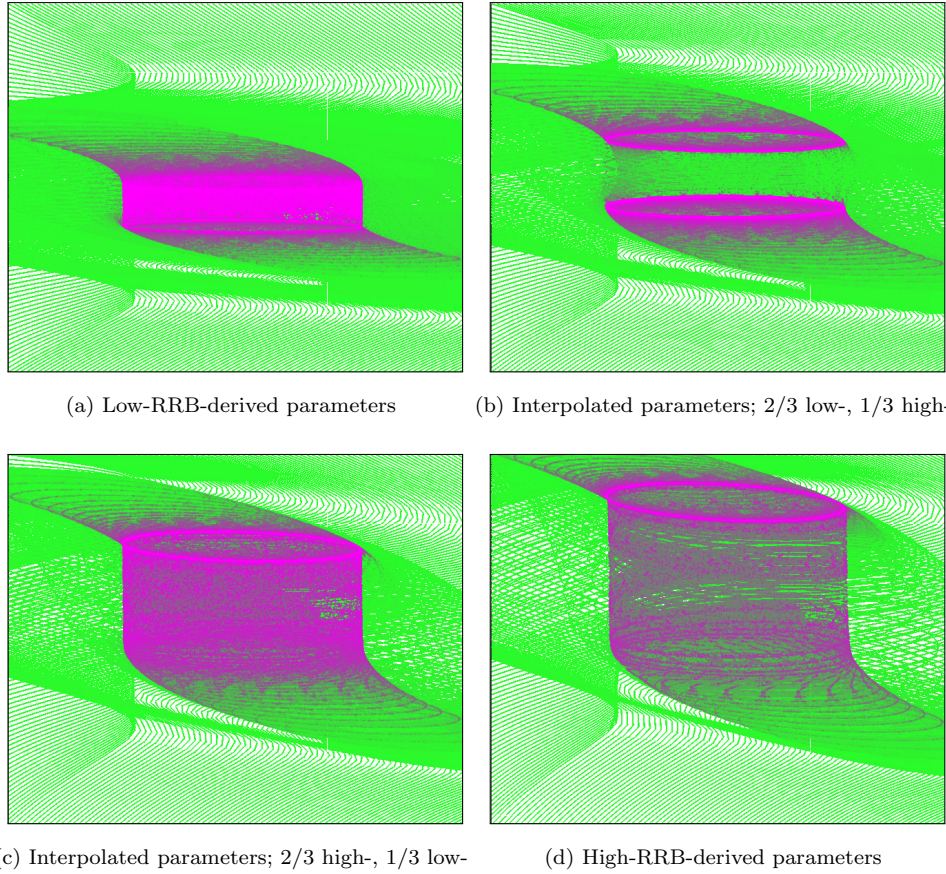
Figure 3.59: Extension of the model with the nonlinear term $-\frac{\phi z^3}{|z|}$ appended to $\dot{z}$. This nonlinear term, along with the time inhomogeneity added in the prior section in the form of a positive ω, results in dynamic equilibrium behavior, represented by green—magenta color mapping of t of phase trajectories and point plots.
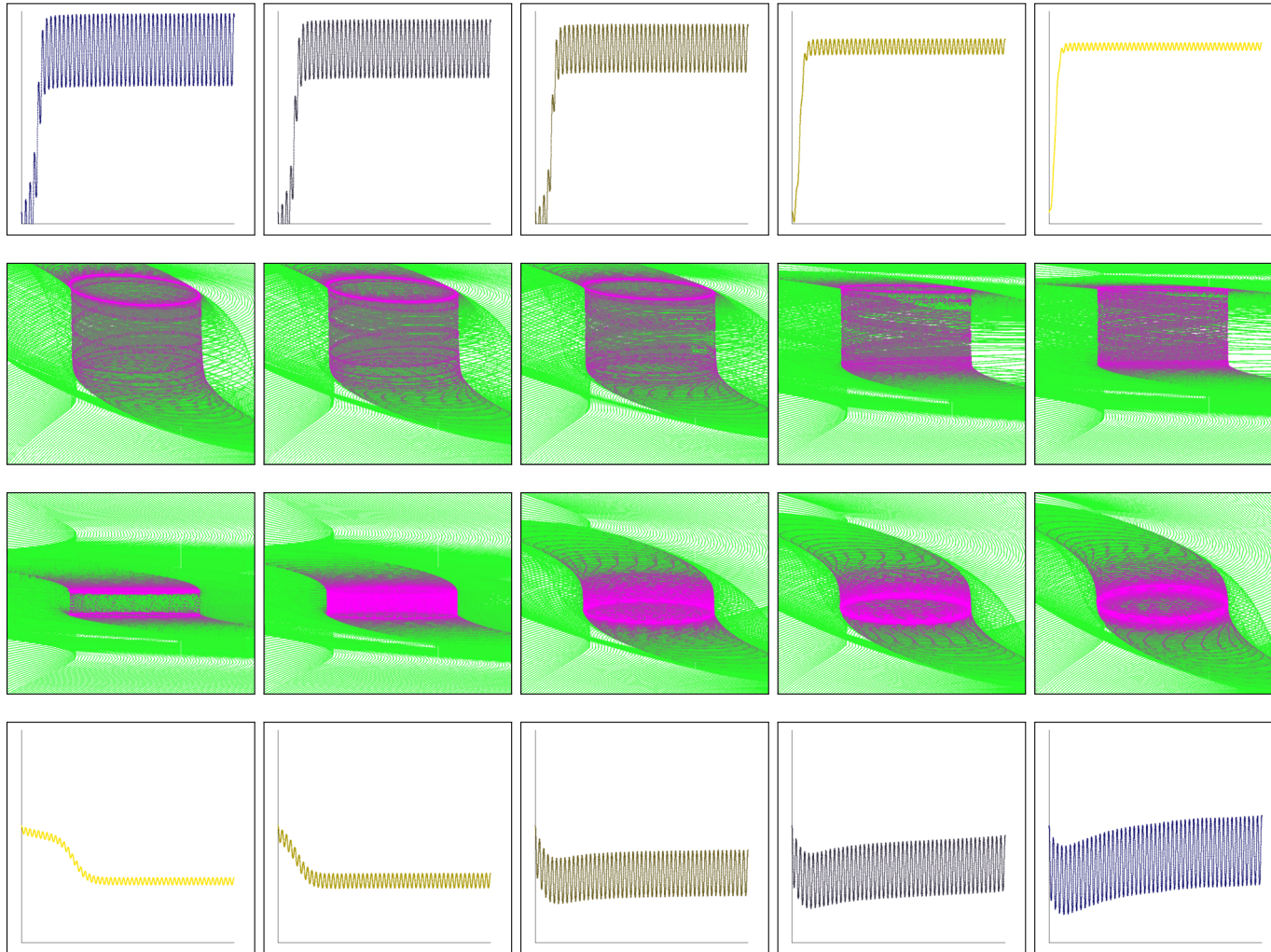
Figure 3.60: Comparison of hub nonlinear dynamics.

The top two and bottom two rows of figure 3.60 are paired as in figure 3.54. The top two rows depict, first, z time series from a single initial condition with the same parameters and model simulation as the second row. In fact, the data used to construct the time series corresponding to each of the two middle row phase portraits were also used to construct the phase portraits themselves. While the traditional time series representation allows facile recognition of oscillatory and drift behaviors, the phase portraits summarize far more information by varying the initial conditions and showing the eventual equilibrium state, given the regularly varying stimulus input, reached by phase trajectories from multiple initial conditions. However, aspects of the graphs can be usefully related. For example, when the apparent equilibrium state in the phase portrait comprises elliptical trajectories, the greater the minor axis of the ellipse, the greater the amplitude of the oscillation of z in the time series. This indeed shows the influence of the executive subnetwork on the calculated z, as a higher f and stronger executive influence, in the form of executive—motor coupling, yield a greater effect of stimulus input on z. However, as the empirical parameter values (table 3.16) and previous model output show, the executive influence increase is lesser in the high-RRB derived model realization than the corresponding increase in motor reinforcement strength. Hence, the true high-RRB subject subcategory model (top two rows, middle column) shows both a higher average z and higher amplitude oscillations in z than the approximate low-RRB counterpart (bottom two rows, second column approximates actual low-RRB subject subcategory empirical parameter values, with $f = \{1, 0.8073, 0.6667, 0.2167, 0.1084\}$ for the top two rows and $f = \{0.1084, 0.2167, 0.6667, 0.8073, 1\}$ for the bottom two, those being identical to the ones used in figure 3.54. Values for r and s are the actual low- and high-RRB subject subcategory derived empirical values for the bottom two and top two rows, respectively, with the second column, bottom-two-row f-value of 0.2167 approximating the empirical one of 0.2003, with the present values derived from manipulation of the network's cerebellar and cingulate hubs' connectivity values in constant proportion (table 3.21)).

Figure 3.61: Explanation of figure 3.60 on the preceding page, showing t-color-mapped phase portraits along with corresponding time series plots of the same data and the relationship between the representations.
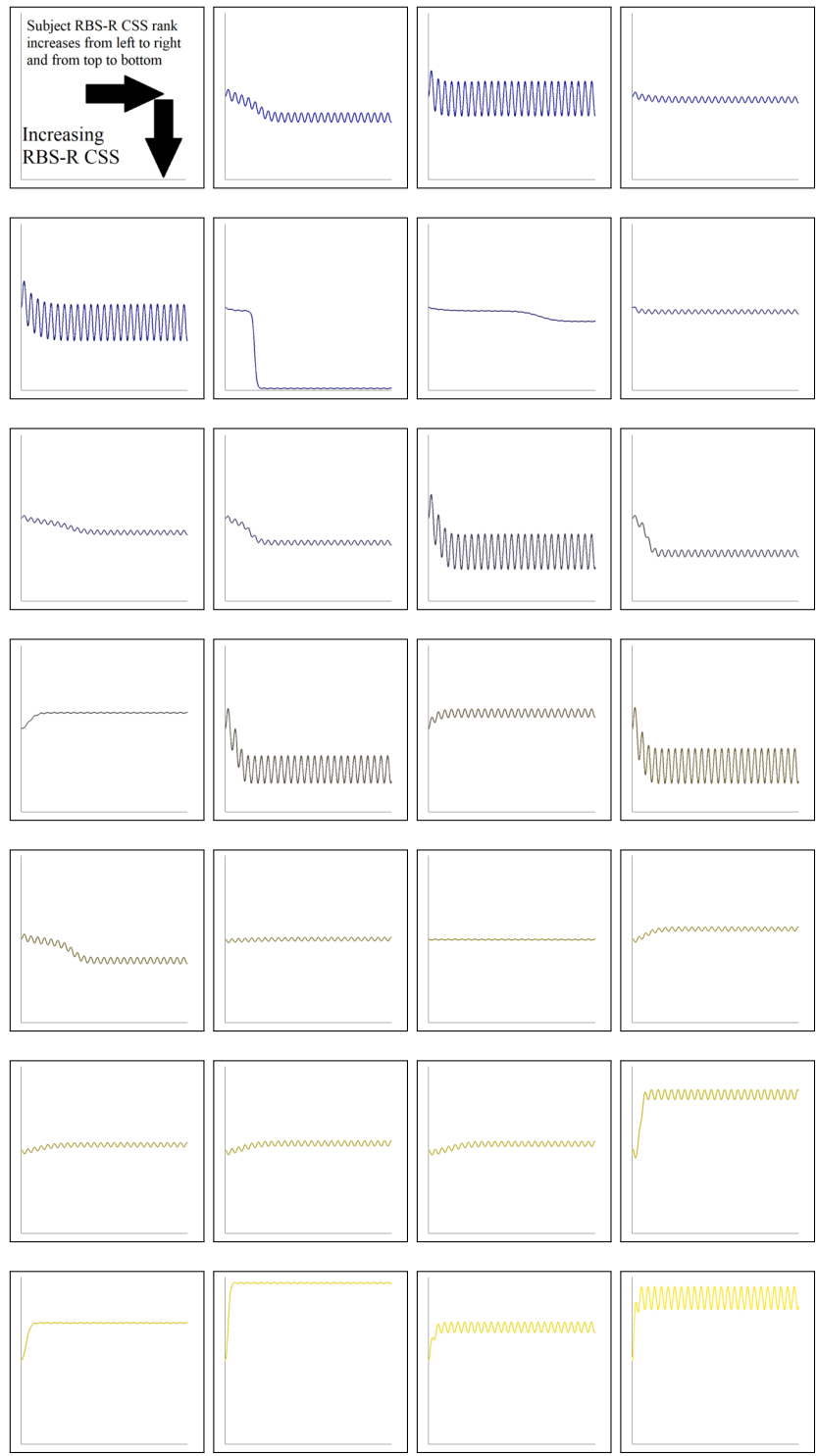
Figure 3.62: Subject-level nonlinear time series.

Subject time series representations in figure 3.62 are analogous to those described in figures 3.60 and 3.61. Color mapping is according to the scheme described in figure 3.7.5. Oscillation magnitude in the z direction, apparent equilibrium z value around which model z fluctuates, and the impulse-like behavior of z in t following simulation initiation, all could form aspects of model relevance, as will be quantitatively tested in following figures. The phase portraits and their color mapping in figure 3.64 is likewise that described in figure 3.7.5. As discussed in figure 3.60, correlations in qualitative aspects between the time series and phase portrait representations can be made. Notice it is especially clear in the nonlinear, dynamic stimulus, t-color-mapped phase portraits that the models based on connectivity values from subjects 5 and 25 exhibit dynamical regimes consistent with the implication as prediction outliers in regression modeling, both in, for example, figure 3.41, using the static stimulus, linear model realization, and in figure 3.68(a) and (c), generated from the present dynamic stimulus, nonlinear model extension While the present model, nor any variation, can account for such subject-specific discrete differences, a more robust and inclusive underlying functional brain network identified via large subject samples and repeated testing, though not by necessity a substantially more complex nonlinear dynamical model of such a network, conceivably could resolve regimes of patterned brain activity at the subject level While machine learning classifiers promise seemingly limitless pattern identification capabilities, pattern *generation*, from relatively more complex underlying data into simpler discrete macro-scale arrangements that nevertheless correspond closely to the underlying organic system behavior, facilitates human understanding of the relevant phenomena more directly, and may well lead to an easing of the burden of our robot overlords, and electrical grid, should the resulting models be, and they might be expected to be, relatively computationally efficient.

Figure 3.63: Explanation of figures 3.62 and 3.64 on the prior and following pages, respectively.
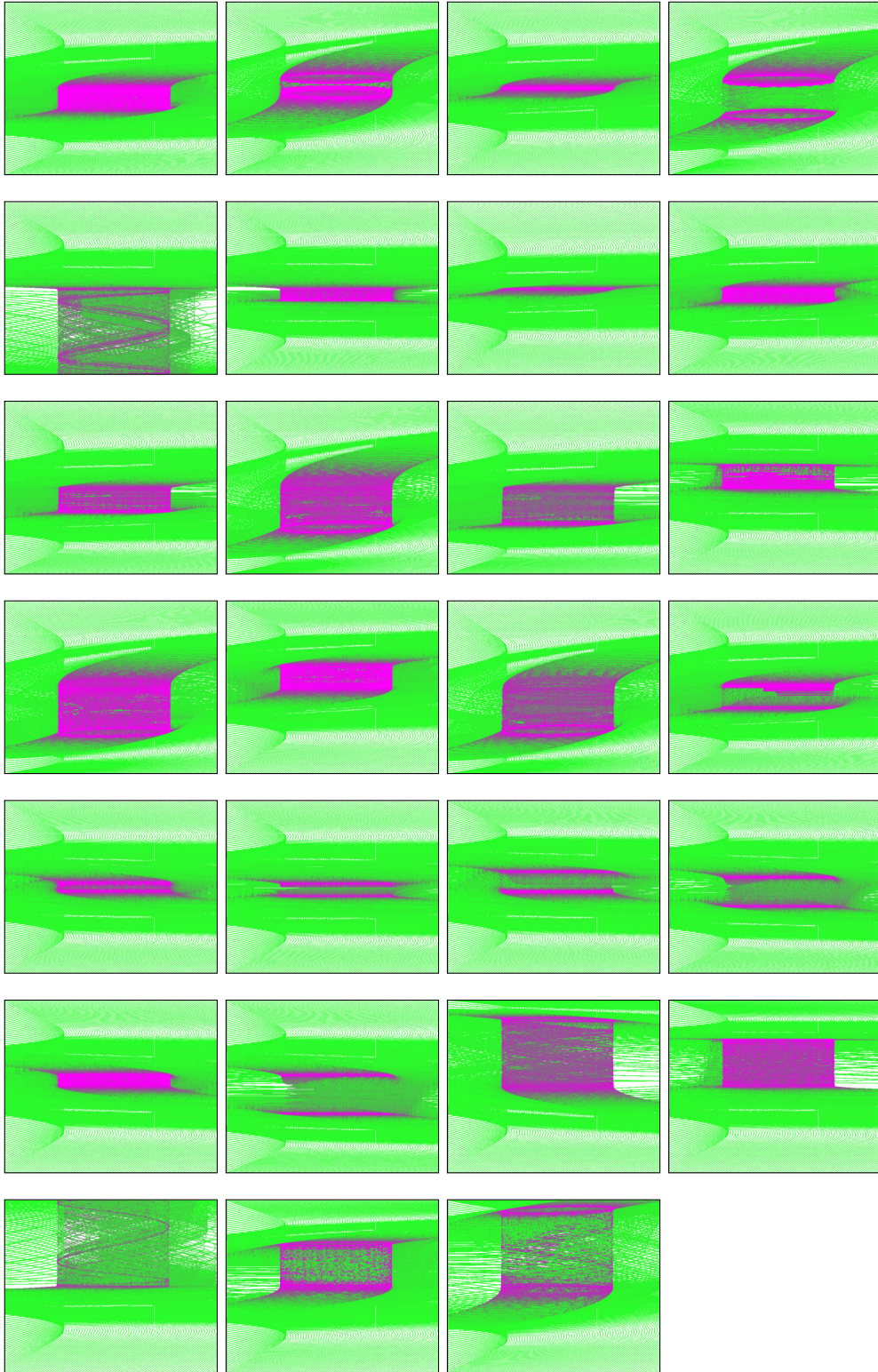
Figure 3.64: Subject-level nonlinear phase portraits, ordered as in fig. 3.62.

194
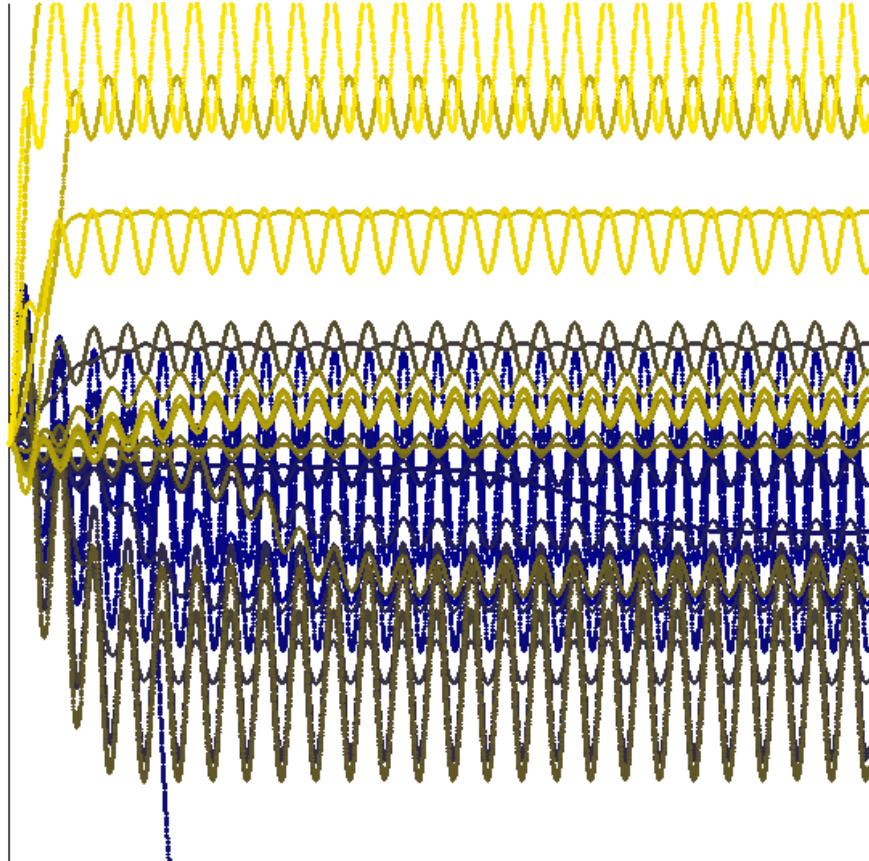
Figure 3.65: Composite graph of all subject time series with the nonlinear dynamical model modification and initial conditions $\{y, z\} = \{1, 1\}$ Color mapping is blue to yellow for subject id (RRB CSS rank) from 1 to 27. Amplitude of dynamic stimulus input increased to 64 to emphasize differences in trajectories in z (vertical axis) in time. Metrics based on this nonlinear dynamical model variation produce metrics of z with superior correlation with subject RBS-R CSS compared to those from the static nonlinear version in figure 3.66, as shown in table 3.22 in the third row.
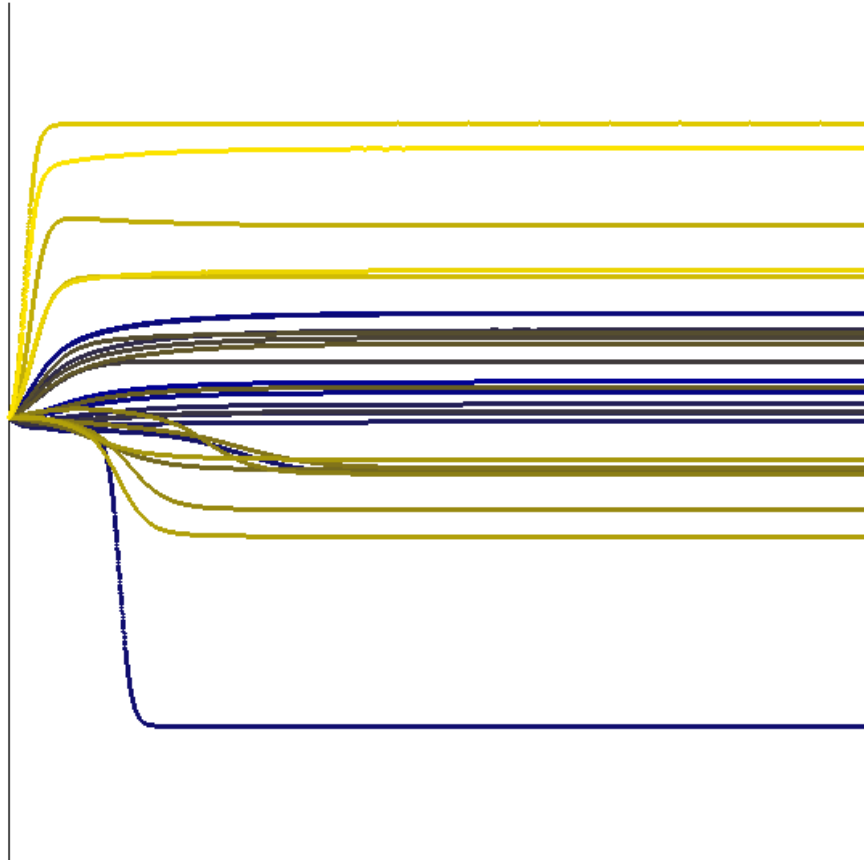
Figure 3.66: Composite graph of all subject time series with the original dynamical model and initial conditions $\{y, z\} = \{1, 1\}$ Color mapping is blue to yellow for subject id (RRB CSS rank) from 1 to 27. Amplitude of static stimulus input is 1, as in the prior static subject-level analyses. The static, equilibrium measure of z this model yields correlates poorly with RBS-R CSS in comparison to the dynamic version shown in the time series in figure 3.65, as shown in table 3.22 in the second row.

Table 3.22: Comparison of single-regressor linear model fit between subject RBS-R CSS and various instantaneous and averaged metrics based on z. $\hat{z}$ is the metric devised and evaluated in section 3.7.3. While $\bar{z}$ is a more successful regressor when measured across the first 5 of 100 time steps (with model output sampled every 0.01 time steps) across initial conditions, the difference is negligible, as table 3.23 shows. While the correlation between t and z for the first 5 time steps is even more strongly correlated with subject RBS-R CSS, it falls just short of significance in the J-test, also shown in table 3.23.

Measure	Time step	R^2	p
$\hat{z}$, linear static model	t_0	0.591	2.81e-06 ***
$\bar{z}$, nonlinear static model	t_f	0.2395	0.009573 **
$\bar{z}$, nonlinear dynamic model	$[\mathbf{t_0, t_{0.05f}})$	**0.5927**	**2.67e-06 *****
$\bar{z}$, nonlinear dynamic model	$(t_{0.95\mathrm{f}}, t_\mathrm{f}]$	0.5822	3.69e-06 ***
$\bar{z}$, nonlinear dynamic model	$[t_0, t_\mathrm{f}]$	0.5843	3.46e-06 ***
skew(z), nonlinear dynamic model	$[t_0, t_{0.05\mathrm{f}})$	0.537	1.38e-05 ***
skew(z), nonlinear dynamic model	$(t_{0.95\mathrm{f}}, t_\mathrm{f}]$	0.004191	0.748
skew(z), nonlinear dynamic model	$[t_0, t_\mathrm{f}]$	0.5238	1.99e-05 ***
corr(z, t), nonlinear dynamic model	$[\mathbf{t_0, t_{0.05f}})$	**0.6328**	**7.08e-07 *****
corr(z, t), nonlinear dynamic model	$(t_{0.95\mathrm{f}}, t_\mathrm{f}]$	0.02653	0.417
corr(z, t), nonlinear dynamic model	$[t_0, t_\mathrm{f}]$	0.5326	1.56e-05 ***
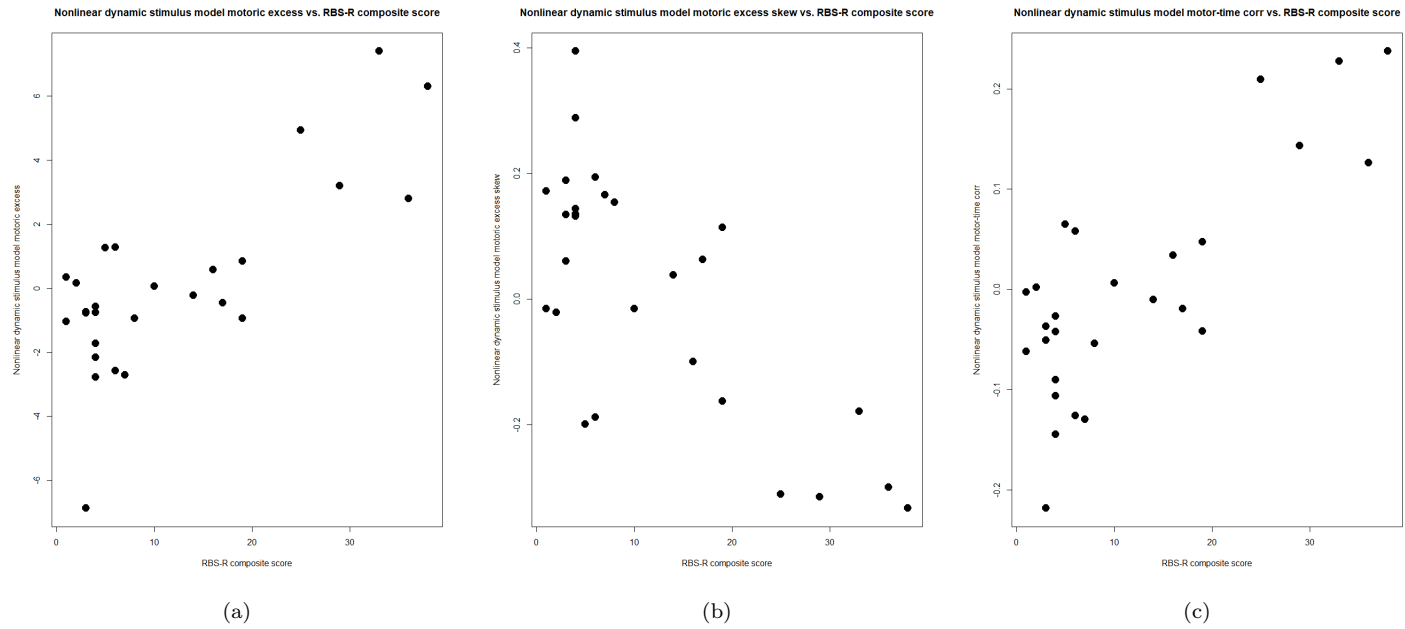
Figure 3.67: Scatter plots of subject-level RBS-R CSS vs. the raw regressor data for linear models summarized in the (a) third, (b) sixth, and (c) ninth rows of table 3.22. (a) The nonlinear dynamic average $\bar{z}$ for $t < 5$ regressor yields a trivially higher R^2 than the statistic $\hat{z}$, but predicts the same subject (ID no. 5) inaccurately. (b) Skewness is negatively correlated with subject RBS-R CSS, indicating a more top-heavy distribution of z with higher RB manifestation, as would be expected. (c) The time-correlation of z through the first five time steps is the most strongly correlated regressor tested with subject RBS-R CSS. This supports the further validity of the nonlinear model modification.

Table 3.23: Comparison between the performance of three regressors: $\hat{\bar{z}}$ (table 3.17 and figure 3.41), $\bar{z}$ restricted to the first 5 discrete time steps (out of 100 in the dynamic stimulus nonlinear model instantiations), and $\mathrm{corr}(z, t)$, again restricted to the first 5 discrete time steps. While the $\hat{\bar{z}}$ regressor yielded the lowers R^2 in terms of the full model, its performance was intermediate with respect to its predictions of left out observations in leave-one-out cross-validation. The $\mathrm{corr}(z, t)$ regressor was superior on every measure, but its predictions did not significantly improve those of the $\hat{\bar{z}}$ regressor model when included as additional regressors ($p = 0.06179$).

Measure	R^2 (full)	RMSE	R^2 (CV)	MAE	p	(J test against $\hat{\bar{z}}$)
$\hat{\bar{z}}$	0.591	7.7561	0.5210	6.1875	N/A	N/A
$\bar{z} \| t < 0.05 t_f$	0.5927	7.8197	0.5153	6.3530	0.6147	0.6902
$\mathrm{corr}(z, t) \| t < 0.05 t_f$	0.6328	7.3072	0.5732	6.1886	0.06719 .	0.3666

Table 3.24: Regression of subject RRB-severity category (low = -1, high = 1) on regressors of differing provenience. Comparison of stepwise model performance between power regression models (table 3.8), linear regression models using the same connectivity data, and linear models using subject-wise nonlinear dynamical model spatiotemporal summary statistics as regressors. The first model row is for the linear regression of RBS-R CSS on $\hat{z}$ (table 3.17, figure 3.41). In every stepwise sequential replacement regression model, the regression model using the dynamical model summary statistic regressors is superior by every listed measure. Graphs of the first three model steps for the connectivity linear regression models and the dynamical model output summary statistics models are shown in figures 3.68 and 3.69.

Data type	Form	Step	RMSE	R^2	MAE
Model output	Linear	N/A	0.2722	0.5146	0.2209
Connectivity	Power	I	0.5705	0.4636	0.4478
Connectivity	Linear		0.6036	0.4048	0.4295
Model output	**Linear**		**0.5042**	**0.5812**	**0.4203**
Connectivity	Power	II	0.4830	0.6154	0.4075
Connectivity	Linear		0.4673	0.6412	0.3974
Model output	**Linear**		**0.3693**	**0.7765**	**0.2746**
Connectivity	Power	III	0.4092	0.7273	0.3416
Connectivity	Linear		0.5576	0.5062	0.4034
Model output	**Linear**		**0.3326**	**0.8181**	**0.2474**
Connectivity	Power	IV	0.4002	0.7392	0.3226
Connectivity	Linear		0.5519	0.5210	0.4164
Model output	**Linear**		**0.3135**	**0.8385**	**0.2276**
Connectivity	Power	V	0.4116	0.7259	0.3251
Connectivity	Linear		0.4318	0.7006	0.3384
Model output	**Linear**		**0.3127**	**0.8405**	**0.2200**

(a) Step I   (b) Step II   (c) Step III
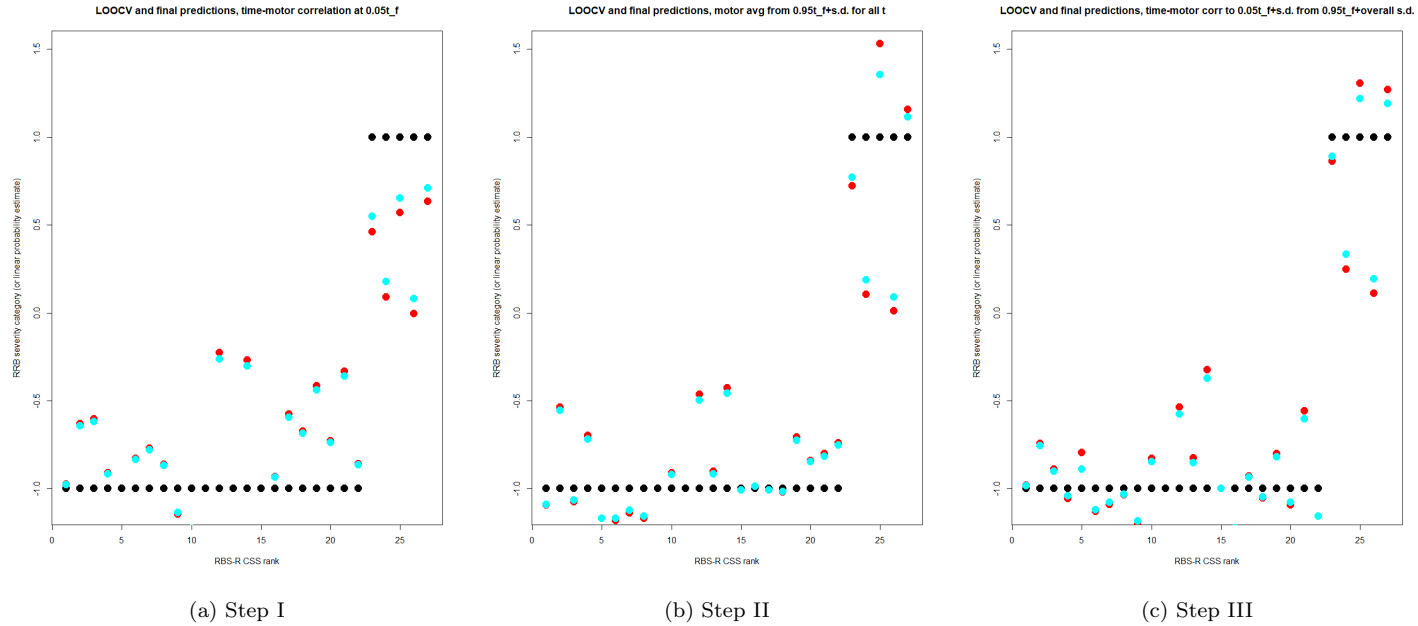
Figure 3.68: Nonlinear dynamical model output regressor stepwise linear regression model predictions of subject RRB severity category for left-out observations during leave-one-out cross-validation (red) and after full model construction (cyan) for the first three stepwise model iterations. Only three iterations are shown as the multiple R^2 and root-mean-square error are superior for the third iteration using nonlinear dynamical model output statistic regressors compared with the fourth and fifth iterations of linear and power regression models using subject connectivity (Pearson correlation) data. This supports the validity of the dynamical model overall and of the nonlinear extension. Regressors were (a) $\mathrm{corr}(z,t)|t < 0.05t_f$; (b) $\{\bar{z}|t \geq 0.99t_f\} + \{\sigma(z)|\forall t \in [t_0, t_f]\}$ (c) $\{\mathrm{corr}(z,t)|t < 0.05t_f\} + \{\sigma(z)|t > 0.95t_f\} + \{\sigma(z)|\forall t \in [t_0, t_f]\}$. The step I model final predictions have no errors in sign (predictions are all negative for low- and positive for high-RRB subjects), whereas the predictions of left-out points have one sign error. The step II and III models have no sign errors before or after cross-validation prediction and training, cf. fig 3.69.

(a) Step I   (b) Step II   (c) Step III
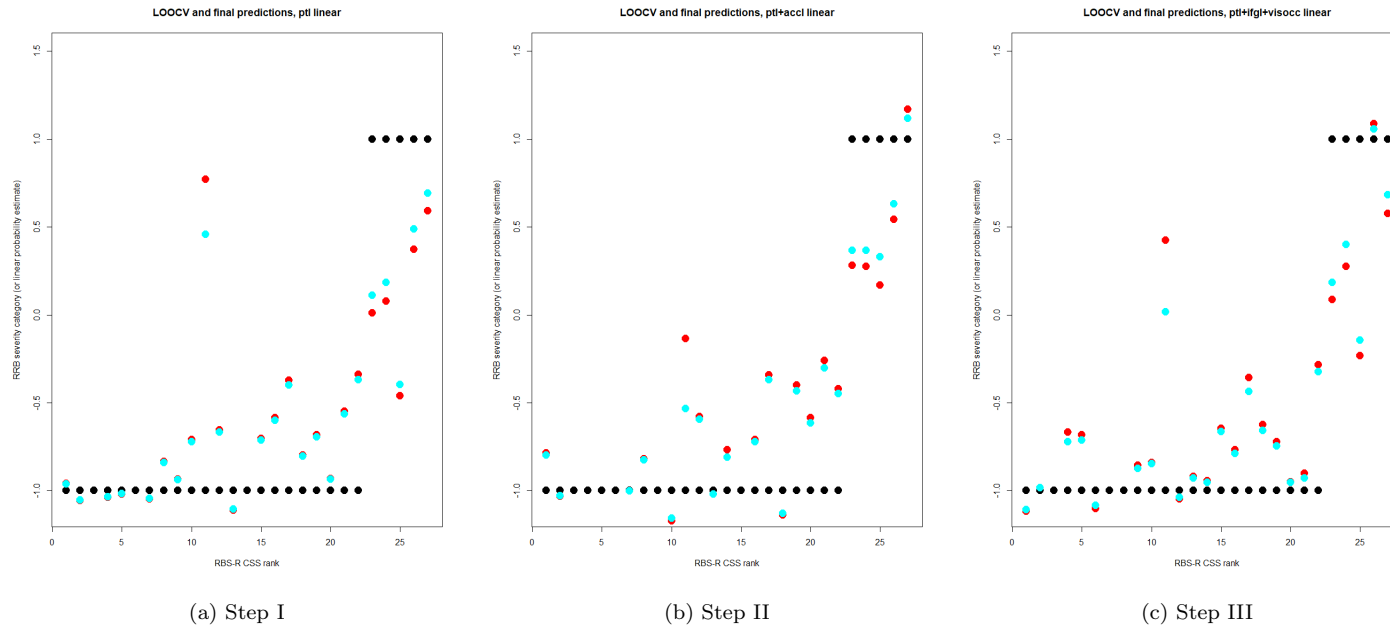
Figure 3.69: Subject functional connectivity (Pearson correlation) regressor stepwise linear regression model predictions of subject RRB severity category for left-out observations during leave-one-out cross-validation (red) and after full model construction (cyan) for the first three stepwise model iterations. Regressors were (a) L PT —cingulate; (b) L PT —cingulate + L N acc—L SMA; (c) L PT—cingulate + L IFG—R occipital + Vis —L IFG. The step I LOOCV predictions have two sign errors, as opposed to one in the pre-training step I model in figure 3.68, and the final predictions have two sign errors as well, compared to zero for the dynamical model output regressor step I model. The step II model has no sign prediction errors. The step III model pre- and post-training predictions both have two sign errors, the increase a result of the model selection algorithm not optimizing for this metric. Notice the different order of inclusion of potential regressors in this linear model stepwise iteration compared to the power regression results of table 3.7.

3.7.6 Model extension: stochastic perturbation

The model system 3.11 abstracts two important features, one of the input to the nervous system and one of the nervous system itself: time-varying stimulus activation of sensory subnetworks and nonlinearity of the time dynamics of brain function in response to that external stimulus activation. However, the modeling of stimulus input as the value of a sinusoidal function at each given t is, in addition to being entirely deterministic, unrealistically trivial in its predictable (lack of) variation across time. While restricting stimulus input to a measure in $\mathbb{R}$ is, even disregarding the trivial functional form used in the prior model iterations, itself an oversimplification at the neurocognitive level, modeling stimulus input at the level of individual sensory systems exceeds the hypothetical functional network's (from which the dynamical model in all iterations is substantially derived) theoretical resolution, since putative "sensory" ROIs are grouped together irrespective of their specific sensory modality or modalities, and relatively few primary sensory areas were able to be implicated in the network arrangement effected in section 3.6. However, the final dynamical model extension in this section is posited to address both the temporal and neurocognitive oversimplification in prior model iterations. The extended model is described by

$$
\begin{aligned}
\dot{x} &= -\omega \sin(\omega t) + \text{RW}(t) - \left[\sum_{l=1}^{4} \left((0.5^l) \text{RW}(t - l) \right) \right] \\
\dot{y} &= cx - \delta y \\
\dot{z} &= r|z| + sz - fy - \frac{\phi z^3}{|z|},
\end{aligned}
\tag{3.12}
$$

where

$\text{RW} =$ the random walk function with $\text{RW}(t)$ uniformly distributed across [-1, 1] and

$l =$ a time lag.

Hence, modeled sensory subnetwork input now comprises a stochastic differential equation representing its time behavior; this straightforwardly addresses the temporal oversimplification. And, because the model stimulus function is only an input to the model, whereas its output is activation in executive and motor (non-sensory) networks, the stochastic input also resolves the neurocognitive oversimplification within the model abstraction because stimulus function values are no longer recoverable to the infinite past given known t and initial and current model conditions due to the independent stochastic component of the stimulus function value at every t. Because historical values of the stimulus input function are unrecoverable and, therefore, unobservable, no claim can be made within the model universe regarding their modal composition. Conversely, when the stimulus function is entirely deterministic and its values, therefore, recoverable to the arbitrary past, its temporal

autocorrelation could be argued to indicate isolability to a single sensory subnetwork with discrete neuromodulatory behavior in response to sensory input (of that single modality). The decoupling of the modeled stimulus input (and therefore sensory subnetwork activation) with its past facilitates the interpretation that the values are composites representing putative net effects on executive subnetwork activation via an unknown and unobserved functional relationship. Theoretical synthesis the two disparate sources of modeled stimulus input is accomplished by considering the deterministic component as internally generated stimulus input from genetically determined homeostatic rhythms (e.g., circadian cycles), and the stochastic component as encapsulating all other stimulus factors. The stochastic input likewise decouples model output even further from the statistical correlations that, along with *a priori* conjecture as to relevant neurocognitive mechanisms, formed the basis for the hypothetic network construction and subsequent dynamical model iterations.

While figure 3.64 shows prominent dynamic equilibrium behavior in phase space for most subjects, the introduction of the stochastic component of stimulus input in this model extension abrogates the possibility of discrete equilibrium regimes or other stable behaviors through time. For comparison, analogous phase portraits to those in figure 3.64 are shown at the group level in figures 3.70 and 3.71; in this case, multiple model runs are depicted, with a given realization of the random walk function compared between the high- (top) and low-RRB severity category model parameterizations in each pair. Again, as in the prior depictions, color mapping of phase trajectories and overlaid point plots is from early t (mint green) to late t (magenta). Because the same 100 time steps underlie every model run, the differences in the distribution of green and magenta in phase space are as significant as the trajectories themselves in assessing modeled dynamical activity within the functional brain subnetworks. Note spatiotemporal patterns do emerge within parameterizations, and between parameterizations for a given random walk function realization, because the dynamical properties of the executive and reinforcement motor subnetworks remains intact, and stochastic stimulus input is constrained to within the magnitude range of the deterministic stimulus component, yielding apparently aggregately quasi-stable stimulus- and subgroup-dependent spatiotemporal regime genera.

At the subject level, 20 runs of the model were executed per subject. Figure 3.73 depicts time series per-subject as in figure 3.62, with the same color mapping from low (medium blue) to high (aureolin) RBS-R CSS rank. In this case, however, multiple time series iterations are plotted per-subject corresponding to different values of the random walk function. Likewise, figure 3.75 depicts per-subject phase portraits akin to figure 3.64. Again, discrete realizations ("runs") of the model for different randomizations of the random walk function values are depicted. In this case, however,

because each of the 20 runs would have as many corresponding phase trajectories as each per-subject plot in 3.64, the trajectories are omitted, and only discrete points from the model output are plotted. Color mapping is as in the preceding nonlinear model extension phase portraits, however, the background is black (#000000) to increase the contrast between the individual points plotted and the coordinate plane.

Per-subject model output, specifically that as depicted in figures 3.73 and 3.75, was extracted, and summary statistics were calculated. Specifically, the mean, standard deviation, skewness, kurtosis, and correlation between z and t were calculated for each subject for each of the 20 runs, for the entire run. All such values are listed starting in table A.5 in the appendix. The values are depicted for each subject against that subject's RBS-R CSS for each individual model run in line graphs, one graph for each statistical measurement, in figures 3.76 and 3.77. The mean per subject across all 20 runs is overlaid on the same line graphs in figures 3.78 and 3.79. Only the averaged standard deviation values seem to suggest a direct linear relationship between RBS-R CSS and the average statistical measure. However, note that, for the mean, the divergence between the most extreme runs, those with the maximum and minimum values across runs, seems to increase with increasing RBS-R CSS. Hence, a statistic, the **divergent mean product** , was constructed as the product of the means from the two most extreme model runs, that is, those with the global maximum and minimum values for $\bar{x}$. The relationship between this statistic and subject RBS-R CSS is shown in figure 3.80, against the plot of all values of $\bar{z}$ as in the upper left plot in figures 3.76 and 3.78, with the most extreme runs plotted in white (#ffffff).

Regression statistics are summarized in table 3.25 for univariate regression models of RBS-R CSS on the average values of each of the five summary statistics (mean, s.d., skewness, kurtosis, $cor(z,t)$) calculated for each model run, as well as for on the divergent mean product statistic. Both the mean(s.d.(z)) and divergent mean product statistic regressors were superior in univariate regression to all regressors summarized in table 3.22, with the latter being the superior of the two. Leave-one-out cross-validation analysis was performed for the divergent mean product regressor, with results plotted in figure 3.81. Comparison of the resulting model with all of the next best analogous univariate models, including that of the mean(s.d.(z)) statistic from the present model extension, is summarized in table 3.26. It is notable both that the divergent mean product regression model has a high R^2 relative to the other univariate models, and also that it has a higher R^2 than the four-regressor model of RBS-R CSS on the four empirical connections identified and validated in sections 3.2 and 3.3, respectively; thus, the stochastic model has produced at least one measure that correlates more strongly with subject RBS-R CSS than do all of the connectivity values, in

combination with individual coefficients, initially found to be *themselves* correlated with subject RBS-R CSS.

Additionally, table 3.27 shows that, while decidedly lesser in statistical significance, one of the five summary statistic regressors for each subscale score from the stochastic model output in this section more strongly predicted subject ADOS-G social and communication scores than did the same four empirical connectivity values, *plus* the *a priori* identified left nucleus accumbens—left supplementary motor area connection. The analysis yielding these results was performed as a preliminary inquiry into whether or not the current results suggest a "core autistic neurocognitive phenotype," across core deficit domains, might be suggested by the dynamically modeled brain activity to an extent exceeding that intimated by the behavioral measure scores or connectivity values (associated with RBS-R CSS) themselves. An encompassing test of each univariate regression model, ADOS-G social subscale score on mean(kur(z)) and ADOS-G comm. subscale score on mean(cor(z, t)), against the five-connection regression models suggested that the univariate models using the stochastic dynamical model extension statistic was, in fact, superior to the five-connection model. While the model $p-$ values for the two relevant models in isolation are at the threshold of significance given the multiple comparisons, their superiority to the five-regressor model is less ambiguous. While there is no intrinsic reason beyond the aforementioned potential for the existence of a "core autistic (neurocognitive) phenotype" to conjecture that the relevant ADOS-G subscale scores should correlate with the subject connectivity values for the five connections, the salient point is that this is no less true for the summary statistic regressors, and yet, in the case of both of the ADOS-G subscale scores tested, *one of the five* summary statistic regressors explains more of the score variance by itself than do *all five* of the (no more likely *a priori* to be uncorrelated) connectivity value regressors in a single model. These observations together thus fail to rule out the possibility of an extended core ASD neurocognitive phenotype.
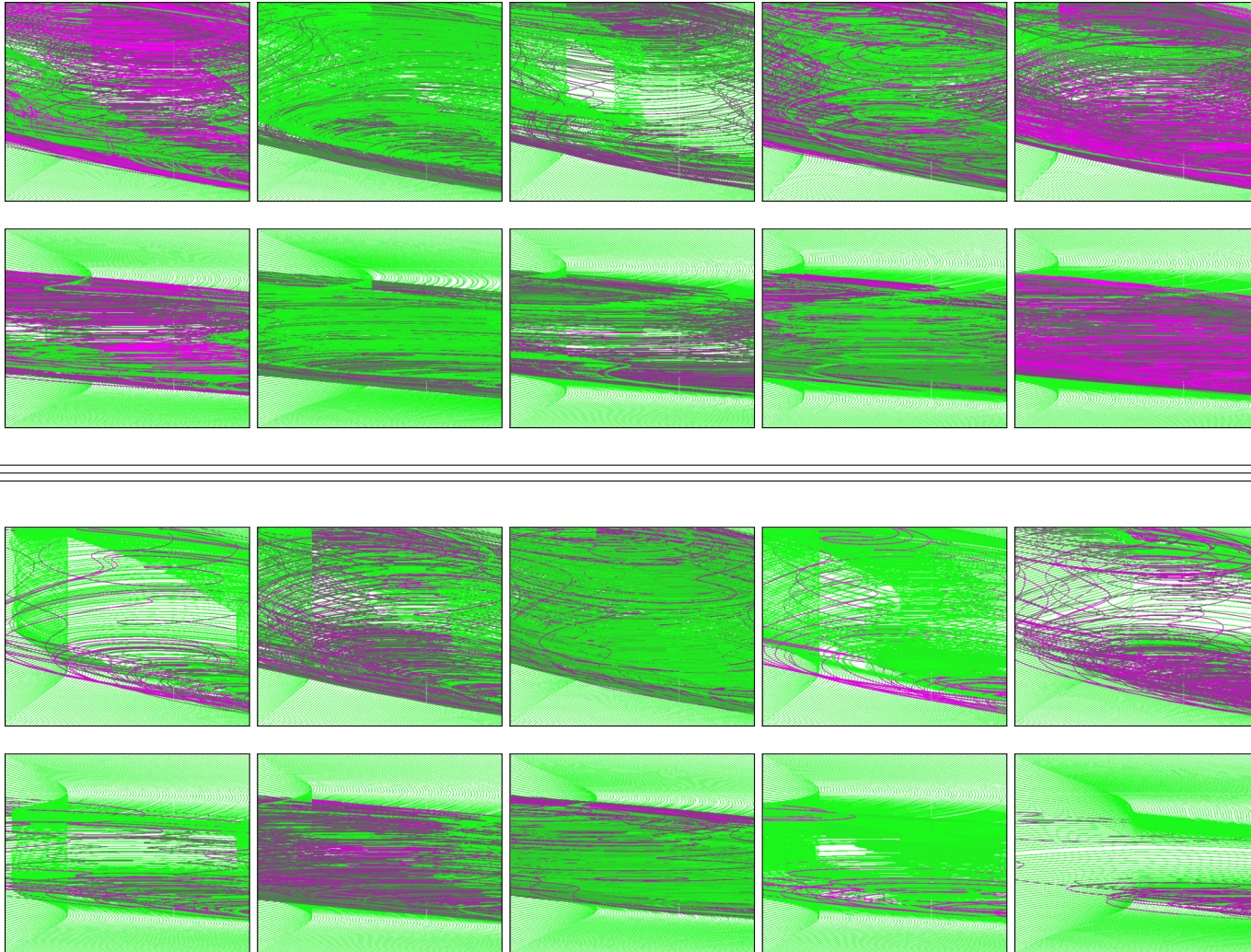
Figure 3.70: Paired high-/low-RRB stochastic portraits; ref. fig. 3.7.6.
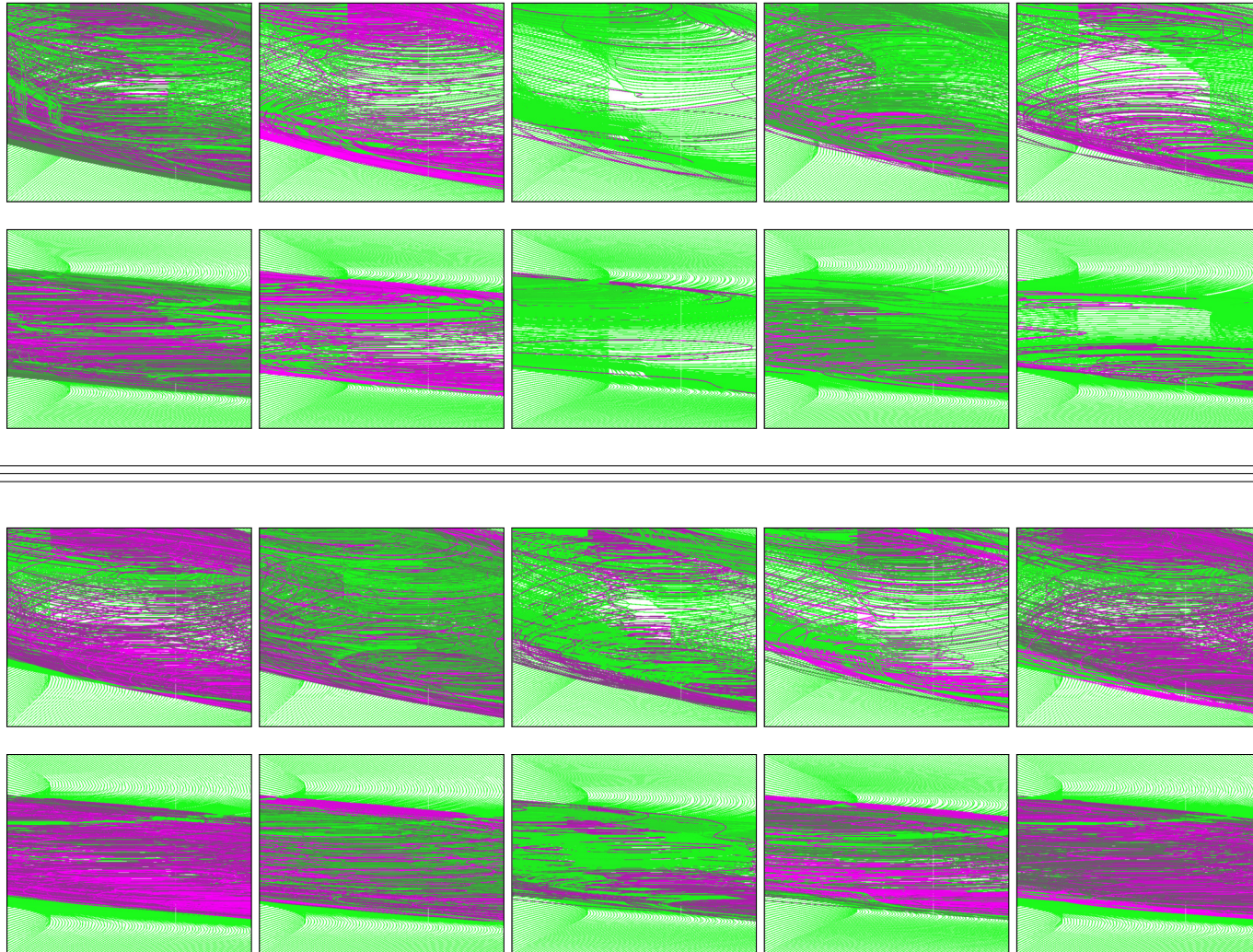
Figure 3.71: Paired stochastic portraits cont.; ref. fig. 3.7.6.

Unlike in figure, e.g., 3.60, all of the phase portraits in figures 3.70 and 3.71 are actual RBS-R severity-category derived model iterations, this time adding the random walk stochastic term. Because of the addition of this term, each individual phase portrait represents one unique realization of model behavior given the randomly determined stochastic portion of the stimulus input the modeled sensory networks. High-RRB derived parameters are depicted in the top five phase portraits of each pair of rows with five portraits in each row, the lower row depicting low-RRB-derived-parameter model behavior under the same stochastic input. Thus, each pair of vertically matched high- and low-realizations depict differences specific to the behavioral category model parameters and the behavior they impart on the model *given specific stochastic perturbation.*

Figure 3.72: Group level stochastic-input model extension, description of phase portraits with stochastic stimulus input (figs. 3.70 and 3.71.)

Subject RBS-R CSS rank increases from left to right and from top to bottom

Increasing RBS-R CSS
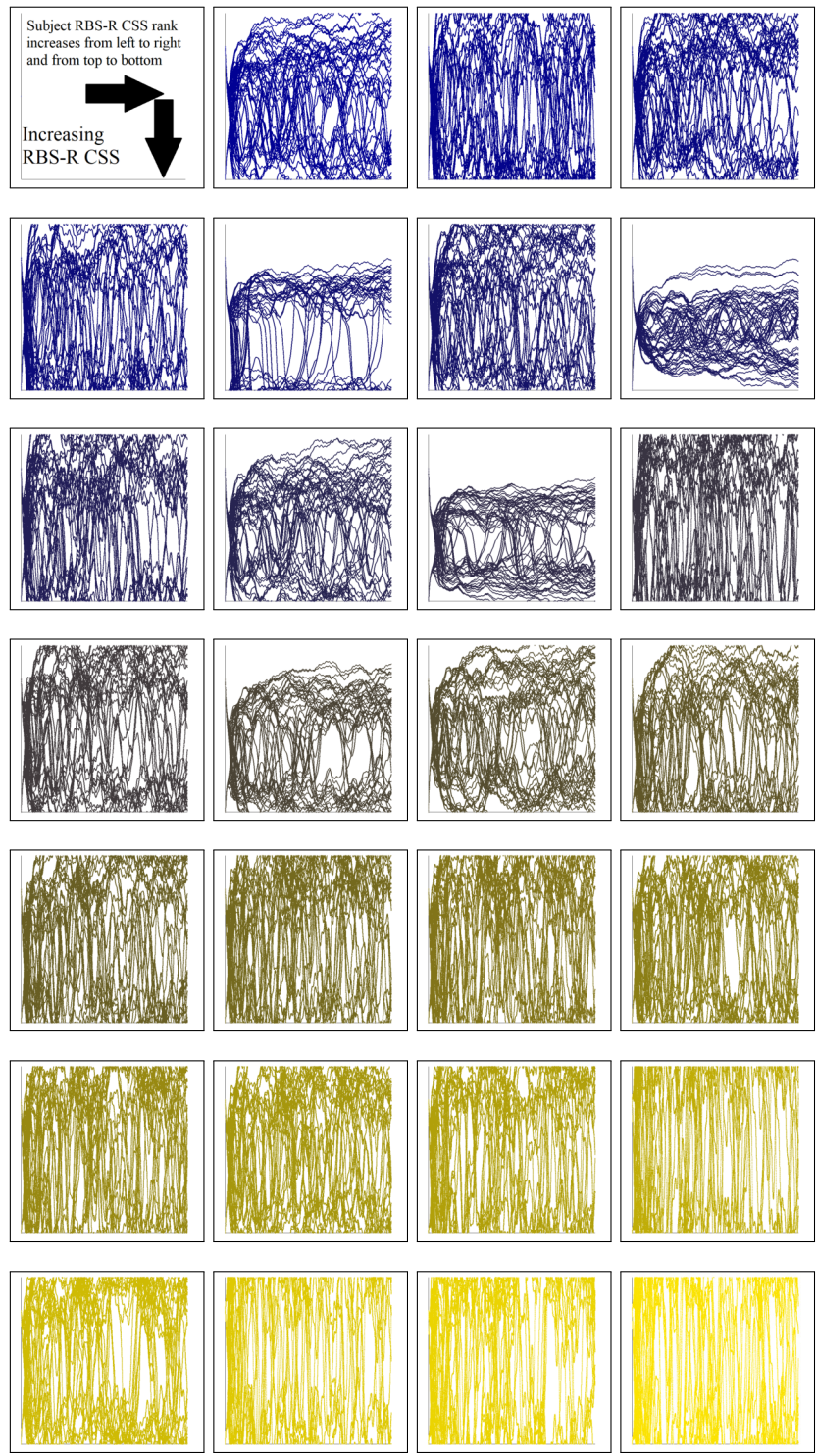
Figure 3.73: Subject-level stochastic time series; ref. 3.74.

Figures 3.73 and 3.75 are analogous to figures 3.62 and 3.62. The subject-level time series in this case, rather than representing a dynamic equilibrium regime, depict distinct realizations across 20 runs of the model with independent generation of the stochastic stimulus input, across initial conditions corresponding to those used for the phase portraits. The subject-level phase portraits, color mapped as in figure 3.64, are depicted on a higher contrast coordinate plane background because only individual model output data points are plotted rather than phase trajectories proper; this allows resolution of detail while plotting many runs with different stochastic stimulus input. Plotting all complete phase trajectories would result in excessive overlap given the 20 runs. While the time series tend to diverge for all subjects, a behavior resulting from the random walk input used to introduce stochasticity to the stimulus function, the phase portraits, conversely, again show a qualitatively distinct spatiotemporal pattern for the five "high-RRB" category subjects. While no static or dynamic equilibria are reached, trends can be observed in the data point distribution consistent with the established theoretical framework used to interpret values of y and z through time in phase space.

Figure 3.74: Explanation of figures 3.73 and 3.75 on the prior and following pages, respectively.
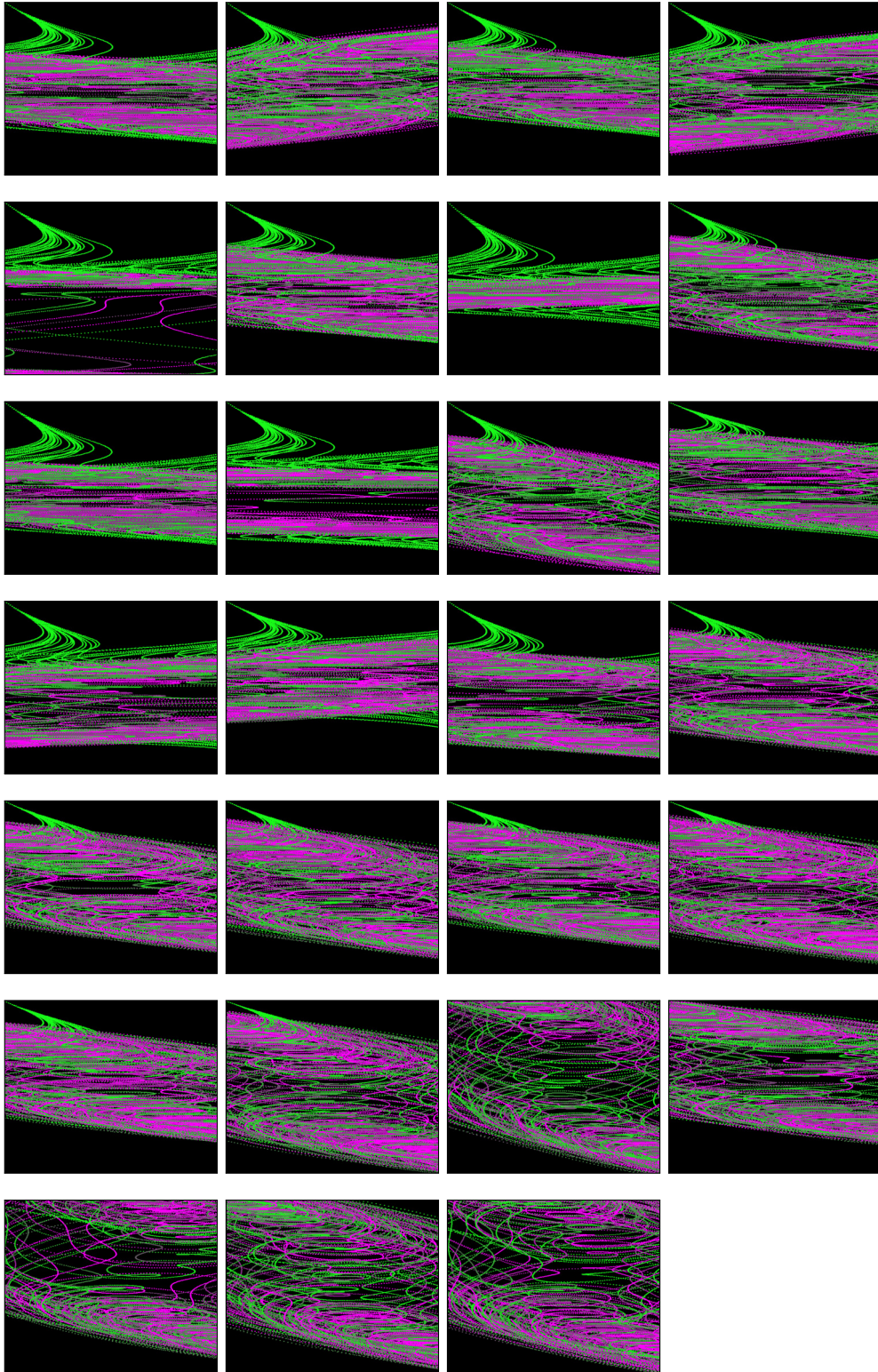
Figure 3.75: Subject-level stochastic phase portraits, ordered as in fig. 3.73; ref. 3.74.
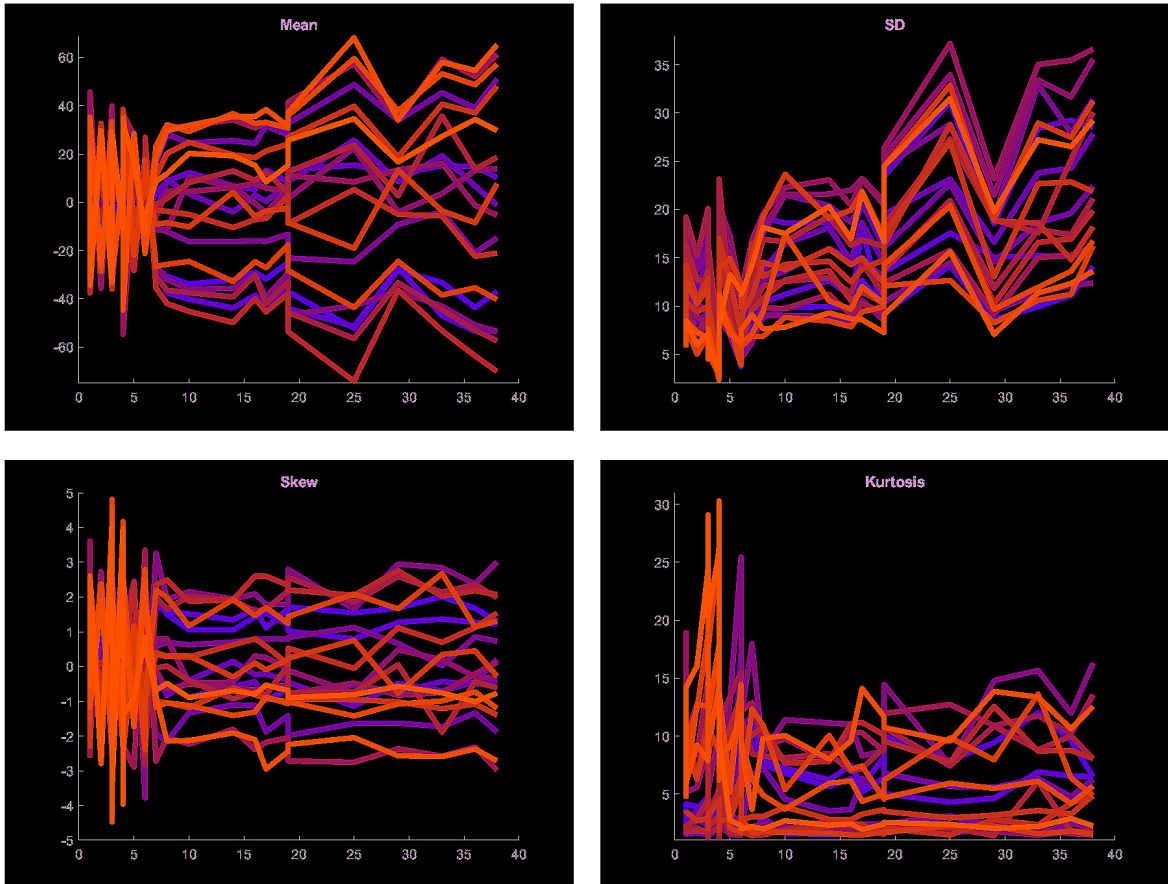
Figure 3.76: Plots of subject RBS-R CSS and stochastic model statistics, horizontal axis subject RBS-R CSS, vertical axis statistics calculated from model output with the stochastic stimulus input. The twenty runs of the model with unique random-walk function values, are identified by run number color mapping from violet (pure, #7f00ff) to orange (pure, #ff7000) for comparison of runs between plots.
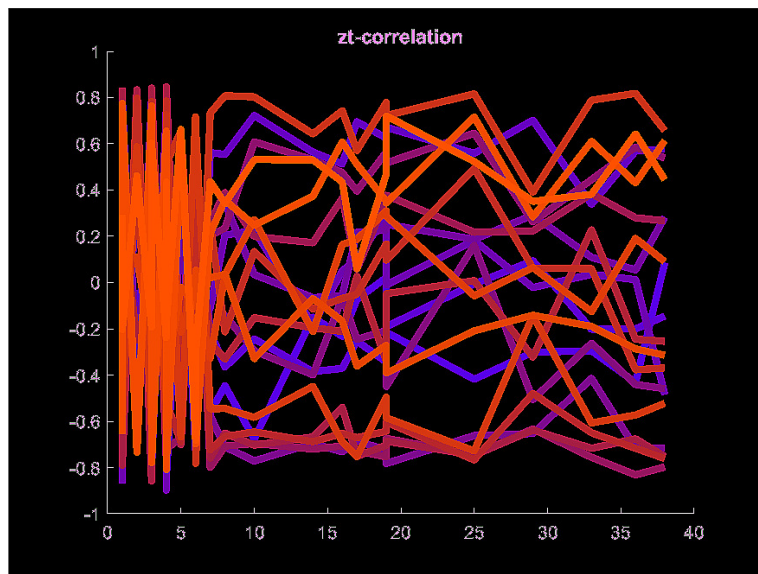
Figure 3.77: Plot of subject RBS-R CSS with stochastic model z—t Pearson correlation. Run color mapping is as in figure 3.76.) for comparison of runs between line graphs.
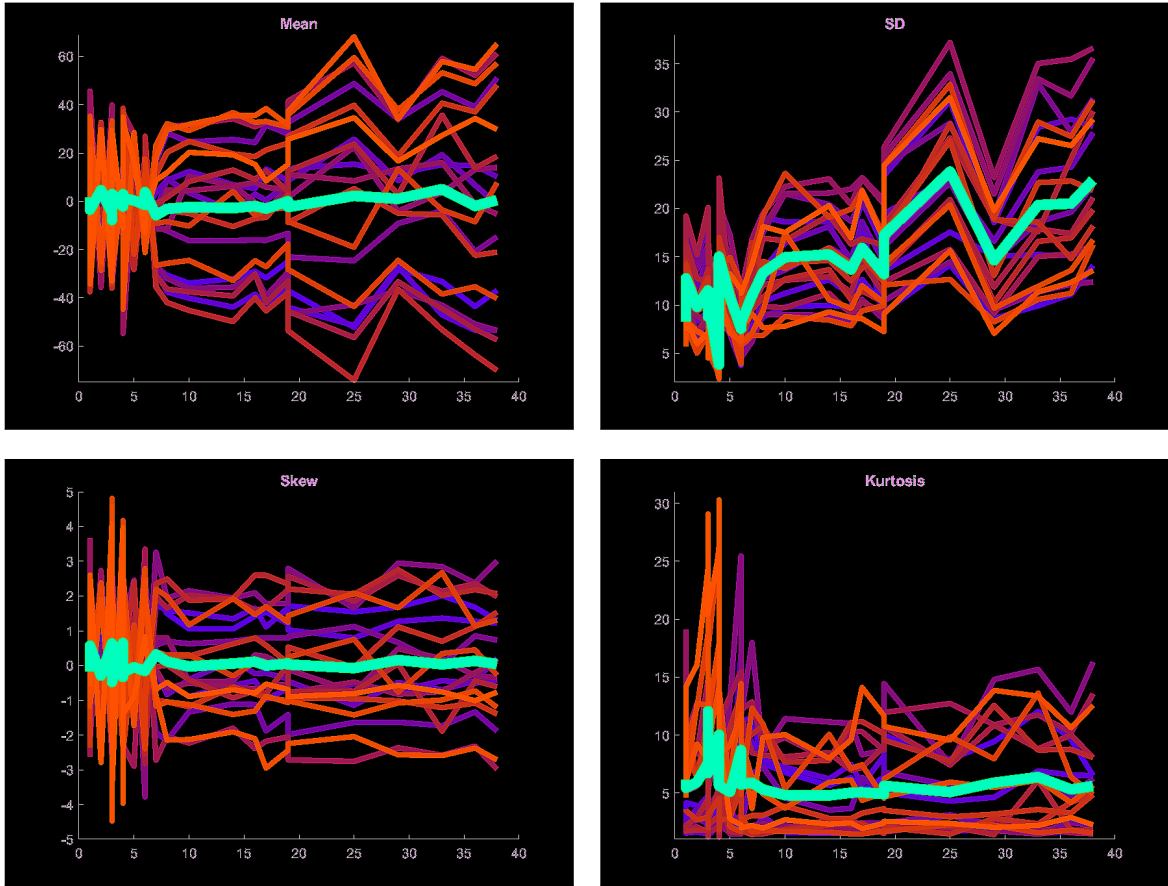
Figure 3.78: The mean values of the 20 runs for each subject (in terms of RBS-R CSS on the horizontal axis) from figure 3.76 in mint green (#00FFC0).
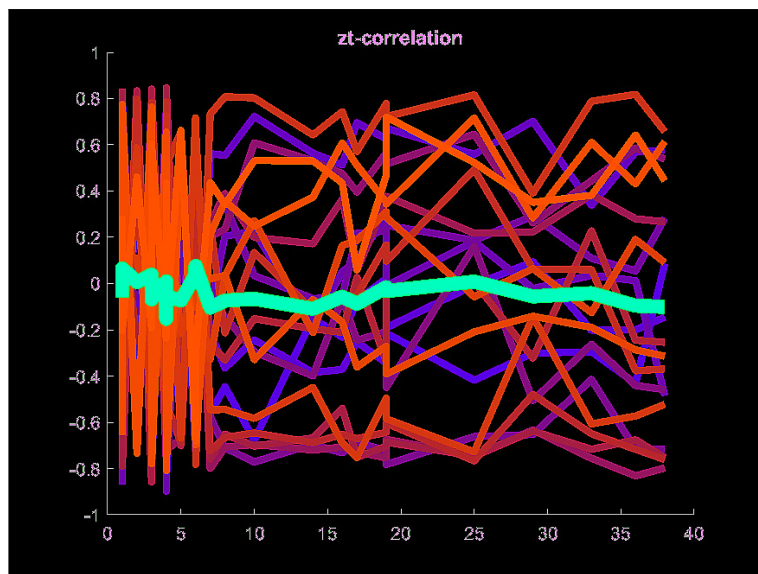
Figure 3.79: The mean correlation of subject RBS-R CSS with stochastic model extension z—t Pearson correlation across the twenty runs in mint green.
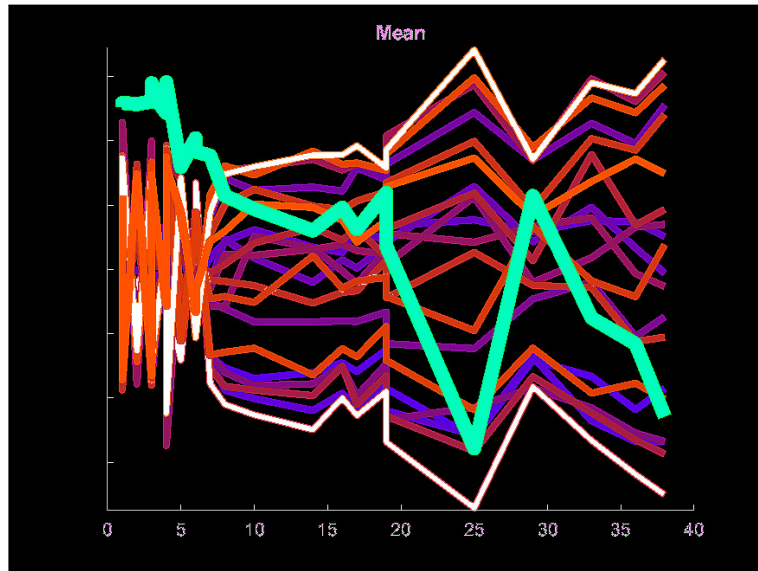
Figure 3.80: Correlation of subject RBS-R CSS with $\bar{z}$ peak difference across all twenty runs, scaled and shifted to fit in the same window as the values of $\bar{z}$ as first shown in figure 3.76. The divergence, observed qualitatively, between the highest and lowest mean values(white) across runs with increasing RBS-R CSS motivated calculating this statistic.

The horizontal spacing due to increasing gaps in numerical scores at higher measured RRB intensity understates the actual strength of the correlation of this statistic with subject RBS-R CSS; The Spearman's rank correlation ρ test's of the variables p-value $= 8.265$e-11, indicating extremely high consistency between the ordering of the statistic and the behavioral score, and see also table 3.25 for regression testing results.

Table 3.25: (A) Various statistics used as regressors, all averaged across the twenty runs of the stochastic model and depicted in the preceding figures, for predicting subject RBS-R CSS. The divergent mean product regressor ($\bar{z}_{\min} \cdot \bar{z}_{\max}$) is the best single regressor identified across all model forms, and notably, is derived from model output with substantial stochastic influences on dynamical behavior. (B) Power-regression probability model using the divergent mean product regressor, cf. table 3.7.

(A) Linear regression of subject RBS-R CSS on averaged stochastic dynamical model statistics

Measure	Estimate	Std. Error	t-value	p-model	R^2
$\mathrm{mean}(\bar{z})$	0.5692	0.6990	0.814	0.423	0.02584
$\bar{z}_{\min} \cdot \bar{z}_{\max}$	**-0.0066782**	**0.0007023**	**-9.509**	**8.77e-10 *****	**0.7834**
$\mathbf{mean(\sigma(z))}$	**1.8555**	**0.2561**	**7.246**	**1.36e-07 *****	**0.6774**
$\mathrm{mean}(\mathrm{skew}(z))$	.004	8.222	0.244	0.809	0.00237
$\mathrm{mean}(\mathrm{kur}(z))$	-2.365	1.194	-1.981	0.05865 .	0.1357
$\mathrm{mean}(\mathrm{cor}(z,t))$	-59.256	38.556	-1.537	0.1369	0.08633

(B) Power regression of subject RRB severity category on $\bar{z}_{\min} \cdot \bar{z}_{\max}$

Measure	Estimate	Std. Error	t-value	p-model	R^2
$\bar{z}_{\min} \cdot \bar{z}_{\max}$	6.4357	0.9719	6.622	6.15e-07 ***	0.6226
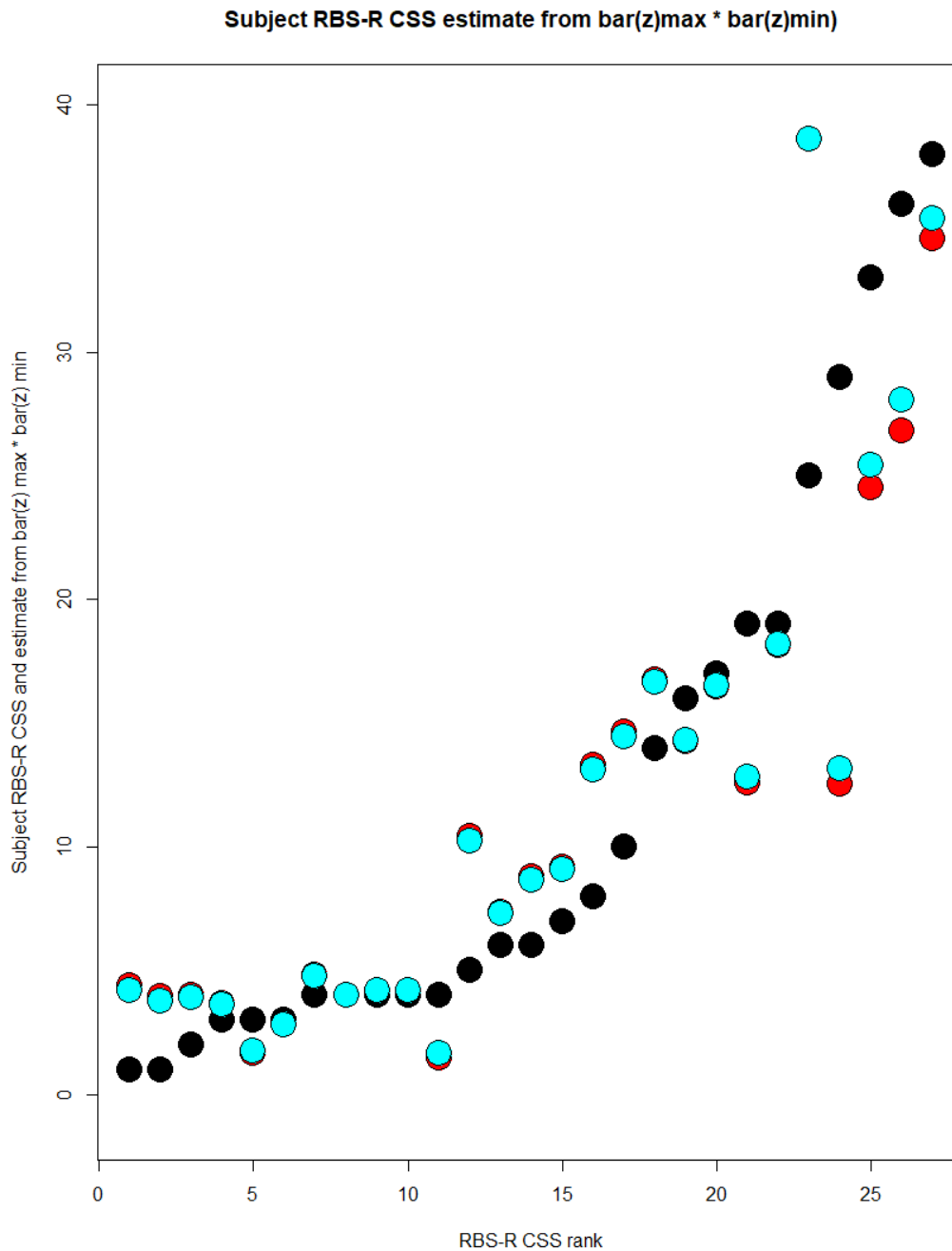
Figure 3.81: Using the product of the two most-diverging averaged values for mean z through the 100 model time steps (evaluated at intervals of 0.01) in regression prediction of RBS-R CSS provides dramatically better fit than any other single regressor, and multiple other combinations of regressors: Using all four empirically identified connections in linear regression prediction of RBS-CSS yields an unadjusted R^2 of 0.731. Only by including the *a posteriori* left nucleus accumbens connection, and thus five total regressors, does the full linear regression on subject connectivity values exceed the predictive power of the product of the divergent average alone, albeit substantially ($R^2 = 0.9029$).

Table 3.26: J-tests of divergent mean product regressor against next best model. The divergent mean product regression model is superior in terms of p-value and both unadjusted (given below), and even more so in terms of adjusted, R^2. The divergent mean product regression even significantly improves upon one including all four empirically identified connectivity values as regressors, albeit that model likewise does so with the divergent mean product regression model mutually.

Model or regressor	p	R^2	Improvement from divg. mod	Improvement to divg. mod	Orig. ref . table
Linear static $\hat{\hat{z}}$	2.809e-06	0.591	2.908e-5 ***	0.1128	3.17
$\mathrm{corr}(z,t)\|t < 0.05t_f$	7.076e-07	0.6328	0.0001157 ***	0.1181717	3.22
$\mathrm{mean}(\sigma(z))$	1.361e-07	0.6774	0.001132 **	0.267840	
OLS(ptl.cing + ifgl.occr + visocc.ifgl + atfuscl.dmnlpr	4.834e-06	0.731	0.0001458 ***	0.0007532 ***	3.6 log-transformed power regression form given)
Divg. mod	8.773e-10	0.7834	—	—	3.25

Table 3.27: Correlations of ADOS-G social and comm scores with stochastic model statistics. Considering each ADOS-G subscore separately and adjusting for five comparisons within each set of regression statistics, the $\text{mean}(\text{cor}(z, t))$ regression model is significant after multiple comparisons correction for the communication subscore. (B) For both subscores, the best regression model (M1) on single stochastic model output statistics is not significantly worse than the encompassing model (ME) including as regressors the five connections used in the stepwise regression analysis in table 3.7 first identified in the initial whole-brain ROI-to-ROI (section 3.2) and seed-based (section 3.3) connectivity analyses. Each five-connection model (M2), however, is significantly worse than the encompassing model.

(A) Comparison of regression models for ADOS-G subscale scores.

Regressor:	$\text{mean}(\bar{z})$	$\text{mean}(\sigma(z))$	$\text{mean}(\text{skew}(z))$	$\text{mean}(\text{kur}(z))$	$\text{mean}(\text{cor}(z, t))$	5 connections
ADOS-G social score						
p-value (model)	0.7538	0.5816	0.2237	**0.01752**	0.9062	0.7373
R^2	0.004007	0.01231	0.05863	**0.2056**	0.0005664	0.1156
ADOS-G comm score						
p-value (model)	0.6456	0.3634	0.6840	0.8985	**0.006264**	0.2948
R^2	0.008594	0.03315	0.006739	0.0006637	**0.2627**	0.2388

(B) Encompassing (ME) test [215] of best univariate (M1) and 5-connection (M2) models.

	Social	Comm
M1 vs. ME	0.59712	0.37501
M2 vs. ME	0.01967 *	0.01908 *

CHAPTER 4
DISCUSSION AND CONCLUSION

4.1 RATIONALE AND ASSESSMENT OF METHODOLOGICAL APPROACH

The results of the present study demonstrate the viability of employing a hybrid approach to the assessment of correlations between functional measures of resting-state brain activity and symptom manifestation in a neuropsychological disorder when such measures are available in rs-fMRI datasets. Particularly, the methodological approach incorporated traditional rs-fcMRI analysis with exploratory seed-based surveyal of connectivity to and from putative nodes in a hypothesized brain network of functional relevance to the particular symptom manifestation, the network itself being iteratively constructed by observation of the functional connectivity values between the putative nodes in the exploratory survey and successively guiding subsequent surveyal and search for further connections and nodes resulting in a discrete and fully interconnected functional network topology, with connectivity values from both the initial traditional analysis and the exploratory network construction procedure ultimately manifesting in a model system of putative brain activity consisting of differential equations with nonlinear, time-inhomogeneous, and stochastic member equations, which was solved numerically via software implementation, and then evaluated in light of its own intrinsic behavior as well as its correlation to the particular symptom manifestation measures. Individual, discrete analyses comprising this approach in its entirety were thus:

(i) model-free whole-brain functional connectivity analysis

(ii) calculation of seed-based connectivity metrics on both the connections identified in the previous step and those chosen *a priori* based on prior observations

(iii) regression-based analysis of the ensemble significance of the identified connections in the prior two steps by comparison to homologously derived connectivity measures based on randomization of the underlying data

(iv) iterative seed-based connectivity analysis considering effects sizes only (threshold-free) guided by *a priori* hypotheses of the neurocognitive relevance to RRB manifestation in order to generate a hypothetical functional network to be used in

222

(v) dynamical modeling of the hypothetical brain network's behavior by a system of differential equations representing the time derivatives of network subcomponent activity with parameter values calculated from the real underlying functional connectivity data in order to generate plausible hypotheses regarding

(vi) statistical correlation between model output and quantitative (categorical or ordinal, in this case) measures of symptom manifestation within the neuropsychological diagnosis (ASD).

Functional connections are therefore the objects of the original whole-brain search, and their modeled behavior constitutes the raw data used to generate statistics for the final assessments in each of the dynamical model realizations. Importantly, this study identified *increasing* statistical correlation between the relevant behavioral measures contained in the subject data with model output generated by successive model forms that were *decreasingly* analytically connected to that subject data. Incorporating dynamic stimulus input, introducing nonlinear reactivity of a component subnetwork, and perturbing model dynamical behavior with extrinsic stochastic influences all tended to increase the explanatory power of statistics calculated from model output used as regressors in attempted reconstruction of actual subject behavioral measures. Ultimately, by regressing the primary measure of interest, the RBS-R composite scale score per subject, on a particular statistic (the divergent mean product; page 205) generated from the full model with time inhomogeneous, nonlinear, and stochastic behavior components, a greater unadjusted R^2 was calculated for the resulting linear regression with one independent variable than for an alternative regression model of RBS-R CSS on *all four* connectivity values identified as significant in the initial model-free whole-brain connectivity analysis that remained significant after the seed-based analysis step assessing the same ROIs. This result is salient not only because the one-variable regression outperformed the four-variable regression, but because all four of the regressors in the latter model were identified *specifically because they were correlated with the independent variable* (RBS-R CSS) in both regression models. This permits formulation of a preliminary hypothesis with respect to the dynamical modeling approach used: Dynamical modeling such as that effected in this thesis might potentially be able to capture some relevant aspects of dynamic brain function in neuropsychological disorder symptom manifestation. At worst, it captures relevant statistical correlations and, particularly if such results can be substantially reproduced using further analogous data, such statistical correlations imply the greater plausibility of real biological significance of modeled output than of an essential lack thereof. Of the most direct relevance to the central theoretical question developed in chapter 1, that of the fundamental nature of ASD as a disorder and diagnosis, particular model

output from the most complex model form outperformed *five*-regressor models for the prediction of symptom severity measures in the other two core deficit domains of ASD. While neither any of the five connections nor the model output presents with *a priori* rationale for conjectural proposition of any relationship to measures of symptom severity outside the RRB domain, the connections and model output *equally* lack such rationale, and hence, as with the case of modeling RBS-R CSS via regression on the divergent mean product and other statistical measures from model output, the modeled dynamical behavior of the brain realized via the chosen approach facially demonstrates at least the possibility of capturing substantially brain-wide (including cerebrum and cerebellum) spatiotemporal patterns of neural activity significantly associated with, and statistically accounting for the majority of the variance in, the available measure of symptom manifestation within one ASD core deficit domain (RRBs), and less substantially, but still significantly, aspects of such brain-wide activity correlated with manifestation of symptoms from the other two core deficit domains. While, given the model construction process, there is little reason to doubt the existence of *at least some* real relationship between *at least some* model output and actual subject behavioral inventory measures for RRBs, skepticism is warranted for the existence of any real relationship between model output and behavioral inventory measures for the other core deficit domains; while it is true the model output decisively outperformed much more extensive sets of regressors comprising the entirety of the initially identified functional connectivity values in predicting behavioral inventory measures in those two symptom categories, the model output regressors were themselves at the threshold of significance depending on the adjustment to the *p*-values chosen. However, the results still strongly encourage the tandem pursuit of further insight into whether (i) dynamical modeling such as in this thesis truly encapsulates measures of brain activity of real biological significance to the precipitating behavioral observations and (ii) whether such dynamical modeling can independently identify the extent of the similarity and/or distinctiveness of the neurocognitive phenotype of individuals with ASD diagnoses or analogous clinically-defined populations of persons.

4.2 BRIEF SUMMARY OF FINDINGS FROM EACH ANALYSIS STEP

In the initial ROI-level analysis, significantly RRB-associated connectivity values were found between (i) left planum temporale and left supplementary motor area; (ii) left planum temporale and salience anterior cingulate network; (iii) left pars triangularis and visual occipital network; (iv) right lateral parietal default mode network (consisting primarily of right angular gyrus) and left anterior temporal fusiform cortex. Seed-based assessment of these connections using standard statistical thresholding settings eliminated the connection between the left planum temporale and left supplementary motor

area as insignificant.

Subject-level connectivity values for each connection, taken as the Pearson correlation between the time series of the selected seed and the central voxel in the most significantly connected cluster for each seed for each subject, were extracted and visually inspected for qualitative patterns in the data. Based on the observation that for all four of the empirically-derived connections, and an additional connection identified *a priori* between the left nucleus accumbens and left Brodmann area 6, exhibited predictable qualitative changes at the literature-derived threshold for high RRB symptom severity, a linear probability (functional form) or power-regression probability (analytical form) model was constructed in order to investigate whether or not RRB-severity class could be predicted by either (i) an arbitrary combination of the connections as regressors, or (ii) specifically the interaction effects between *all* of the empirically-derived connections (the most restrictive predictor that incorporates all of the information from all such connections). In each case, the empirical model was a statistically significant improvement on the one derived from the initial spurious score distribution.

Step-wise sequential replacement of individual regressors in the full power regression model, including the four empirical and one *a priori* connections as possible regressors, indicated that the connection value that best independently predicted subject RRB-severity class was the one between right lateral parietal default mode network and left anterior temporal fusiform cortex, an empirically derived seed. Hence, the strict superiority of the exclusively *a priori* seed-based approach to analysis over the ROI-based empirical approach is rebutted. More integral to the research question, multiple functionally identified roles for the ROIs forming the nodes of the putative network have plausible associations with RRBs and/or other core ASD deficits, as discussed in section 4.3.

After confirmation of the statistical significance of the entire putative network comprising the identified ROIs, exploratory seed-based connectivity metrics were conducted to identify nodes that might integrate the whole network via functional and/or anatomical connectivity, with the resulting network shown in section 3.6 as figure 3.21. The network consisted primarily of three functional sub-network divisions: (i) a sensory/sensory association subnetwork comprising visual cortex, fusiform cortex, planum temporale, and orbitofrontal cortex (categorized as sensory association given no identified functional connections to sensory cortex of lower hierarchical levels) (ii) an executive/salience subnetwork comprising frontal pole, anterior cingulate cortex, and default mode network, and (iii) a motor subnetwork comprising precentral gyrus and supplementary motor area. Additionally, the network comprised two essential mediators of network-wide functional activity: nucleus accumbens, underlying putative reward reinforcement of motoric behavior, and cerebellum, modulating acti-

vation between subnetwork divisions. The network topology was used to inform composition of a dynamical model, shown in figure 3.2, which produced output in iterations of increasing complexity that was more and more statistically correlated with, but less and less analytically associated with, subject RBS-R CSS, or, that is, subject RRB manifestation severity.

Dynamical model assessment qualitatively suggests that RRBs in part result from greater intrinsic and reward reinforcement of motor cortex activation separate from motor cortex activation associated with executively-mediated goal-oriented responses to stimuli, and a stronger functional coupling between all network subcomponents. Regression analysis of the final (stochastic) model implementation suggests that RRBs might also correspond to greater standard deviation in the measure of excess motor activation, suggesting not only greater overall reinforcement of motor cortex activation concomitant with more severe RRB manifestation, but greater variability and lability of activity within motor cortex as well. Similarly, the composite divergent mean product statistic and regressor suggested increasing divergence of trajectories in phase space, in terms of extrema with greater absolute magnitudes, similarly correlates to RRB symptom severity. This measure obviously bears some analogy to standard deviation, but considers only the most extreme trajectories in phase space, rather than variability resulting from all trajectories. While other statistics generated from final model iteration output were less successful in predicting RRB symptom severity, model output statistics were of overall much greater predictive power across symptom domain inventory measurements than the functional connectivity values identified originally as explicitly correlated with RRB severity, thus precluding the rejection of a hypothesized core ASD neurocognitive phenotype in terms of brain functional dynamics associated with symptom manifestation.

4.3 FUNCTIONAL SIGNIFICANCE OF CONNECTIONS IDENTIFIED

All of the identified functional connections from the primary connectivity analysis have function potentially significant in RRB manifestation based on prior research, whether directly identifying the specific connections and their valences in ASD RRB manifestation, or via functionally relevant associations. First, given that the imaging data is of subjects at rest, the default mode network observations should be considered. Within the set of identified connections, those to, from, or wholly within parts of the default mode network tend to corroborate theories about altered DMN connectivity in individuals with autism spectrum disorder. A significant increase in intra-DMN connectivity has been identified in OCD-associated compulsive behavior [182]. The prior result identified such connectivity between posterior cingulate and ventromedial prefrontal cortex, compared to our finding of potentially comparable connectivity correlations between bilateral cingulate

and paracingulate gyri (CG, PCG) and left planum temporale, the latter located near, though not coterminous with, the temporoparietal junction, a proposed DMN-associated region. With appropriate caution due to the fact that the specific ROIs are not identical, only functionally related, the identification of intra-DMN connectivity encompassing proximal and functionally related areas of cingulate and left association cortex significantly positively correlated with repetitive behavior severity in a distinct disorder, that is, ASD, to an analogous finding in the literature specific to OCD affirms the broad role of extended DMN function in this class of behavioral pathology, and is likewise consistent with previously identified increased within-DMN connectivity concomitant with greater general ASD symptom severity [176].

Right angular gyrus comprises the other default mode network structure identified, and was identified in the initial whole-brain search specifically as the lateral parietal default mode network ROI. While left angular gyrus (see below) appears to have multiple higher-level language functions, the functional role of left planum temporale (PT), plausibly DMN associated due to its proximity to temporoparietal junction, is even more straightforward, forming the functionally defined Wernicke's area which is the core receptive language processing area that complements the productive-oriented Broca's area. The left PT—cingulate cortex connection (spanning multiple bilateral cingulate regions) contains two regions associated with the perception of coherent motion [252]. As discussed below, multiple other ROIs identified in significantly RRB-correlated connections also have associations with multimodal spatial perception, and, while not necessary motion perception, the execution of coherent patterns of motion at a fundamental level (that is, not goal-oriented action plans).

The other, and most specific, identified connection involving the DMN, in this case the *trans*-DMN left fusiform cortex to portions of right angular gyrus, is more novel, but nevertheless implicates several plausible mechanisms for RRBs and has been functionally associated with them [124]. Most generally, the dorsal stream, incorporating parietal and premotor cortex and including specifically angular gyrus, effects cortical representation of object locations and calculates how potential courses of action would interact spatially with those objects in those locations. It is contrasted with the ventral stream, which incorporates medial temporal and limbic structures, and demonstrates a preference for object identity and function representation [238]. Fusiform and cingulate cortex, located medially, are functionally involved in ventral stream cognitive processing. The fusiform face area (FFA) is a well-established region in fusiform gyrus that shows preferential activation to human face stimuli, and has been implicated in ASD social deficits. This region, however, typically shows *right* lateralization, and is localized to the portion of the fusiform gyrus around the temporooccipital junction [253], rather than in the anterior part of fusiform cortex, as found in the ROI-level search

(section 3.2). However, before network-level thresholding of the ROI-level results, right posterior temporal fusiform cortex was also identified as an ROI with significantly positively RRB-associated connectivity, but to cerebellar regions, which were excluded from the initial analysis. Increased FFA (right)—executive control network connectivity was found via fMRI in subjects viewing social rewards in comparison with FFA—DMN connectivity [254], whereas the connection identified in the present study suggested weaker left FG—right DMN and angular gyrus connectivity in individuals with higher prevalence of RRBs. Right angular gyrus has been associated with the representation of intended versus actual consequences of self-initiated actions [255], indicating potential significance to the types of motor behaviors denoted as RRBs, but further research is warranted into the potential association of the specific connection identified with RRBs more generally. Seed-based connectivity analysis, before correction for multiple comparisons, did identify significantly negatively RRB-correlated connectivity between right frontal pole (FP) and both left and right fusiform cortex, although the voxel clusters were small in size. Nevertheless, the potential significance of FP in immediate action execution [256] provides an at least cursory rationale for further investigation, in addition to that pertaining to other frontal regions associated with physical action planning, in the context of RRBs. Most substantially, perhaps, is that FP activity has been found to be predictive of actions before subjects are consciously aware of their own intention to perform said actions [257]; regardless of the many implications of this finding, it suggests that RRBs, which are not deliberately planned to attain specific goals but rather apparently spontaneous, compulsive, and purposeless, may well impute functional significance to a region with such a functionally identified role. As might be noted in figure 3.6, table 3.13, equation 3.4, and, most explicitly, in table A.2, the connectivity values at the subject and group levels between FG and FP were incorporated into the model parameter derivation (and associated functional network specification).

Given the supervisory role of right AG, the functional connectivity between it and left FG, and between FG and FP with the latter's role in spontaneous action execution, the connections between these regions offers rationale for further characterization in RRBs; differences in time-domain behavior of fusiform gyrus has been associated with RRBs in ASD, specifically, decreased variability of temporal dynamics [124]. The specific connection identified (left FG - right AG) too is perhaps more nebulous in light of the literature, but reduced FG connectivity in ASD rs-fcMRI has been identified [178]. And indeed, there are again multiple plausible mechanisms that could associate the differences in functional connectivity between the two structures with RRB manifestation. Left FG itself, most intriguingly, has been found to be a highly specific trimodal sensory integration center in object manipulation tasks [258], integrating visual, auditory, and haptic sensory information of ma-

nipulable objects. ASD is associated with sensory abnormalities within and across modalities [259], and hence, cortical processing centers that integrate information from multiple distinct modalities are of interest regarding a putative ASD "core phenotype." Structural plasticity in AG is associated with motor learning that requires spatial coordination, for example, jogging [260], and hence, the repeated performance of stereotyped motions too likely involves AG to some extent. AG, like FG, is multimodal with respect to its sensory substrates. Therefore, connectivity between the two regions doubly implicates multisensory processing, already well documented to frequently be aberrant in ASD.

Hypoconnectivity in visual cortex in ASD has been identified via rs-fcMRI [178], consistent with present results. Visual-specific processing centers associated with reading (Wernicke's area/PT and AG) and in coherent motion detection (CG and Wernicke's area), multimodal visual areas (left FG) associated with object perception all imply that RRBs may involve differences in perceptual processing centers of cortex, a finding consistent with the fact that the visual occipital (VOcc) network itself formed a significant ROI in one of the empirically identified connections, in this case to left inferior frontal gyrus (IFG), specifically, when correcting for multiple comparisons, between left IFG—right VOcc. Moreover, left IFG contains Broca's area, constituting the third strongly language-associated region identified in the present results after AG and PT. This connection in particular forms part of the dorsal visual stream, which is associated with the execution of precision-requiring manual actions [261]. As with the previously discussed connections, this provides a direct and specific rationale for the investigation of these two areas and their interactions with respect to RRBs: Given their stereotyped nature, they are executed with a high degree of "precision" even if with no apparent utility or purpose. Visual cortex exhibits functional significance spanning ASD core deficit categories; reduced visual cortex—salience network connectivity, consistent with that identified as associated with RRB severity in the present research results, has been observed to correlate with sensory abnormalities in ASD. Furthermore, circumscribed restoration of function to specifically this set of connections correlates with *exacerbation* of social deficits, additionally providing a mechanism of heterogeneous presentation not inconsistent with the observed weak negative correlation between RRB severity and communication deficit severity noted in the present results [262].

The *a priori* identified connection between left nucleus accumbens (NAcc) and left Brodmann area 6 (BA6) further supports assignment of significance to motor coordination-specific brain areas in RRB neurocognitive theories; BA6 overlaps with the supplementary motor area, which is involved in the planning of coordinated movement. Recent advances in high-resolution DTI techniques applied in human neuroimaging have revealed significant connections via corona radiata to the pyramidal

tract. This directly facilitates functional involvement of BA6/SMA in the actual execution of co-ordinated movements via anatomical connections, lending yet more theoretical justification for the plausible conclusion that such mechanisms are significant to RRB manifestation. Furthermore, while FP is functionally associated with spontaneous movements, BA6 has greater functional specificity to planned movement, albeit also to coordinated movement generally, as in the case of FP, and also the IFG—right VOcc connection. In the case of BA6, though, the other node of the connected pair is part of the striatal reward circuit, of paramount significance to contemporary explanations of the putative broader ASD cognitive and behavioral phenotype [263], and to specifically motoric behaviors. In view of the positive correlation between RRB severity and the strength of this connection, this result has the most straightforward putative mechanism: RRBs are more strongly reinforcing to individuals who demonstrate them more intensely. While the data in this study are of the task-free state, as SMA is involved in not only the execution, but the planning of coordinated movements, this is consistent with a hypothesis that high-RRB severity is at least in part dependent on a cognitive mechanism that reinforces the *intent* to perform such actions, which itself would suggest activation of reward pathways upon the actual execution of the actions. Functional and anatomical similarities are shared in skin picking in Prader-Willi syndrome in increased connectivity between basal nuclei (putamen) and sensorimotor cortex, and aberrant amygdalostriatal and hypothalamostriatal functional connectivity [190].

The cerebellar hub identified in the hypothetical network in 3.6 has significant connectivity to left fusiform cortex and right lateral parietal default mode network, which comprises parts of right angular and right supramarginal gyri. The specific interest of this pattern of connectivity with respect to ASD RRBs is that right angular gyrus has been associated with "out of body experiences [264]" through a mechanism thought to involve anomalous integration of vestibular and somatosensory information. The putative circuit comprising cerebellum, fusiform cortex, and angular gyrus substantially overlaps functionally with these roles, and hence the presence of this circuit within the larger network likewise implicates changes in the self-perception of the body in sensory terms, an association that could conceivably subserve an impulse to engage in RRBs as they result in somatosensory and vestibular feedback to the one initiating them, which may consequently result in reward pathway activation, or suppress anxiogenic influences or feelings of restlessness.

Further evidence for the significance of cerebellum as a mediator comes in the fact that it, along with other sensorimotor areas identified here, is implicated in differential activation between real and imagined movement, in which cerebellum itself does not seem to participate in imagined movement, while sensorimotor cortical areas do [265]. Given the fact that motor planning, spatial perception,

haptic feedback, and self-awareness of bodily motion have been functionally encompassed by the ROIs identified, as noted above, overlap with a functional network that differentiates between the imagining and execution of coordinated movements, perhaps especially in the context of an MRI scanner in which subjects are told not to move, and yet some of those who graciously volunteered to lend their brains for this present study have a particular proclivity for doing so, is a potentiality that further reinforces conjectures of the fundamental significance of the network nodes identified in subserving ASD RRB manifestation in some capacity.

Functional brain connections identified in this research correspond also to many identified in ASD neurocognitive research more generally. Results of a single study particularly consistent with the present ones are those identifying the dynamic functional connectivity associations between left pars triangularis, left middle occipital gyrus, left middle orbitofrontal cortex, right supramarginal gyrus, left cerebellum VIII, and cerebellum X, and autism spectrum disorder diagnosis. The listed ROIs correspond to, from this study, left pars triangularis (identical), visual occipital cortex (overlapping), orbitofrontal cortex (overlapping), right lateral parietal default mode network (overlapping), left cerebellum VIII (identical), and cerebellum X (identical). In addition to these six areas of consistent findings, the study also identified left postcentral gyrus and left supramarginal gyrus. Thus, the present study mutually identified six of the eight ROIs functionally implicated in ASD in the comparison study. Importantly, the ROIs in the study were identified in terms of dynamical functional behavior [266]. However, the association was with ASD diagnosis, as noted, not RRBs specifically. Nevertheless, the present results and those of this source do encourage further investigation of functional and dynamic connectivity associations between these ROIs, both in ASD generally and in RRB presentation in the disorder.

From these cumulated patterns, summarized in figure 4.1, emerges a coherent constellation of functional relationships between the relevant ROIs that has multiple identified physiological mechanisms which facilitate its correlation with RRB manifestation in ASD. Moreover, in one important respect, they are compatible with the existence of a "core phenotype" in ASD, although not one that is necessarily clear or straightforward. The fact that the majority of major language areas were implicated in the present results (figure 4.2) accords with the observation that there was, it was determined, a statistically significant relationship between subject RBS-R CSS and ADOS-G communication score in the present results. Furthermore, the lack of such an association between RBS-R CSS and ADOS-G social score is likewise consistent with this formulation: few areas directly related to social interactions were explicitly identified, although the potential significance of the fusiform face area cannot be entirely dismissed given its pre-network-thresholding identification in

the initial ROI-level analysis (section 3.2). However, the relationship between symptom severity in the communication and repetitive behavior domains was a *negative* one; the connectivity results do not suggest in any substantive way that they represent a compensatory mechanism between the two deficits, neither a coextensive one, but the preservation of, or even excellence in, cognitive and behavioral capacities with adaptive utility despite some general pattern of neurocognitive traits typically construed as deficits *is* consistent with adaptive accounts of aspects of ASD evolutionary etiology, the notion of which is discussed under assortative mating theories of ASD in section 1.2.2.

These results therefore permit a coherent narrative account of a putative brain network that presents with significant alterations within a subject population of those diagnosed with ASD as RRB severity increases, and in turn, an account of a plausible behavioral and cognitive ASD phenotype that comprises co-varying (but not linearly co-varying) measures of symptom severity. While the results are *not* tantamount to the isolation of a consistent and discrete pattern in which all three ASD core deficits reliably co-vary with one another, they are nevertheless not entirely inconsistent with the possible existences of such a cohesive, albeit frequently apparently idiosyncratic, varied phenotype. In a sense, that is, ASD neurocognitive diversity may well, given the size of the relevant population, correspond in at least qualitative respects with that of the population exhibiting putatively typical neurocognitive characteristics. Thus, we can neither rule in, nor rule out, a "unitary" pattern of connectivity alterations that correlates strongly with inclusive ASD symptom severity measures, but we can posit that at least one network discretely associated with two of the core deficits, if in an unexpected way for at least one of the deficits, manifests in these results. The negative correlation between the two behavioral measures actually, especially in light of the multiple language-associated ROIs identified when calculating connectivity metrics associated with a distinct symptom category, arouse novel inference as to the potential functional, if not behavioral in the expected manner, significance of the identified network in aspects of both RRB and communication deficit manifestation in ASD, although, as yet, no explication of such significance can be forthcoming.

4.3.1 Evaluation of identified connections in the context of ASD RRB FC research

Tables 1.5 and 1.6 summarize some of the connectivity results observed in past studies of their correlations with ASD and RRBs, respectively. Table 1.5, capitulating intrinsic grey matter connectivity, exhibits overlap with multiple of the ROIs comprising nodes of the identified network: precentral gyrus, posterior parietal cortex, temporoparietal junction (that is, at the boundary of planum temporale), and orbitofrontal cortex. While there is no direct comparison possible given the specific connectivity metrics in each case, plausible accounts can be given. For example, decreased mean

separation distance among motor areas, as identified in the summaries above, is not inconsistent with the present results, as such would facilitate intrinsic motoric correlations in activation of relevant cortex. Additionally, as multiple RRB-associated intrinsic grey matter connectivity differences were identified, they will be covered in turn.

Orbitofrontal cortex, temporoparietal junction (that is, the border of planum temporale), posterior parietal cortex, and precentral gyrus reflect RRB-associated differences in intrinsic grey matter connectivity and also in corticocortical or corticostriatal functional connectivity as assessed here.

More extensive contextualization of functional connectivity results can proceed in light of table 1.6; given the numerous regions identified across methodologies, substantial overlap exists with the connections herein identified. All primary dorsolateral frontal areas, salience/anterior cingulate, inferior frontal gyrus, angular gyrus, cerebellar divisions, caudate nucleus and putamen of striatum, Wernicke's area, fusiform gyrus, precentral gyrus (primary motor cortex), and medial prefrontal cortex (coextensive with paracingulate gyrus) appear both in the present results as either originally identified nodes of significant connections or in the hypothetical network, and in table 1.6's summary of RRB-associated connectivity changes. While the results in the table are not all for ASD, both the ASD-specific and common features of RRBs in the multiple disorders presenting some manifestation of them are of interest, and the whole of the results summarized are hence considered. Connection valence will next be compared between the summary table and present results.

The extent of non-analogy of many of the connections described and connectivity analysis methods employed in the full summary constrains the mutuality of interpretation with some aspects of the findings in this thesis, but some observations and patterns correspond rather directly to both other relevant research findings and specifically those in this thesis. First, decreased functional connectivity between posterior cingulate and lateral parietal default mode network (angular and part of supramarginal gyri) was observed in the qualitative network seed-based search and is depicted in figure 3.18 and is exactly identical to the pattern in the summary table, also using RBS-R as the behavioral measure. Partial overlap with increased salience network resting state functional connectivity with higher RRB severity was seen specifically between anterior cingulate and planum temporale. Likewise, the inverse pattern has also been observed, and is represented in the anterior cingulate connectivity to visual cortex in these results. The table summarizes many more results in the basal ganglia than were observed in this analysis, but the connected node in some cases is an ROI identified here: fusiform gyrus (albeit right) and primary motor cortex are noted to have altered functional connectivity with basal nuclei with RRB severity. The present results thus do tend to corroborate, in light of all of the above, important aspects of connectivity priorly identified to covary

233

with RRB severity. Full incorporation of the spectrum of the RRB-relevant connectivity findings informing this thesis generally into an incipient, to the field, but specifically to this researcher, theoretical framework that relates current and, to the greatest extent possible, prior findings bearing on the research question writ large, commences section 4.5.

- Left planum temporale—cingulate cortex: Positive correlation between connectivity and both ASD severity, and specifically RRB severity consistent with prior research regarding compulsive behavior in OCD that also identified increased within-DMN connectivity strength for greater symptom severity; **perception of coherent motion** and **language**; consistent with within-DMN hyperconnectivity

- Left inferior frontal gyrus—right visual occipital network: Functionally associated with precision manual movements, of which RRBs are plausibly an aberrant subtype; **execution of precise motions**; **language** and **visual processing**; indicative of **long-range hypoconnectivity**

- Left fusiform cortex—right angular gyrus; bilateral fusiform cortex—right frontal pole: Functionally associated with spontaneous motor behavior, sensory integration in object manipulation, comparison of intended and actual results of actions; **execution and monitoring of motor behaviors**; **language**, **visual**, and **multimodal sensory integration**; **DMN to extra-DMN connectivity**; indicative of **long-range hypoconnectivity**

- Left nucleus accumbens—left Brodmann area 6: Reinforcement and reward pathway, planning as well as execution of coordinated movement, direct connection to descending motor pathway; **reward/reinforcement** and **motor planning/execution**

Figure 4.1: Summary of plausible relations of empirically and *a priori* identified connections to RRB severity

- Spontaneous actions and coordinated movement: Brodmann area 6 (supplemental motor area), inferior frontal gyrus-to-occipital cortex connection, right angular gyrus, frontal pole

- Vestibular and somatosensory processing/out-of-body experiences: Right angular gyrus, cerebellum, fusiform cortex

- Multimodal sensory integration: Angular gyrus, fusiform gyrus, cingulate gyrus

- Reward processing: Nucleus accumbens

- Visual processing: Visual occipital network, angular gyrus, fusiform gyrus, Wernicke's area/planum temporale

- Language areas: Broca's area/inferior frontal gyrus, Wernicke's area/planum temporale, angular gyrus

Figure 4.2: Summary of functional cognitive/behavioral processing roles of identified connections and ROIs of plausible significance to RRB severity.

4.4 CLEAR IMPLICATIONS OF ALTERED BRAIN NETWORK DYNAMICS IN ASD RRBS

The substantial alterations in the dynamic behavior within the proffered model when using no precise parameters except those derived directly from the connectivity analysis were furthermore found to pertain to the known manifestation of RRBs in ASD via quantitative abstraction in the model. That is, functional activation in salience, executive, and motor-reinforcement subnetworks based on the calculated network connection strengths and a simple, time-varying stimulus input function, both in the simple linear system and in the nonlinear model system, corresponds to subject behavioral measures of relevance (RBS-R CSS or subgroup). The relative simplicity of the model definition (though not all of its parameter derivations) in comparison with the visually busy schematic representation of the network, despite the fact that the latter actually implicates relatively few total brain areas, shows that there are plausibly large-scale, self-organizing principles that underlie the manifestation of RRBs in ASD under various conditions, to various extents, and in various manners. This comports to expectation, as such dynamics are now thought to underlie in the brain essentially every behavioral function of recognizable specificity. Physiological plausibility is further enhanced by the fact that RRB-associated differences in dynamical behavior of several of the identified cortical areas in the network topology have been recently observed [124].

Furthermore, the dynamical model successfully predicted subject-level RRB severity, in the form of subject RBS-R CSS, with increasing success in concert with increasing model complexity and incorporation of more substantial extrinsic sources of influence on its spatiotemporal behavior. Beyond this incipient success, functional model parameters, such as a putative measure of executive/salience network influence on behavior, correspond straightforwardly to electrophysiological measures consistent with response inhibition deficits in daily life among individuals who have been diagnosed with ASD [267]. That is, while model behavior from a system intentionally contrived to minimize the dimensionality of its inputs and outputs is of absolutely no analogy to electrophysiological (or other) recordings of actual humans, these recordings yield, at present, values, sometimes many, stored as binary computer data. It is the valence of the computational effort—human and machine, abstract data representation, concrete data representation—on charts at conferences, and correlation with real neurocognitive systems that is (it is hoped) shared. At present, the interest is in establishing extrinsic model validity, or the lack of it, and further refining its analytical form, the latter generally construed as comprising as great an increase in power and utility with as little an increase in complexity as possible (it is the modeled system, not the model system, that is complex). Because such

a goal rests on at least cursory success of the approach, the remainder of the discussion turns first toward the neurocognitive, given such is the field of this research, next toward potential epidemiological and nosological, and, at last, to conceivable eventual clinical applications of the implementation of said approach.

In summary, whole-brain connectivity analysis apparently successfully identified multiple functionally related and interconnected brain regions. Then, after various efforts were directed towards ensuring, and then increasing, statistical confidence in the results, incorporation into a model neurocognitive network of conjectured significance to the category of deficits, RRBs, as diagnostically defined in the disorder, ASD, was achieved. Along with *a priori*-identified nodes, and those identified in functionally and anatomically guided seed-based searches across cortex and cerebellum to identify overlapping functional divisions, whole-brain, hypothesis-free connectivity analysis yielded the constituent network nodes. The network, identified in the first place in terms of the functional relationships between its components, was topologically organized such that the interactions between discrete smaller-scale aggregates of a few functional units within it could be modeled in terms of the reciprocal dynamical influences between them. A dynamical model followed from this, with parameter values derived from the connectivity metrics used originally to construct the network, between ROIs and along all paths between functional subnetworks for low- and high-RRB subject subgroups, yielding a system of differential equations that intuitively calculated output conceived as an abstracted extrinsic physiological correlate of motor RRB propensity and motoric behavioral lability. Such output correlated with real subject behavioral measures, confirmed via cross-validation analysis, in both linear, and nonlinear system variations. Given the wide anatomical distribution of the hypothesized network across cortical, subcortical, and cerebellar areas in the brain, this compels hypotheses such as that ASD symptoms are in the aggregate contingent on influences arising out of the whole complexity of the brain, a system that intrinsically dynamically reorganizes itself into transient equilibrium states based on cognitive and behavioral needs and conditions, and therefore ASD symptoms can, like the gross dynamical behavior of the whole brain, be conceptualized and explained as arising from particular transitions between qualitative regimes of dynamical behavior in a time-dependent system (the extended functional network, specifically the actual brain functional behavioral from which it is putatively abstracted, the latter itself also within the universe) realized follow appropriate perturbations within multiple functionally interdependent subsystems (individual functional connections) that collectively spontaneously shift the system from one metastable configuration into another upon reaching a critical threshold. In a simplistic, but not inappropriate conception, the observation that 35% and 70% of the model's time derivatives' mere initial

238

values across phase space correlated to net motor cortex excitation for the aggregated low- and high-RRB-severity subject subgroup-derived model implementations suggests the potential for an equilibrium-shift etiology dependent on the complexity of the neurocognitive agent from whom it arises. Furthermore, and more specifically, graphical depictions of the data suggested that especially severe restrictive and repetitive behavior extent might be an emergent phenomenon in which a trend towards a certain pattern of functional connectivity in the brain eventually reaches a critical point where the typical network is substituted with an equivalent antinetwork. Most importantly, without the high-RRB subgroup, little could be said about the connectivity pattern associated with RRBs in this dataset, because the present data are consistent with a (relatively) distinct phase transition in putative network dynamics rather than a linear or other gradual change. The fact that intrinsic brain activity is theorized to be related to task-specific activity through various mechanisms, and itself is postulated to represent a large portion of the brain's overall metabolic activity, the identification of networks associated with disease states in this way provides a plausible method for elucidating real changes in intrinsic brain dynamics that lead to observed symptoms in clinical and real-life contexts [163]. The plausibility of this idealization is more consistent with the known temporal dynamics of the brain as a system with distributed interdependent subcomponents than those that implicate functional or anatomical changes in one or a few cortical areas as underlying ASD pathophysiology: Even if ASD did arise from such a mechanism, the functional implications of the mechanism would not be constrained to the affected structures. An intrinsic organismal bias towards homeostatic regimes would engage multiple compensatory physiological responses resulting in widespread downstream alterations to overall brain structure and function. This is consistent with, though not proven by, a decreased threshold for reinforcement motor activation combined with increased executive network influence in the dynamical model. For RRBs to arise as a result of multiple discrete anatomical differences in circumscribed brain areas would imply the separability of the ensemble of changes to the motor reward, intrinsic motor, and executive control functional circuits, but this is inconsistent with the mere fact that to these circuits are functionally interconnected with both each other and themselves, as exemplified by the possibility of multifold reciprocity between subnetworks functionally mediated by cerebellum in the proposed network functional connection topology.

As promised, the full neurocognitive assessment is now turned to, albeit by synthesizing the posited analytical approach with brain metrics with particularly analogous attributes. Diminished frequency-dependent higher-level cortical feedback modulation of distinct feedforward somatosensory streams was observed to potentiate the feedforward output directed from primary to secondary somatosensory cortex, resulting in exaggerated measured MEG response following a carefully de-

signed tactile stimulus with specific temporal structure in children and young adults diagnosed with ASD [268]. This corresponds in the spatial (between brain regions) domain to the modeled association between executive network influence on motor network (model parameter f) with damping of intrinsic motor activity under appropriate stimulus input conditions, but a concomitant greater activation lability of motor cortex with respect to stimulus magnitude necessarily follows, thus yielding, paradoxically, values for "executive control" generally much lower for the low-RRB subject subgroup. This indeed fits the general mechanistic principle in that, though the model considers positive executive and salience activation due to positive stimulus input to represent an increase in executive control over motoric output from cortex, a tighter coupling of sensory and association cortex with motor cortex, consistent with this construal of "increased executive control," could equally be interpreted as "exaggerated stimulus responsivity," as actual observations show to be possible in fairly exact terms. And thus, in light of the face validity of the model established vis-à-vis the contained preliminary evaluation spanning several quantitative and qualitative milieux, section 4.5 below reorients finally the discussion of results towards the brain and ASD-associated cognitive theories relatively exclusively.

4.5   AN "RRB NETWORK?"

The present results suggest a pattern of altered cortical connectivity associated with high RRB trait presence. Specifically, a fairly consistent pattern of connectivity value sign inversion above the threshold RRB trait level, fostering ambitions towards further characterization of such a pattern in terms of the brain functional connections encompassed by it. This ensued after initial consideration and testing of the independent statistical significance of the observed connectivity correlations in light of the iterative and numerical approach taken in preliminary analysis. Of note, divisions of cerebellum were identified as forming a functional hub between network subdivisions as conceived in the posited topological functional relationship in the hypothetical network, consistent with recent lines of evidence; in addition to anatomical differences and intrinsic connectivity differences within cerebellum, incipient evidence has reinforced confidence in a pattern of consistent alterations of corticocerebellar connectivity in ASD [269].

The network identified comprises nodes with functional significance previously identified in the literature with respect to RRB-like behavior in other disorders, as well to relatively specific plausible neurocognitive mechanisms that might underlie RRBs. Furthermore, none of the nodes or connections identified were inconsistent with the proposed general pattern of motor-, reward-, and sensory integration-associated cortical areas forming the functional cognitive basis high RRB symptom pres-

ence. While currently, these results in concert are subject to many limitations, including appropriate caution in interpretation in addition to, for the time being, no validation of the results using external data, statistical modeling and testing results necessitate that the more reckless interpretation is that there is *no* significant association between RRB severity and the identified brain connections and the network which they are proposed to form.

The inherent advantage of the network search and formation process, informed to the extent possible by anatomical, physiological, and cognitive factors bearing on its plausibility, is that, since the largest functional connectivity effect sizes between candidate ROIs considered for inclusion as network nodes guide the search, along with connectivity overlap with prior nodes, rather than "significance" construed and operationalized however, the resultant network should accompany surer assertions of neurocognitive relevance than one elucidated via block box techniques. Moreover, since the ensemble connectivity patterns in subnetworks are extracted, abstracted, and dimensionally reduced, significance can be evaluated in terms of functional behavior independent of the network search. Hence, to satisfy the criterion of surer assertions of neurocognitive relevance, they follow.

4.5.1 Implications of network-level findings on "theories of autism"

With alterations within the default mode network, between the default mode network and other nodes, and between nodes entirely outside the default mode network all identified, several patterns of which correspond to prior findings, the most plausible interpretation of these results in the aggregate is that changes in the connection dynamics between nodes in an underlying brain network, of which at least some of the identified ROIs comprise at least a part, form the neurocognitive basis of RRB manifestation and presentation in ASD, and furthermore, that these changes in connection dynamics are likely to be associated with, if not causally bound to, symptom presentation in the other core deficit categories. This tends to be confirmatory of putative "connectivity theories of autism," themselves consistent with an etiopathogenesis of synaptogenetic origin. The individual connections identified in the initial whole-brain ROI-level functional connectivity analysis have been discussed in terms of functional significance in section 4.3.1, but the entire-network functional arrangement, especially given the findings of significance from the modeling derived from it, merits further targeted commentary as to its theoretical implications on autism neurocognitive heterogeneity and manifestation, and therefore, on putative theories of autism. The most salient feature of the proposed functional network is the centrality, in terms of node degree (functionally significant connections to other network nodes) of the putative cerebellum hub. As cerebellum has been repeatedly implicated in psychopathology across diagnoses and symptoms, its functional significance,

in ASD in general, and in RRBs both in ASD and other neurocognitive disorders, will be discussed in some detail.

Cerebellum's centrality in the hypothetical network is unsurprising given its multiple roles across cognitive domains. These include ones related to symptoms that have been clinically associated with cerebellar lesions, which include, quoted here at length:

> . . . hyperactivity, impulsiveness, disinhibition, anxiety, **ritualistic and stereotypical behaviors**, illogical thought and lack of empathy, . . . aggression . . . irritability . . . ruminative and **obsessive behaviors**, dysphoria and depression, tactile defensiveness and sensory overload, apathy, childlike behavior, and inability to comprehend social boundaries and assign ulterior motives [270, p. 253] (emphasis added).

It hence seems improbable for cerebellum to *lack* a major role in ASD deficit manifestation and its neural substrate. While RRB-related deficits are emboldened, the list also includes symptoms similar to those in the other two core deficits of ASD, suggesting that the putative "cerebellar theory of autism" possesses substantial functional neurocognitive explanatory power. Most substantially confirming this putative cerebellar role is the fact that conditional knockout models in mice inactivating *PTEN* within only cerebellar Purkinje neurons, the output cells of cerebellar cortex to deep cerebellar nuclei with a morphology characterized by effusive dendritic arborization and consequent diversiform enmeshment with afferents of cells (parallel and climbing fiber neurons) themselves transducing afferents of cerebellar cortex, resulted in substantial presence of ASD-analogous behaviors across ASD core deficit domains [88]. Similarly, deficits in only the RRB core deficit domain were observed in Purkinje neuron *Shank2* knockout mice [89]. Comparison between mice genetic lines with high or low social behavior administered buthionine sulfoximine to reduce antioxidant activity and induce oxidative stress presented with lesser presence of antioxidant species and increased oxidation of fat and protein in cerebellum in the low-sociality mice concurrent with exaggerated RRB-like behavior, in comparison to increased compensatory antioxidant activity in cerebellum in the high-sociality mice [91]. Increased Purkinje cell ablation, up to and including total postnatal loss of all Purkinje neurons, was likewise associated with less exploratory and greater repetitive motor behavior in mice models [90]. Further reinforcing an RRB-specific, beyond general ASD-associated, role of cerebellum in humans is the correlation between vermis VI-VII hypoplasia observed via sMRI and restricted interest inferred through exploratory behavior in an environment designed for explorative play [271]. These vermal loci specifically, as discussed in section 3.6.1, were first associated with hypoplasia in ASD four decades ago [87]. An additional finding that adds particular significance

to findings regarding these lobules (VI and VII) is that lobules VIII through X, but *not* lobules VI through VII, presented with hypoplasia in sMRI analysis of boys with ADHD [272]. While this allows no conclusions so specific, it is consistent with the possibility that gross cerebellar dysfunction, arising out of disrupted neural ontogeny, underlies features of both ASD and ADHD, and that the boundary between the disorders, at the very least, in vermal hypoplasia, but also likely in symptom manifestation, is mediated by the specific pattern of gross alterations that proceed from the initial disruption, whatever its ultimate etiology; such a possibility tends to account for both the distinctive and overlapping features between the two neurodevelopmental disorders. Further establishing the substantial functional relationships across sensory and cognitive modalities between cerebrum and cerebellum, hemispheric and vermal lobes VIII of cerebellum were found to demonstrate resting state functional connectivity to distributed neocortical functional divisions, including from vermal to visual cortex, from hemispheric to auditory cortex and task-positive and salience networks, and from lobule to sensorimotor and default mode networks. Broadly, significant portions of these corticoneocerebellar functional relationships are recapitulated here, with connectivity of cerebellum VIII L/R to default mode and salience networks, motor cortex, and motor association areas [273].

Further findings of significance to the results, and in combination with them significant to ASD heterogeneity and its potential explanations, are numerous. Cerebellar injury is known to be associated with language deficits, which manifest in ASD as deficits in sociocommunication, but isolation of response-time and accuracy components in a language task involving patients with cerebellar injury and putatively typical controls demonstrated that executive function integrity, and not just disruption of motor function, must underlie aspects of cerebellum-related language deficits [274]; this comports with the implication of both language areas and cerebellum broadly in association with a particular discrete ASD deficit, RRB, found in this thesis. While the relationship between language and RRB scores on behavioral inventories was not the expected one, being weak and negative, the functional significance of frontal executive areas and their mediating influence on more specifically motor areas of frontal cortex accords with the generally broad significance of cerebellar pathology to deficits across cognitive domains. Even if cerebellum does not fully synthesize all outstanding issues of ASD heterogeneity (a tall order, to be sure), the increasingly broad swathe of symptoms associated with damage to it, and the increasing understanding of its multiple roles in cognition, behavior, and memory [275], these three inextricably linked in contending with most environmentally relevant challenges, suggests at the very least that no such eventuality is conceivable with respect to a synthetic theory of ASD *without* further elucidation and contextualization of cerebellum's role in the disorder. Sources of inertia detrimental to this task still exist, however. While cerebellum does

have functionally and anatomically segregated motor-specific roles, also inferred through cerebellar anatomical pathology [276], this fact in itself is not an impediment. Rather, it is the continued popular conception, not entirely absent in academic neuroscience, that cerebellum is "a motor structure." For example, though explicitly with commentary on absolutely no other matter concerning the specific text, cerebellum has very recently (2020) been assigned to the chapter on motor systems in a textbook on structural and functional neuroanatomy [277], consistent with earlier editions of the same text. The cerebellum does indeed have many conveniently orderly relationships between structure and function, making such a notion as its "motorness" convenient, at a minimum, pedagogically. But it is a structure, as ASD is a neurodevelopmental disorder, of contrasts, and in both cases, the same heuristic arguments for the simultaneous broadening and deepening, as well as synthetic aggregating, of existing research exist. Further research on ASD-cerebellum associations, in sum, seems to decorate every potential avenue of ASD heterogeneity related discovery with the further promise of both a more detailed understanding of the extent, and a more coherent understanding of the core implications, of ASD heterogeneity. In this way, while a "cerebellar theory of autism" may seem facially suspect, as any and all putative theories of autism, to some extent, must, it, along with a better understanding of the self-organizing dynamical features of brains (in ASD and in general) is, in fact, like the neural circuit and connectivity theories with which it forms overlapping explanatory frameworks for interpretation of ASD neurocognitive research, and indispensable theoretical tool.

Contextualizing the specific cerebellar ROIs and connections identified in the present study, cerebellar vermal lobules VIII-X were found to be reduced in area in children with ASD compared to controls of putatively typical neurocognition, with IQ scores as a noted confound [278]. This dysplasial pattern is of potential relevance to gait alterations seen in ASD and other conditions, and gait abnormalities may bridge cerebellar and basal ganglial dysplasia and dysfunction in ASD, with differences in gait of subjects diagnosed with ASD compared to that of controls of putatively typical neurocognition being well-studied [279–282]. Additionally, vermal functional connectivity to sensorimotor cortex has been correlated with multiple gait-specific outcomes in Parkinson disease [283]. Given the repeated implication of vermal dysplasia in ASD, this enhances the preference for inclusion of cerebellar dysfunction in accounts of gait differences in subjects with ASD.

The RRB-cerebellum relationship identified tends to at a minimum intimate essential compatibility with the connectivity and neural circuit, and hyper-systemizing and assortative mating, theories of autism. However, importantly, the functional diversity of cerebellum renders the putative cerebellar theory of autism specifically no less compatible with other at least nominally plausible theories. For example, cerebellum—amygdala connectivity has been identified as positively associated with

ASD [38], and while the relationship identified in this thesis was a negative relationship between RRB intensity and the same connection, the near necessity of at least *a* cerebellar theory of autism, that is, a theory synthesizing the role of cerebellum in ASD deficits, along with connectivity observed between cerebellum and another structure which underlies a storied theory of autism, suggests the latter, that is, the amygdala theory of autism, is less "incorrect" than it is incomplete. One semantic adjustment would be to render such theories instead as, for example, "autism theory of the amygdala," "autism theory of the cerebellum," and, despite the marginality of the theory in this case, "autism theory of mirror neurons." A putative "autism theory" or "ASD theory," rather than one (or many) "*of* autism," might be conceived as an analytical framework from which anatomical, functional, and physiological variation in human nervous systems can be apprehended in terms of correlations with the general "autistic phenotype," comprising the whole of the clinical heterogeneity of the formally defined disorder, as well as the body of established and more-or-less plausible narratives incorporating aspects of the formal disorder into the broader context of human social behavior and organization, Western and other systems of medicine, and human biological and cultural evolution.

Such an analytical framework as ASD theory need not be so constrained to *Homo sapiens* either, as intraspecific variation in the relevant neuroanatomy and associated function can be productively viewed through the same lens, and not only the sense of the translational neuroscience extensively discussed so far. As extensive as the RRB-cerebellum association is, and as fruitful as research on its function and role in ASD is therefore likely to remain, further motivation to study the structures possible roles, again beyond the already substantial associations established in extant ASD research, comes in the observation that the generalized cognitive functionality of cerebellum is at this point, among the primates, a matter of "nearly complete consensus [99, abstract]." Cerebellum's role in cognition is also apparently an ancestral trait, at least among the mammals, given a cognitive-cerebellar functional relationship across cognitive domains in rodents [99]. Thus, if the structure is significantly implicated in ASD, it is also significantly implicated in putative evolutionary theories of autism, such as the assortative mating theory. Both the latter and significant clinical evidence observed in cerebellar injury implicate RRB-like behavior. However, beyond the apparently basal (though long-marginalized) broad cognitive function of cerebellum, telencephalization in the great apes, especially humans, has been accompanied by corresponding expansion of neocerebellum [284] in evolutionary time. Thus, in addition to containing the majority of neurons in the brain, cerebellum in great apes demonstrates specialized structure and function corresponding to overall cognitive needs. A further relevant contrast is proffered by birds, in whom relative mesencephaliza-

tion and metencephalization has *not* seen concomitant expansion of the analog of neocortex through evolutionary time [285], implying the driving force behind hominoid neocerebellarization was neocorticalization first and not vice versa. An analogy can be drawn, however, between the fundamental behavioral relevance of the divergent courses of cerebellar evolution between the putative ancestors of the extant great apes and those of the extant dinosaurs: rapid calculation needed for flight drove mesencephalization and metencephalization without relative telencephalization, while the benefits in heterogeneous and asymmetric processing inherent in telencephalization drove that pattern, and a downstream effect of telencephalization has been neocerebellarization. Neocerebellum, in fact, contains representations of every intrinsic functional cortical network [284]; this would be necessary for the true functional ubiquity of cerebellum, and, given the tendency of selective pressure to optimize tissue metabolic expense, putatively sufficient also, though functional neuroimaging has independently demonstrated this as well. The inextricability of cerebral and cerebellar evolution, and the latter's extensive involvement so far observed with RRBs, seem to establish it securely as an important target for research in the immediate to medium term.

As such a close relationship between the "big and little brains" might suggest, cerebellum has been implicated broadly in aspects cognitive flexibility and attention to stimuli of environmental and behavioral salience [286, 287]. More directly, there is behavioral evidence of correlation between cerebellar function, the presence of ASD traits, and cognitive flexibility in terms of verbal set-shifting ability in a non-clinical population [288]. Furthermore, and specific to RRB presentation, subjects who underwent surgery to remove tumors in the posterior fossa, the region of the cranium in which cerebellum resides, were later to found to exhibit impairments in rapid task switching [289], consistent with perseveration in a given regime of motor behavior once it is started. A complication of this paradigm restricts this task-switching deficiency associated with cerebellar insult to only tasks requiring cognitive conflict resolution [290]; this observation links deficits in salience detection and attention to those in task switching, highlighting a possible specific mechanism relating cerebellum structure to its RRB-related function. The interrelationship between cerebellar and basal ganglia function across cognitive domains contextualizes another observation relevant to task- and attention-switching in ASD and other neurocognitive disorders: attention deficits associated with cerebellar insult have been observed to be inseparable from action coordination components, while the same is not true of those sustaining insult to basal ganglia [238, 291]. In schizophrenia, as well, another candidate spectrum disorder [292], weaker corticoneocerebellar connectivity correlated with slower processing speeds based on behavioral measures [246]. Of potential relevance to future treatment modalities in ASD informed by cerebellar function is that, at least in the case of cerebellar focal

lesions, rehabilitative therapy is at least somewhat effective in mitigating functional impairments caused by cerebellar injury [293].

While accelerating research output on a particular neural structure within a research area does imply the functional significance of that structure, as repeatedly noted, brain structures universally are not independent modules but rather to some extent arbitrary parcellations of a structure whose fundamental function is utterly reciprocal and integrative. Hence, conclusions about the significance of cerebellum are best contextualized in terms of their relationship to the rest of the brain. Returning to the amygdala theory once more, the structure's critical role in emotion, a cognitive process of profound behavioral relevance, and therefore of profound relevance in research on psychopathology, further instructing interpretation of results from ASD research in the context of existing theories, including marginal ones. While its role has been left underdeveloped in the present model, despite appearing in the functional network, amygdala has been implicated in the modulation of stimulus—response information streams to anterior (motor) cerebellum, thereby modulating cerebellarly mediated motor learning [294, 295]. In other disorders of neurocognitive symptomatology, comorbidity of mental disorders with ASD, like other facets of ASD, is heterogeneous, but simple anatomical correlations with amygdalar volume are predictive of comorbid psychopathology in ASD [296]. Hence, this "rudimentary" neuroanatomical and functional theory of ASD encapsulates explanatory power that has surely not yet been fully revealed.

With respect to heterogeneity writ large, perhaps the central consideration in assessing more-or-less marginal or nominal theories of autism is that the ubiquity of the cognitive functions subserved by most discrete neuroanatomical structures and most discrete functional networks invoked by such theories necessarily will yield insight into heterogeneity because such structures and networks are all but certainly associated with aspects of symptoms in other psychopathology as well. Again, for its conceptual utility, amygdala, and for its ambiguous relation to ASD, schizophrenia, provide an apt illustration of this. First, if not explicitly combined into a single disorder in the same way, schizophrenia-like symptoms clearly present along a continuum of diagnostic intensity in separate but related symptom domains [292] that includes schizoid and schizotypal personality disorders, schizophreniform disorder, and schizoaffective disorder and schizophrenia [22]; one might also include other psychotic disorders (brief psychotic disorder and delusional disorder, and, though not in the DSM-5, shared delusional disorder and paraphrenia [297–299]). Next, schizophrenia and ASD have been posited to have varying relationships to one another. One view is that they are at least to a certain extent at least crudely quantitative, genetic, and neuroanatomical "opposites" [300]. On the other hand, they have been conflated with one another, and, perhaps independent of this,

viewed as related disorders, or forms of the same disorder [301], though the DSM-5 makes no such possibility evident in its definitions of the disorders. Both disorders do share one qualitative fact regarding brain connectivity. Whole-brain functional connectivity in schizophrenia comprises functional connections that are weaker, more diverse, and more global than in TD [302], consistent with long-range hypoconnectivity in ASD. Given both have affective components, amygdala differences are unsurprisingly found in bother disorders; some of the functional differences are associated with polygenic risk factors for ASD in subjects with schizophrenia [301]. Here, it can be seen that, at the boundary of the symptomatological extent between these two disorders, both genetic and functional brain differences in a mutually implicated structure are found in a pattern consistent with both shared features and diagnostic distinctiveness.

Though amygdala theory can be construed in meaningful respects as a "marginal" theory of autism, it is equally true that "disproving" is a notion of indefinite connotation, because there will not come a point when ASD is determined to completely, and both as a disorder, and as all the associated human experiences, totally unrelated in any way, shape, or form to structural or functional variation in amygdala, and the putative theory can still inform research even of direct relevance to potential therapeutic intervention. The mere implication of amygdala function in ASD means that modulation of its behavior will effect corresponding modulation of aspects of neurocognition and of associated ASD symptom domains when the two are related, as has been found in the case of oxytocin administration as a therapeutic intervention in ASD inferred via rs-fcMRI between amygdala and the cortical social brain [303]. While the amygdala theory is a basal phylogenetic radiation in ASD neural theory evolution, nonapeptide pharmacotherapeutic intervention seems at this point likely to be the first approved for treatment of ASD generally [10], establishing the true magnitude of the clinical and societal impact such research involving amygdala may proffer, despite its placement low in the chronological and conceptual hierarchy of autism neuroanatomical/functional theories. Relevant, perhaps, is the ecological success of alligators today in terms of their popular conception as being fundamentally unaltered across tens of millions of years of evolutionary time. The alligator is not a candidate for some grandiose, exhaustive metric of anatomical, neural, and evolutionary sophistication and ecological dominance, but also seem if anything to have persuasively solidified their argument to success through perseveration.

Consideration of cerebellum and amygdala in turn with respect to the implications of the current result on the theories of autism leads to the emergence of at least four general principles regarding the relationship between psychopathology of any etiology and specific anatomical or functional divisions of the brain:

- Any anatomical structure with putative function qualitatively related to ASD deficits will be associated, anatomically, or functionally through activation and/or connectivity, with ASD deficits

- Any such structure will likely be implicated in analogous symptoms in other disorders

- Specific delineation, or overlap, along diagnostic boundaries between disorders with similar symptoms can be better specified by studying differential neuroanatomy/function of such structures

- Wider functional dispersion (e.g., cerebellum) of any such structure will implicate in a greater variety of associations with a greater variety of symptoms within and between disorders

These principles emerge in part due to the fact that any anatomical or functional division of the brain at this point extensive enough for significant measurement via fMRI, given its limitations, will have a substantial enough impact on general cognition that a qualitative relationship between its function and symptom presentation in a diagnosis comprising cognitive symptomatology renders an actual functional relationship per functional neuroimaging analysis essentially inevitable at realistic values for sample sizes. Hence, all theories of autism implicating functional or structural divisions of the brain are nearly certain to be part, but only part, of pathophysiological explanation of autism in its entirety; one need not concern themself with, in an effort to fully assimilate neurocognitive research of ASD, the Brodmann area 1 theory of autism, the Brodmann area 2 theory of autism, the Brodmann area 3 theory of autism, and so on, repeated say for the Harvard-Oxford atlas of brain ROIs used in this thesis along with other parcellation schemes. Doing would, at some point, begin to result in diminishing marginal returns, as the degrees of freed in putative autism theory space would, rather than assist in consolidating theoretical effort, compound it.

Because cognitive functions implicated in ASD (metarepresentation, central coherence, social motivation, systemizing, empathizing, theory of mind, sensory sensitivity, etc.) are likewise conceived in terms general enough that they are unlikely to at some future point wholly escape any association with ASD, these too can be viewed to comprise proper subsets of ASD symptomatological heterogeneity. Ultimately, per the principles above, the precise relationships between the brain, symptoms, and diagnoses will become clearer with further research, but these results, and the ones that motivated the experimental design leading to them in the first place, do indicate the utility of an approach contingent on questions, rather than theories, and an analytical scheme that incorporates both specific hypotheses and incorporation of *a posterior* results from initial exploratory analyses to do so. Evidence directly urging consideration of the inter-theory relationships is readily

identifiable as well, at least in those syntheses including "neural" components: Direct covariation across (intrinsically manifoldly functionally interconnected) brain structures in the form of noted differences in anatomical covariance within and between cerebrum, cerebellum, and amygdala in sensory networks has been observed, confirming further that brain structure and function do not vary in an itemized manner, nor do any brain areas at all behave atomically. [304].

4.6 LIMITATIONS

While there are multiple conceptual impeti encouraging of the use of both the resting state and within-clinical-subject variation in carrying out functional connectivity analysis, the present analysis looked at only one of the three putative core deficits of ASD. Given that the relationships between symptom severity within and across core deficit domains and the corresponding functional brain differences are certain to not be totally independent, analyzing substantially only one, as was the case with the present rs-fcMRI analysis, necessarily limits the maximum explanatory power of the results in the larger context of ASD theoretical discourse. This conceptual issue has been specifically and extensively addressed in recent literature [121], and this trend is likely to accelerate; the noted reference is, in the view of this thesis and the extensive literature perusal conducted for it, at least among those most significant in both total ASD heterogeneity incorporation explicitly into its analysis, and likewise, therefore, correspondingly so in the plausibility of mechanisms explaining it so derived. Additionally, as noted in the Background, "function," in terms of specific role in cognition and/or behavior, is not readily abstracted from rs-fcMRI; this necessitates extrinsic knowledge from task-based paradigms, brain injury studies, animal lesion studies, and so on. But the significant findings herein are discussed in terms of functional connectivity; this construal thus requires, and not only due to the fact that no task-specific data was analyzed in this thesis for the subjects, at least some level of conjecture as to the connectivity—function—neuroanatomy relationship above and beyond what simulated dynamical behavior of the relevant ROIs and network, even if it reflected only real effects, might reveal. Most importantly, these results urge validation on more and larger sets of analogous subject data, deemphasizing functional network or dynamical model refinement theretofore. The results of this experiment, particularly dynamical model output, rightly construed, cannot be directly evaluated in light of their real or potential relationship to any of the etiopathogenesis of ASD, its epidemiology, presentation or heterogeneity, clinical intervention targeted towards its symptom presentation, real human experience, and so on. Efforts at such syntheses, though, have been made in light of brain connectivity analysis [46], and seem, as of now, to be the ultimate basic science goal of research on ASD heterogeneity and its correlates. The tangent begun in this

dissertation may evolve, though not in the manner of an alligator, towards viability for such holistic application, but the probability that further pursuits informed by the current findings will significantly alter their preliminary hypotheses as they stood at the conclusion and submission of this manuscript is 1, to any desired precision. Nevertheless, multiple avenues of particular promise for refinement, including through contradiction, of the current results seem clear.

While the dynamical model developed in this thesis outputs perhaps one of the most conceptually simple abstraction of neural mass function, that is, changes in activation within functional subnetworks over time, simulation of functionally diverse structures, in this case, cerebellum, abstracting cognitively and environmentally relevant informational measures and transforming them, has been proposed as a method of assessing brain function in light of modeled processing of plausible information-theoretic inputs [305]. Thus, regarding the nature of the model abstraction itself, further contextual validation of the model predictions is an important objective in determining the extent to which the present findings can be generalized. Such refinement can consist of expanding and improving the parameter generating data, that is, the underlying functional network and associated connectivity, the parameter definitions themselves, the form of the system equations, the interpretation of the model output, additional time or partial derivatives, and so on, though again with the intent to simultaneously optimize conceptual utility and economy. For example, the model, even in the final stochastic extension, remains relatively simple, if incorporating modestly diverse abstracted forms of discrete aspects of dynamic neurocognitive functional behaviors, but so too therefore does its calculated output with respect to the entire range of possible cognitive and behavioral quantitative abstractions of potential relevance to the research question.

Neuroimaging of ASD specifically also has been frequently critiqued in terms of an apparent lack of cohesive findings across similar studies. It is true that, given the substantial prior results that provide a theoretically consistent contextualization of the present ones, the methods employed do seem to have qualitative and quantitative indications of external validity, increasing confidence in their real significance to the disorder and its manifestation, and therefore can too likewise be construed to point towards potential further avenues of research using similar methods. Though, while large and significant correlations were found between various model outputs and the relevant behavioral metric, functional connectivity findings even within populations of individuals diagnosed with ASD have been noted to be, in addition to proliferating, frequently inconsistent across studies and imaging sites [306]. Hence, while the present results are sufficient to spur theoretical interest in, and to provide experimental justification for, further research in the same vein, they do not explicitly confirm, rebut, or significantly alter any other results or proposals derived from neurocognitive

research on ASD or related research, not even in the case of strongly debatable ones with, in the best case, significance at the threshold of identification. This, again, proceeds from the very nature of nervous systems and their essentially innumerable degrees of freedom. This does not, however, mean that *no* results, nor even that none which consist only of model-driven results, cannot so alter the landscape of plausibility of ASD research and theory. Indeed, in the optimistic case, generalized, extensive application of the framework minimally represented herein may accomplish this in small measure, even better if the framework is concurrently dynamically altered as appropriate.

While such conclusory optimism might guide further efforts, it is simultaneously true that, even beyond those already identified, some experimental issues of fundamental significance to analyses such as this have been left totally unaddressed. For example, while Pearson correlation, the functional connectivity measure used in this study is a well-validated measure as applied to fMRI data, other metrics, for example, dynamic time warping, have been posited as superior, especially notably in rs-fcMRI analysis of differences in ASD [307]. Dynamic time warping was found to be both more sensitive and more specific to ASD deficit—functional connectivity associations, and, further discouraging its employment, Pearson correlation was found to correlate more strongly with confounding physiological signals such as respiration. This emphasizes the potential "room for improvement" that might be conceived, and without validation across both the relevant alternative connectivity metrics and larger sample spaces, and each of these along with the other, can *not* be achieved; a handful of even very significant p-values a significant finding does not make.

Nevertheless, it is asserted that the dynamical approach minimally represented here is not constrained by any particular systemic shortcomings related to neurocognitive research in ASD, and is generalizable across neuroimaging, behavioral, and other underlying data types. In final evaluation, the dynamical model chosen incorporates brain-wide functional connectivity values and behavioral associations, for all connections with sufficiently large effect sizes that could be incorporated into a working hypothetical network arrangement, that is, having at least one connection in common with the rest of the entire functional network at the stage of analysis it is actually identified in. This approach ameliorates, to an extent, issues with reduced statistical power, and potential idiosyncrasy, of localized or *a priori* determined sets of functional or anatomical ROIs, because it produces, essentially, via model output, new statistics, which may in turn be evaluated independently of any individual connection p-values, although such metrics should correlate with model output fit for models with straightforward interpretation.

Employing whole-brain fc analysis is also more physiologically plausible because alterations in brain structure or function, given the fundamental manifold interconnectedness of brains, are never

entirely spatially localized [308]. A direct application of this paradigm can be seen in its employment in a data-driven approaches to whole-brain fc that has recently successfully been used to identify neuromarkers and risk factors of ASD [309, 310]. Indeed, the application of whole-brain analytical methods to large subject populations data sets, particularly, ones representative of the observed heterogeneity in ASD, offers perhaps the greatest promise for cohering specifically the (heterogeneous) neurocognitive aspects of the disorder, as has increasingly been done within this domain [311]. Further substantiating the potential of this approach to further illuminate the neurocognitive component of ASD pathophysiology in humans is substantial converging evidence from multiple mucine models implying discrete ASD connectotypes [312], not inconsistent with the various formulations of discrete ASD subtypes discussed in the Background. And, as whole-brain, large-sample rs-fcMRI experimental approaches will help generate the substrate from which conclusions about the neurocognitive heterogeneity of ASD and its clinical and nosological implications can be made, machine learning classification techniques provide a method of evaluating the significant search costs exploratory data analysis of such massive quantities of information might otherwise impose. Complicating this, though their statistical power and utility still render them an indispensable analytical technique in future synthetic analyses of results such as those of this thesis, is the fact that machine learning classificatory algorithm performance is dependent on sample heterogeneity across the dimensions of the data to be classified [313].

While much of this context does proffer support of the methods used in this thesis in general, and of those used in specific to the extent practical given the criteria whose satisfaction was being sought, improvements are conceivable across every relevant dimension, and if nothing else, the analysis effected here should succeed in generating an improved one subsequently.

4.7 FUTURE DIRECTIONS

The results of this study, taken together, imply a functional brain network that underlies RRBs in ASD and overlaps with known functional changes both in ASD and RRBs more generally. Specifically, its relevant measurement, the connection strengths (Pearson correlations in this case) between its nodes (structural or functional ROIs), vary consistently with RRB severity. These measurements can be parameterized, as was done, such that they can inform model implementations, increasing neurocognitive plausibility, streamlining model development, and improving model output, where parameterization is rationally executed. While not all canonical conclusions given the broad range of realistic interpretations of the observed model behavior and features, general observations consisted of, in potentially slightly modified forms in some cases, these observations:

- Greater influence of reward pathways on excess motor cortex activation $\implies$ increased reinforcement of repetitive motor behavior

- Greater intrinsic correlation between primary and supplementary motor cortex activation $\implies$ greater descending motor lability and likelihood of spontaneous or exuberant motor behavior

- Reduced regulation, despite larger absolute modeled influence, of motor cortex activation by incoming sensory streams $\implies$ greater intractability and behavioral inertia in repetitive motor patterns

- Increased executive network influence on motor structures inferred via functional relationship mediated by cerebellar node $\implies$ increased volitional cognitive resources directed towards motor behavior

- Predominance of intrinsic motor correlation and reward reinforcement of motor behavior compared to stronger executive—motor coupling in terms of effect sizes $\implies$ synthetic result of aggregate changes in network are increased spontaneous compared to planned motor behavior despite the tighter executive coupling to motor areas

- Greatest subject behavioral measure correlation with abstracted model measure of time correlation of motor cortex excess activation in the nonlinear dynamic case $\implies$ Potential for time-course specificity of repetitive motor cortex activation and behaviors

Figure 4.3: Hypothesized behavioral significance of findings.

The network identified comprises regions most readily associable with RRBs in ASD, however, it also included a large number of previously implicated functional language areas of cortex in ASD communication deficits. Further assessment of the potential neurocognitive relationship between language and RRB deficits in ASD merits effort, especially given the observed weak, but statistically significant, negative correlation between RRB and communication impairment severity.

Finally, given that, when investigating functional connectivity associated with one core ASD deficit (RRBs), multiple extensive regions associated with another core ASD deficit (communication) were identified, but with fewer and more ambiguous social-emotional deficit-associated regions being identified, these results tend to suggest the plausibility of the view that ASD as a whole cannot be explained as an *exclusively* sociocognitive disorder, even if they do not directly contradict the possibility that it is *primarily* one. That two deficits seem to cross-implicate one another in terms of brain functional connectivity, but the third appears neither in strictly behavioral-measure regression analysis, nor in the functional connectivity results, is most consistent with RRB and communication deficits forming inextricable and unisolable components of any putative "core" ASD phenotype, as predicted by theoretical approaches that view at least certain aspects of the disorder as adaptive, in isolation.

Beyond functional relationships between brain regions known to be associated with specific cognitive tasks from evidence in lesion studies, functional activation studies, and translational neuroscience research with model species, the complex time-dependent interrelationships within and between functionally segregated areas of cortex characterizes the fundamental dynamical behavior of brains as cognitive systems. In this study, a dynamical model that incorporated all, and only, the significant results from the functional connectivity analysis, successfully predicted and characterized the time-dependent changes in brain behavior within and between networks that associated with increased motor behavior, taken to plausibly represent specifically repetitive behavior. While fMRI suffers from being extremely sluggish with respect to the timescale of neurocognitive functioning, a model such as the one proposed, constructed, and confirmed as valid, uses results from analyses on (slow) fMRI time series, but is scale-free with respect to time because it is iterated arbitrarily with respect to the related rates of change in functional behavior in component subnetworks, though this does not correspond to any known physiological mechanism, rather being significant to the abstraction itself barring specific independent validation.

Postulated clinical applications of rs-fcMRI research on ASD are already proliferating. Potential targets for stimulotherapeutic intervention in treatment of ASD deficits have been identified [314]. Indeed, rs-fcMRI, combined with the herein and other methods of assessing dynamical behavior of

interconnected brain functional subdivisions constitutes an avenue of direct possible relevance to such therapies given any therapeutic stimulation will, rather than have temporally static and spatially circumscribed activity, result in dynamic perturbations dependent on the intrinsic dynamical properties of the target system, the human brain. This, in fact, is the explicit case when the converse application is made use of: Rather than identification of target nodes for therapeutic stimulation, a measure of functional connectivity, wavelet decomposition via synchronization likelihood, one metric of time series interdependence, applied electrophysiological recordings, was used to assess the success of virtual-reality based therapy, with significant correlations between clinical and functional connectivity measures [315]. The approach has shown clinically significant therapeutic potential in other disorders as well, such as in schizophrenia [316].

As ASD heterogeneity at this time remains substantially unexplained, further assessment of brain connectivity, activation, and dynamics, effected through diverse approaches, though hopefully trending generally towards larger sample sizes and greater ease of reproduction and validation, is warranted more than ever. The still rapid pace of increases in computer power can enhance evaluation of large neuroimaging datasets relevant to the research question, novel connectivity metrics may increase the physiological relevance of results, publicly accessible data sets, such as used in this thesis, can enhance reproducibility and elucidate methodological differences where they arise, complex systems methods can reduce the numerical complexity of observed brain (and other) behaviors drastically without seriously degrading the fidelity of the patterns of interest (ideally), and further incorporation of all of the above with ASD research on human behavior and genetics, and of animal models of increasing sophistication and, it seems now, nearly arbitrary possibilities, will all likewise continue to shed light on dimensions of human neurocognitive diversity. Inherent to ASD is a vast range of such diversity, perhaps rivaling that seen in the population exhibiting putatively typical cognition. The potential to foster understanding of human cognition generally, of nervous systems generally, of evolution generally, of human neurocognitive difference generally, and all the other innumerable virtues accumulated neurocognitive research on diverse manifestations of the human mind will surely not soon cease manifesting, vindicate all the vast efforts directed thereunto. Even if research on ASD neurocognitive heterogeneity repeatedly yielded insights barely more definite than those that would be gleaned from identically researching *human* neurocognitive heterogeneity, the merit of the enterprise is undiminished. In the worst case, effort directed to the former goal contributes equally to the latter.

This is certainly not to say convergence across multiple lines of inquiry and evidence is not strongly desired, as ground truth social benefit, whether through improved clinical intervention,

facilitation of informed, substantive and practical empathy between neurocognitively diverse populations and individuals, or demonstrable brass-tacks economic benefits from enhanced utilization of unique human capabilities, is easier to correlate with such convergence, and so is government research support. The present results encourage further research of similar type, as a few questions remain without answers, but in no way do they encourage research of one type to the detriment of any other addressed in the background, experimental design and results, and interpretation whatsoever. The heterogeneity of ASD can only reflect heterogeneity in biopsychosocial mechanisms, to which no conceivable methodology is sufficient save "all of the above."

APPENDICES

APPENDIX A

CODE EXAMPLES AND DATA TABLES

A.1 FUNCTIONAL CONNECTIVITY ANALYSIS CODE AND DATA

Spurious connectivity and regression model generation Spurious regression model generation was effected via identical methods to actual regression modeling of connectivity data, as in section 3.5. Fundamental is that this approach provided a realistic "outgroup comparison" in terms of statistical comparisons to known true-negative results. The randomization of subject behavioral scores, calculation of FC, and formulation of mirroring regression models to increase confidence in the initial connectivity results established the rationale for the further qualitative network search and characterization as in section 3.6. Actual randomized subject RBS-R CSS assignment and calculated connectivity values are given below, which can be used with the publicly available ABIDE II KUL database to yield the spurious regression models in section 3.5.

Subject ID	Original RBS-R CSS	Reassigned RBS-R CSS
1	1	3
2	1	6
3	2	4
4	3	5
5	3	6
6	3	1
7	4	25
8	4	19
9	4	4
10	4	2
11	4	1
12	5	7
13	6	10
14	6	3
15	7	29
16	8	33
17	10	8
18	14	4
19	16	3
20	17	4
21	19	19
22	19	14
23	25	17
24	29	36
25	33	38
26	36	4
27	38	16

Table A.1: Subject RBS-R CSS scores were randomly reassigned using random.org, a source of random number generation based on atmospheric noise, as shown.

ID	RBS-R	p-c	i-o	v-i	a-d	r1	r2	r3	r4
1	1	-0.06	0.15	0.14	0.06	-0.37	-0.26	-0.32	-0.70
2	1	-0.09	0.02	-0.06	-0.01	-0.41	-0.57	-0.19	-0.26
3	2	-0.21	0.18	0.29	0.09	-0.53	-0.39	-0.31	-0.16
4	3	-0.09	-0.06	0.19	0.13	-0.36	-0.51	-0.02	-0.33
5	3	-0.08	-0.09	0.02	0.00	-0.31	-0.49	0.07	-0.13
6	3	-0.23	-0.01	0.17	0.16	-0.22	-0.47	-0.42	-0.27
7	4	-0.09	0.44	0.13	0.22	-0.10	-0.43	-0.40	-0.15
8	4	-0.01	0.31	0.31	0.34	-0.27	-0.18	-0.45	-0.19
9	4	-0.05	0.06	0.25	0.14	-0.05	-0.02	-0.06	-0.20
10	4	0.04	0.09	0.03	-0.05	-0.12	-0.34	-0.40	0.02
11	4	0.51	0.08	0.01	0.04	-0.32	-0.60	-0.13	-0.19
12	5	0.06	0.24	0.27	0.10	-0.20	-0.43	-0.30	-0.14
13	6	-0.11	-0.02	-0.03	0.15	-0.22	-0.78	-0.45	-0.27
14	6	-0.21	-0.08	0.04	0.01	-0.19	-0.30	-0.07	-0.17
15	7	0.04	-0.01	-0.04	0.22	-0.21	-0.67	-0.18	-0.42
16	8	0.09	0.13	0.19	0.03	0.08	-0.19	-0.23	-0.13
17	10	0.17	0.02	0.17	0.13	-0.14	-0.10	-0.11	-0.35
18	14	0.00	-0.06	-0.10	0.01	-0.01	-0.07	0.32	-0.12
19	16	0.05	0.03	-0.09	-0.11	-0.14	-0.37	0.02	0.07
20	17	-0.05	0.06	0.00	0.18	-0.19	-0.22	0.29	0.18
21	19	0.10	0.15	-0.17	-0.14	0.34	-0.22	0.31	-0.15
22	19	0.18	-0.07	-0.09	0.07	-0.08	-0.09	0.26	0.04
23	25	0.37	-0.15	-0.10	-0.19	0.06	0.19	0.17	0.06
24	29	0.40	-0.22	-0.06	-0.22	0.05	0.09	0.04	-0.01
25	33	0.17	-0.16	-0.06	-0.04	0.26	0.00	0.08	0.04
26	36	0.52	-0.50	-0.42	-0.23	0.34	0.11	0.39	0.21
27	38	0.60	-0.22	-0.28	-0.26	0.29	0.00	0.45	0.26

Table A.2: Functional connectivity values were calculated using the randomly reassigned subject RBS-R CSSs in an identical manner as was used for the ROI-level functional connectivity analysis. The results are given in this table, with connectivity values for every subject, or, in the case of the randomized values, pseudo-subject, for the four most significant ROI-level functional connections identified empirically. Subject functional connections left to right are planum temporale-cingulate, IFG to occipital, visual to IFG, and fusiform to default mode. In this table, the functional connectivity associated with the randomized RBS-R CSS reassignment is presented in the same order as the true data, that is, as opposed to the order in table A.1 in which the new assignment of RBS-R CSS was presented in the order of the actual subjects to whom it was spuriously assigned. Spurious connectivity values are derived from the most significant connections depicted in figure 3.14.

Long-transformed power regression model construction   Log transformation of raw connectivity values and RRB-severity contrast variable was performed as shown in `R`. This was done so that traditional linear regression functions could be used to generate power regression models, deemed to be more physiologically plausible than were linear regression models themselves. Log transformation ensured ease of both analysis and representation of the models and associated data, although it must be noted statistics on model performance are relative to the log-transformed variables and their relationship in the model as implemented. Note that this method would fail if a Pearson correlation coefficient for a particular connection were exactly -1, but this can be accounted for when necessary.

```
subj <- read.csv("subjectdata.csv")
logptl <- log(subj$ptl.cing + 1)
logifgl <- log(subj$ifgl.occr + 1)
logvisocc <- log(subj$visocc.ifgl + 1)
logatfuscl <- log(subj$atfuscl.dmnlpr + 1)
logaccl <- log(subj$accl.ba6l + 1)
loghi <- log(subj$hi + 2)
subj.log <- data.frame(loghi, logptl, logifgl, logvisocc, logatfuscl, logaccl)
model <- lm(loghi ~ logptl, data = subj.log)
sumamry(model)
```

Leave-one-out cross-validation implementation   LOOCV was effected using the `R` package `Caret` (https://cran.r-project.org/web/packages/caret/index.html). In the case of the probability models in which subject RRB-severity category subgroup membership was predicted, for example, the binary contrast `hi` was regressed on, in this case, the step I regression incorporating `ptl`, or planum temporale connectivity, as the regressor. Plots were effected, and data extracted, calling, in this case with the model results being assigned to `step1`, `step1$pred$pred` and `step1$finalModel$fitted.values`.

```
ctrl <- trainControl(... "LOOCV", savePredictions = "all"...,

returnData = TRUE)

#training parameters

step1 <- caret::train(hi~ptl, data = ...,  ..."lm", trControl = ctrl)

assignment of training model data to a variable

plot(stats$ID, stats$high, type="p", xlab = "RBS-R CSS rank",

     ylab=..., pch=19, main = ..., cex=2, ylim=c(-1.1, 1.5), xlim=c(1,27) )

#plotting of actual subject RRB-severity category subgroup membership

against ID (RBS-R CSS rank)

points(stats$ID, step1$pred$pred, cex=2, pch=19, col=rgb(1,0,0))

#plotting of cross validation predictions

points(stats$ID, step1$finalModel$fitted.values, cex=2, pch=19, col=rgb(0,1,1))

#plotting of final model predictions
```

A.2 DYNAMICAL MODEL CODE AND DATA

Dynamical model parameter definition and calculation   The calculation of r and s was relatively straightforward, as shown in equation 3.3, and the code snippets correspond to the equation.

```
r = sn + nm + sn*ms + nm*ms;

s = ms;
```

The calculation of f likewise mirrors the notation in equation 3.4. This calculation takes every path from putative sensory areas to motor areas without backtracking (although continuing through one motor area to the next is allowed). Because input from the putative sensory periphery passes through executive, salience, default mode, and cerebellar hubs to reach the putative motor network, there are multiple interaction values that represent the extrapolated Pearson correlation that would result from all within-network one-way paths from "extra-motor," where model input is in the form of stimulus drive or function, to "motor" ROIs.

```
f = fg*(p2f+p2f2)*cp2*sc + v*pv*cp*sc + fg*(p2f+p2f2)*cp2*mc ...
    + v*pv*cp*mc + fg*(p2f+p2f2)*cp2*mc2 + v*pv*cp*mc2 ...
    + fg*(p2f+p2f2)*cp2*sc*ms + v*pv*cp*sc*ms + fg*(p2f+p2f2)*cp2*mc*ms ...
    + v*pv*cp*mc*ms + fg*(p2f+p2f2)*cp2*sc*sn*nm + v*pv*cp*sc*sn*nm ...
    + fg*(p2f+p2f2)*cp2*mc*nm*sn + v*pv*cp*mc*nm*sn ...
    %from sensory to fp via cerebellum
    + fg*(af*ca*sc + af*ca*mc + af*ca*mc2 + af*ca*sc*ms + af*ca*mc*ms ...
    + af*ca*sc*sn*nm + af*ca*mc*nm*sn) ...
    %from sensory (fus) to dmn via cerebellum
    + fg*(cf*sc + cf*mc + cf*mc2 + cf*sc*ms + cf*mc*ms + cf*sc*sn*nm + ...
    + cf*mc*nm*sn + cf2*sc + cf2*mc + cf2*mc2 + cf2*sc*ms + cf2*mc*ms ...
    + cf2*sc*sn*nm + cf2*mc*nm*sn) ... %from sensory (fus) via cerebellum
    + v*(ev2*et*st + ev2*et*st*ms + ev2*et*st*sn*nm*ms) ...
    %from sensory (vis) via acc
    + o*(co*sc + co*mc + co*mc2 + co*sc*ms + co*mc*ms + co*sc*sn*nm ...
    + co*mc*nm*sn) ... % from sensory (ofc) via cerebellum
    + t*(st + st*ms + st*sn*nm); %from sensory (pt) direct
```

Visual examples of the parameter calculation procedure occur in figures A.2 and A.3. In the latter example, not the functional relationship modeled is that input across cerebellar or cingulate

hubs to motor cortex is calculated by including all possible stopping points, maximizing the effect of external inputs, whatever that effect may be.

Figure A.1: Node labels for the subsequent figures.
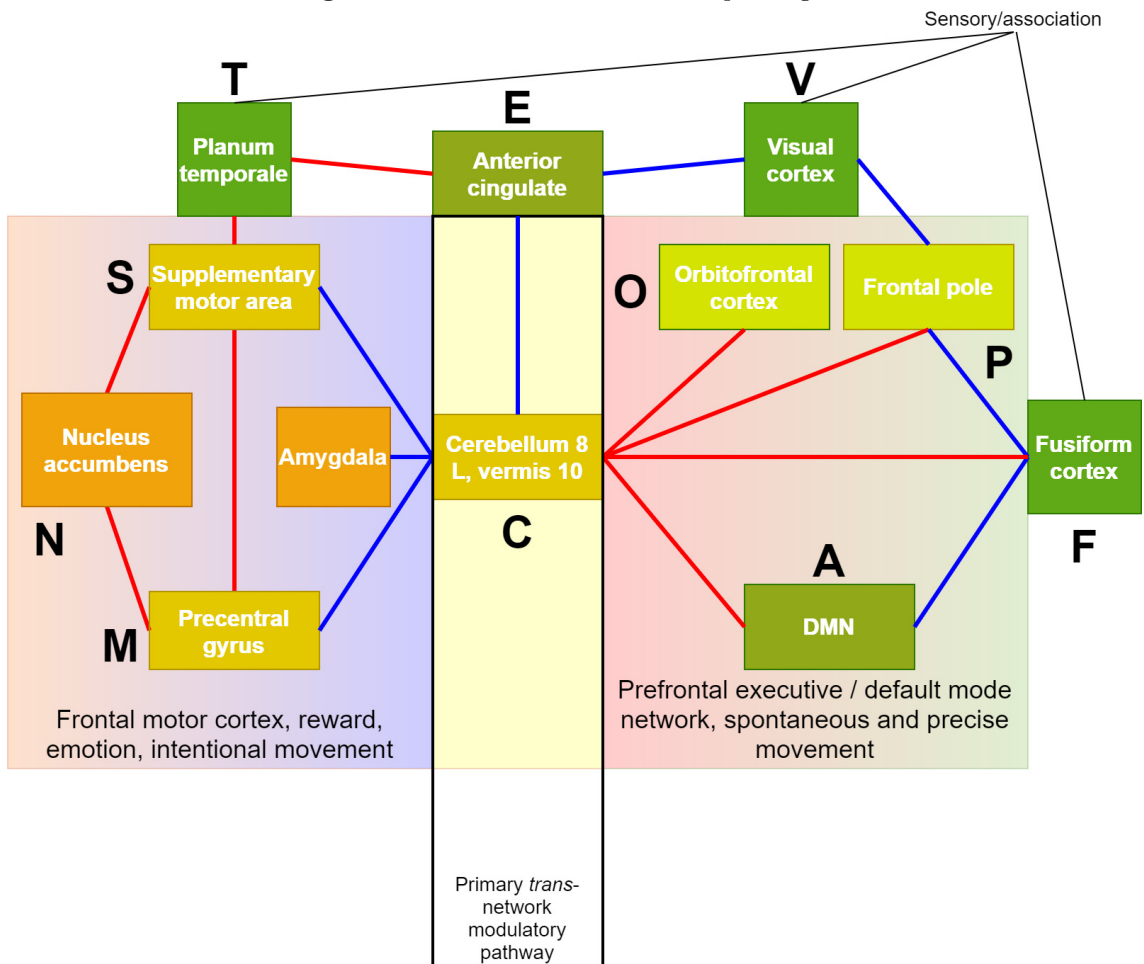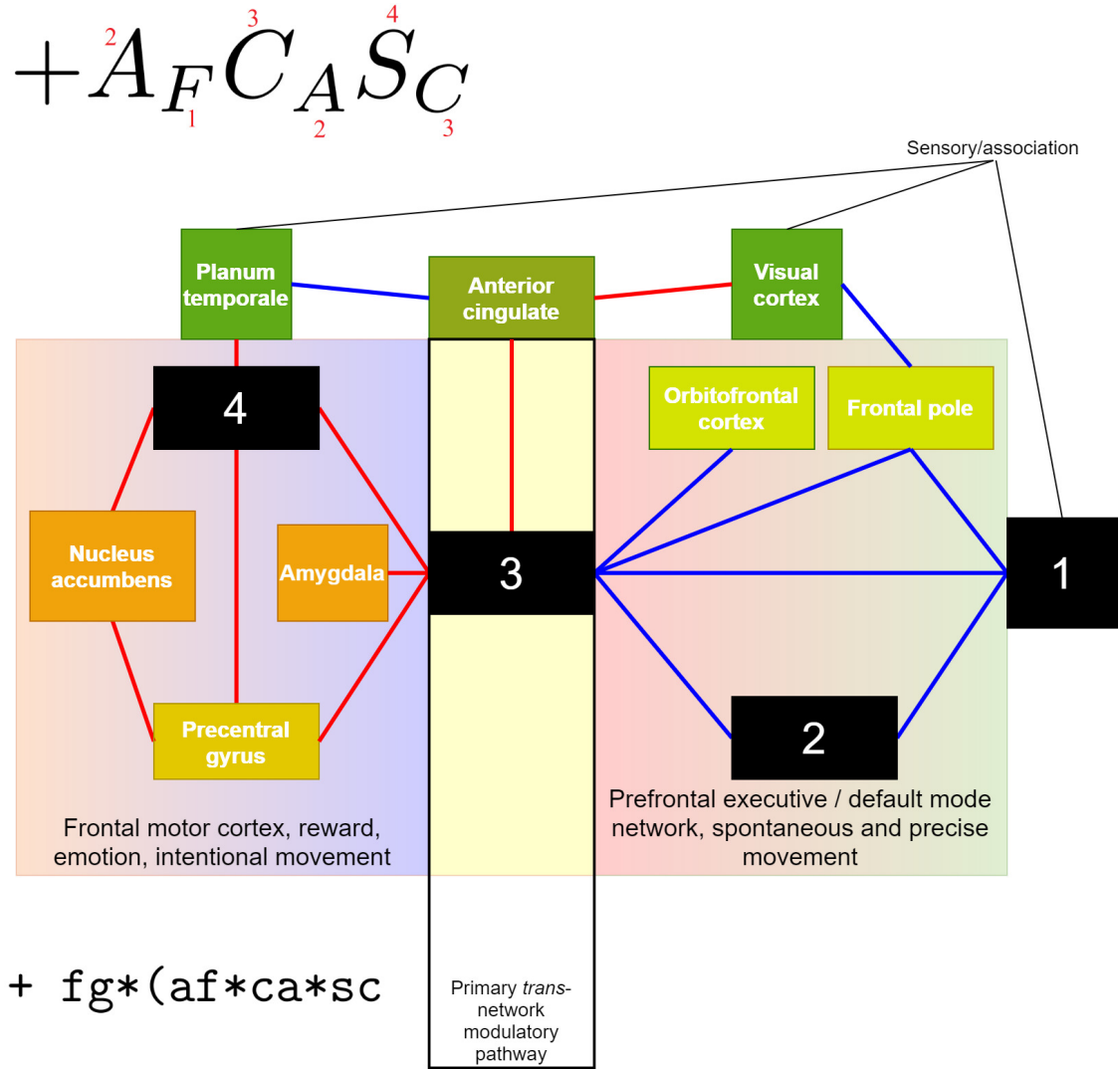
$$+\overset{2}{A}_F\overset{3}{C}_A\overset{4}{S}_C$$

$$\underset{1}{}\underset{2}{}\underset{3}{}$$

+ fg*(af*ca*sc

$$+\overset{2}{C}_{FR}\underset{1}{\overset{3}{S}_C}\underset{2}{\overset{3}{S}_N}\underset{4}{\overset{4}{N}_M}\underset{5}{} + \underset{2}{C}_{FR}\underset{1}{\overset{3}{M}_C}\underset{2}{\overset{4}{N}_M}\underset{3}{\overset{5}{S}_N}\underset{4}{}$$
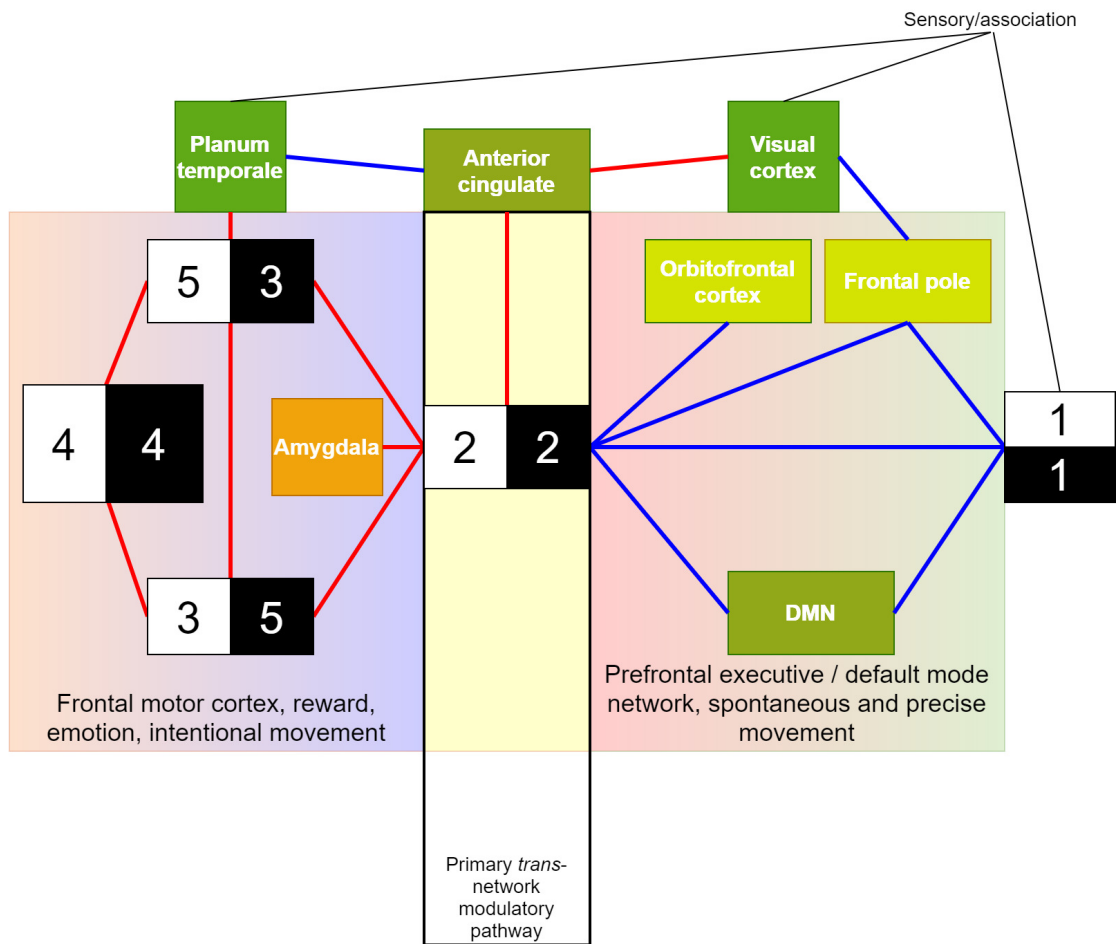

```
+ af*ca*sc*sn*nm + af*ca*mc*nm*sn) ...
```

Subject functional network connectivity values   Connectivity values for all of the indicated variable names corresponding to the hypothetical network diagram are given starting in table A.2, as are parameter values for calculated from them for r, s, and f. Subject ID is RBS-R CSS rank from low to high.

ID	sn	nm	ms	p2f	p2f2	pv	cp
1	-0.2304	0.0728	0.1712	0.2877	0.0054	0.0500	0.0678
2	0.0186	0.0147	0.1601	0.1139	-0.1202	-0.1489	0.1085
3	0.0694	-0.0368	-0.0442	0.0618	0.1660	0.2706	0.0099
4	0.0920	-0.2013	0.3135	-0.0772	0.1459	-0.0276	0.1495
5	-0.4061	-0.1180	0.6635	0.0973	-0.1099	0.1405	0.1567
6	-0.0673	-0.0685	0.0628	0.1879	0.1693	0.2171	0.0230
7	-0.1642	-0.1347	-0.3166	0.1746	0.0512	0.4956	0.2534
8	-0.1511	0.0088	0.0655	0.3157	0.0150	0.3407	-0.0578
9	-0.1464	-0.1659	0.0795	0.1720	-0.1296	0.2583	-0.0006
10	-0.0828	-0.1755	0.3484	0.0705	0.1175	-0.0795	0.0735
11	-0.0771	-0.3847	0.1150	0.2659	0.0021	0.1373	0.1045
12	0.1372	0.0480	0.1764	0.0591	-0.1841	0.2518	0.0534
13	-0.2475	-0.0206	0.4067	0.1070	-0.1265	-0.0600	0.2229
14	0.0496	0.1312	0.1816	0.2084	0.0796	-0.1474	-0.0386
15	-0.1035	-0.2451	0.2994	0.3563	0.0488	-0.2338	0.0461
16	-0.0880	-0.0494	0.1897	0.0872	0.3308	0.0835	0.1632
17	-0.0235	0.0354	0.0709	0.0381	-0.2655	0.1833	-0.0197
18	0.0408	-0.0777	0.1072	-0.1379	-0.1276	-0.1535	0.2337
19	-0.0330	0.1207	0.1745	0.1801	-0.1529	-0.0838	-0.0157
20	-0.0641	0.0073	0.2526	-0.1221	-0.0244	-0.0278	0.0080
21	0.0504	0.1201	0.0330	-0.0552	-0.0259	0.0323	0.0376
22	-0.0918	-0.0101	0.3359	-0.0170	-0.3398	-0.0604	-0.0341
23	0.2582	0.1489	0.5429	-0.1247	-0.0888	-0.1609	-0.1680
24	0.1605	0.1946	0.3443	-0.3466	-0.2494	-0.0481	0.0097
25	0.2686	0.3071	0.6564	0.1569	-0.2666	-0.1607	-0.1936
26	0.1277	0.1645	0.3481	-0.1912	-0.2597	-0.3649	-0.0908
27	0.0861	0.3192	0.6612	-0.3055	-0.3700	-0.3937	-0.0953

Table A.3: Connectivity values for individual subjects along with calculated parameter values, node names corresponding to figure 3.33.

ID	cp2	sc	mc	mc2	af	ca	cf	ev2
1	-0.1725	0.2149	0.1484	0.1013	0.0632	-0.5427	0.1484	0.0645
2	-0.1258	0.2168	0.1352	0.1877	-0.0086	-0.3030	-0.1314	0.0450
3	-0.1490	0.0037	0.1733	0.1188	0.0890	-0.1959	0.0307	0.1614
4	-0.2126	0.2981	0.1647	0.1002	0.1349	-0.1702	-0.0762	-0.0912
5	-0.1026	0.0813	0.0408	-0.0501	-0.0002	-0.3407	0.1967	0.1806
6	-0.2882	0.1525	-0.0738	-0.0425	0.1614	-0.0340	0.0219	0.0387
7	-0.0045	0.2147	0.0687	-0.0128	0.2249	-0.1953	-0.0963	0.0257
8	-0.1320	-0.0054	0.3148	0.2912	0.3375	-0.0731	-0.0460	-0.1992
9	-0.1214	0.0320	0.2056	0.0947	0.1369	-0.3449	0.0579	0.0735
10	-0.2630	0.1721	0.0637	0.2617	-0.0532	-0.2997	-0.0469	0.0609
11	-0.1730	0.1642	0.1101	0.0905	0.0424	-0.3637	0.0252	-0.0599
12	-0.0809	-0.0032	0.1637	0.0935	0.0992	-0.2437	0.1200	-0.0473
13	-0.2073	0.2397	0.1427	0.1090	0.1458	-0.1870	-0.1695	0.0827
14	-0.1840	0.1353	0.2917	0.0890	0.0114	-0.1141	0.1740	0.2221
15	-0.0689	0.2137	0.3165	0.2127	0.2211	-0.1302	0.1088	-0.2142
16	-0.1828	0.2028	0.1730	0.0631	0.0321	-0.1519	-0.0659	-0.0251
17	-0.1259	0.0723	-0.0983	0.0050	0.1328	-0.3179	-0.0785	-0.0100
18	-0.1079	0.0476	0.0860	-0.0687	0.0124	-0.1076	-0.0555	-0.1821
19	-0.1421	-0.1015	0.1835	0.0949	-0.1099	-0.0498	0.1213	-0.4229
20	-0.0654	0.0131	-0.0057	0.0062	0.1800	-0.1521	0.2090	-0.0832
21	-0.1807	0.1593	0.0898	-0.0268	-0.1447	0.0470	0.0193	-0.0463
22	-0.0159	0.0767	0.1107	0.0896	0.0655	0.0548	0.1047	-0.2065
23	-0.1231	0.0725	-0.0108	0.0179	-0.1950	-0.0522	0.0774	-0.1083
24	-0.0841	0.0311	-0.0225	-0.0385	-0.2242	-0.2024	0.1119	-0.0886
25	0.0425	-0.0728	-0.1074	-0.0850	-0.0431	0.1273	-0.0795	-0.4372
26	0.0571	-0.0678	-0.0156	-0.1470	-0.2273	0.1743	0.1497	-0.3499
27	0.0001	-0.0936	-0.0887	-0.0783	-0.2565	0.0033	0.3516	-0.2250

ID	et	st	co	cf2	r	s	f
1	0.0497	0.1929	-0.0869	-0.2140	-0.1846	0.1712	0.1015
2	-0.0601	0.0567	-0.1031	-0.3599	0.0386	0.1601	-0.2963
3	-0.2256	0.2785	-0.1414	-0.1151	0.0312	-0.0442	0.1769
4	0.0095	0.1308	-0.1355	-0.3060	-0.1435	0.3135	-0.2221
5	-0.0160	0.0232	-0.0587	-0.1405	-0.8719	0.6635	0.0429
6	-0.0915	0.1738	-0.2352	-0.0067	-0.1443	0.0628	0.1714
7	0.0236	0.0100	-0.1296	-0.0866	-0.2042	-0.3166	-0.0363
8	-0.0162	0.3323	-0.0437	0.0446	-0.1516	0.0655	0.2722
9	0.0375	0.1353	-0.0785	-0.1102	-0.3370	0.0795	0.0844
10	0.1377	0.3336	-0.2198	-0.4327	-0.3484	0.3484	0.0277
11	0.5879	0.4607	-0.1322	-0.1168	-0.5148	0.1150	0.3995
12	0.0924	0.1585	-0.0507	-0.0908	0.2178	0.1764	0.1804
13	0.1721	0.1908	-0.1752	-0.1419	-0.3771	0.4067	-0.0662
14	-0.0863	-0.0075	-0.2258	-0.0461	0.2137	0.1816	-0.0962
15	0.0457	0.4536	-0.1800	-0.3402	-0.4529	0.2994	0.1569
16	0.2152	0.3304	-0.0678	-0.0027	-0.1635	0.1897	0.2880
17	0.2007	0.3485	0.0468	0.0076	0.0127	0.0709	0.3731
18	0.0775	0.4056	-0.0381	-0.2616	-0.0409	0.1072	0.4128
19	0.0963	0.2596	-0.1082	0.1113	0.1030	0.1745	0.3158
20	-0.0444	0.3239	0.0448	-0.0457	-0.0712	0.2526	0.4100
21	0.1662	0.2720	0.0392	0.0567	0.1761	0.0330	0.3093
22	0.2454	0.3503	-0.0164	-0.0066	-0.1362	0.3359	0.4763
23	0.2650	0.5428	0.0841	0.3451	0.6280	0.5429	0.8997
24	0.4839	0.2577	0.0940	0.1416	0.4773	0.3443	0.3276
25	0.2439	0.4159	-0.0030	0.0947	0.9536	0.6564	0.6342
26	0.5347	0.6916	0.0522	-0.0260	0.3940	0.3481	0.7340
27	0.5932	0.7242	0.0457	0.2460	0.6733	0.6612	0.7980

Calculation of the statistic $\hat{\dot{z}}$ Calculation of putative averaged motor activation, the independent variable against which subject RBS-R CSS was regressed in the linear homogeneous model form, followed the analytical formulation given in equation 3.6. The loop to do so, and actual coordinate bounds across which model output was summed, are shown below.

```
%Note: w in the code is evaluated as the linear, not angular, frequency
[x,y,z]=meshgrid(j,-20:2:20,-20:2:20);
U = -2*pi*w*sin(2*pi*w*x);
V = c.*x - n.*y;
H = mact*(r.*abs(z) + s.*z - f.*y);
for ii = 1:length(y)/2
    for ij = 1:length(z)/2
        zdothat = zdothat + H(2*ii,2*ij);
    end
end
```

Nonlinear model extension summary statistic calculations and tables Values of nonlinear, in-homogeneous dynamical model summary statistics used for regression analysis are given starting in table A.2. Results were obtained after first iterating the dynamical model

```
[t,dynamic]=ode45(model,tvals,[k,yvals,zvals]);
yout = transpose(dynamic(:,2));
zout = transpose(dynamic(:,3));


stats = [tvals.' yout.' zout.']


zmean = mean(stats(:,3), 'omitnan');
zsd = std(stats(:,3), 'omitnan');
zskew = skewness(stats(:,3));
ztcor = corr(stats, 'Rows', 'pairwise');


% etc.
```

ID	rbsr	high	avg.0	sd.0	ske.0	kur.0	cor.t0
1	1	-1	-0.2088	13.4244	-0.0081	1.5081	-0.0127
2	1	-1	0.5309	13.3653	-0.0489	1.5336	0.045
3	2	-1	0.1136	12.9805	-0.0077	1.5893	0.0085
4	3	-1	0.2125	13.6863	-0.0439	1.4811	0.0238
5	3	-1	-2.3047	15.0725	-0.0019	1.3685	-0.1276
6	3	-1	-0.2423	13.2033	0.0036	1.546	-0.0175
7	4	-1	-0.1507	12.4927	-0.0108	1.695	-0.0186
8	4	-1	-0.1969	13.2064	-0.0023	1.5449	-0.014
9	4	-1	-0.4735	13.2589	-0.0052	1.5373	-0.0318
10	4	-1	-0.2197	13.779	-0.0391	1.4694	-0.0057
11	4	-1	-0.7811	13.3865	-0.003	1.5199	-0.055
12	5	-1	0.378	13.4532	-0.0036	1.5026	0.025
13	6	-1	-0.4384	13.9352	-0.0237	1.4436	-0.0202
14	6	-1	0.4955	13.453	-0.016	1.5065	0.0348
15	7	-1	-0.3698	13.6911	-0.0453	1.4829	-0.0166
16	8	-1	-0.2169	13.4714	-0.0039	1.4992	-0.0136
17	10	-1	-0.0245	13.2134	0.0046	1.5439	-0.002
18	14	-1	-0.0899	13.2901	0.0038	1.5299	-0.007
19	16	-1	0.1348	13.4332	0.0024	1.505	0.0085
20	17	-1	-0.1857	13.6011	0.0061	1.4777	-0.012
21	19	-1	0.2119	13.1407	0.0047	1.5572	0.015
22	19	-1	-0.3476	13.7929	0.0101	1.4493	-0.0226
23	25	1	1.3955	14.4617	-0.0029	1.3876	0.0775
24	29	1	1.0162	13.9154	-0.0146	1.44	0.0617
25	33	1	2.4926	15.132	0.0108	1.3788	0.1377
26	36	1	0.9911	13.8674	-0.0252	1.4521	0.0621
27	38	1	2.1436	14.8009	-0.0213	1.4132	0.1231

Table A.4: Summary statistics calculated from nonlinear inhomogeneous dynamical model output, mean, s.d., skewness, kurtosis, correlations between model variables, given for different time ranges, from 0 to 1, 0 to 5, 95 to 100, 99 to 100, and from 0 to 100.

ID	cor.x0	avg.1	sd.1	ske.1	kur.1	cor.t1	cor.x1	avg.2
1	0.0297	-1.0391	8.4548	0.172	2.9186	-0.0619	0.152	-4.6455
2	0.1034	0.3406	9.5797	-0.015	2.0505	-0.0027	0.4337	1.667
3	0.0183	0.1518	7.6428	-0.0212	3.8568	0.0018	0.0955	0.0652
4	0.1074	-0.7748	10.3705	0.0608	1.7883	-0.051	0.4496	-2.8738
5	-0.0073	-6.866	12.8333	0.1892	1.5675	-0.2186	0.0127	-20.471
6	-0.0004	-0.7332	7.9447	0.1346	3.4744	-0.0368	-0.0026	-2.405
7	0.0139	-0.5761	7.103	0.1317	4.7576	-0.0268	0.0699	-0.065
8	0.0149	-0.7586	7.9779	0.1433	3.429	-0.0425	0.0747	-2.852
9	0.0161	-1.7198	8.1942	0.2883	3.2263	-0.0901	0.082	-5.5566
10	0.1078	-2.154	10.7484	0.135	1.7391	-0.1063	0.4505	-9.266
11	0.0242	-2.7817	8.6614	0.3941	2.8714	-0.1449	0.1148	-8.4038
12	-0.0046	1.2546	8.4134	-0.1989	2.9749	0.0648	-0.0231	4.5986
13	0.0879	-2.5818	10.6316	0.194	1.8123	-0.1261	0.3849	-10.4553
14	0.024	1.2789	8.493	-0.1875	2.8964	0.0578	0.1239	5.2449
15	0.1085	-2.7123	10.6713	0.1655	1.7832	-0.1296	0.4507	-10.0146
16	0.0207	-0.9403	8.4571	0.1536	2.9167	-0.0542	0.1039	-3.1207
17	-0.0109	0.055	7.9435	-0.0152	3.4601	0.0063	-0.0582	0.1822
18	-0.0026	-0.2219	8.0527	0.0385	3.3295	-0.0103	-0.0138	-0.5672
19	-0.0132	0.5818	8.3366	-0.0995	3.0228	0.0338	-0.0663	2.2166
20	-0.0127	-0.4608	8.6487	0.0632	2.7262	-0.0193	-0.0637	-1.9019
21	-0.0174	0.8435	7.8977	-0.1624	3.5285	0.0474	-0.0888	2.7826
22	-0.0158	-0.9406	9.0799	0.114	2.4087	-0.0419	-0.0728	-3.2301
23	-0.0329	4.9284	11.2614	-0.31	1.7873	0.2094	-0.1542	15.6279
24	-0.0029	3.1936	9.635	-0.3144	2.2303	0.1435	-0.0222	10.9547
25	0.0089	7.3896	13.0886	-0.1785	1.5651	0.2276	-0.0077	21.4641
26	0.0329	2.7978	9.5471	-0.2995	2.2594	0.1262	0.1472	9.8738
27	0.0859	6.3009	12.7119	-0.3326	1.6117	0.2376	0.2987	17.7201

ID	sd.2	ske.2	kur.2	cor.t2	cor.x2	avg.t	sd.t	ske.t
1	0.3288	1.3409	7.1194	-0.2973	-0.0095	-4.7809	0.234	0.2432
2	1.5148	-0.7678	2.7309	0.3173	0.03	2.1903	0.8588	0.2331
3	0.1433	0.0398	1.5203	-0.0553	-0.0293	0.0646	0.1496	-0.0261
4	3.9296	0.388	1.3376	-0.205	0.0417	-5.1815	2.8305	2.0536
5	0.0145	-0.0982	1.5411	0.0162	-0.4136	-20.4662	0.0134	-0.4336
6	0.8798	2.1339	5.6044	-0.2499	-0.0366	-2.7599	0.0103	-0.0829
7	0.0974	0.0679	1.5186	-0.1015	0.0279	-0.0818	0.1021	0.3203
8	0.1345	0.4302	2.6635	-0.2492	-0.0067	-2.9081	0.1096	0.1895
9	0.1127	0.0453	1.5216	-0.0606	0.094	-5.5704	0.1142	0.18
10	0.8456	0.0525	1.5205	-0.0425	0.1743	-9.4631	0.861	0.3244
11	0.1666	0.061	1.5263	-0.0513	0.161	-8.433	0.1666	0.2533
12	1.7363	-2.2601	6.111	0.2538	0.0352	5.2602	0.0265	-0.1897
13	0.6781	0.0678	1.5255	-0.0302	0.2009	-10.6181	0.6839	0.3379
14	0.1994	0.0599	1.5383	-0.0504	0.0861	5.2072	0.2033	0.2811
15	0.8466	0.0596	1.524	-0.0282	0.1883	-10.2129	0.857	0.3118
16	2.358	0.8018	1.6622	0.0147	-0.0055	-2.9249	2.4233	0.6104
17	0.9417	-0.0249	1.0341	-0.0282	0.0035	0.1109	0.9351	0.1286
18	1.4292	0.0314	1.002	-0.004	-0.0019	-0.5813	1.4284	0.0501
19	2.1647	-0.7718	1.6048	0.0103	0.0064	2.2093	2.1635	-0.7582
20	3.2283	0.5915	1.3542	-0.0442	-0.0013	-2.2282	3.1104	0.8287
21	0.1257	-0.0546	1.5304	0.1016	-0.0227	2.8052	0.1302	-0.2244
22	4.2469	0.6671	1.4487	-0.0383	0.0009	-3.6147	4.0964	0.8841
23	0.2685	-0.0844	1.5351	0.0248	-0.3183	15.6971	0.26	-0.3504
24	0.0189	-0.0637	1.5284	0.0352	-0.2215	10.9582	0.0187	-0.2522
25	0.0335	0.1028	1.541	-0.0176	0.4289	21.4524	0.0309	0.4614
26	0.2605	0.0505	1.5241	-0.0455	0.193	9.8172	0.2597	0.2698
27	0.6293	0.0884	1.5318	-0.0203	0.3631	17.509	0.5943	0.4179

ID	kur.t	cor.tt	cor.xt	favg	fsd	fske	fkur	fcort
1	1.4742	-0.9884	-0.1573	-2.644	3.3438	0.892	7.489	-0.1904
2	1.463	-0.9909	-0.2978	0.5206	3.8981	-0.14	5.2023	0.0555
3	1.4579	-0.987	-0.141	0.1139	1.8818	-0.008	51.767	-0.0161
4	5.9363	-0.4856	-0.064	-1.9794	5.43	0.2547	2.3803	-0.0594
5	1.6919	0.9598	-0.0991	-16.7941	8.0312	1.8477	4.7918	-0.4777
6	1.5057	0.9897	0.0952	-1.5578	2.2686	1.0462	27.3204	-0.1543
7	1.5122	-0.9906	-0.1691	-0.1657	1.6316	-0.1979	84.6809	0.0797
8	1.462	-0.9898	-0.1471	-1.8041	2.3683	1.213	23.66	-0.1872
9	1.5233	-0.9872	-0.0598	-4.513	2.8111	2.3369	17.0162	-0.3433
10	1.5468	-0.9817	-0.116	-6.3525	5.7575	1.2358	3.6438	-0.4001
11	1.5566	-0.9837	-0.0347	-7.155	3.4737	2.609	12.6056	-0.3846
12	1.5318	0.9874	0.066	3.2431	3.202	-1.1274	8.9591	0.1994
13	1.5638	-0.9801	-0.0978	-6.9727	6.1567	1.1386	3.1138	-0.3781
14	1.5242	-0.9872	-0.2281	3.2171	3.42	-1.0617	7.33	0.2432
15	1.5382	-0.9804	-0.1274	-7.5612	5.5394	1.5365	4.6114	-0.4215
16	1.3905	0.002	0.0018	-2.7791	3.2776	1.0594	8.1991	-0.1274
17	1.0522	0.0304	0.0217	0.1661	2.1748	-0.1517	31.1703	0.0134
18	1.0035	0.0144	-0.0021	-0.5078	2.3535	0.3014	23.2361	-0.0308
19	1.5841	-0.0596	-0.0307	1.9391	2.9925	-0.9276	10.4168	0.1101
20	1.6919	0.0629	0.0499	-1.603	3.7914	0.5424	4.6035	-0.0736
21	1.4823	0.9896	0.1756	1.8418	2.3146	-1.2751	25.609	0.2127
22	1.7861	0.094	0.0925	-2.8598	4.7394	0.6321	2.7731	-0.0794
23	1.6108	0.9716	-0.0704	12.7789	6.5067	-1.9789	5.5588	0.3934
24	1.5547	0.981	-0.045	8.4098	4.9552	-1.6385	5.1316	0.4399
25	1.7097	-0.9566	0.0993	18.3678	7.7063	-2.2277	6.419	0.4557
26	1.5526	-0.9819	-0.0608	7.5873	4.816	-1.7181	5.4939	0.3462
27	1.6462	-0.9672	-0.0369	14.4515	7.7212	-1.916	5.138	0.3859

ID	fcorx	statavg	subject
1	0.1561	3.542	-184.6028
2	0.2786	8.3339	38.6149
3	0.1312	2.7909	31.1981
4	0.2487	8.2888	-143.5361
5	-0.0174	-20.5165	-871.8784
6	-0.005	-2.962	-144.3063
7	0.0826	0.7399	-204.2054
8	0.1057	1.9705	-151.63
9	0.1016	1.3852	-337.035
10	0.2565	7.1313	-348.3894
11	0.1227	1.4711	-514.7919
12	-0.0245	4.9396	217.7949
13	0.2216	6.6153	-377.1275
14	0.1327	6.9577	213.693
15	0.2676	6.2027	-452.9338
16	0.1117	3.1693	-163.5448
17	-0.092	-2.6561	12.6843
18	-0.0184	-2.4957	-40.8615
19	-0.0783	-2.8975	102.9624
20	-0.0602	-5.4231	-71.1863
21	-0.1238	-1.9147	176.118
22	-0.0588	-7.2952	-136.1748
23	-0.1253	14.434	628.0188
24	-0.025	10.8469	477.2538
25	0.0408	21.57	953.6364
26	0.1198	11.2896	393.974
27	0.166	19.8243	673.3037

Values of stochastic model extension output starting in table A.5. Results are from twenty separate iterations of the model extensions, according to

```
rng = rand(105);
tsteps = [0:0.01:100];
```

...

```
% Full model definition of time derivatives of x,y,z
g = @(t,P)[-2*pi*w*(sin(2*pi*w*t))+cos(2*pi*rng(step,round(t+5))) ...
-0.5*cos(2*pi*rng(step,round(t+4)))-0.25*cos(2*pi*rng(step,round(t+3))) ...
-0.125*cos(2*pi*rng(step,round(t+2)))- ...
0.0625*cos(2*pi*rng(step,round(t+1))); ...
c*P(1)-n*P(2);mact*(r*abs(P(3))+s*P(3)-f*P(2) ...
-(.075*(P(3))^3)/abs(P(3)))];
```

```
for p=1:27 %27 subjects
%calculate subject values for f, r, s
for step = 1:20 %20 randomized value runs
%solve model for values of rng
stattable = [runz.']; %value of z at each time step
substattable(:,20*(p-1)+step+1) = stattable(:,2);
%20 columns per subject, 20 subjects, 540 data columns
end
end
%full output table stored in variable "data"
```

...

```
%stat calcluations from model output
for subject = 1:27
for run = 1:20
avgs(subject,run+1) = mean(data(:,1+run+(subject-1)*20));
sds(subject,run+1) = std(data(:,1+run+(subject-1)*20));
```

```
skews(subject,run+1) = skewness(data(:,1+run+(subject-1)*20));

kurts(subject,run+1) = kurtosis(data(:,1+run+(subject-1)*20));

ztcor(subject,run) = corr(data(:,1),data(:,1+run+(subject-1)*20));

%yields table below of stochastic model stats

%rows are subjects, columns are runs, stored per stat

%combined in table below

%28 rows (titles + 27 subjects)

%107 columns

%(titles + 5 stats * 20 runs + 5 avgs + mean divg. stat)

end

end

.
```

id	zt1	zt2	zt3	zt4	zt5	zt6	zt7
1	-0.3894	-0.1050	-0.1621	-0.8686	-0.3245	0.1401	-0.6662
2	-0.1181	0.1503	-0.2186	0.7999	0.6445	-0.5672	0.6968
3	0.2289	-0.1030	-0.2699	-0.6495	-0.2796	0.6851	-0.6875
4	0.3761	0.1401	0.4227	0.6979	0.2503	-0.5444	0.7972
5	-0.2047	-0.4907	-0.3634	-0.7390	-0.4075	0.3916	-0.6136
6	0.0342	0.0884	0.2116	-0.8047	-0.5430	0.4332	-0.7437
7	0.2521	0.1318	-0.3929	0.7121	0.5936	-0.2385	0.7485
8	0.1288	-0.5560	-0.3712	-0.8982	-0.4478	0.6527	-0.6437
9	-0.2420	0.1710	0.1678	-0.8698	-0.4322	0.3366	-0.8040
10	0.3683	-0.3914	-0.1747	-0.7890	-0.6777	0.1374	-0.6448
11	0.2283	-0.1507	0.2211	-0.8486	-0.6776	0.6358	-0.3846
12	-0.5209	-0.1499	0.4329	0.2609	0.2290	-0.5151	-0.3202
13	0.0885	0.3229	-0.7306	0.2042	-0.4381	0.5056	0.4104
14	0.6632	0.4209	-0.7642	-0.2417	0.3150	0.6716	0.1667
15	-0.5615	-0.2112	0.5623	-0.1082	0.2824	-0.5763	-0.1906
16	-0.4466	-0.3657	0.5540	0.2046	0.3434	-0.7104	-0.1424
17	-0.6765	-0.2439	0.7228	0.2261	0.0345	-0.7715	-0.2956
18	-0.1493	-0.3851	0.5640	-0.1831	-0.0653	-0.6951	-0.3987
19	-0.2330	-0.3713	0.5135	0.0505	-0.0576	-0.7320	-0.0649
20	-0.0725	-0.2528	0.6954	0.1013	0.2167	-0.6846	-0.2456
21	0.0220	-0.3438	0.6248	0.2918	0.2277	-0.7255	-0.2080
22	-0.2146	-0.1912	0.6717	-0.0099	0.2522	-0.7825	-0.4490
23	-0.4183	-0.0062	0.5585	0.1815	0.1868	-0.6621	0.1611
24	-0.3014	0.0944	0.7022	-0.0215	0.2922	-0.6528	-0.5061
25	-0.2952	-0.2025	0.3387	0.0357	0.1091	-0.4148	-0.2623
26	-0.4325	-0.2007	0.5684	0.0123	0.0548	-0.7174	-0.4408
27	0.0865	-0.1445	0.5780	-0.4852	0.2830	-0.7149	-0.4590

Table A.5: Summary statistics calculated from nonlinear stochastic dynamical model output, mean, s.d., skewness, kurtosis, correlations of z with t, across 20 randomized runs.

id	zt8	zt9	zt10	zt11	zt12	zt13	zt14	zt15
1	0.0137	-0.5893	0.5505	0.8420	-0.3904	-0.4722	0.7073	0.7215
2	0.0040	0.5239	-0.2475	-0.7915	0.2850	0.3159	-0.6066	-0.4236
3	0.4194	-0.6984	0.5735	0.8338	-0.2485	-0.5932	0.7989	0.4102
4	-0.1707	0.5654	-0.5370	-0.8584	-0.0274	0.4873	-0.6095	-0.5281
5	0.1534	-0.4116	0.4589	0.7628	-0.1724	-0.4942	0.5846	0.1024
6	0.0328	-0.6258	0.5786	0.8413	-0.3944	-0.6619	0.7836	0.5731
7	-0.2965	0.7058	-0.6912	-0.7625	0.3194	0.4647	-0.6468	-0.6055
8	-0.4415	-0.6906	0.3924	0.7662	-0.2037	-0.4339	0.7858	0.7262
9	0.0903	-0.6435	0.6025	0.8209	0.0809	-0.5194	0.7836	0.5387
10	-0.5214	-0.6100	-0.0649	0.8000	-0.2751	-0.3374	0.5474	-0.0357
11	-0.4534	-0.7198	0.3060	0.8473	-0.3622	-0.5184	0.6684	0.5151
12	0.4858	-0.6722	0.4291	-0.7013	-0.3990	-0.6898	-0.2630	0.6551
13	-0.4148	0.3930	-0.3943	0.5880	0.1847	0.5728	0.4670	-0.4314
14	-0.3841	0.5675	-0.2172	0.6260	0.3828	0.6160	-0.1720	-0.7823
15	0.2037	-0.7998	0.2609	-0.7598	-0.2596	-0.7239	0.2555	0.7330
16	0.2345	-0.7073	0.3893	-0.6515	-0.3308	-0.6657	-0.2132	0.8082
17	0.6087	-0.6961	0.1995	-0.7035	-0.1519	-0.6460	0.1346	0.8030
18	0.5308	-0.7199	0.1723	-0.6677	-0.1958	-0.6886	-0.1146	0.6427
19	0.4754	-0.7072	0.3644	-0.5395	-0.2117	-0.6523	-0.0686	0.7432
20	0.3957	-0.7270	0.0577	-0.7514	0.0266	-0.6711	-0.0506	0.5711
21	0.5646	-0.7542	0.3597	-0.7036	-0.3395	-0.6433	0.1679	0.7786
22	0.5174	-0.6741	0.3777	-0.6860	-0.0479	-0.6038	0.0967	0.7220
23	0.6458	-0.7456	0.2174	-0.7463	0.0080	-0.7671	0.4938	0.8160
24	0.2630	-0.6330	0.2230	-0.6381	-0.3227	-0.4796	0.0631	0.3906
25	0.4451	-0.7560	0.3842	-0.7169	0.2282	-0.6500	0.0598	0.7886
26	0.5856	-0.8317	0.2800	-0.6759	-0.2450	-0.7166	-0.3774	0.8181
27	0.5384	-0.7974	0.2669	-0.7532	-0.2540	-0.7612	-0.3693	0.6568

id	zt16	zt17	zt18	zt19	zt20	mean1	mean2	mean3
1	0.5273	0.1873	-0.5704	-0.6550	0.2932	5.4840	-9.0358	-9.7243
2	-0.4319	0.1236	0.6013	0.7764	-0.2048	-20.6082	21.0932	13.6802
3	0.5878	0.1081	-0.7307	-0.7347	0.4632	14.5389	-11.6145	-13.4724
4	-0.6278	-0.2746	0.6498	0.7654	-0.1942	-6.5283	15.0622	19.5387
5	0.5746	0.3021	-0.3892	-0.5262	0.1041	-6.4651	-20.4665	-20.7199
6	0.5294	0.3582	-0.5666	-0.7802	0.6052	11.6956	-10.8100	-7.9140
7	-0.5215	-0.4772	0.0746	0.6559	-0.2391	-2.5531	4.2251	1.7802
8	0.6254	0.6080	-0.6085	-0.8097	0.2892	13.0611	-24.5157	-21.7520
9	0.4886	0.4006	-0.4514	-0.7681	0.4354	4.7864	-8.0025	-9.6567
10	0.1582	0.2116	-0.3631	-0.6642	0.2709	4.9852	-11.8813	-10.3252
11	0.5855	0.3691	-0.4030	-0.7835	-0.1727	20.3811	-24.9669	-15.1790
12	-0.6692	-0.2135	-0.0200	0.5280	0.6629	-24.0449	-24.7510	4.7064
13	0.7170	-0.0391	-0.1044	-0.4455	-0.6821	12.2640	15.5585	-7.7964
14	0.6764	-0.0696	0.0534	-0.6985	-0.3074	20.8791	23.3030	-3.6825
15	-0.5469	-0.3270	0.0209	0.2129	0.4369	-27.0792	-28.0396	3.5942
16	-0.5443	0.0333	0.0360	0.3565	0.3419	-30.6299	-37.5980	8.6879
17	-0.5837	0.2719	-0.3295	0.2481	0.5318	-33.9259	-40.1644	12.3575
18	-0.4492	-0.2117	-0.0690	0.3733	0.5305	-32.0694	-43.8404	6.8881
19	-0.6896	0.1645	-0.1659	0.6082	0.4353	-29.0457	-38.5043	5.2888
20	-0.7530	0.1865	-0.3613	0.5115	0.0595	-31.7677	-42.6608	13.3561
21	-0.4951	0.3107	-0.2703	0.3517	0.4688	-24.9666	-34.9012	8.5047
22	-0.5848	0.2868	-0.3917	0.3434	0.7212	-37.0166	-43.9493	13.5245
23	-0.7286	-0.0570	-0.2089	0.7157	0.5233	-52.2988	-51.4627	15.4027
24	-0.1434	0.0642	-0.1412	0.2833	0.3510	-28.1371	-27.2145	11.6574
25	-0.6070	-0.1258	-0.1897	0.6103	0.3818	-33.2741	-47.0837	15.1840
26	-0.5730	0.1910	-0.2868	0.4310	0.6431	-43.6025	-53.4978	14.7698
27	-0.5221	0.0904	-0.3146	0.6142	0.4444	-36.9351	-53.4957	10.1885

id	mean4	mean5	mean6	mean7	mean8	mean9	mean10	mean11
1	-7.9528	3.3264	-0.4023	-12.2858	13.4486	-28.9095	24.0827	7.5156
2	2.1972	2.1681	-10.2935	22.6891	-18.1473	45.6994	-34.4630	-10.6843
3	-0.3378	7.2014	10.7851	-12.1367	19.5400	-35.6416	30.0695	10.3317
4	-1.5543	-8.3755	-7.5762	19.7481	-22.3694	39.8934	-35.9140	-11.7853
5	-17.0610	-8.0560	-9.5252	-23.1325	3.0253	-28.8099	12.7754	-7.6361
6	-2.0106	1.3052	6.1073	-16.2851	16.4216	-34.5180	29.2106	6.9369
7	-1.6940	0.2809	-1.7542	4.8651	-7.1430	14.3425	-14.2397	-3.8955
8	-3.7043	2.1776	8.9885	-19.7219	8.2337	-44.3391	34.8356	7.6079
9	-9.2306	1.9719	1.5433	-14.9380	11.5366	-27.8194	21.8424	4.4955
10	-3.6262	-4.2978	-3.7479	-10.6398	2.6513	-18.5627	9.0814	-0.5056
11	-12.7664	-5.0179	8.5918	-23.4991	7.8516	-54.7563	36.7979	11.7310
12	12.5121	23.2528	-4.4864	-24.6283	2.8487	10.2606	27.4648	-25.9469
13	-3.4297	-18.4632	2.4242	16.4297	-2.6712	-9.4994	-20.3737	15.5954
14	-3.0674	-4.3227	8.3934	20.2812	5.2782	-4.3552	-15.4211	22.0239
15	-4.1672	16.4819	-10.3639	-26.3544	-11.2763	-5.8751	21.8915	-30.7026
16	9.2205	28.3181	-12.2134	-31.9791	-11.6780	4.7029	31.0615	-36.3894
17	3.5372	24.5911	-16.2957	-36.0928	10.3861	4.3935	31.6099	-37.5169
18	-4.0329	25.5802	-16.2981	-35.5856	6.5620	6.2209	34.2573	-39.2376
19	2.9643	24.3653	-16.0572	-30.0877	-0.4440	7.7742	30.8738	-30.0729
20	0.4140	31.6367	-16.1784	-39.3036	-4.4529	5.9055	32.8608	-41.9698
21	7.5818	27.8637	-13.2346	-29.3846	5.9593	4.6171	30.5493	-33.0180
22	8.5387	32.6970	-23.0968	-46.7151	1.5627	11.1490	41.5377	-45.5742
23	25.7768	48.7745	-24.6241	-42.8517	22.5465	8.4419	57.4671	-56.4953
24	8.5525	34.0545	-9.1982	-36.9037	-4.0744	13.4602	33.8582	-33.3469
25	19.3178	45.4002	-3.9298	-43.0769	3.6366	16.0734	59.2245	-44.5799
26	6.7005	39.0847	-20.8442	-50.9062	13.1557	-1.3011	52.1751	-52.9990
27	-1.2540	51.1246	-14.7184	-53.5289	13.9898	-5.3147	61.2799	-57.4064

id	mean12	mean13	mean14	mean15	mean16	mean17	mean18	mean19
1	4.6093	-4.7233	23.0096	14.3757	18.4808	15.6447	-23.6681	-20.0449
2	-10.7623	4.6743	-37.4941	-16.5911	-34.0378	-25.2368	35.4441	34.6495
3	8.8510	-5.6197	32.7916	13.3454	27.6814	20.7960	-28.7144	-25.1760
4	-17.0412	6.5133	-36.0623	-17.1016	-34.1053	-27.8868	33.3859	28.2186
5	-3.2065	-18.0233	12.7688	-0.3248	9.7267	8.8753	-25.3666	-25.5020
6	6.5957	-11.1615	29.3797	15.0426	25.8771	22.5413	-30.1702	-27.3316
7	-3.8253	0.7998	-11.8114	-6.1722	-11.3713	-9.2609	7.4620	7.4678
8	14.5864	-3.6425	37.2802	22.0955	33.3226	31.4527	-36.8403	-34.5734
9	8.0465	-4.6912	18.7734	10.9893	16.1031	14.8937	-20.6113	-20.5290
10	2.2098	-6.2276	11.7891	-0.1118	8.4890	9.2330	-15.0350	-15.3765
11	15.4230	-10.5671	38.5870	16.9788	37.2138	33.3639	-41.8294	-44.7806
12	5.4567	-28.3090	-10.3476	19.0692	-7.7647	-21.9583	27.4383	28.5828
13	-5.2588	18.6614	8.2210	-14.5030	4.1847	12.1804	-21.0618	-19.8677
14	2.4913	26.9878	3.6772	-9.3706	9.8422	17.5251	-17.1638	-21.3026
15	-1.1580	-35.5460	-3.2223	10.9149	-9.1592	-26.5392	23.3646	17.8735
16	1.6288	-41.9662	-3.7391	20.2631	-8.4027	-25.7270	32.1959	29.5811
17	8.2125	-45.2227	-5.0536	24.8753	-10.2799	-24.4999	29.3138	31.9029
18	12.9880	-49.8236	-10.4778	19.6579	4.1958	-32.8227	36.7801	35.4989
19	9.0671	-39.9400	-7.1509	18.5497	-5.8394	-24.6075	32.6750	35.5482
20	12.6456	-45.4419	-6.6542	21.2745	-3.6130	-27.1405	33.0870	38.4420
21	3.8803	-37.8686	2.6446	24.1083	-2.4948	-17.6286	30.7961	31.6187
22	12.5412	-53.6438	-8.8678	26.9926	-8.4112	-28.2719	35.8198	37.3074
23	23.6965	-74.1724	5.2997	39.8151	-19.0413	-43.6315	59.5950	68.2329
24	2.7343	-36.4479	-4.9827	18.7684	13.3574	-24.4712	37.9101	34.1319
25	35.7427	-53.2043	-5.6671	40.6591	-3.5961	-38.4616	53.3330	58.0370
26	13.7275	-63.7062	-22.4172	37.0819	-8.4906	-35.4054	48.6820	54.6213
27	18.6910	-70.1160	-21.0467	48.1916	7.7140	-40.3275	57.3485	65.3314

id	mean20	sd1	sd2	sd3	sd4	sd5	sd6	sd7
1	22.5815	9.2493	9.2135	7.9323	12.3621	10.6563	11.1847	7.6408
2	-34.3045	11.8243	13.929	13.9522	17.8016	17.3295	17.2396	11.7332
3	29.8191	9.716	10.9428	8.3169	14.8648	11.8447	13.7183	10.4388
4	-33.106	15.1982	13.2894	9.2742	18.2566	14.9651	16.1904	9.225
5	11.2303	13.4797	8.4446	6.0405	11.3922	13.4785	12.4679	6.3126
6	29.5519	12.875	13.5789	10.7198	15.2461	13.3713	14.1385	8.5688
7	-11.3298	3.7728	4.0196	3.8072	4.7205	4.816	4.4412	3.118
8	34.9702	10.3867	12.7487	10.1101	20.5484	17.8051	16.5402	9.8801
9	18.2631	7.3439	9.2478	8.4567	11.7594	9.6955	9.2069	5.939
10	11.1041	4.2741	6.1488	5.0139	9.2762	7.448	8.1742	4.5534
11	32.7593	15.0149	18.2821	16.5993	21.2173	21.4167	20.278	11.0254
12	17.0863	9.5887	9.6537	13.0672	8.5669	10.444	13.5994	6.962
13	-13.0808	3.7134	4.8421	9.972	9.6125	7.7123	9.9051	3.9043
14	-5.6061	4.6495	5.1395	10.7832	7.79	12.2444	10.4353	4.5212
15	8.6845	7.1054	7.769	14.1348	11.414	9.4972	13.9277	6.2195
16	11.8753	8.7166	10.3573	19.0872	13.6435	12.7225	17.5037	9.0461
17	20.2736	9.8266	11.2101	18.6146	16.4425	13.6386	21.5386	9.0166
18	19.2816	9.9666	12.6297	18.6361	18.1442	15.9796	20.4142	8.9186
19	15.3027	9.7511	11.0319	17.0824	14.6117	14.7566	18.6671	8.1008
20	8.4321	18.22	12.6556	20.7292	18.6458	14.7863	20.7781	10.5911
21	15.2917	8.5272	9.8483	16.07	14.3959	13.0012	17.1958	8.475
22	25.7227	9.3058	13.5232	23.4293	19.4753	16.0739	24.4272	10.4378
23	34.6409	14.1667	17.5647	31.1744	23.1693	22.6826	28.8468	14.4791
24	16.6729	8.615	15.0495	18.5399	16.6122	14.5767	19.2059	9.4734
25	27.3133	9.9213	15.2316	28.4176	23.7904	18.6255	32.9369	11.3571
26	34.3166	11.1128	15.0939	29.2563	24.2841	19.623	27.9385	12.1479
27	29.7516	14.0945	15.9943	28.5121	27.8478	22.4255	31.372	12.3913

id	sd8	sd8	sd10	sd11	sd12	sd13	sd14	sd15
1	5.9947	6.8182	5.6852	12.4396	9.7095	8.841	6.753	7.447
2	11.7517	9.6008	9.3022	19.2175	16.3726	14.7799	10.4103	14.2676
3	6.4324	8.8849	7.2992	15.1796	12.7572	10.1072	9.4212	10.6483
4	8.8531	8.1651	8.7249	20.0896	12.4232	13.6619	9.9438	12.8284
5	9.64	6.2349	6.0309	14.3425	13.7555	7.348	6.1742	12.1739
6	11.3003	8.4014	6.6584	16.6743	11.2984	10.724	8.1812	10.0557
7	3.4018	3.7261	4.305	5.7107	3.5556	3.609	3.7884	4.199
8	15.0259	9.9712	9.7642	17.5628	11.8352	11.9784	10.356	10.3603
9	5.2968	6.7819	6.2738	10.7902	5.3529	9.2203	5.5495	5.9029
10	6.5199	5.0202	5.4733	9.8401	6.629	6.4227	3.8435	8.1662
11	20.4589	11.919	8.6766	23.1649	15.3281	16.4843	11.3664	17.0059
12	17.2688	15.673	7.0446	10.6654	13.773	8.4236	8.2291	12.4779
13	11.2185	10.0789	6.1598	5.1226	10.9208	5.2127	5.343	7.3664
14	11.481	11.3484	6.0352	5.6843	10.4947	6.3628	7.8567	9.0603
15	13.8131	16.8439	7.0623	9.8581	12.3329	9.5217	16.4931	11.0804
16	18.0169	19.5237	9.8437	12.1027	16.9176	10.8127	13.0488	14.5378
17	21.5321	22.2883	9.7151	12.561	16.672	12.6812	14.3259	13.7806
18	21.6072	23.0751	11.2167	12.9323	19.2967	13.6739	14.6372	15.9215
19	22.0232	20.4095	9.0784	11.3111	16.298	10.5521	12.4869	14.2806
20	23.2037	23.1198	10.3066	14.466	16.8612	11.4536	13.8514	14.9887
21	20.8802	20.4658	9.2341	11.1557	16.1774	10.2888	14.7886	12.3247
22	25.4695	26.3616	12.3767	13.9054	18.3424	13.75	16.3791	17.5329
23	33.9545	37.211	15.7671	20.9243	27.3203	20.5818	28.7824	27.0115
24	21.5044	23.2014	9.1513	11.8527	18.9157	10.231	18.8336	13.0569
25	33.423	35.0275	15.0436	17.8972	17.6013	16.5968	18.5797	22.6895
26	31.6821	35.4663	15.2581	17.3951	25.1744	16.954	14.8156	22.8494
27	35.5793	36.6233	16.1703	21.1388	30.0921	19.8843	18.21	21.8683

id	sd16	sd17	sd18	sd19	sd20	skew1	skew2	skew3
1	6.7727	7.0274	6.2856	5.713	7.3045	-0.9869	0.7444	0.6273
2	12.6258	7.9218	8.4968	8.3636	8.4501	1.1832	-1.1659	-0.7549
3	10.2519	5.0166	7.2663	7.3062	5.9736	-0.7563	0.8794	0.8433
4	11.8299	7.0074	6.6558	6.6977	7.1403	0.6497	-1.0062	-1.0635
5	7.8154	4.7416	5.548	5.7887	4.5179	-0.0061	2.3293	3.5678
6	8.6683	5.0742	7.6718	7.6817	5.7454	-1.2145	0.7355	0.5149
7	4.5886	2.8915	2.3581	2.5128	3.1895	0.7252	-0.7352	-0.3765
8	11.2834	7.6887	8.399	10.1785	6.7383	-0.9675	1.3791	0.934
9	6.3985	4.0164	4.8255	5.7119	5.5996	-1.1029	0.6263	0.8843
10	3.9838	3.4945	4.2141	4.8139	3.1616	-1.8746	1.8256	2.2918
11	13.8824	10.0615	8.8447	11.1665	8.0538	-1.0209	1.1414	0.6651
12	14.9321	8.0394	7.5644	7.112	13.2467	0.4145	0.9412	-0.2878
13	12.2565	3.8803	5.86	6.2417	11.556	-2.4178	-2.0274	0.8373
14	9.895	5.7686	6.0782	7.5292	11.1973	-1.7594	-1.98	0.8185
15	15.0783	6.8285	7.0848	9.0915	14.1717	2.0301	1.7488	-0.6412
16	19.2602	6.8434	9.3729	7.626	18.1441	1.4984	1.5871	-0.5331
17	23.6414	8.815	17.4294	7.8082	17.5174	1.0542	1.5137	-0.8851
18	19.0837	8.4372	10.5415	9.2975	20.3045	1.0512	1.3445	-0.5785
19	19.9404	7.85	9.6599	8.6869	16.9603	1.4229	1.6534	-0.4382
20	21.9037	9.4025	12.0105	8.589	21.8224	1.5342	1.1154	-0.9735
21	17.0829	9.9418	10.2336	7.2368	16.7019	1.207	1.6616	-0.6651
22	24.498	12.0916	14.2849	9.0922	24.4679	1.7151	1.0234	-0.8633
23	32.8613	12.6597	20.3763	15.6358	31.5136	1.5453	0.7929	-0.5287
24	19.0253	8.2632	9.6777	7.0596	19.7816	1.6812	1.27	-0.7374
25	28.9656	10.5818	11.9426	11.3601	27.2345	2.0108	1.3647	-0.4348
26	27.4736	11.2219	13.6101	12.3375	26.5211	1.676	1.2718	-0.5149
27	31.2249	16.2697	16.7681	13.6031	29.2422	1.2986	1.2196	-0.4153

id	skew4	skew5	skew6	skew7	skew8	skew9	skew10	skew11
1	0.6716	-0.7817	0.2284	0.8262	-2.2722	3.6807	-2.6273	-0.7442
2	-0.1248	0.327	0.4366	0.3734	1.5981	-2.164	2.0634	0.5404
3	-0.2122	-0.9134	-0.6289	0.5476	-0.9852	2.7337	-1.7068	-0.6477
4	0.2391	0.8348	0.1986	-0.7566	2.2091	-2.6109	2.9837	0.4629
5	1.3902	0.0604	0.2525	2.9884	-1.4054	4.6771	-3.7936	0.3536
6	-0.0362	-0.6118	-0.0271	0.7329	-1.2657	2.7116	-2.5733	-0.3437
7	0.3405	0.2165	-0.3591	-0.4482	1.8914	-2.3608	2.8634	0.363
8	-0.1451	-0.6208	-0.4654	0.6173	-1.0206	3.0748	-1.0349	-0.5309
9	0.5589	-0.841	-0.0049	1.3548	-1.9809	3.1234	-1.7645	-0.4526
10	-0.06	0.1351	0.4626	1.9401	-1.1193	3.8619	-2.6115	-0.0144
11	0.6192	-0.2493	-0.543	1.0578	-0.9452	2.6164	-2.3006	-0.5222
12	-1.1717	-1.5241	0.4921	2.4563	-0.0852	-0.7962	-2.8981	1.3527
13	0.2176	2.3508	-0.6111	-3.7809	-0.0503	1.0767	3.3519	-2.8334
14	0.8018	0.5555	-0.7743	-1.8155	-0.6504	0.8686	2.7358	-2.4662
15	-0.1358	-1.9384	0.5865	3.2605	0.7946	-0.1238	-2.7208	1.9863
16	-0.8372	-2.1566	0.6958	1.9414	0.8	-0.6497	-2.0387	1.648
17	-0.3985	-1.3346	0.6274	2.1506	-0.4639	-0.5053	-2.233	2.0304
18	0.1446	-1.1054	0.7018	1.9423	-0.4496	-0.6194	-1.8089	1.9123
19	-0.2313	-1.1257	0.7805	2.0946	0.3069	-0.6741	-2.3912	1.5881
20	-0.2182	-1.8781	0.7975	1.784	0.2571	-0.5961	-2.1781	1.6497
21	-0.3832	-1.4131	0.7891	1.7857	-0.0495	-0.5388	-2.0529	2.1718
22	-0.4542	-1.9893	0.8386	2.7951	-0.113	-0.7866	-2.7175	2.5681
23	-1.1446	-1.6363	1.1211	1.6488	-0.7618	-0.4747	-2.7575	1.8464
24	-0.4881	-1.6297	0.6634	2.9487	0.4845	-0.8269	-2.3682	2.5945
25	-0.6996	-1.731	0.0295	2.8458	0.1958	-0.7534	-2.5808	2.1374
26	-0.4382	-1.3359	0.8524	2.3707	-0.2979	-0.2079	-2.321	2.3605
27	0.2042	-1.8894	0.7313	3.0054	-0.3537	0.1277	-2.9865	1.977

id	skew12	skew13	skew14	skew15	skew16	skew17	skew18	skew19
1	-0.8724	0.1108	-1.6281	-0.6104	-2.3556	-1.6139	2.3436	2.4933
2	0.8082	0.0702	2.5636	0.8563	2.3564	1.7451	-0.6912	-1.177
3	-1.1454	0.125	-1.4994	-0.5076	-1.5546	-1.9349	2.3801	1.9056
4	1.3494	-0.4432	2.6302	0.6326	2.7117	3.5412	-2.2695	-1.6699
5	-0.3316	2.2957	-3.4653	-0.773	-2.7128	-4.296	4.8106	4.5711
6	-0.9327	0.4149	-1.7595	-0.6005	-2.7143	-3.0756	2.1766	1.8676
7	1.1754	0.1097	3.0665	0.51	2.0314	4.0082	-2.3038	-1.65
8	-1.7013	-0.0844	-1.79	-0.1752	-2.5441	-2.1457	2.5627	1.3295
9	-2.3722	-0.136	-1.9912	-0.5061	-2.1052	-2.7358	3.9145	2.4828
10	-1.0377	0.6759	-3.8263	-0.4022	-2.6795	-3.1871	4.1717	3.1447
11	-1.5577	0.1482	-1.6114	-0.416	-2.4857	-1.5978	2.6089	1.7734
12	-0.4197	2.4128	1.0581	-0.7612	0.4636	1.1769	-1.1696	-1.7346
13	0.346	-2.5561	-1.7796	1.6224	-0.5319	-2.3973	2.7974	2.4511
14	-0.1362	-2.0359	-0.2358	0.9443	-0.9763	-0.9365	1.7705	2.0664
15	-0.0377	2.362	0.3367	-0.9978	0.4014	2.198	-1.1736	-0.8635
16	0.0135	2.4904	0.29	-1.0464	0.2972	1.9877	-1.0439	-2.1475
17	-0.4092	1.8759	0.2709	-1.1866	0.3056	1.1685	-1.1226	-2.131
18	-0.9324	1.9236	0.6245	-0.6144	-0.3034	1.9279	-1.4103	-1.9086
19	-0.724	2.6021	0.7975	-0.8151	0.0995	1.4631	-1.308	-2.1053
20	-0.8066	2.596	0.5827	-0.9166	-0.0954	1.6968	-0.8785	-2.9541
21	0.0159	2.3434	0.0683	-1.0127	0.1958	1.2415	-1.0671	-2.4442
22	-0.7535	2.2037	0.5302	-0.9309	0.2394	1.4357	-1.0174	-2.245
23	-0.7442	2.0486	-0.0526	-0.9519	0.7543	2.0883	-1.4214	-2.0463
24	0.0525	2.7563	1.1145	-1.0194	-0.7691	1.6584	-1.0763	-2.5707
25	-1.8893	2.0202	0.6971	-1.2129	0.3464	2.6774	-0.9904	-2.5926
26	-0.4437	2.1837	1.1238	-1.0843	0.453	1.1377	-0.728	-2.374
27	-0.6081	2.0686	1.5398	-1.3982	-0.2822	1.3113	-1.2059	-2.7199

id	skew20	kurt1	kurt2	kurt3	kurt4	kurt5	kurt6	kurt7
1	-0.6184	2.9083	2.2993	2.6936	1.9872	2.3937	1.6542	3.3968
2	2.6064	4.145	3.2843	2.5403	1.5274	1.6875	1.8806	3.3749
3	-2.7947	3.9124	2.6701	3.634	1.6268	2.7745	1.9924	2.8108
4	4.0925	1.9863	2.9036	4.7433	1.4707	2.3567	1.714	3.6426
5	-4.4765	1.1978	7.2384	16.1727	3.2979	1.1911	1.2587	15.1227
6	-3.5242	3.5891	2.3293	1.9913	1.3356	1.9657	1.8378	3.7347
7	3.9755	3.5374	3.4075	3.0206	2.2136	2.0399	2.9532	5.0683
8	-3.3074	3.4607	4.5463	4.3381	1.3944	1.9235	1.8771	3.7081
9	-0.8505	3.2011	1.9656	2.85	1.9164	2.3167	1.7026	5.9965
10	-3.9651	7.4153	5.8934	8.5673	1.2565	1.5267	1.5381	9.5967
11	-1.4078	3.657	2.984	2.2319	1.9938	1.6054	1.9556	4.9308
12	-0.9007	4.3696	4.5439	1.5479	3.7736	5.3926	1.9017	13.0013
13	0.8321	17.0788	11.6583	2.015	1.4675	8.0771	2.0686	25.4748
14	0.5238	11.1115	11.2094	1.9637	2.5227	1.9921	2.2896	11.5882
15	-0.684	11.5813	9.3427	1.7302	1.4152	6.6853	1.9337	17.975
16	-0.485	7.5572	7.8605	1.6248	2.9857	7.2315	2.1591	8.4882
17	-0.8933	6.7629	7.2237	2.1639	1.5983	4.556	2.0898	11.4056
18	-0.6954	5.6329	6.2114	1.7703	1.4918	3.5176	2.3705	11.1276
19	-0.7934	6.3256	7.4683	1.6187	1.5539	3.6683	2.4737	11.0161
20	-0.5334	5.1634	5.7038	2.2918	1.5804	6.334	2.3906	8.3016
21	-0.6878	6.3881	8.2029	1.9518	1.8689	5.0637	2.3967	8.6818
22	-0.896	9.9629	5.0168	2.0903	1.9244	6.7862	2.4075	14.4388
23	-0.8093	7.8901	4.2899	1.6321	3.0985	5.6431	3.1068	7.4721
24	-0.57	9.4279	4.6188	1.9739	1.7871	5.5597	2.2065	14.7947
25	-0.7584	12.0356	6.9045	1.4705	1.9715	6.3252	1.5331	15.6576
26	-1.0125	9.5847	6.5391	1.6929	1.5725	4.7565	2.4488	11.9691
27	-0.7646	6.4915	6.4993	1.5512	1.4627	6.2573	2.1491	16.2925

id	kurt8	kurt9	kurt10	kurt11	kurt12	kurt13	kurt14	kurt15
1	9.1617	19.1396	13.0643	2.0636	2.3448	1.7326	7.7931	3.5702
2	5.1575	9.8569	10.2505	1.9234	2.1878	1.6978	11.3018	3.4671
3	5.5685	12.6994	8.3715	2.0479	2.8917	1.8031	6.2364	2.6639
4	9.0309	12.7038	14.7801	1.6268	4.4777	1.7619	11.6216	2.9038
5	3.3325	26.6619	18.8418	1.2887	1.2251	7.5631	17.5102	1.9763
6	5.2097	13.4552	11.9142	1.5647	2.6176	2.2101	7.8178	3.0799
7	10.2113	12.4777	14.2426	2.1081	5.4266	3.0324	16.0412	4.5427
8	2.6445	14.8955	5.2098	1.91	5.0124	1.5824	7.4024	3.1847
9	8.2932	15.8577	7.7737	1.8661	9.3694	1.8056	10.0247	4.1736
10	2.775	20.6866	9.8821	1.1945	2.7999	2.3975	21.6794	1.8059
11	2.5163	13.2031	11.0491	1.9012	4.5255	1.6049	7.2582	2.6354
12	1.4638	2.1299	13.3841	6.0547	1.6595	10.757	3.9338	2.834
13	1.4452	3.0905	15.4954	14.6458	1.5224	13.4165	6.5315	5.4644
14	2.0399	2.3965	12.1775	11.6507	1.6787	9.0827	1.8144	2.7377
15	2.1788	1.5776	12.8661	8.4704	1.4655	10.0896	1.3726	3.0408
16	2.3339	1.9069	9.0161	8.2434	1.4577	10.748	1.8054	3.0473
17	2.0612	1.7557	9.7846	8.1138	1.8748	7.6548	1.7474	3.8669
18	1.8907	1.9597	7.8266	8.4729	2.6615	7.8078	2.2189	2.8071
19	1.7897	1.9204	10.3641	6.9615	2.2022	11.0785	2.4493	2.7951
20	1.6419	1.8362	10.289	7.178	2.3925	11.1699	2.2794	3.2522
21	1.7158	1.8216	8.6829	9.0544	1.4871	10.1115	1.5809	3.6429
22	1.6254	2.2171	11.9431	10.7317	2.2745	9.5642	2.0306	3.4938
23	2.3537	1.6719	12.7268	7.4131	2.0728	7.7443	1.4536	2.9297
24	1.7527	2.3245	10.8875	10.8685	1.4085	12.5702	2.7999	3.1679
25	1.4372	1.9655	11.741	8.801	6.0827	8.7034	2.3311	3.5728
26	1.8238	1.5613	10.2132	10.0113	1.7684	8.7607	4.2071	3.27
27	1.682	1.4693	13.557	8.0239	1.832	8.0481	4.859	4.8527

id	kurt16	kurt17	kurt18	kurt19	kurt20	meanmean	meansd	meanskew
1	9.5694	5.2804	14.0226	13.161	4.5754	1.7906	8.2515	-0.1692
2	8.9981	9.4815	5.7558	6.0144	14.216	-3.5164	12.7685	0.5725
3	6.2649	12.3493	12.7313	9.2232	16.0527	4.6519	9.8193	-0.2936
4	10.3785	18.7695	12.5895	7.8468	24.3855	-4.8523	11.521	0.6358
5	9.7023	25.0427	28.0649	25.3393	29.0941	-7.7947	8.7864	0.3018
6	10.7363	17.345	11.7393	9.3374	20.4401	3.0232	10.3317	-0.4763
7	8.6844	26.3134	17.8795	14.0957	25.8239	-2.1913	3.8266	0.6522
8	10.0072	10.7042	13.8956	6.1768	19.0116	2.9761	11.9581	-0.3318
9	8.5243	16.9144	23.1466	12.5726	7.5019	0.8883	7.1685	-0.1949
10	13.6311	18.0412	23.6585	15.85	30.3027	-2.0397	5.8236	-0.1134
11	9.8107	6.528	13.9886	8.3071	9.9121	1.3158	15.0123	-0.2014
12	2.067	5.9127	5.1279	9.1163	2.7406	0.3221	10.8166	-0.049
13	1.665	14.3911	14.44	11.8336	2.2603	-1.5243	7.544	-0.1551
14	2.8694	4.8863	9.4994	9.2294	1.9765	3.8195	8.2177	-0.1341
15	1.6493	12.3253	6.3106	3.6503	2.1813	-5.8339	10.9664	0.3194
16	1.733	10.9297	4.8901	9.8004	1.9657	-3.1394	13.3564	0.1156
17	1.6739	5.3591	3.6959	10.0354	2.6801	-2.3799	14.9528	-0.0283
18	1.6093	10.0593	5.9249	7.9941	2.3032	-2.8139	15.2357	0.0573
19	1.4671	7.1262	6.1268	9.5779	2.4072	-1.967	13.6769	0.1101
20	1.456	7.4258	4.3679	14.1123	1.9177	-3.0564	15.9193	-0.0008
21	1.7144	4.5302	4.9827	11.663	2.3898	-0.0041	13.2013	0.0583
22	1.6851	6.1951	4.6543	10.7348	2.538	-2.4077	17.2612	0.0291
23	2.249	9.8513	5.9286	9.5566	2.3669	2.2556	23.8342	-0.0742
24	2.2047	7.9414	5.4721	13.8542	2.0156	1.0191	14.6313	0.1584
25	1.554	13.6288	6.0977	13.3537	2.191	5.0524	20.3612	0.0341
26	1.7747	6.3672	4.1632	10.6095	2.8808	-1.9428	20.5108	0.1336
27	1.532	4.8636	5.6942	12.563	2.2428	0.4734	22.9656	0.043

id	meankurt	meanztcor	meanprod
1	6.1406	-0.0605	94.6788
2	5.4374	0.0656	161.961
3	5.9162	0.0057	141.4805
4	7.5847	0.039	183.7957
5	12.0561	-0.0689	459.6285
6	6.7125	-0.0025	305.0628
7	9.156	-0.0107	5.9728
8	6.1443	-0.0565	125.9333
9	7.3886	0.0093	96.3054
10	10.0249	-0.1528	95.7584
11	5.6299	-0.0549	473.1989
12	5.0856	-0.0725	-809.1486
13	8.7021	0.0387	-370.7584
14	5.7358	0.0761	-574.9109
15	5.8921	-0.1048	-635.3312
16	5.2892	-0.0738	-1241.4059
17	4.8052	-0.0659	-1442.7355
18	4.7829	-0.109	-1768.6842
19	5.0195	-0.0569	-1419.7962
20	5.0542	-0.0874	-1746.875
21	4.8966	-0.0157	-1197.3583
22	5.6157	-0.0323	-2001.3111
23	5.0725	0.0084	-5060.999
24	5.8818	-0.0556	-1244.0342
25	6.3679	-0.0419	-3087.8184
26	5.2987	-0.0957	-3479.7151
27	5.5962	-0.1008	-4580.7798

A.3 FULL CIRCLE: CORTICAL SURFACE PROJECTIONS OF CONNECTIVITY ASSOCIATIONS WITH DYNAMICAL MODEL OUTPUT

Subject RBS-R CSS was used to identify connections in a whole-brain search, which were used to identify further connections until a functionally plausible hypothetical network model was sufficiently populated with nodes, the network model then being used to generate parameter values for a dynamical model putatively representing cortical activity, and here, subject-level calculated output from that model is used to identify functional connectivity associations, in this case, from the putative network cerebellar hub to the rest of the brain. Bivariate Pearson correlation connectivity from an averaged seed comprising left and right cerebellum XIII and vermis X is depicted in each case for qualitative comparison with the inflated cortical surface projection depictions used in the rest of this thesis.

First, RBS-R CSS associated connectivity of the same kind is shown (figure A.3) for contextualization, followed by connectivity associated with the measure of the time correlation of z in the dynamical model (figure A.3), followed by connectivity associated with the skewness of z from the dynamical model output (figure A.3), which is negatively correlated with RBS-R CSS, followed by connectivity associations with the final time step value of $\bar{z}$ in the static stimulus linear model realization (figure A.3), followed by connectivity associations with the stochastic model mean divergence regressor (figure A.3). Note that, for the first (RBS-R CSS) and last (stochastic model mean divergence) figures, the heatmaps are effectively inverses of one another, given the very strong correlation of the stochastic model mean divergence regressor with subject RBS-R CSS and the negative value of the regression coefficient.
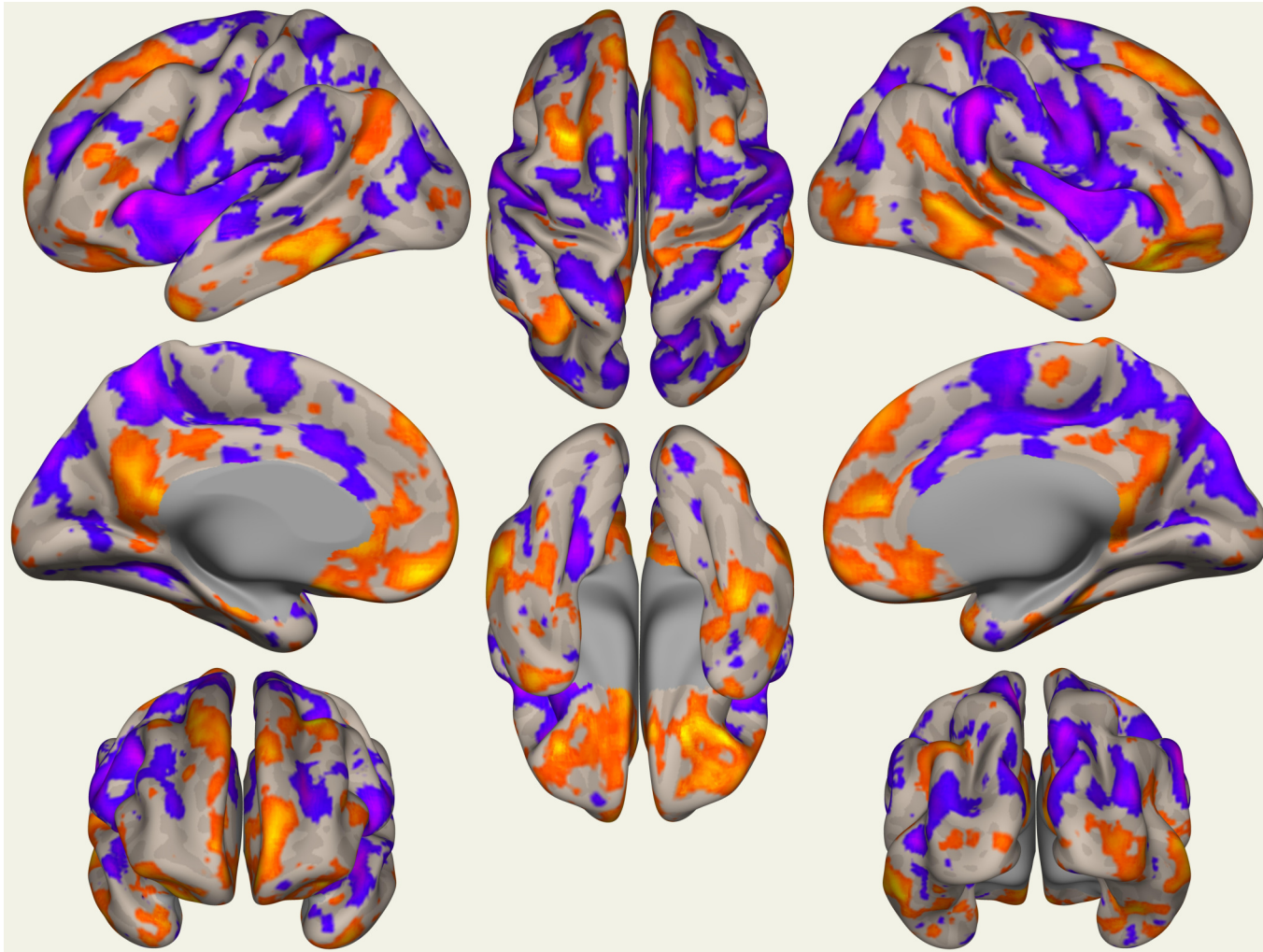
Figure A.4: Reference RBS-R associated cerebellum—whole brain FC cortical surface projection
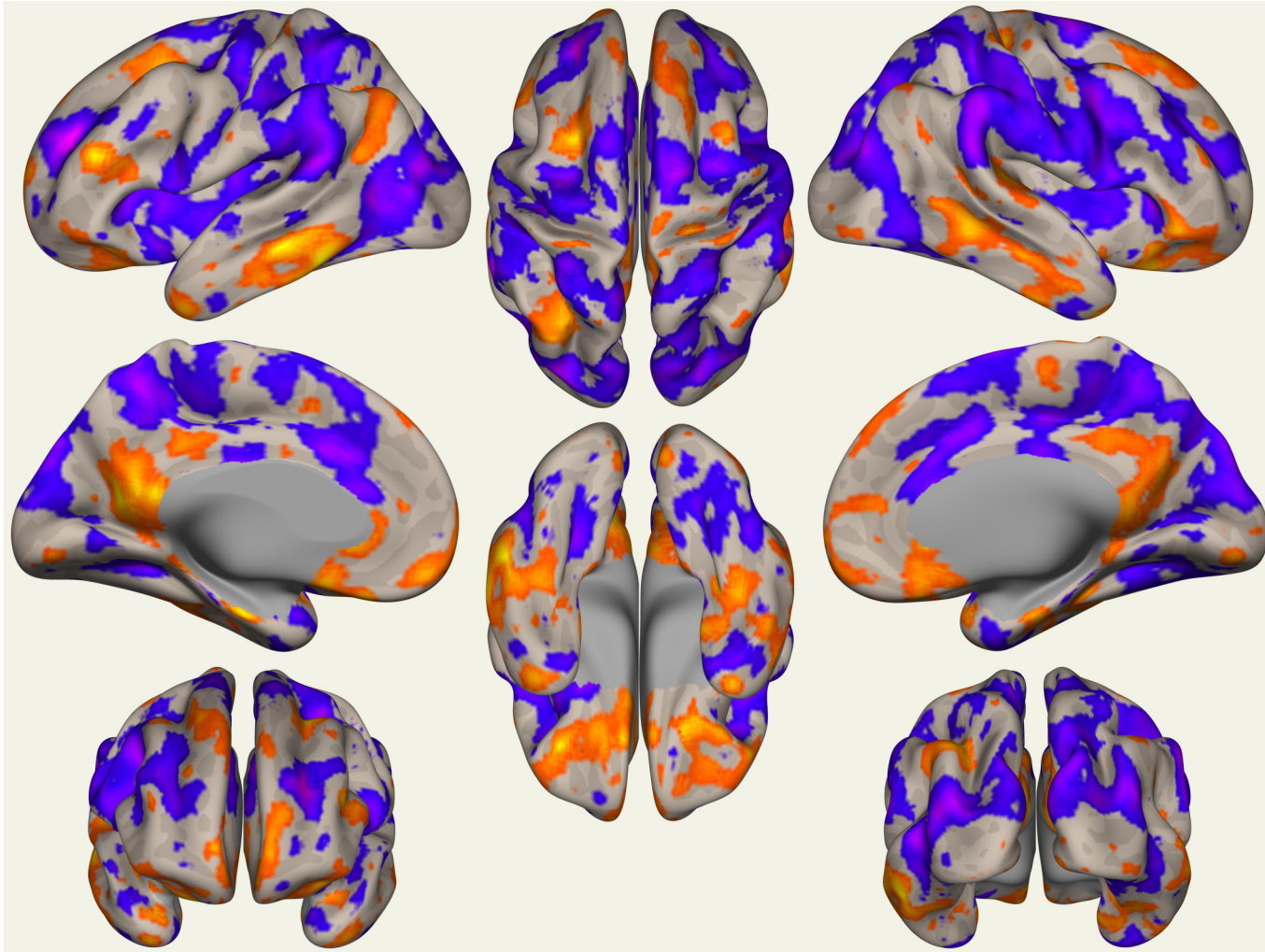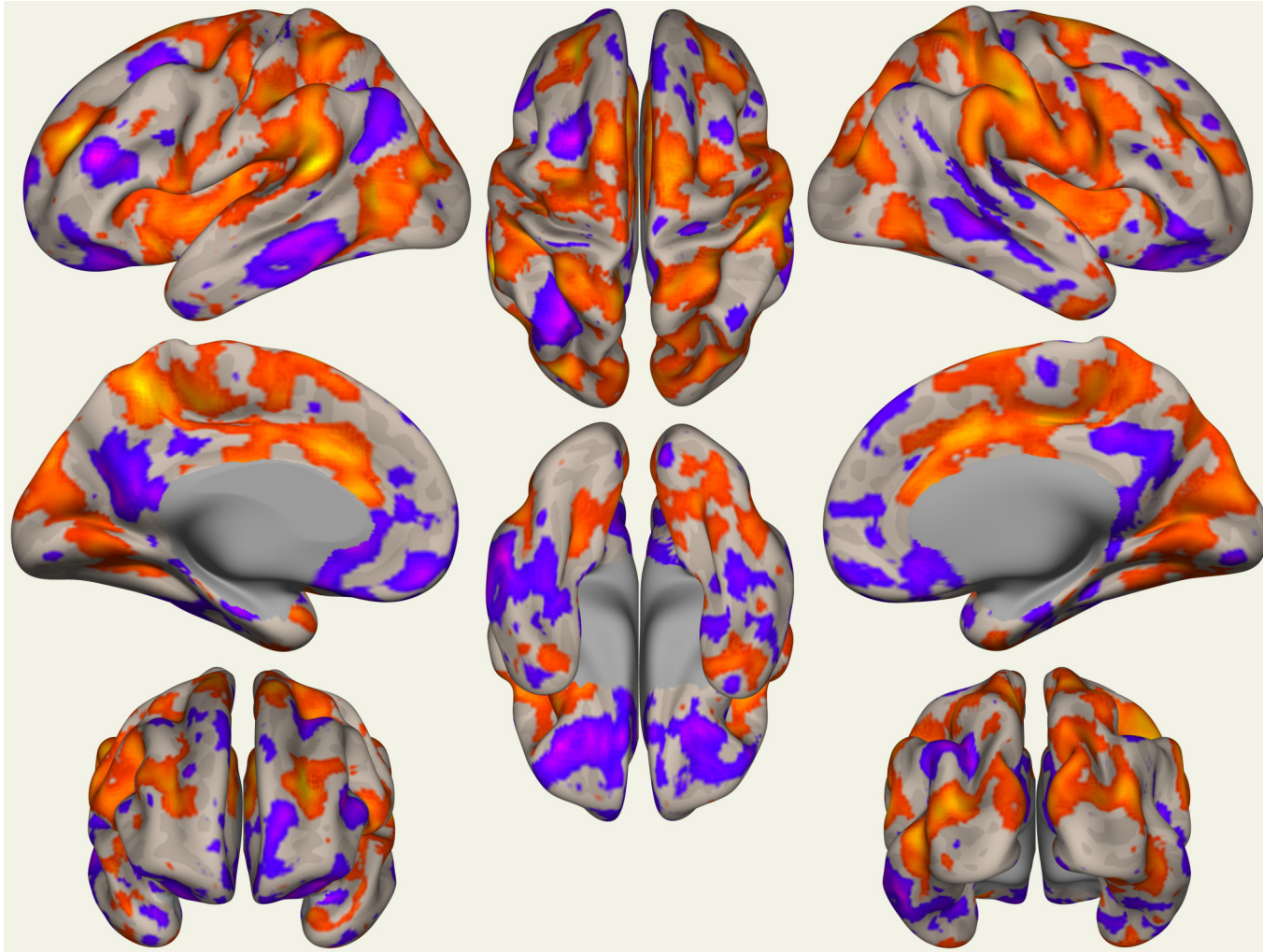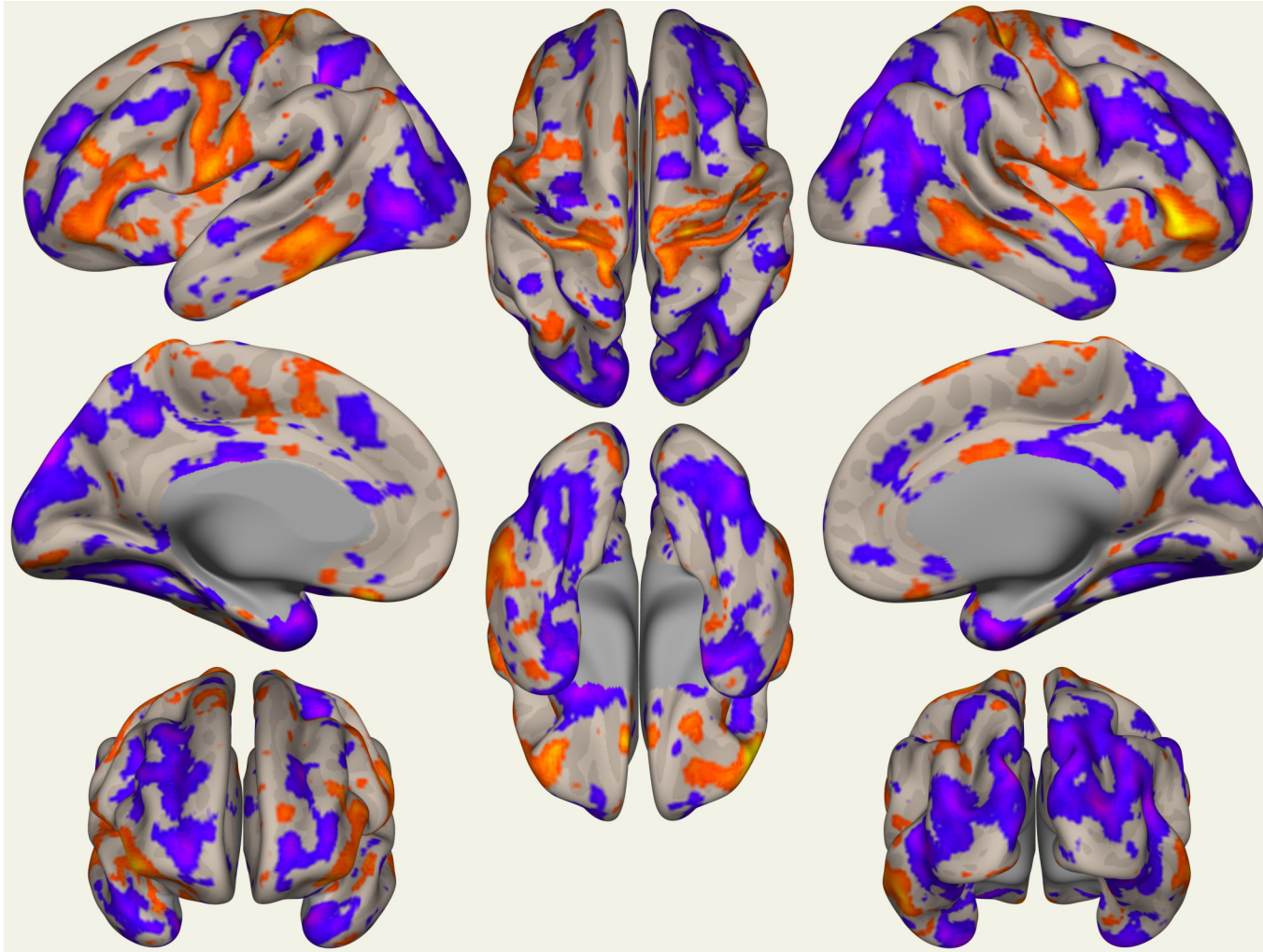
Figure A.5: $\bar{z}|[t_0, t_{0.05f})$ associated cerbellum—whole brain FC cortical surface projection
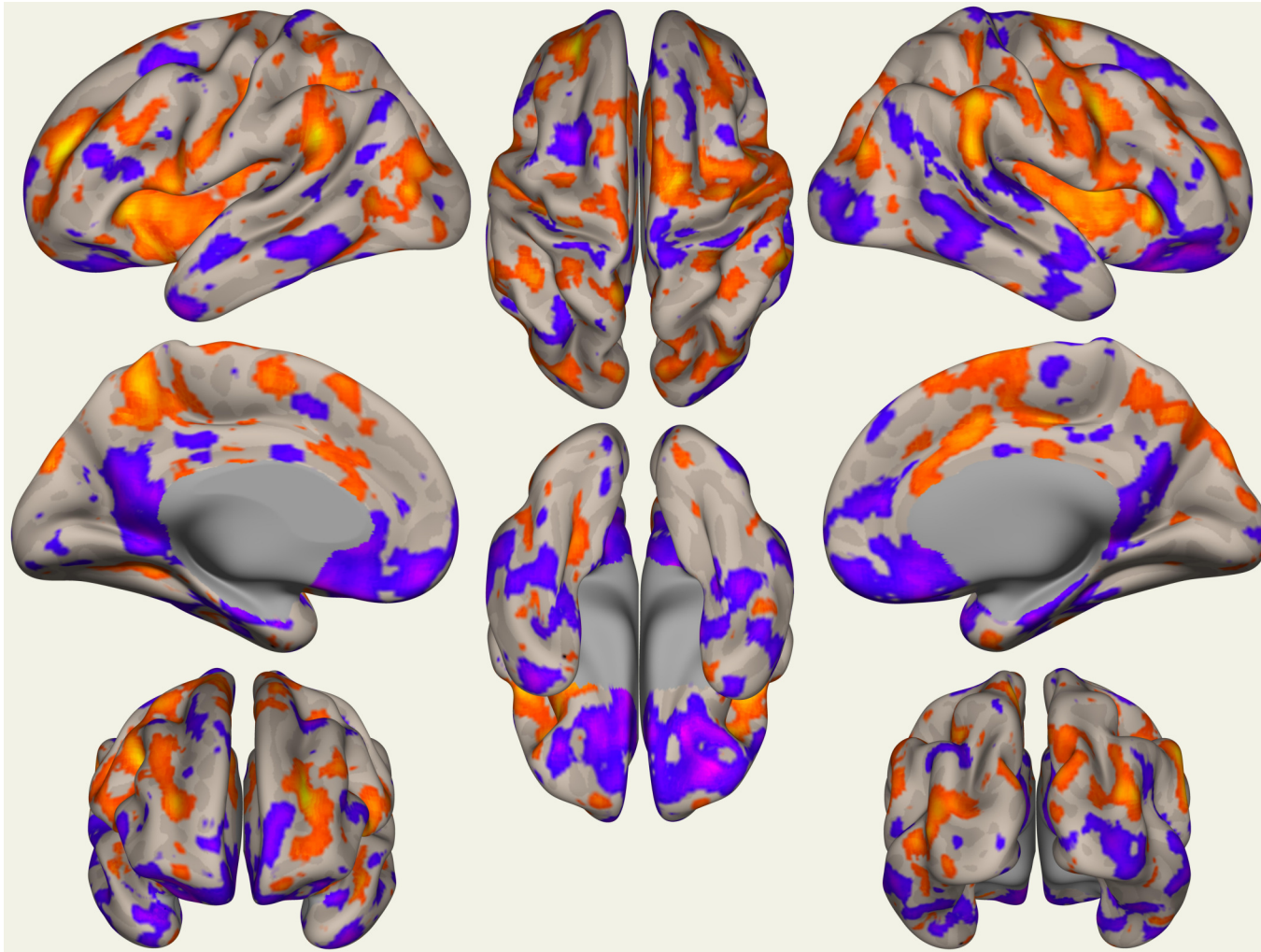
Figure A.6: skew$(z)|[t_0, t_{0.05f})$ associated cerbellum—whole brain FC cortical surface projection

Figure A.7: Static $\bar{z}|t_\mathrm{f}$ associated cerebellum—whole brain FC cortical surface projection

Figure A.8: Stochastic model $\bar{z}_{\min} \cdot \bar{z}_{\max}$ associated cerebellum—whole brain FC cortical surface projection

Analogously generated cortical surface projections of connectivity from the hypothetical network's cerebellar hub to the rest of the brain, in this case associated with ADOS-G communication subscale score (figure A.3) and ADOS-G social subscale score (figure A.3).
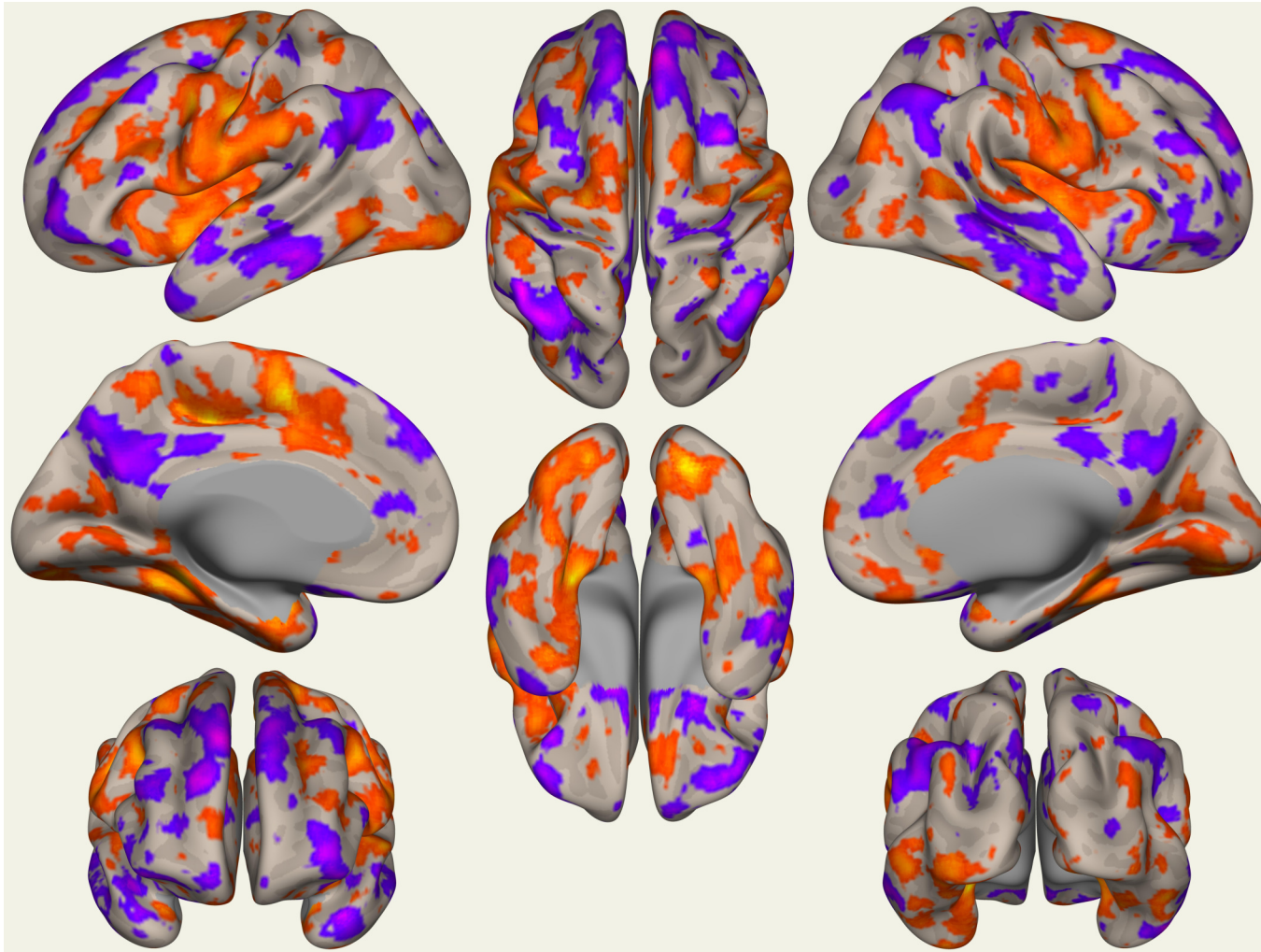
Figure A.9: ADOS-G comm associated cerebellum—whole brain FC cortical surface projection

Figure A.10: ADOS-G soc associated cerebellum—whole brain FC cortical surface projection

BIBLIOGRAPHY

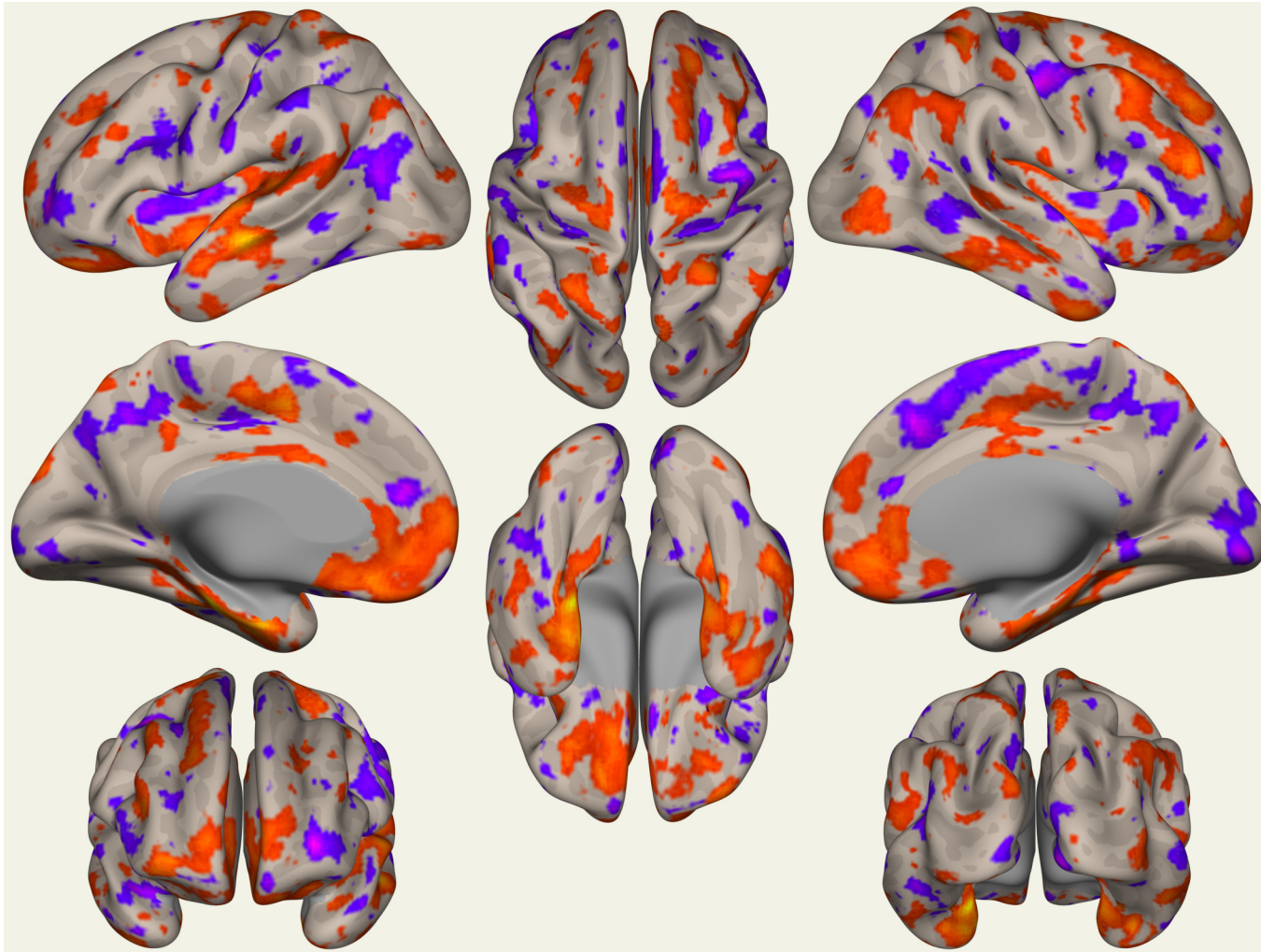[1] Catherine Lord, Mayada Elsabbagh, Gillian Baird, and Jeremy Veenstra-Vanderweele. "Autism spectrum disorder". In: *The Lancet* 392.10146 (2018), pp. 508–520.

[2] Janet Cakir, Richard E Frye, and Stephen J Walker. "The lifetime social cost of autism: 1990–2029". In: *Research in Autism Spectrum Disorders* 72 (2020), p. 101502.

[3] Johnny L Matson and Alison M Kozlowski. "The increasing prevalence of autism spectrum disorders". In: *Research in Autism Spectrum Disorders* 5.1 (2011), pp. 418–425.

[4] Angelica Ronald and Rosa A Hoekstra. "Autism spectrum disorders and autistic traits: a decade of new twin studies". In: *American Journal of Medical Genetics Part B: Neuropsychiatric Genetics* 156.3 (2011), pp. 255–274.

[5] Joachim Hallmayer, Emma J Glasson, Carol Bower, Beverly Petterson, Lisa Croen, Judith Grether, and Neil Risch. "On the twin risk in autism". In: *The American Journal of Human Genetics* 71.4 (2002), pp. 941–946.

[6] Christine M Pennesi and Laura Cousino Klein. "Effectiveness of the gluten-free, casein-free diet for children diagnosed with autism spectrum disorder: based on parental report". In: *Nutritional neuroscience* 15.2 (2012), pp. 85–91.

[7] Christopher Newell, Marc R Bomhof, Raylene A Reimer, Dustin S Hittel, Jong M Rho, and Jane Shearer. "Ketogenic diet modifies the gut microbiota in a murine model of autism spectrum disorder". In: *Molecular autism* 7.1 (2016), pp. 1–6.

[8] Nermin Eissa, Mohammed Al-Houqani, Adel Sadeq, Shreesh K Ojha, Astrid Sasse, and Bassem Sadek. "Current enlightenment about etiology and pharmacological treatment of autism spectrum disorder". In: *Frontiers in neuroscience* 12 (2018), p. 304.

[9] Katherine KM Stavropoulos and Leslie J Carver. "Research review: social motivation and oxytocin in autism–implications for joint attention development and intervention". In: *Journal of Child Psychology and Psychiatry* 54.6 (2013), pp. 603–618.

[10] Federico Bolognani, Marta del Valle Rubido, Lisa Squassante, Christoph Wandel, Michael Derks, Lorraine Murtagh, Jeff Sevigny, Omar Khwaja, Daniel Umbricht, and Paulo Fontoura. "A phase 2 clinical trial of a vasopressin V1a receptor antagonist shows improved adaptive behaviors in men with autism spectrum disorder". In: *Science translational medicine* 11.491 (2019).

[11] Leo Kanner et al. "Autistic disturbances of affective contact". In: *Nervous child* 2.3 (1943), pp. 217–250.

[12] Lisa Campisi, Nazish Imran, Ahsan Nazeer, Norbert Skokauskas, and Muhammad Waqar Azeem. "Autism spectrum disorder." In: *British Medical Bulletin* 127.1 (2018).

[13] Stelios Georgiades, Peter Szatmari, and Michael Boyle. "Importance of studying heterogeneity in autism". In: *Neuropsychiatry* 3.2 (2013), p. 123.

[14] Catherine Lord and Somer L Bishop. "Autism spectrum disorders and commentaries: Diagnosis, prevalence, and services for children and families". In: *Social Policy Report* 24.2 (2010), pp. 1–27.

[15] David G Amaral, Cynthia Mills Schumann, and Christine Wu Nordahl. "Neuroanatomy of autism". In: *Trends in neurosciences* 31.3 (2008), pp. 137–145.

[16] Timothy M Krahn and Andrew Fenton. "The extreme male brain theory of autism and the potential adverse effects for boys and girls with autism". In: *Journal of bioethical inquiry* 9.1 (2012), pp. 93–103.

[17] Simon Baron-Cohen, Alan M Leslie, Uta Frith, et al. "Does the autistic child have a "theory of mind"". In: *Cognition* 21.1 (1985), pp. 37–46.

[18] Blythe A Corbett, Deanna M Swain, Cassandra Newsom, Lily Wang, Yanna Song, and Dale Edgerton. "Biobehavioral profiles of arousal and social motivation in autism spectrum disorders". In: *Journal of Child Psychology and Psychiatry* 55.8 (2014), pp. 924–934.

[19] Rajesh K Kana, Lauren E Libero, and Marie S Moore. "Disrupted cortical connectivity theory as an explanatory model for autism spectrum disorders". In: *Physics of life reviews* 8.4 (2011), pp. 410–437.

[20] Ali A Danesh and Wafaa A Kaf. "DPOAEs and contralateral acoustic stimulation and their link to sound hypersensitivity in children with autism". In: *International journal of audiology* 51.4 (2012), pp. 345–352.

[21] Jose O Maximo, Elyse J Cadena, and Rajesh K Kana. "The implications of brain connectivity in the neuropsychology of autism". In: *Neuropsychology review* 24.1 (2014), pp. 16–31.

[22] American Psychiatric Association et al. *Diagnostic and statistical manual of mental disorders (DSM-5®)*. American Psychiatric Pub, 2013.

[23] Allen J Frances, Marc Galanter, Herbert D Kleber, et al. *Diagnostic and Statistical Manual of Mental Disorders: DSM-IV-TR®*. American Psychiatric Pub, 2000.

[24] Yvonne MY Han and Agnes S Chan. "Disordered cortical connectivity underlies the executive function deficits in children with autism spectrum disorders". In: *Research in developmental disabilities* 61 (2017), pp. 19–31.

[25] Frank DeStefano. "Vaccines and autism: evidence does not support a causal association". In: *Clinical Pharmacology & Therapeutics* 82.6 (2007), pp. 756–759.

[26] Klaus W Lange, Joachim Hauser, and Andreas Reissmann. "Gluten-free and casein-free diets in the therapy of autism". In: *Current Opinion in Clinical Nutrition & Metabolic Care* 18.6 (2015), pp. 572–575.

[27] Rhoshel Krystyna Lenroot and Pui Ka Yeung. "Heterogeneity within autism spectrum disorders: what have we learned from neuroimaging studies?" In: *Frontiers in human neuroscience* 7 (2013), p. 733.

[28] Robert B Dudas, Chris Lovejoy, Sarah Cassidy, Carrie Allison, Paula Smith, and Simon Baron-Cohen. "The overlap between autistic spectrum conditions and borderline personality disorder". In: *PLoS One* 12.9 (2017), e0184447.

[29] Sula Wolff. "The history of autism". In: *European child & adolescent psychiatry* 13.4 (2004), pp. 201–208.

[30] James C Harris. "The origin and natural history of autism spectrum disorders". In: *Nature neuroscience* 19.11 (2016), pp. 1390–1391.

[31] Simon Baron-Cohen, Howard A Ring, Sally Wheelwright, Edward T Bullmore, Mick J Brammer, Andrew Simmons, and Steve CR Williams. "Social intelligence in the normal and autistic brain: an fMRI study". In: *European journal of neuroscience* 11.6 (1999), pp. 1891–1898.

[32] Sebastian B Gaigg and Dermot M Bowler. "Differential fear conditioning in Asperger's syndrome: implications for an amygdala theory of autism". In: *Neuropsychologia* 45.9 (2007), pp. 2125–2134.

[33] Isabel Dziobek, Stefan Fleck, Kimberley Rogers, Oliver T Wolf, and Antonio Convit. "The 'amygdala theory of autism'revisited: linking structure to behavior". In: *Neuropsychologia* 44.10 (2006), pp. 1891–1899.

[34] Robert James R Blair. "Fine cuts of empathy and the amygdala: dissociable deficits in psychopathy and autism". In: *The Quarterly Journal of Experimental Psychology* 61.1 (2008), pp. 157–170.

[35] Natalia M Kleinhans, Todd Richards, Kurt Weaver, L Clark Johnson, Jessica Greenson, Geraldine Dawson, and Elizabeth Aylward. "Association between amygdala response to emotional faces and social anxiety in autism spectrum disorders". In: *Neuropsychologia* 48.12 (2010), pp. 3665–3670.

[36] Tiziana Zalla and Marco Sperduti. "The amygdala and the relevance detection theory of autism: an evolutionary perspective". In: *Frontiers in human neuroscience* 7 (2013), p. 894.

[37] Xiaonan Guo, Xujun Duan, Zhiliang Long, Heng Chen, Yifeng Wang, Junjie Zheng, Youxue Zhang, Rong Li, and Huafu Chen. "Decreased amygdala functional connectivity in adolescents with autism: A resting-state fMRI study". In: *Psychiatry Research: Neuroimaging* 257 (2016), pp. 47–56.

[38] Joshua K Lee, David G Amaral, Marjorie Solomon, Sally J Rogers, Sally Ozonoff, and Christine Wu Nordahl. "Sex Differences in the Amygdala Resting-State Connectome of Children With Autism Spectrum Disorder". In: *Biological Psychiatry: Cognitive Neuroscience and Neuroimaging* 5.3 (2020), pp. 320–329.

[39] Lei Li, Changchun He, Taorong Jian, Xiaonan Guo, Jinming Xiao, Ya Li, Heng Chen, Xiaodong Kang, Huafu Chen, and Xujun Duan. "Attenuated link between the medial prefrontal cortex and the amygdala in children with autism spectrum disorder: Evidence from effective connectivity within the "social brain"". In: *Progress in Neuro-Psychopharmacology and Biological Psychiatry* (2020), p. 110147.

[40] Lauri Nummenmaa, Andrew D Engell, Elisabeth Von Dem Hagen, Richard NA Henson, and Andrew J Calder. "Autism spectrum traits predict the neural response to eye gaze in typical individuals". In: *Neuroimage* 59.4 (2012), pp. 3356–3363.

[41] Lennart Gustafsson. "Inadequate cortical feature maps: A neural circuit theory of autism". In: *Biological psychiatry* 42.12 (1997), pp. 1138–1147.

[42]   Caleb Andrew Doll and Kendal Broadie. "Impaired activity-dependent neural circuit assembly and refinement in autism spectrum disorder genetic models". In: *Frontiers in cellular neuroscience* 8 (2014), p. 30.

[43]   Sacha B Nelson and Vera Valakh. "Excitatory/inhibitory balance and circuit homeostasis in autism spectrum disorders". In: *Neuron* 87.4 (2015), pp. 684–698.

[44]   Harry T Chugani, Michael E Behen, Otto Muzik, Csaba Juhász, Ferenc Nagy, and Diane C Chugani. "Local brain functional activity following early deprivation: a study of postinstitutionalized Romanian orphans". In: *Neuroimage* 14.6 (2001), pp. 1290–1301.

[45]   Jocelyn J LeBlanc and Michela Fagiolini. "Autism: a "critical period" disorder?" In: *Neural plasticity* 2011 (2011).

[46]   L Carroll, DA Menassa, S Braeutigam, JM Dawes, Z Krsnik, I Kostovic, E Coutinho, JM Dewing, CA Horton, and D Gomez-Nicola. "Autism spectrum disorders: multiple routes to, and multiple consequences of, abnormal synaptic function and connectivity". In: *Neuroscientist* 27.1 (2020).

[47]   BJ Wilkes and MH Lewis. "The neural circuitry of restricted repetitive behavior: Magnetic resonance imaging in neurodevelopmental disorders and animal models". In: *Neuroscience & Biobehavioral Reviews* 92 (2018), pp. 152–171.

[48]   Coralie Chevallier, Catherine Molesworth, and Francesca Happe. "Diminished social motivation negatively impacts reputation management: autism spectrum disorders as a case in point". In: *PloS one* 7.1 (2012).

[49]   Kwanguk Kim, M Zachary Rosenthal, Mary Gwaltney, William Jarrold, Naomi Hatt, Nancy McIntyre, Lindsay Swain, Marjorie Solomon, and Peter Mundy. "A virtual joy-stick study of emotional responses and social motivation in children with autism spectrum disorder". In: *Journal of autism and developmental disorders* 45.12 (2015), pp. 3891–3899.

[50]   Hilde M Geurts, Mariolein Luman, and Catharina S Van Meel. "What's in a game: the effect of social motivation on interference control in boys with ADHD and autism spectrum disorders". In: *Journal of Child Psychology and Psychiatry* 49.8 (2008), pp. 848–857.

[51]   Summer Bottini. "Social reward processing in individuals with autism spectrum disorder: A systematic review of the social motivation hypothesis". In: *Research in Autism Spectrum Disorders* 45 (2018), pp. 9–26.

[52] Caitlin C Clements, Alisa R Zoltowski, Lisa D Yankowitz, Benjamin E Yerys, Robert T Schultz, and John D Herrington. "Evaluation of the social motivation hypothesis of autism: A systematic review and meta-analysis". In: *JAMA psychiatry* 75.8 (2018), pp. 797–808.

[53] Heather D Garman, Christine J Spaulding, Sara Jane Webb, Amori Yee Mikami, James P Morris, and Matthew D Lerner. "Wanting it too much: An inverse relation between social motivation and facial emotion recognition in autism spectrum disorder". In: *Child Psychiatry & Human Development* 47.6 (2016), pp. 890–902.

[54] Jessica Bradshaw, Lynn Kern Koegel, and Robert L Koegel. "Improving functional language and social motivation with a parent-mediated intervention for toddlers with autism spectrum disorder". In: *Journal of Autism and Developmental Disorders* 47.8 (2017), pp. 2443–2458.

[55] Simon Baron-Cohen. "Empathizing, systemizing, and the extreme male brain theory of autism". In: *Progress in brain research*. Vol. 186. Elsevier, 2010, pp. 167–175.

[56] Mark Brosnan, Rajiv Daggar, and John Collomosse. "The relationship between systemising and mental rotation and the implications for the extreme male brain theory of autism". In: *Journal of autism and developmental disorders* 40.1 (2010), pp. 1–7.

[57] Christine M Falter, Kate C Plaisted, and Greg Davis. "Visuo-spatial processing in autism—testing the predictions of extreme male brain theory". In: *Journal of autism and developmental disorders* 38.3 (2008), pp. 507–515.

[58] Ingeborg Hauth, Yvette GE de Bruijn, Wouter Staal, Jan K Buitelaar, and Nanda N Rommelse. "Testing the extreme male brain theory of autism spectrum disorder in a familial design". In: *Autism Research* 7.4 (2014), pp. 491–500.

[59] David M Greenberg, Varun Warrier, Carrie Allison, and Simon Baron-Cohen. "Testing the Empathizing–Systemizing theory of sex differences and the Extreme Male Brain theory of autism in half a million people". In: *Proceedings of the National Academy of Sciences* 115.48 (2018), pp. 12152–12157.

[60] Simon Baron-Cohen. "Testing the extreme male brain (EMB) theory of autism: Let the data speak for themselves". In: *Cognitive neuropsychiatry* 10.1 (2005), pp. 77–81.

[61] Simon Baron-Cohen. "Two new theories of autism: hyper-systemising and assortative mating". In: *Archives of Disease in Childhood* 91.1 (2006), pp. 2–5.

[62] Simon Baron-Cohen. "The hyper-systemizing, assortative mating theory of autism". In: *Progress in Neuro-Psychopharmacology and Biological Psychiatry* 30.5 (2006), pp. 865–872.

[63] Simon Baron-Cohen. "The evolution of empathizing and systemizing: Assortative mating of two strong systemizers and the cause of autism". In: *Oxford Handbook of Evolutionary Psychology*. 2007.

[64] Martina Siracusano, Valentina Postorino, Assia Riccioni, Leonardo Emberti Gialloreti, Monica Terribili, Paolo Curatolo, and Luigi Mazzone. "Sex Differences in Autism Spectrum Disorder: Repetitive Behaviors and Adaptive Functioning". In: *Children* 8.5 (2021), p. 325.

[65] L. Brizendine. *The Male Brain: A Breakthrough Understanding of How Men and Boys Think*. Harmony/Rodale, 2010. ISBN: 9780307589392. URL: https://books.google.com/books?id=7nRSO9OUYwEC.

[66] Simon Baron-Cohen. "Autism and the technical mind". In: *Scientific American* 307.5 (2012), pp. 72–75.

[67] Hays Golden. *Childhood autism and assortative mating*. University of Chicago, Division of the Social Sciences, Department of Economics, 2013.

[68] Rosa A Hoekstra, Meike Bartels, Catharina JH Verweij, and Dorret I Boomsma. "Heritability of autistic traits in the general population". In: *Archives of pediatrics & adolescent medicine* 161.4 (2007), pp. 372–377.

[69] Evi van der Zee and Jan JL Derksen. "The power of systemizing in Autism". In: *Child Psychiatry & Human Development* 52.2 (2021), pp. 321–331.

[70] Lindsay M Oberman and Vilayanur S Ramachandran. "The simulating social mind: the role of the mirror neuron system and simulation in the social and communicative deficits of autism spectrum disorders." In: *Psychological bulletin* 133.2 (2007), p. 310.

[71] Lindsay M Oberman, Edward M Hubbard, Joseph P McCleery, Eric L Altschuler, Vilayanur S Ramachandran, and Jaime A Pineda. "EEG evidence for mirror neuron dysfunction in autism spectrum disorders". In: *Cognitive brain research* 24.2 (2005), pp. 190–198.

[72] Nouchine Hadjikhani, Robert M Joseph, Josh Snyder, and Helen Tager-Flusberg. "Anatomical differences in the mirror neuron system and social cognition network in autism". In: *Cerebral cortex* 16.9 (2006), pp. 1276–1282.

[73] Mirella Dapretto, Mari S Davies, Jennifer H Pfeifer, Ashley A Scott, Marian Sigman, Susan Y Bookheimer, and Marco Iacoboni. "Understanding emotions in others: mirror neuron dysfunction in children with autism spectrum disorders". In: *Nature neuroscience* 9.1 (2006), pp. 28–30.

[74] Justin HG Williams, Gordon D Waiter, Anne Gilchrist, David I Perrett, Alison D Murray, and Andrew Whiten. "Neural mechanisms of imitation and 'mirror neuron'functioning in autistic spectrum disorder". In: *Neuropsychologia* 44.4 (2006), pp. 610–621.

[75] Antonia F de C Hamilton, Rachel M Brindley, and Uta Frith. "Imitation and action understanding in autistic spectrum disorders: how valid is the hypothesis of a deficit in the mirror neuron system?" In: *Neuropsychologia* 45.8 (2007), pp. 1859–1868.

[76] Victoria Southgate and Antonia F de C Hamilton. "Unbroken mirrors: Challenging a theory of autism". In: *Trends in cognitive sciences* 12.6 (2008), pp. 225–229.

[77] Alan M Leslie and Uta Frith. "Metarepresentation and autism: How not to lose one's marbles." In: (1987).

[78] Claire Hughes and James Russell. "Autistic children's difficulty with mental disengagement from an object: Its implications for theories of autism." In: *Developmental psychology* 29.3 (1993), p. 498.

[79] Tiffany D Rogers, Eric McKimm, Price E Dickson, Dan Goldowitz, Charles D Blaha, and Guy Mittleman. "Is autism a disease of the cerebellum? An integration of clinical and pre-clinical research". In: *Frontiers in systems neuroscience* 7 (2013), p. 15.

[80] V. Lyons and M. Fitzgerald. *Asperger Syndrome: A Gift Or a Curse?* Biomedical books. Nova Biomedocal Books, 2005. ISBN: 9781594543876. URL: https://books.google.com/books?id=eMunoqn0iU8C.

[81] Marta Fernández, Teresa Sierra-Arregui, and Olga Peñagarikano. "The Cerebellum and autism: More than motor control". In: *Behavioral Neuroscience*. IntechOpen, 2019.

[82] Eiji Hoshi, Léon Tremblay, Jean Féger, Peter L Carras, and Peter L Strick. "The cerebellum communicates with the basal ganglia". In: *Nature neuroscience* 8.11 (2005), pp. 1491–1493.

[83] Catherine J Stoodley. "The cerebellum and neurodevelopmental disorders". In: *The Cerebellum* 15.1 (2016), pp. 34–37.

[84] Ilan Dinstein, Karen Pierce, Lisa Eyler, Stephanie Solso, Rafael Malach, Marlene Behrmann, and Eric Courchesne. "Disrupted neural synchronization in toddlers with autism". In: *Neuron* 70.6 (2011), pp. 1218–1225.

[85] Eric Courchesne, Alan J Lincoln, Beverly A Kilman, and Robert Galambos. "Event-related brain potential correlates of the processing of novel visual and auditory information in autism". In: *Journal of autism and developmental disorders* 15.1 (1985), pp. 55–76.

[86] Eric Courchesne and Karen Pierce. "Why the frontal cortex in autism might be talking only to itself: local over-connectivity but long-distance disconnection". In: *Current opinion in neurobiology* 15.2 (2005), pp. 225–230.

[87] Eric Courchesne, Rachel Yeung-Courchesne, JR Hesselink, and TL Jernigan. "Hypoplasia of cerebellar vermal lobules VI and VII in autism". In: *New England Journal of Medicine* 318.21 (1988), pp. 1349–1354.

[88] Dario Cupolillo, Eriola Hoxha, Alessio Faralli, Annarita De Luca, Ferdinando Rossi, Filippo Tempia, and Daniela Carulli. "Autistic-like traits and cerebellar dysfunction in Purkinje cell PTEN knock-out mice". In: *Neuropsychopharmacology* 41.6 (2016), pp. 1457–1466.

[89] Seungmin Ha, Dongwon Lee, Yi Sul Cho, Changuk Chung, Ye-Eun Yoo, Jihye Kim, Jiseok Lee, Woohyun Kim, Hyosang Kim, Yong Chul Bae, et al. "Cerebellar Shank2 regulates excitatory synapse density, motor coordination, and specific repetitive and anxiety-like behaviors". In: *Journal of Neuroscience* 36.48 (2016), pp. 12129–12143.

[90] Loren A Martin, Dan Goldowitz, and Guy Mittleman. "Repetitive behavior and increased activity in mice with Purkinje cell loss: a model for understanding the role of cerebellar pathology in autism". In: *European Journal of Neuroscience* 31.3 (2010), pp. 544–555.

[91] Ahmed Nadeem, Sheikh F Ahmad, Naif O Al-Harbi, Sabry M Attia, Musaad A Alshammari, Khalid S Alzahrani, and Saleh A Bakheet. "Increased oxidative stress in the cerebellum and peripheral immune cells leads to exaggerated autism-like repetitive behavior due to deficiency of antioxidant response in BTBR T+ tf/J mice". In: *Progress in Neuro-Psychopharmacology and Biological Psychiatry* 89 (2019), pp. 245–253.

[92] John P Hegarty, Dylan J Weber, Carmen M Cirstea, and David Q Beversdorf. "Cerebro-cerebellar functional connectivity is associated with cerebellar excitation–inhibition balance in autism spectrum disorder". In: *Journal of autism and developmental disorders* 48.10 (2018), pp. 3460–3473.

[93] Russell G Port, Lindsay M Oberman, and Timothy PL Roberts. "Revisiting the excitation/inhibition imbalance hypothesis of ASD through a clinical lens". In: *The British journal of radiology* 92.1101 (2019), p. 20180944.

[94] Stefano Berto, Alex Treacher, Emre Caglayan, Danni Luo, Jillian R Haney, Michael J Gandal, Daniel H Geschwind, Albert Montillo, and Genevieve Konopka. "Association between resting-state functional brain connectivity and gene expression is altered in autism spectrum disorder". In: *medRxiv* (2021).

[95] Eliana Roldan Gerschcovich, Daniel Cerquetti, Eduardo Tenca, and Ramon Leiguarda. "The impact of bilateral cerebellar damage on theory of mind, empathy and decision making". In: *Neurocase* 17.3 (2011), pp. 270–275.

[96] Chris I De Zeeuw, Stephen G Lisberger, and Jennifer L Raymond. "Diversity and dynamism in the cerebellum". In: *Nature Neuroscience* 24.2 (2021), pp. 160–167.

[97] Dewen Hu, Hui Shen, and Zongtan Zhou. "Functional asymmetry in the cerebellum: a brief review". In: *The Cerebellum* 7.3 (2008), pp. 304–313.

[98] Anila M D'Mello, John DE Gabrieli, and Derek Evan Nee. "Evidence for hierarchical cognitive control in the human cerebellum". In: *Current Biology* 30.10 (2020), pp. 1881–1892.

[99] Megan L Shipman and John T Green. "Cerebellum and cognition: does the rodent cerebellum participate in cognitive functions?" In: *Neurobiology of learning and memory* 170 (2020), p. 106996.

[100] Sarah V Clark, Eric S Semmel, Holly A Aleksonis, Stephanie N Steinberg, and Tricia Z King. "Cerebellar-subcortical-cortical systems as modulators of cognitive functions". In: *Neuropsychology Review* (2021), pp. 1–25.

[101] Murat Golpinar, Emre Demir, et al. "Global research output of the cerebellum: Yesterday, today, and tomorrow". In: *Journal of The Anatomical Society of India* 69.3 (2020), p. 155.

[102] Huda Y Zoghbi and Mark F Bear. "Synaptic dysfunction in neurodevelopmental disorders associated with autism and intellectual disabilities". In: *Cold Spring Harbor perspectives in biology* 4.3 (2012), a009886.

[103] Manuel Casanova and Juan Trippe. "Radial cytoarchitecture and patterns of cortical connectivity in autism". In: *Philosophical Transactions of the Royal Society B: Biological Sciences* 364.1522 (2009), pp. 1433–1436.

[104] Marlies E Vissers, Michael X Cohen, and Hilde M Geurts. "Brain connectivity and high functioning autism: a promising path of research that needs refined models, methodological convergence, and stronger behavioral links". In: *Neuroscience & Biobehavioral Reviews* 36.1 (2012), pp. 604–625.

[105] Lynn Waterhouse. *Rethinking autism: Variation and complexity*. Academic Press, 2013.

[106] Kevin A Pelphrey, Sarah Shultz, Caitlin M Hudac, and Brent C Vander Wyk. "Research review: constraining heterogeneity: the social brain and its development in autism spectrum disorder". In: *Journal of Child Psychology and Psychiatry* 52.6 (2011), pp. 631–644.

[107] Heather Cody Hazlett, Michele D Poe, Amy A Lightbody, Guido Gerig, James R MacFall, Allison K Ross, James Provenzale, Arianna Martin, Allan L Reiss, and Joseph Piven. "Teasing apart the heterogeneity of autism: Same behavior, different brains in toddlers with fragile X syndrome and autism". In: *Journal of neurodevelopmental disorders* 1.1 (2009), pp. 81–90.

[108] Lies De Fossé, Steven M Hodge, Nikos Makris, David N Kennedy, Verne S Caviness Jr, Lauren McGrath, Shelley Steele, David A Ziegler, Martha R Herbert, Jean A Frazier, et al. "Language-association cortex asymmetry in autism and specific language impairment". In: *Annals of Neurology: Official Journal of the American Neurological Association and the Child Neurology Society* 56.6 (2004), pp. 757–766.

[109] Marieke Langen, Hugo G Schnack, Hilde Nederveen, Dienke Bos, Bertine E Lahuis, Maretha V de Jonge, Herman van Engeland, and Sarah Durston. "Changes in the developmental trajectories of striatum in autism". In: *Biological psychiatry* 66.4 (2009), pp. 327–333.

[110] Donald C Rojas, Eric Peterson, Erin Winterrowd, Martin L Reite, Sally J Rogers, and Jason R Tregellas. "Regional gray matter volumetric changes in autism associated with social and repetitive behavior symptoms". In: *BMC psychiatry* 6.1 (2006), pp. 1–13.

[111] Eric Hollander, Evdokia Anagnostou, William Chaplin, Katherine Esposito, M Mehmet Haznedar, Elizabeth Licalzi, Stacey Wasserman, Latha Soorya, and Monte Buchsbaum. "Striatal volume on magnetic resonance imaging and repetitive behaviors in autism". In: *Biological psychiatry* 58.3 (2005), pp. 226–232.

[112] Claudia L Hilton, Jacquelyn D Harper, Rachel Holmes Kueker, Andrea Runzi Lang, Anna M Abbacchi, Alexandre Todorov, and Patricia D LaVesser. "Sensory responsiveness as a predictor of social severity in children with high functioning autism spectrum disorders". In: *Journal of autism and developmental disorders* 40.8 (2010), pp. 937–945.

[113] Sarah Brieber, Susanne Neufang, Nicole Bruning, Inge Kamp-Becker, Helmut Remschmidt, Beate Herpertz-Dahlmann, Gereon R Fink, and Kerstin Konrad. "Structural brain abnormalities in adolescents with autism spectrum disorder and patients with attention deficit/hyperactivity disorder". In: *Journal of Child Psychology and Psychiatry* 48.12 (2007), pp. 1251–1258.

[114] Nanda NJ Rommelse, Hilde M Geurts, Barbara Franke, Jan K Buitelaar, and Catharina A Hartman. "A review on cognitive and brain endophenotypes that may be common in autism spectrum disorder and attention-deficit/hyperactivity disorder and facilitate the search for pleiotropic genes". In: *Neuroscience & Biobehavioral Reviews* 35.6 (2011), pp. 1363–1396.

[115] Ekaterina Staikova, Hilary Gomes, Vivien Tartter, Allyssa McCabe, and Jeffrey M Halperin. "Pragmatic deficits and social impairment in children with ADHD". In: *Journal of Child Psychology and Psychiatry* 54.12 (2013), pp. 1275–1283.

[116] Silvio Scarone, Cristina Colombo, Simin Livian, Massimo Abbruzzese, Paolo Ronchi, Marco Locatelli, Giuseppe Scotti, and Enrico Smeraldi. "Increased right caudate nucleus size in obsessive-compulsive disorder: detection with magnetic resonance imaging". In: *Psychiatry Research: Neuroimaging* 45.2 (1992), pp. 115–121.

[117] David R Rosenberg, Matcheri S Keshavan, Kirsten M O'Hearn, Elizabeth L Dick, Werner W Bagwell, Andrew B Seymour, Debra M Montrose, Joseph N Pierri, and Boris Birmaher. "Frontostriatal measurement in treatment-naive children with obsessive-compulsive disorder". In: *Archives of general psychiatry* 54.9 (1997), pp. 824–830.

[118] Bradley S Peterson, Prakash Thomas, Michael J Kane, Lawrence Scahill, Heping Zhang, Richard Bronen, Robert A King, James F Leckman, and Lawrence Staib. "Basal ganglia volumes in patients with Gilles de la Tourette syndrome". In: *Archives of general psychiatry* 60.4 (2003), pp. 415–424.

[119] Marieke Langen, Alexander Leemans, Patrick Johnston, Christine Ecker, Eileen Daly, Clodagh M Murphy, Flavio dell'Acqua, Sarah Durston, Declan GM Murphy, AIMS Consortium, et al. "Fronto-striatal circuitry and inhibitory control in autism: findings from diffusion tensor imaging tractography". In: *Cortex* 48.2 (2012), pp. 183–193.

[120] Finale Doshi-Velez, Yaorong Ge, and Isaac Kohane. "Comorbidity clusters in autism spectrum disorders: an electronic health record time-series analysis". In: *Pediatrics* 133.1 (2014), e54–e63.

[121] Natasha Bertelsen, Isotta Landi, Richard AI Bethlehem, Jakob Seidlitz, Elena Maria Busuoli, Veronica Mandelli, Eleonora Satta, Stavros Trakoshis, Bonnie Auyeung, Prantik Kundu, et al. "Imbalanced social-communicative and restricted repetitive behavior subtypes of autism spectrum disorder exhibit different neural circuitry". In: *Communications biology* 4.1 (2021), pp. 1–13.

[122] Francesca Happé, Angelica Ronald, and Robert Plomin. "Time to give up on a single explanation for autism". In: *Nature neuroscience* 9.10 (2006), pp. 1218–1220.

[123] Lynn Waterhouse, Eric London, and Christopher Gillberg. "ASD validity". In: *Review Journal of Autism and Developmental Disorders* 3.4 (2016), pp. 302–329.

[124] Gerardo Noriega. "Brain Functional Connectivity Dynamics in Autism in the Context of Restrictive, Repetitive and Stereotyped Behaviors". In: *2021 10th International IEEE/EMBS Conference on Neural Engineering (NER)*. IEEE. 2021, pp. 359–363.

[125] Seok-Jun Hong, Joshua T Vogelstein, Alessandro Gozzi, Boris C Bernhardt, BT Thomas Yeo, Michael P Milham, and Adriana Di Martino. "Towards neurosubtypes in autism". In: *Biological psychiatry* (2020).

[126] Jessica H Schroeder, Mary Desrocher, James M Bebko, and M Catherine Cappadocia. "The neurobiology of autism: Theoretical applications". In: *Research in Autism Spectrum Disorders* 4.4 (2010), pp. 555–564.

[127] Jenna M Traynor and Geoffrey BC Hall. "Structural and functional neuroimaging of restricted and repetitive behavior in autism spectrum disorder". In: *Journal of Intellectual Disability-Diagnosis and Treatment* 3.1 (2015), pp. 21–34.

[128] Claire J McKinnon, Adam T Eggebrecht, Alexandre Todorov, Jason J Wolff, Jed T Elison, Chloe M Adams, Abraham Z Snyder, Annette M Estes, Lonnie Zwaigenbaum, Kelly N Botteron, et al. "Restricted and repetitive behavior and brain functional connectivity in infants at risk for developing autism spectrum disorder". In: *Biological Psychiatry: Cognitive Neuroscience and Neuroimaging* 4.1 (2019), pp. 50–61.

[129] James W Bodfish, Frank J Symons, Dawn E Parker, and Mark H Lewis. "Varieties of repetitive behavior in autism: Comparisons to mental retardation". In: *Journal of autism and developmental disorders* 30.3 (2000), pp. 237–243.

[130] Anna Fetta, Elisa Carati, Laura Moneti, Veronica Pignataro, Marida Angotti, Maria Chiara Bardasi, Duccio Maria Cordelli, Emilio Franzoni, and Antonia Parmeggiani. "Relationship between Sensory Alterations and Repetitive Behaviours in Children with Autism Spectrum Disorders: A Parents' Questionnaire Based Study". In: *Brain sciences* 11.4 (2021), p. 484.

[131] Dionisio A Amodeo, Brandon Oliver, Alma Pahua, Kristianna Hitchcock, Alexa Bykowski, Devon Tice, Aya Musleh, and Bryce C Ryan. "Serotonin 6 receptor blockade reduces repetitive behavior in the BTBR mouse model of autism spectrum disorder". In: *Pharmacology Biochemistry and Behavior* 200 (2021), p. 173076.

[132] Wouter G Staal, Mariken de Krom, and Maretha V de Jonge. "Brief report: the dopamine-3-receptor gene (DRD3) is associated with specific repetitive behavior in autism spectrum disorder (ASD)". In: *Journal of autism and developmental disorders* 42.5 (2012), pp. 885–888.

[133] Wouter G Staal. "Autism, DRD3 and repetitive and stereotyped behavior, an overview of the current knowledge". In: *European Neuropsychopharmacology* 25.9 (2015), pp. 1421–1426.

[134] Gabriella E DiCarlo, Jenny I Aguilar, Heinrich JG Matthies, Fiona E Harrison, Kyle E Bundschuh, Alyssa West, Parastoo Hashemi, Freja Herborg, Mattias Rickhag, Hao Chen, et al. "Autism-linked dopamine transporter mutation alters striatal dopamine neurotransmission and dopamine-dependent behaviors". In: *The Journal of clinical investigation* 129.8 (2019), pp. 3407–3419.

[135] Sheryl S Moy, Natallia V Riddick, Viktoriya D Nikolova, Brian L Teng, Kara L Agster, Randal J Nonneman, Nancy B Young, Lorinda K Baker, Jessica J Nadler, and James W Bodfish. "Repetitive behavior profile and supersensitivity to amphetamine in the C58/J mouse model of autism". In: *Behavioural brain research* 259 (2014), pp. 200–214.

[136] Denis Pavăl. "A dopamine hypothesis of autism spectrum disorder". In: *Developmental neuroscience* 39.5 (2017), pp. 355–360.

[137] Jon E Grant, Eric Leppink, and Samuel Chamberlain. "Body focused repetitive behavior disorders and perceived stress: Clinical and cognitive associations". In: *Journal of Obsessive-Compulsive and Related Disorders* 5 (2015), pp. 82–86.

[138] Mandy AL Mostert-Kerckhoffs, Wouter G Staal, Renske H Houben, and Maretha V de Jonge. "Stop and change: Inhibition and flexibility skills are related to repetitive behavior in children and young adults with autism spectrum disorders". In: *Journal of autism and developmental disorders* 45.10 (2015), pp. 3148–3158.

[139] Eric W Leppink, Sarah A Redden, and Jon E Grant. "Impulsivity in body-focused repetitive behavior disorders: Disparate clinical associations between three distinct measures". In: *International journal of psychiatry in clinical practice* 20.1 (2016), pp. 24–31.

[140] Parasuraman Padmanabhan, Anu Maashaa Nedumaran, Sachin Mishra, Ganesh Pandarinathan, Govindaraju Archunan, and Balázs Gulyás. "The Advents of Hybrid Imaging Modalities: A New Era in Neuroimaging Applications". In: *Advanced Biosystems* 1.8 (2017), p. 1700019.

[141] Michal Teplan et al. "Fundamentals of EEG measurement". In: *Measurement science review* 2.2 (2002), pp. 1–11.

[142] Marie D Bomba and Elizabeth W Pang. "Cortical auditory evoked potentials in autism: a review". In: *International Journal of Psychophysiology* 53.3 (2004), pp. 161–169.

[143] Nicole Bruneau, Sylvie Roux, Jean Louis Adrien, and Catherine Barthélémy. "Auditory associative cortex dysfunction in children with autism: evidence from late auditory evoked potentials (N1 wave–T complex)". In: *Clinical Neurophysiology* 110.11 (1999), pp. 1927–1934.

[144] Raffaele Ferri, Maurizio Elia, Nivedita Agarwal, Bartolo Lanuzza, Sebastiano A Musumeci, and Giovanni Pennisi. "The mismatch negativity and the P3a components of the auditory event-related potentials in autistic low-functioning subjects". In: *Clinical neurophysiology* 114.9 (2003), pp. 1671–1680.

[145] Yvonne Groen, Albertus A Wijers, Lambertus JM Mulder, Brenda Waggeveld, Ruud B Minderaa, and Monika Althaus. "Error and feedback processing in children with ADHD and children with Autistic Spectrum Disorder: an EEG event-related potential study". In: *Clinical neurophysiology* 119.11 (2008), pp. 2476–2493.

[146] Frank H Duffy, Aditi Shankardass, Gloria B McAnulty, and Heidelise Als. "A unique pattern of cortical connectivity characterizes patients with attention deficit disorders: a large electroencephalographic coherence study". In: *BMC medicine* 15.1 (2017), p. 51.

[147] Klaus Kessler, R Al Seymour, and Gina Rippon. "Brain oscillations and connectivity in autism spectrum disorders (ASD): new approaches to methodology, measurement and modelling". In: *Neuroscience & Biobehavioral Reviews* 71 (2016), pp. 601–620.

[148] Nicole M Gage, Bryna Siegel, and Timothy PL Roberts. "Cortical auditory system maturational abnormalities in children with autism disorder: an MEG investigation". In: *Developmental Brain Research* 144.2 (2003), pp. 201–209.

[149] Arvind K Shukla and Utham Kumar. "Positron emission tomography: An overview". In: *Journal of medical physics/Association of Medical Physicists of India* 31.1 (2006), p. 13.

[150] Gerd Muehllehner and Joel S Karp. "Positron emission tomography". In: *Physics in Medicine & Biology* 51.13 (2006), R117.

[151] Mônica Zilbovicius, Nathalie Boddaert, Pascal Belin, Jean-Baptiste Poline, Philippe Remy, Jean-François Mangin, Lionel Thivard, Catherine Barthélémy, and Yves Samson. "Temporal lobe dysfunction in childhood autism: a PET study". In: *American Journal of Psychiatry* 157.12 (2000), pp. 1988–1993.

[152] NR Zürcher, ML Loggia, JE Mullett, C Tseng, A Bhanot, L Richey, BG Hightower, C Wu, AJ Parmar, RI Butterfield, et al. "[11 C] PBR28 MR–PET imaging reveals lower regional

brain expression of translocator protein (TSPO) in young adult males with autism spectrum disorder". In: *Molecular psychiatry* (2020), pp. 1–11.

[153]   Arthur Lefevre, Raphaëlle Mottolese, Jérôme Redouté, Nicolas Costes, Didier Le Bars, Marie-Maude Geoffray, Marion Leboyer, and Angela Sirigu. "Oxytocin fails to recruit serotonergic neurotransmission in the autistic brain". In: *Cerebral Cortex* 28.12 (2018), pp. 4169–4178.

[154]   Mina Fukai, Tetsu Hirosawa, Mitsuru Kikuchi, Yasuomi Ouchi, Tetsuya Takahashi, Yuko Yoshimura, Yoshiaki Miyagishi, Hirotaka Kosaka, Masamichi Yokokura, Etsuji Yoshikawa, et al. "Oxytocin effects on emotional response to others' faces via serotonin system in autism: a pilot study". In: *Psychiatry Research: Neuroimaging* 267 (2017), pp. 45–50.

[155]   Joshua J Green and Eric Hollander. "Autism and oxytocin: new developments in translational approaches to therapeutics". In: *Neurotherapeutics* 7.3 (2010), pp. 250–257.

[156]   Craig M. Bennett, Abigal A. Baird, Michael B. Miller, and George L. Wolford. "Neural correlate of intersepecies perspective taking in the post-mortem Atlanting Salmon: An argument for multiple comparisons correction". In: *University of California, Santa Barbara* (2009).

[157]   Martin A. Lindquist. "The statistical analysis of fMRI data". In: *Statistical Science* 23.4 (2008), pp. 439–464.

[158]   Rümeysa İnce, Saliha Seda Adanır, and Fatma Sevmez. "The inventor of electroencephalography (EEG): Hans Berger (1873–1941)". In: *Child's Nervous System* (2020), pp. 1–2.

[159]   Edgar Douglas Adrian. *Brain rhythms*. 1944.

[160]   Rosaleena Mohanty, William A Sethares, Veena A Nair, and Vivek Prabhakaran. "Rethinking measures of functional connectivity via feature extraction". In: *Scientific reports* 10.1 (2020), pp. 1–17.

[161]   Michael D Fox and Michael Greicius. "Clinical applications of resting state functional connectivity". In: *Frontiers in systems neuroscience* 4 (2010), p. 19.

[162]   Timothy P Meehan and Steven L Bressler. "Neurocognitive networks: findings, models, and theory". In: *Neuroscience & Biobehavioral Reviews* 36.10 (2012), pp. 2232–2247.

[163]   Dongyang Zhang and Marcus E Raichle. "Disease and the brain's dark energy". In: *Nature Reviews Neurology* 6.1 (2010), pp. 15–28.

[164]   Michael Greicius. "Resting-state functional connectivity in neuropsychiatric disorders". In: *Current opinion in neurology* 21.4 (2008), pp. 424–430.

[165] Aarthi Padmanabhan, Charles J Lynch, Marie Schaer, and Vinod Menon. "The default mode network in autism". In: *Biological Psychiatry: Cognitive Neuroscience and Neuroimaging* 2.6 (2017), pp. 476–486.

[166] Way KW Lau, Mei-Kei Leung, and Ruibin Zhang. "Hypofunctional connectivity between the posterior cingulate cortex and ventromedial prefrontal cortex in autism: Evidence from coordinate-based imaging meta-analysis". In: *Progress in Neuro-Psychopharmacology and Biological Psychiatry* 103 (2020), p. 109986.

[167] R Cameron Craddock, Paul E Holtzheimer III, Xiaoping P Hu, and Helen S Mayberg. "Disease state prediction from resting state functional connectivity". In: *Magnetic Resonance in Medicine: An Official Journal of the International Society for Magnetic Resonance in Medicine* 62.6 (2009), pp. 1619–1628.

[168] Janine Bijsterbosch, Stephen M Smith, and Christian F Beckmann. *An introduction to resting state fMRI functional connectivity*. Oxford University Press, 2017.

[169] Jessica S Damoiseaux and Michael D Greicius. "Greater than the sum of its parts: a review of studies combining structural connectivity and resting-state functional connectivity". In: *Brain structure and function* 213.6 (2009), pp. 525–533.

[170] Kaat Alaerts, Daniel G Woolley, Jean Steyaert, Adriana Di Martino, Stephan P Swinnen, and Nicole Wenderoth. "Underconnectivity of the superior temporal sulcus predicts emotion recognition deficits in autism". In: *Social cognitive and affective neuroscience* 9.10 (2014), pp. 1589–1600.

[171] Paul Broca. "Perte de la parole, ramollissement chronique et destruction partielle du lobe antérieur gauche du cerveau". In: *Bull Soc Anthropol* 2.1 (1861), pp. 235–238.

[172] Steven L Bressler. "Large-scale cortical networks and cognition". In: *Brain Research Reviews* 20.3 (1995), pp. 288–304.

[173] Karl Spencer Lashley. "Mass action in cerebral function." In: *Science* (1931).

[174] Steven L Bressler and JA Scott Kelso. "Cortical coordination dynamics and cognition". In: *Trends in cognitive sciences* 5.1 (2001), pp. 26–36.

[175] Steven L Bressler and Vinod Menon. "Large-scale brain networks in cognition: emerging methods and principles". In: *Trends in cognitive sciences* 14.6 (2010), pp. 277–290.

[176] Lucina Q Uddin, Kaustubh Supekar, Charles J Lynch, Amirah Khouzam, Jennifer Phillips, Carl Feinstein, Srikanth Ryali, and Vinod Menon. "Salience network–based classification and prediction of symptom severity in children with autism". In: *JAMA psychiatry* 70.8 (2013), pp. 869–879.

[177] Mark Tommerdahl, Vinay Tannan, Jameson K Holden, and Grace T Baranek. "Absence of stimulus-driven synchronization effects on sensory perception in autism: Evidence for local underconnectivity?" In: *Behavioral and Brain Functions* 4.1 (2008), pp. 1–9.

[178] Zhiliang Long, Xujun Duan, Dante Mantini, and Huafu Chen. "Alteration of functional connectivity in autism spectrum disorder: effect of age and anatomical distance". In: *Scientific reports* 6.1 (2016), pp. 1–8.

[179] Christine Ecker, Lisa Ronan, Yue Feng, Eileen Daly, Clodagh Murphy, Cedric E Ginestet, Michael Brammer, Paul C Fletcher, Edward T Bullmore, John Suckling, et al. "Intrinsic gray-matter connectivity of the brain in adults with autism spectrum disorder". In: *Proceedings of the National Academy of Sciences* 110.32 (2013), pp. 13222–13227.

[180] Michal Assaf, Kanchana Jagannathan, Vince D Calhoun, Laura Miller, Michael C Stevens, Robert Sahl, Jacqueline G O'Boyle, Robert T Schultz, and Godfrey D Pearlson. "Abnormal functional connectivity of default mode sub-networks in autism spectrum disorder patients". In: *Neuroimage* 53.1 (2010), pp. 247–256.

[181] Christopher S Monk, Scott J Peltier, Jillian Lee Wiggins, Shih-Jen Weng, Melisa Carrasco, Susan Risi, and Catherine Lord. "Abnormalities of intrinsic functional connectivity in autism spectrum disorders". In: *Neuroimage* 47.2 (2009), pp. 764–772.

[182] Kathrin Koch, Tim J Reeß, Oana G Rus, Deniz A Gürsel, Gerd Wagner, Götz Berberich, and Claus Zimmer. "Increased default mode network connectivity in obsessive–compulsive disorder during reward processing". In: *Frontiers in psychiatry* 9 (2018), p. 254.

[183] Adriana Di Martino, Clare Kelly, Rebecca Grzadzinski, Xi-Nian Zuo, Maarten Mennes, Maria Angeles Mairena, Catherine Lord, F Xavier Castellanos, and Michael P Milham. "Aberrant striatal functional connectivity in children with autism". In: *Biological psychiatry* 69.9 (2011), pp. 847–856.

[184] Angela E Abbott, Annika C Linke, Aarti Nair, Afrooz Jahedi, Laura A Alba, Christopher L Keown, Inna Fishman, and Ralph-Axel Müller. "Repetitive behaviors in autism are linked to imbalance of corticostriatal connectivity: a functional connectivity MRI study". In: *Social cognitive and affective neuroscience* 13.1 (2018), pp. 32–42.

[185] Irene Dupong and Adrina Di Martino. "Hyper-connectivity of the striatum related to restricted and repetitive behaviors' severity in children with ASD". In: *bioRxiv* (2020).

[186] Safiye Çavdar, Merve Özgür, Yasemin Kuvvet, Hüsniye Bay, and Evren Aydogmus. "Cortical, subcortical and brain stem connections of the cerebellum via the superior and middle cerebellar peduncle in the rat". In: *Journal of integrative neuroscience* 17.3-4 (2018), pp. 609–618.

[187] Bradley J Wilkes, Carly Bass, Hannah Korah, Marcelo Febo, and Mark H Lewis. "Volumetric magnetic resonance and diffusion tensor imaging of C58/J mice: neural correlates of repetitive behavior". In: *Brain imaging and behavior* 14.6 (2020), pp. 2084–2096.

[188] JM Traynor, KAR Doyle-Thomas, LC Hanford, NE Foster, A Tryfon, KL Hyde, E Anagnostou, AC Evans, L Zwaigenbaum, GBC Hall, et al. "Indices of repetitive behaviour are correlated with patterns of intrinsic functional connectivity in youth with autism spectrum disorder". In: *Brain research* 1685 (2018), pp. 79–90.

[189] Curtis L Carter. "Improvisation in dance". In: *The Journal of Aesthetics and Art Criticism* 58.2 (2000), pp. 181–190.

[190] Jesus Pujol, Laura Blanco-Hinojo, Susanna Esteba-Castillo, Assumpta Caixas, Ben J Harrison, Marta Bueno, Joan Deus, Mercedes Rigla, Didac Macia, Jone Llorente-Onaindia, et al. "Anomalous basal ganglia connectivity and obsessive–compulsive behaviour in patients with Prader Willi syndrome". In: *Journal of psychiatry & neuroscience: JPN* 41.4 (2016), p. 261.

[191] Catherine Lord, Michael Rutter, Pamela C DiLavore, Susan Risi, Katherine Gotham, Somer L Bishop, et al. "ADOS". In: *Autism diagnostic observation schedule. Manual. Los Angeles: WPS* (1999).

[192] A. Fuchs. *Nonlinear Dynamics in Complex Systems: Theory and Applications for the Life-, Neuro- and Natural Sciences.* Springer complexity. Springer Berlin Heidelberg, 2012. ISBN: 9783642335525. URL: https://books.google.com/books?id=h0U85ConqXAC.

[193] A Megremi. "Autism spectrum disorders through the lens of complex-dynamic systems theory". In: *Open Access Autism* 22.2 (2014), pp. 1–10.

[194] Dipanjan Roy and Lucina Q Uddin. "Atypical core-periphery brain dynamics in autism". In: *Network Neuroscience* 5.2 (2021), pp. 295–321.

[195] Jose O Maximo, Cailee M Nelson, and Rajesh K Kana. ""Unrest while Resting"? Brain entropy in autism spectrum disorder". In: *Brain research* 1762 (2021), p. 147435.

[196] Lucina Q Uddin. "Brain mechanisms supporting flexible cognition and behavior in adolescents with autism spectrum disorder". In: *Biological psychiatry* 89.2 (2021), pp. 172–183.

[197] Paul L Nunez and Ramesh Srinivasan. "A theoretical basis for standing and traveling brain waves measured with human EEG with implications for an integrated consciousness". In: *Clinical neurophysiology* 117.11 (2006), pp. 2424–2435.

[198] Gerald Edelmann and Guilio Tonini. "A universe of consciousness". In: *New York: Basic* (2000).

[199] Emmanuelle Tognoli and JA Scott Kelso. "The metastable brain". In: *Neuron* 81.1 (2014), pp. 35–48.

[200] JS Griffith. "On the stability of brain-like structures". In: *Biophysical journal* 3.4 (1963), pp. 299–308.

[201] Melanie Mitchell. "Ubiquity symposium: biological computation". In: *Ubiquity* 2011.February (2011).

[202] José Luis Pérez Velázquez and Roberto Fernández Galán. "Information gain in the brain's resting state: a new perspective on autism". In: *Frontiers in neuroinformatics* 7 (2013), p. 37.

[203] Takamitsu Watanabe and Geraint Rees. "Brain network dynamics in high-functioning individuals with autism". In: *Nature Communications* 8.1 (2017), pp. 1–14.

[204] Leanna M Hernandez, Jeffrey D Rudie, Shulamite A Green, Susan Bookheimer, and Mirella Dapretto. "Neural signatures of autism spectrum disorders: insights into brain network dynamics". In: *Neuropsychopharmacology* 40.1 (2015), pp. 171–189.

[205] Carlos Gómez, Joseph Troy Lizier, Michael Schaum, Patricia Wollstadt, Christine Grützner, Peter Uhlhaas, Christine M Freitag, Sabine Schlitt, Sven Bölte, Roberto Hornero, et al. "Reduced predictable information in brain signals in autism spectrum disorder". In: *Frontiers in neuroinformatics* 8 (2014), p. 9.

[206] Xiaonan Guo, Xujun Duan, Heng Chen, Changchun He, Jinming Xiao, Shaoqiang Han, Yun-Shuang Fan, Jing Guo, and Huafu Chen. "Altered inter-and intrahemispheric functional connectivity dynamics in autistic children". In: *Human brain mapping* 41.2 (2020), pp. 419–428.

[207] Rikkert Hindriks, Mohit H Adhikari, Yusuke Murayama, Marco Ganzetti, Dante Mantini, Nikos K Logothetis, and Gustavo Deco. "Can sliding-window correlations reveal dynamic functional connectivity in resting-state fMRI?" In: *Neuroimage* 127 (2016), pp. 242–256.

[208] Joana Cabral, Etienne Hugues, Olaf Sporns, and Gustavo Deco. "Role of local network oscillations in resting-state functional connectivity". In: *Neuroimage* 57.1 (2011), pp. 130–139.

[209] Adriana Di Martino, Chao-Gan Yan, Qingyang Li, Erin Denio, Francisco X Castellanos, Kaat Alaerts, Jeffrey S Anderson, Michal Assaf, Susan Y Bookheimer, Mirella Dapretto, et al. "The autism brain imaging data exchange: towards a large-scale evaluation of the intrinsic brain architecture in autism". In: *Molecular psychiatry* 19.6 (2014), pp. 659–667.

[210] Yoon Phaik Ooi, Shih-Jen Weng, Joe Kossowsky, Heike Gerger, and Min Sung. "Oxytocin and autism spectrum disorders: a systematic review and meta-analysis of randomized controlled trials". In: *Pharmacopsychiatry* 50.01 (2017), pp. 5–13.

[211] Alfonso Nieto-Castanon. "Handbook of functional connectivity magnetic resonance imaging methods in CONN". In: *Hilbert-Press, Boston, MA* (2020).

[212] Hadley Wickham. *ggplot2: Elegant Graphics for Data Analysis*. Springer-Verlag New York, 2016. ISBN: 978-3-319-24277-4. URL: https://ggplot2.tidyverse.org.

[213] Alboukadel Kassambara. *ggpubr: 'ggplot2' Based Publication Ready Plots*. R package version 0.4.0. 2020. URL: https://CRAN.R-project.org/package=ggpubr.

[214] Bin Wang. *bda: Binned Data Analysis*. R package version 15.2.2. 2021. URL: https://CRAN.R-project.org/package=bda.

[215] Achim Zeileis and Torsten Hothorn. "Diagnostic Checking in Regression Relationships". In: *R News* 2.3 (2002), pp. 7–10. URL: https://CRAN.R-project.org/doc/Rnews/.

[216] Thomas Lumley based on Fortran code by Alan Miller. *leaps: Regression Subset Selection*. R package version 3.1. 2020. URL: https://CRAN.R-project.org/package=leaps.

[217] Max Kuhn. *caret: Classification and Regression Training*. R package version 6.0-88. 2021. URL: https://CRAN.R-project.org/package=caret.

[218] Michael D Greicius, Gaurav Srivastava, Allan L Reiss, and Vinod Menon. "Default-mode network activity distinguishes Alzheimer's disease from healthy aging: evidence from functional MRI". In: *Proceedings of the National Academy of Sciences* 101.13 (2004), pp. 4637–4642.

[219] Frank E Harrell Jr and Maintainer Frank E Harrell Jr. "Package 'hmisc'". In: *CRAN2018* 2019 (2019), pp. 235–6.

[220] "Efficient Computation and Testing of the Bergsma-Dassios Sign Covariance". In: (2019).

[221] J Miecznikowski, En-shuo Hsu, Yanhua Chen, and Albert Vexler. "testforDEP: An R Package for distribution-free tests and visualization tools for independence". In: *SUNY University at Buffalo Biostatistics Technical Reports* 1701 (2017), p. 2.

[222] Nia Goulden, Aygul Khusnulina, Nicholas J Davis, Robert M Bracewell, Arun L Bokde, Jonathan P McNulty, and Paul G Mullins. "The salience network is responsible for switching between the default mode network and the central executive network: replication from DCM". In: *Neuroimage* 99 (2014), pp. 180–190.

[223] Daniel E Lidstone, Rebecca Rochowiak, Stewart H Mostofsky, and Mary Beth Nebel. "A Data Driven Approach Reveals That Anomalous Motor System Connectivity is Associated With the Severity of Core Autism Symptoms". In: *Autism Research* (2021).

[224] Randy L Buckner, Fenna M Krienen, Angela Castellanos, Julio C Diaz, and BT Thomas Yeo. "The organization of the human cerebellum estimated by intrinsic functional connectivity". In: *Journal of neurophysiology* 106.5 (2011), pp. 2322–2345.

[225] Philip H-S Jen, Xinde Sun, and Tsutomu Kamada. "Responses of cerebellar neurons of the CF-FM bat, Pteronotus parnellii to acoustic stimuli". In: *Brain research* 252.1 (1982), pp. 167–171.

[226] Catherine J Stoodley and Jeremy D Schmahmann. "Evidence for topographic organization in the cerebellum of motor control versus cognitive and affective processing". In: *cortex* 46.7 (2010), pp. 831–844.

[227] Peter L Strick, Richard P Dum, and Julie A Fiez. "Cerebellum and nonmotor function". In: *Annual review of neuroscience* 32 (2009), pp. 413–434.

[228] Natacha A Akshoomoff and Eric Courchesne. "A new role for the cerebellum in cognitive operations." In: *Behavioral neuroscience* 106.5 (1992), p. 731.

[229] Jeremy D Schmahmann, Julien Doyon, David McDonald, Colin Holmes, Karyne Lavoie, Amy S Hurwitz, Noor Kabani, Arthur Toga, Alan Evans, and Michael Petrides. "Three-dimensional MRI atlas of the human cerebellum in proportional stereotaxic space". In: *Neuroimage* 10.3 (1999), pp. 233–260.

[230] Jan Voogd and Mitchell Glickstein. "The anatomy of the cerebellum". In: *Trends in cognitive sciences* 2.9 (1998), pp. 307–313.

[231] Xavier Guell and Jeremy Schmahmann. *Cerebellar functional anatomy: a didactic summary based on human fMRI evidence.* 2020.

[232] Catherine J Stoodley and Jeremy D Schmahmann. "Functional topography in the human cerebellum: a meta-analysis of neuroimaging studies". In: *Neuroimage* 44.2 (2009), pp. 489–501.

[233] Gloria Castellazzi, Stefania D Bruno, Ahmed T Toosy, Letizia Casiraghi, Fulvia Palesi, Giovanni Savini, Egidio D'Angelo, and Claudia Angela Michela Gandini Wheeler-Kingshott. "Prominent changes in cerebro-cerebellar functional connectivity during continuous cognitive processing". In: *Frontiers in cellular neuroscience* 12 (2018), p. 331.

[234] Daniela Rabellino, Maria Densmore, Jean Théberge, Margaret C McKinnon, and Ruth A Lanius. "The cerebellum after trauma: Resting-state functional connectivity of the cerebellum in posttraumatic stress disorder and its dissociative subtype". In: *Human brain mapping* 39.8 (2018), pp. 3354–3374.

[235] TJH Ruigrok and J Voogd. "Cerebellar influence on olivary excitability in the cat". In: *European Journal of Neuroscience* 7.4 (1995), pp. 679–693.

[236] Kenji Doya. "What are the computations of the cerebellum, the basal ganglia and the cerebral cortex?" In: *Neural networks* 12.7-8 (1999), pp. 961–974.

[237] Jeremy D Schmahmann, Xavier Guell, Catherine J Stoodley, and Mark A Halko. "The theory and neuroscience of cerebellar cognition". In: *Annual review of neuroscience* 42 (2019), pp. 337–364.

[238] Leonard F Koziol, Deborah Ely Budding, and Dana Chidekel. "From movement to thought: executive function, embodied cognition, and the cerebellum". In: *The Cerebellum* 11.2 (2012), pp. 505–525.

[239] Hsiang-Yuan Lin, Daniel Kessler, Wen-Yih Isaac Tseng, and Susan Shur-Fen Gau. "Increased functional segregation related to the salience network in unaffected siblings of youths with attention-deficit/hyperactivity disorder". In: *Journal of the American Academy of Child & Adolescent Psychiatry* (2019).

[240] James A Brissenden, Emily J Levin, David E Osher, Mark A Halko, and David C Somers. "Functional evidence for a cerebellar node of the dorsal attention network". In: *Journal of Neuroscience* 36.22 (2016), pp. 6083–6096.

[241] Aaron Kucyi, Michael J Hove, Joseph Biederman, Koene RA Van Dijk, and Eve M Valera. "Disrupted functional connectivity of cerebellar default network areas in attention-deficit/hyperactivity disorder". In: *Human brain mapping* 36.9 (2015), pp. 3373–3386.

[242] Gordon MG Shepherd. "Corticostriatal connectivity and its role in disease". In: *Nature Reviews Neuroscience* 14.4 (2013), pp. 278–291.

[243] Anila M D'Mello and Catherine J Stoodley. "Cerebro-cerebellar circuits in autism spectrum disorder". In: *Frontiers in neuroscience* 9 (2015), p. 408.

[244] M Fujita. "Adaptive filter model of the cerebellum". In: *Biological cybernetics* 45.3 (1982), pp. 195–206.

[245] Takahiro Ishikawa, Saeka Tomatsu, Jun Izawa, and Shinji Kakei. "The cerebro-cerebellum: could it be loci of forward models?" In: *Neuroscience research* 104 (2016), pp. 72–79.

[246] Sarah V Clark, Amber Tannahill, Vince D Calhoun, Jessica A Bernard, Juan Bustillo, and Jessica A Turner. "Weaker Cerebellocortical Connectivity Within Sensorimotor and Executive Networks in Schizophrenia Compared to Healthy Controls: Relationships with Processing Speed". In: *Brain connectivity* 10.9 (2020), pp. 490–503.

[247] Tingting Xu, Qing Zhao, Pei Wang, Qing Fan, Jue Chen, Haiyin Zhang, Zhi Yang, Dan J Stein, and Zhen Wang. "Altered resting-state cerebellar-cerebral functional connectivity in obsessive-compulsive disorder". In: *Psychological medicine* 49.7 (2019), pp. 1156–1165.

[248] Pierre-Aurélien Beuriat, Shira Cohen-Zimerman, Gretchen NL Smith, Frank Krueger, Barry Gordon, and Jordan Grafman. "A New Insight on the Role of the Cerebellum for Executive Functions and Emotion Processing in Adults". In: *Frontiers in neurology* 11 (2020), p. 1668.

[249] Christian Bellebaum and Irene Daum. "Cerebellar involvement in executive control". In: *The Cerebellum* 6.3 (2007), pp. 184–192.

[250] Eleni A Demetriou, Marilena M DeMayo, and Adam J Guastella. "Executive function in autism spectrum disorder: history, theoretical models, empirical findings, and potential as an endophenotype". In: *Frontiers in psychiatry* 10 (2019), p. 753.

[251] Shruti Japee, Kelsey Holiday, Maureen D Satyshur, Ikuko Mukai, and Leslie G Ungerleider. "A role of right middle frontal gyrus in reorienting of attention: a case study". In: *Frontiers in systems neuroscience* 9 (2015), p. 23.

[252] A Antal, J Baudewig, W Paulus, and P Dechent. "The posterior cingulate cortex and planum temporale/parietal operculum are activated by coherent visual motion." In: *Visual neuroscience* 25.1 (2008), pp. 17–26.

[253] Nancy Kanwisher, Josh McDermott, and Marvin M Chun. "The fusiform face area: a module in human extrastriate cortex specialized for face perception". In: *Journal of neuroscience* 17.11 (1997), pp. 4302–4311.

[254] Amanda V Utevsky, David V Smith, Jacob S Young, and Scott A Huettel. "Large-scale network coupling with the fusiform cortex facilitates future social motivation". In: *Eneuro* 4.5 (2017).

[255] Chlöé Farrer, Scott H Frey, John D Van Horn, Eugene Tunik, David Turk, Souheil Inati, and Scott T Grafton. "The angular gyrus computes action awareness representations". In: *Cerebral cortex* 18.2 (2008), pp. 254–261.

[256] Etienne Koechlin and Alexandre Hyafil. "Anterior prefrontal function and the limits of human decision-making". In: *Science* 318.5850 (2007), pp. 594–598.

[257] Chun Siong Soon, Marcel Brass, Hans-Jochen Heinze, and John-Dylan Haynes. "Unconscious determinants of free decisions in the human brain". In: *Nature neuroscience* 11.5 (2008), pp. 543–545.

[258] Tanja Kassuba, Corinna Klinge, Cordula Hölig, Mareike M Menz, Maurice Ptito, Brigitte Röder, and Hartwig R Siebner. "The left fusiform gyrus hosts trisensory representations of manipulable objects". In: *NeuroImage* 56.3 (2011), pp. 1566–1577.

[259] Grace Iarocci and John McDonald. "Sensory integration and the perceptual experience of persons with autism". In: *Journal of autism and developmental disorders* 36.1 (2006), pp. 77–90.

[260] Mohamed L Seghier. "The angular gyrus: multiple functions and multiple subdivisions". In: *The Neuroscientist* 19.1 (2013), pp. 43–61.

[261] Christos Papadelis, Carola Arfeller, Silvia Erla, Giandomenico Nollo, Luigi Cattaneo, and Christoph Braun. "Inferior frontal gyrus links visual and motor cortices during a visuomotor precision grip force task". In: *Brain research* 1650 (2016), pp. 252–266.

[262] R Joanne Jao Keehn, Ellyn B Pueschel, Yangfeifei Gao, Afrooz Jahedi, Kalekirstos Alemu, Ruth Carper, Inna Fishman, and Ralph-Axel Müller. "Underconnectivity Between Visual and Salience Networks and Links With Sensory Abnormalities in Autism Spectrum Disorders". In: *Journal of the American Academy of Child & Adolescent Psychiatry* 60.2 (2021), pp. 274–285.

[263] Gregor Kohls, Benjamin Yerys, and Robert T Schultz. "Striatal development in autism: repetitive behaviors and the reward circuitry". In: *Biological psychiatry* 76.5 (2014), p. 358.

[264] Olaf Blanke, Stphanie Ortigue, Theodor Landis, and Margitta Seeck. "Stimulating illusory own-body perceptions". In: *Nature* 419.6904 (2002), pp. 269–270.

[265] Dinesh G Nair, Kari L Purcott, Armin Fuchs, Fred Steinberg, and JA Scott Kelso. "Cortical and cerebellar activity of the human brain during imagined and executed unimanual and bimanual action sequences: a functional MRI study". In: *Cognitive brain research* 15.3 (2003), pp. 250–260.

[266] Bo Chen. "A preliminary study of atypical cortical change ability of dynamic whole-brain functional connectivity in autism spectrum disorder". In: *International Journal of Neuroscience* (2020), pp. 1–13.

[267] Veronica Yuk, Benjamin T Dunkley, Evdokia Anagnostou, and Margot J Taylor. "Alpha connectivity and inhibitory control in adults with autism spectrum disorder". In: *Molecular autism* 11.1 (2020), pp. 1–13.

[268] Sheraz Khan, Konstantinos Michmizos, Mark Tommerdahl, Santosh Ganesan, Manfred G Kitzbichler, Manuel Zetino, Keri-Lee A Garel, Martha R Herbert, Matti S Hämäläinen, and Tal Kenet. "Somatosensory cortex functional connectivity abnormalities in autism show opposite trends, depending on direction and spatial scale". In: *Brain* 138.5 (2015), pp. 1394–1409.

[269] Taiane Coelho Ramos, Joana Bisol Balardin, João Ricardo Sato, and André Fujita. "Abnormal cortico-cerebellar functional connectivity in autism spectrum disorder". In: *Frontiers in systems neuroscience* 12 (2019), p. 74.

[270] Jeremy D Schmahmann. "The role of the cerebellum in cognition and emotion: personal reflections since 1982 on the dysmetria of thought hypothesis, and its historical evolution from theory to therapy". In: *Neuropsychology review* 20.3 (2010), pp. 236–260.

[271] Karen Pierce and Eric Courchesne. "Evidence for a cerebellar role in reduced exploration and stereotyped behavior in autism". In: *Biological psychiatry* 49.8 (2001), pp. 655–664.

[272] PC Berquin, JN Giedd, LK Jacobsen, SD Hamburger, AL Krain, JL Rapoport, and FX Castellanos. "Cerebellum in attention-deficit hyperactivity disorder: a morphometric MRI study". In: *Neurology* 50.4 (1998), pp. 1087–1093.

[273] Li Sang, Wen Qin, Yong Liu, Wei Han, Yunting Zhang, Tianzi Jiang, and Chunshui Yu. "Resting-state functional connectivity of the vermal and hemispheric subregions of the cerebellum with both the cerebral cortical networks and subcortical structures". In: *Neuroimage* 61.4 (2012), pp. 1213–1225.

[274] Catherine J Stoodley and Jeremy D Schmahmann. "The cerebellum and language: evidence from patients with cerebellar degeneration". In: *Brain and language* 110.3 (2009), pp. 149–153.

[275] Raymond J Dolan. "A cognitive affective role for the cerebellum". In: *Brain* 121.4 (1998), pp. 545–546.

[276] C Globas, S Bösch, Ch Zühlke, I Daum, J Dichgans, and K Bürk. "The cerebellum and cognition". In: *Journal of neurology* 250.12 (2003), pp. 1482–1487.

[277] J.D. Martin. *Neuroanatomy Text and Atlas, Fifth Edition.* McGraw-Hill Education, 2020. ISBN: 9781259642487. URL: https://books.google.com/books?id=fWCeDAEACAAJ.

[278] Jennifer G Levitt, Rebecca Blanton, Linda Capetillo-Cunliffe, Donald Guthrie, Arthur Toga, and James T McCracken. "Cerebellar vermis lobules VIII-X in autism." In: *Progress in neuro-psychopharmacology & biological psychiatry* 23.4 (1999), pp. 625–633.

[279] Matthew Calhoun, Margaret Longworth, and Victoria L Chester. "Gait patterns in children with autism". In: *Clinical biomechanics* 26.2 (2011), pp. 200–206.

[280] Nicole J Rinehart, Bruce J Tonge, John L Bradshaw, Robert Iansek, Peter G Enticott, and Jenny McGinley. "Gait function in high-functioning autism and Asperger's disorder". In: *European child & adolescent psychiatry* 15.5 (2006), pp. 256–264.

[281] Deirdre Kindregan, Louise Gallagher, and John Gormley. "Gait deviations in children with autism spectrum disorders: a review". In: *Autism research and treatment* 2015 (2015).

[282] Victoria L Chester and Matthew Calhoun. "Gait symmetry in children with autism". In: *Autism research and treatment* 2012 (2012).

[283] Baijayanta Maiti, Kerri S Rawson, Aaron B Tanenbaum, Jonathan M Koller, Abraham Z Snyder, Meghan C Campbell, Gammon M Earhart, and Joel S Perlmutter. "Functional Connectivity of Vermis Correlates with Future Gait Impairments in Parkinson's Disease". In: *Movement Disorders* (2021).

[284] Christophe Habas. "Functional Connectivity of the Cognitive Cerebellum". In: *Frontiers in Systems Neuroscience* 15 (2021), p. 27.

[285] Juan Delius, Martina Siemann, Jacky Emmerton, and Li Xia. *Cognitions of birds as products of evolved brains.* 2001.

[286] P De Bartolo, Laura Mandolesi, F Federico, F Foti, D Cutuli, F Gelfo, and L Petrosini. "Cerebellar involvement in cognitive flexibility". In: *Neurobiology of Learning and Memory* 92.3 (2009), pp. 310–317.

[287] Price E Dickson, James Cairns, Daniel Goldowitz, and Guy Mittleman. "Cerebellar contribution to higher and lower order rule learning and cognitive flexibility in mice". In: *Neuroscience* 345 (2017), pp. 99–109.

[288] Nicole J Ridley, Judi Homewood, and Jenny Walters. "Cerebellar dysfunction, cognitive flexibility and autistic traits in a non-clinical sample". In: *Autism* 15.6 (2011), pp. 728–745.

[289] Andrea Berger, Michelle Sadeh, Gabriel Tzur, Avinoam Shuper, Liora Kornreich, Dov Inbar, Ian J Cohen, Shalom Michowiz, Isaac Yaniv, Shlomi Constantini, et al. "Task switching after cerebellar damage." In: *Neuropsychology* 19.3 (2005), p. 362.

[290] Tom A Schweizer, Chris Oriet, Nachshon Meiran, Michael P Alexander, Michael Cusimano, and Donald T Stuss. "The cerebellum mediates conflict resolution". In: *Journal of cognitive neuroscience* 19.12 (2007), pp. 1974–1982.

[291] Susan M Ravizza and Richard B Ivry. "Comparison of the basal ganglia and cerebellum in shifting attention." In: *Journal of Cognitive Neuroscience* 13.3 (2001), pp. 285–297.

[292] Josef Parnas and Mads Gram Henriksen. "Disordered self in the schizophrenia spectrum: a clinical and research perspective". In: *Harvard review of psychiatry* 22.5 (2014), p. 251.

[293] Tom A Schweizer, Brian Levine, Dmytro Rewilak, Charlene O'Connor, Gary Turner, Michael P Alexander, Michael Cusimano, Tom Manly, Ian H Robertson, and Donald T Stuss. "Rehabilitation of executive functioning after focal damage to the cerebellum". In: *Neurorehabilitation and Neural Repair* 22.1 (2008), pp. 72–77.

[294] Sean J Farley, Jason J Radley, and John H Freeman. "Amygdala modulation of cerebellar learning". In: *Journal of Neuroscience* 36.7 (2016), pp. 2190–2201.

[295] Aryeh H Taub and Matti Mintz. "Amygdala conditioning modulates sensory input to the cerebellum". In: *Neurobiology of learning and memory* 94.4 (2010), pp. 521–529.

[296] Christine Wu Nordahl, Ana-Maria Iosif, Gregory S Young, Alexa Hechtman, Brianna Heath, Joshua K Lee, Lauren Libero, Vanessa P Reinhardt, Breanna Winder-Patel, David G Amaral, et al. "High psychopathology subgroup in young children with autism: associations with biological sex and amygdala volume". In: *Journal of the American Academy of Child & Adolescent Psychiatry* 59.12 (2020), pp. 1353–1363.

[297] THEO C Manschreck. "Delusional disorder and shared psychotic disorder". In: *Comprehensive Textbook of Psychiatry. 7th ed, Baltimore: Williams &Wilkins* (2000), pp. 1243–1264.

[298] Sandeep Grover, Nitin Gupta, and Surendra Kumar Mattoo. "Delusional disorders: an overview". In: *German J Psychiatry* 9 (2006), pp. 62–73.

[299] Alistair Munro. "The classification of delusional disorders". In: *Psychiatric Clinics of North America* 18.2 (1995), pp. 199–212.

[300] Bernard Crespi, Philip Stead, and Michael Elliot. "Comparative genomics of autism and schizophrenia". In: *Proceedings of the National Academy of Sciences* 107.suppl 1 (2010), pp. 1736–1741.

[301] Yue Qin, Jujiao Kang, Zeyu Jiao, Yi Wang, Jiucun Wang, Hongyan Wang, Jianfeng Feng, Li Jin, Fei Wang, and Xiaohong Gong. "Polygenic risk for autism spectrum disorder affects left amygdala activity and negative emotion in schizophrenia". In: *Translational psychiatry* 10.1 (2020), pp. 1–12.

[302] Mary-Ellen Lynall, Danielle S Bassett, Robert Kerwin, Peter J McKenna, Manfred Kitzbichler, Ulrich Muller, and Ed Bullmore. "Functional connectivity and brain networks in schizophrenia". In: *Journal of Neuroscience* 30.28 (2010), pp. 9477–9487.

[303] Kaat Alaerts, Sylvie Bernaerts, Jellina Prinsen, Claudia Dillen, Jean Steyaert, and Nicole Wenderoth. "Oxytocin induces long-lasting adaptations within amygdala circuitry in autism: a treatment-mechanism study with randomized placebo-controlled design". In: *Neuropsychopharmacology* 45.7 (2020), pp. 1141–1149.

[304] Garrett J Cardon, Susan Hepburn, and Donald C Rojas. "Structural covariance of sensory networks, the cerebellum, and amygdala in autism spectrum disorder". In: *Frontiers in neurology* 8 (2017), p. 615.

[305] Bharath Masetty, Reuth Mirsky, Ashish Deshpande, Michael Mauk, and Peter Stone. "Is the Cerebellum a Model-Based Reinforcement Learning Agent?" In: *AAMAS* (2021).

[306] Ye He, Lisa Byrge, and Daniel P Kennedy. "Nonreplication of functional connectivity differences in autism spectrum disorder across multiple sites and denoising strategies". In: *Human brain mapping* 41.5 (2020), pp. 1334–1350.

[307] Annika C Linke, Lisa E Mash, Christopher H Fong, Mikaela K Kinnear, JS Kohli, Molly Wilkinson, Ryan Tung, RJ Jao Keehn, Ruth A Carper, Inna Fishman, et al. "Dynamic time warping outperforms Pearson correlation in detecting atypical functional connectivity in autism spectrum disorders". In: *Neuroimage* 223 (2020), p. 117383.

[308] Weiqi Zhao, Clare E Palmer, Wesley K Thompson, Bader Chaarani, Hugh P Garavan, BJ Casey, Terry L Jernigan, Anders M Dale, and Chun Chieh Fan. "Individual differences in cognitive performance are better predicted by global rather than localized BOLD activity patterns across the cortex". In: *Cerebral Cortex* 31.3 (2021), pp. 1478–1488.

[309] Christiane S Rohr, Shanty Kamal, and Signe Bray. "Building functional connectivity neuromarkers of behavioral self-regulation across children with and without Autism Spectrum Disorder". In: *Developmental cognitive neuroscience* 41 (2020), p. 100747.

[310] Sebastian Urchs. *Subtypes of functional connectivity in autism*. McGill University (Canada), 2020.

[311] Seok-Jun Hong, Mottron Laurent, Bo-yong Park, Oualid Benkarim, Sofie Louise Valk, Casey Paquola, Sara Larivière, Reinder Vos de Wael, Janie Degré-Pelletier, Isabelle Soulieres, et al. "A convergent structure-function substrate of cognitive imbalances in autism". In: *bioRxiv* (2021).

[312] Valerio Zerbi, Marco Pagani, Marija Markicevic, Michela Matteoli, Davide Pozzi, Michela Fagiolini, Yuri Bozzi, Alberto Galbusera, Maria Luisa Scattoni, Giovanni Provenzano, et al. "Brain mapping across 16 autism mouse models reveals a spectrum of functional connectivity subtypes". In: *bioRxiv* (2020).

[313] Maya A Reiter, Afrooz Jahedi, AR Jac Fredo, Inna Fishman, Barbara Bailey, and Ralph-Axel Müller. "Performance of machine learning classification models of autism using resting-state fMRI is contingent on sample heterogeneity". In: *Neural Computing and Applications* 33.8 (2021), pp. 3299–3310.

[314] Yiting Huang, Binlong Zhang, Jin Cao, Siyi Yu, Georgia Wilson, Joel Park, and Jian Kong. "Potential locations for noninvasive brain stimulation in treating autism spectrum disorders—a functional connectivity study". In: *Frontiers in Psychiatry* 11 (2020), p. 388.

[315]   Rosaria De Luca, Antonino Naro, Pia Valentina Colucci, Federica Pranio, Giuseppe Tardiolo, Luana Billeri, Maria Le Cause, Carmela De Domenico, Simona Portaro, Giuseppe Rao, et al. "Improvement of brain functional connectivity in autism spectrum disorder: an exploratory study on the potential use of virtual reality". In: *Journal of Neural Transmission* 128.3 (2021), pp. 371–380.

[316]   Roscoe O Brady Jr, Irene Gonsalvez, Ivy Lee, Dost Öngür, Larry J Seidman, Jeremy D Schmahmann, Shaun M Eack, Matcheri S Keshavan, Alvaro Pascual-Leone, and Mark A Halko. "Cerebellar-prefrontal network connectivity and negative symptoms in schizophrenia". In: *American Journal of Psychiatry* 176.7 (2019), pp. 512–520.